Modulated Coding for Intersymbol Interference Channels

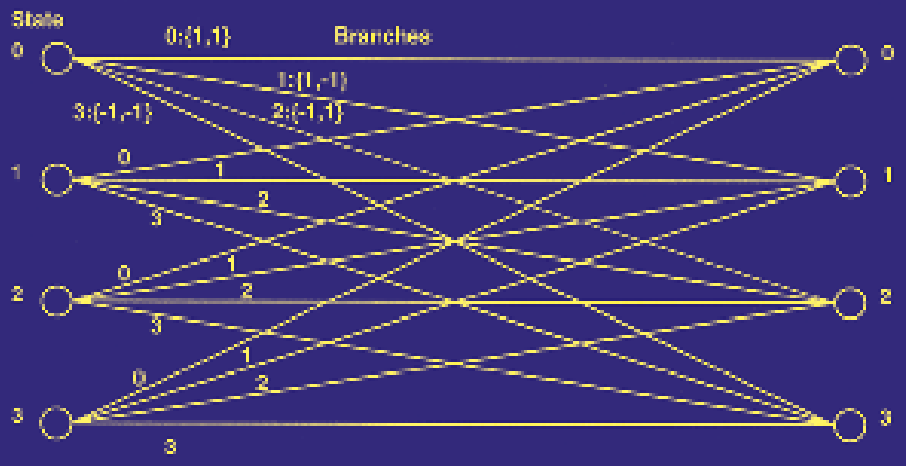

XIANG-GEN XIA

Signal Processing and Communications Series

Modulated Coding for Intersymbol Interference Channels

Signal Processing and Communications

Series Editor

K. J. Ray Liu
University of Maryland
College Park, Maryland

Editorial Board
Sadaoki Furui, *Tokyo Institute of Technology*
Yih-Fang Huang, *University of Notre Dame*
Aggelos K. Katsaggelos, *Northwestern University*
Mos Kaveh, *University of Minnesota*
P. K. Raja Rajasekaran, *Texas Instruments*
John A. Sorenson, *Technical University of Denmark*

1. Digital Signal Processing for Multimedia Systems, *edited by Keshab K. Parhi and Takao Nishitani*
2. Multimedia Systems, Standards, and Networks, *edited by Atul Puri and Tsuhan Chen*
3. Embedded Multiprocessors: Scheduling and Synchronization, *Sundararajan Sriram and Shuvra S. Bhattacharyya*
4. Signal Processing for Intelligent Sensor Systems, *David C. Swanson*
5. Compressed Video over Networks, *edited by Ming-Ting Sun and Amy R. Riebman*
6. Modulated Coding for Intersymbol Interference Channels, *Xiang-Gen Xia*
7. Digital Speech Processing, Synthesis, and Recognition: Second Edition, Revised and Expanded, *Sadaoki Furui*

Additional Volumes in Preparation

Modern Digital Halftoning, *David L. Lau and Gonzalo R. Arce*

Blind Equalization and Identification, *Zhi Ding and Ye (Geoffrey) Li*

Video Coding for Wireless Communications, *King H. Ngan, Chu Yu Yap, and Keng T. Tan*

Modulated Coding for Intersymbol Interference Channels

Xiang-Gen Xia
University of Delaware
Newark, Delaware

MARCEL DEKKER, INC. NEW YORK • BASEL

Library of Congress Cataloging-in-Publication Data

Xia, Xiang-gen

Modulated coding for intersymbol interference channels / Xiang-gen Xia.
p. cm. – (Signal processing ; 6)
Includes bibliographical references and index.
ISBN 0-8247-0459-2 (alk. paper)
1. Signal processing. 2. Coding theory. 3. Modulation (Electronics) 4. Electromagnetic interference. I. Title. II. Signal processing (Marcel Dekker, Inc.) ; 6.

TK5102.92 .X53 2000
621.382'2—dc21

00-060174

This book is printed on acid-free paper.

Headquarters
Marcel Dekker, Inc.
270 Madison Avenue, New York, NY 10016
tel: 212-696-9000; fax: 212-685-4540

Eastern Hemisphere Distribution
Marcel Dekker AG
Hutgasse 4, Postfach 812, CH-4001 Basel, Switzerland
tel: 41-61-261-8482; fax: 41-61-261-8896

World Wide Web
http://www.dekker.com

The publisher offers discounts on this book when ordered in bulk quantities. For more information, write to Special Sales/Professional Marketing at the headquarters address above.

Copyright © 2001 by Marcel Dekker, Inc. All Rights Reserved.

Neither this book nor any part may be reproduced or transmitted in any form or by any means, electronic or mechanical, including photocopying, microfilming, and recording, or by any information storage and retrieval system, without permission in writing from the publisher.

Current printing (last digit):
10 9 8 7 6 5 4 3 2 1

PRINTED IN THE UNITED STATES OF AMERICA

Series Introduction

Over the past 50 years, digital signal processing has evolved as a major engineering discipline. The fields of signal processing have grown from the origin of fast Fourier transform and digital filter design to statistical spectral analysis and array processing, and image, audio, and multimedia processing, and shaped developments in high-performance VLSI signal processor design. Indeed, there are few fields that enjoy so many applications—signal processing is everywhere in our lives.

When one uses a cellular phone, the voice is compressed, coded, and modulated using signal processing techniques. As a cruise missile winds along hillsides searching for the target, the signal processor is busy processing the images taken along the way. When we are watching a movie in HDTV, millions of audio and video data are being sent to our homes and received with unbelievable fidelity. When scientists compare DNA samples, fast pattern recognition techniques are being used. On and on, one can see the impact of signal processing in almost every engineering and scientific discipline.

Because of the immense importance of signal processing and the fast-growing demands of business and industry, this series on signal processing serves to report up-to-date developments and advances in the field. The topics of interest include but are not limited to the following:

- Signal theory and analysis
- Statistical signal processing
- Speech and audio processing
- Image and video processing
- Multimedia signal processing and technology
- Signal processing for communications
- Signal processing architectures and VLSI design

I hope this series will provide the interested audience with high-quality, state-of-the-art signal processing literature through research monographs, edited books, and rigorously written textbooks by experts in their fields.

K. J. Ray Liu

Preface

Intersymbol interference (ISI) mitigation has been an active research area for the last several decades and has played an important role in improving the performance of communication systems. There are mainly two classes of ISI mitigation methods, namely post equalization methods and transmitter assisted equalization methods. The method introduced in this book belongs to the second class. The goal of this book is to introduce modulated codes (MC) for ISI mitigation, recently proposed by the author.

The most results in this book were obtained by my research group in the last few years at the Communications Laboratory, Department of Electrical and Computer Engineering, University of Delaware. The following people in the group have contributed to the results: Pingyi Fan, Weifeng Su, Genyuan Wang, Kai Xiao, Qian Xie, Yong-Jun Alan Zhang, and Guangcai Zhou. Some of the results in this book were also summarized from my joint work with Professor Hui Liu at the Department of Electrical Engineering, University of Washington.

MC encoding and decoding are of three different types: case (i) both encoding and decoding have the ISI channel information; case (ii) neither of the encoding nor decoding has the ISI channel information; and case (iii) encoding does not have the ISI channel information but decoding has the ISI channel information. Case (i) is further split into two subcases: case (i.1) encoding depends on the input information signal constellation; case (i.2) encoding does not depend on the input information signal constellation. All these cases are addressed in this book and organized as follows.

In Chapter 1, we briefly introduce the current ISI mitigation methods, in particular, the methods in the second class as previously mentioned. We also formulate the capacity and the information rates of an ISI channel.

In Chapter 2, we introduce MC and some basic concepts similar to the conventional convolutional codes defined on finite fields. We describe the combination of an MC and an ISI channel. We also introduce and study the coding gain of an MC in an ISI channel compared to the uncoded additive white Gaussian noise (AWGN) channel. Some coding gain results are presented. The results in this chapter are for case (i.1), where the channel information and the input signal constellation are used.

In Chapter 3, we introduce the joint maximum-likelihood sequence estimation (MLSE) encoding and decoding of an MC coded ISI channel. For the MC performance analysis, we introduce the error-pattern trellis and present a spectrum distance calculation algorithm by extending the known bidirectional searching algorithm. We also present an algorithm to search for the optimal MC given an ISI channel. The results in this chapter are also for case (i.1).

In Chapter 4, we introduce some suboptimal MC design results given an ISI channel, which are of case (i.2), i.e., the signal constellation is not needed. The advantage over the design in Chapter 3 is its simplicity. In particular, we introduce MC coded ZF-DFE and MMSE-DFE and their corresponding optimal MC designs. Another suboptimal MC design is also introduced to optimally convert an ISI channel with AWGN into an ISI-free AWGN channel.

In Chapter 5, we study the capacity and information rates of an MC coded ISI channel with AWGN. We show that for any finite tap ISI channel there exist MC such that the MC coded ISI channel has higher information rates than the original ISI channel does at low channel signal-to-noise ratio (SNR). This implies that the achievable transmission data rates of the MC coded ISI channel may be higher than those of the original ISI channel. We introduce a joint turbo and MC encoding and decoding for an ISI channel, which may achieve performance above the AWGN channel capacity at low channel SNR.

In Chapter 6, we extend the MC results to space-time MC encoding and decoding for multiple transmit and multiple receive antenna systems.

In Chapter 7, we study a channel-independent MC coded orthogonal frequency division multiplexing (OFDM) system, which belongs to case (iii), i.e., the MC encoding does not need the ISI channel information while the decoding needs to know the ISI channel. We show that the MC coded OFDM channels may be robust to spectral null and frequency-selective multipath fading channels. We also introduce vector OFDM systems that can be used to reduce the cyclic prefix length over conventional OFDM systems.

In Chapter 8, we study polynomial ambiguity resistant MC (PARMC), which belongs to case (ii), i.e., neither the MC encoding nor the MC decoding needs to know the ISI channel. It is proved that it is necessary and sufficient for an MC to be PARMC for the blind identifiability at the receiver. A block MC is not a PARMC. In this chapter, we also introduce an algebraic blind identification algorithm. Note that PARMC applies to both single antenna and multiple antenna systems. For multiple antenna systems, PARMC may be used as space-time coding.

In Chapter 9, we characterize and construct PARMC by providing the canonical forms.

In Chapter 10, we introduce an optimal criterion for the PARMC design. Although in theory any PARMC is sufficient for canceling an ISI channel, it may have a performance difference when there is additive noise. The optimality studied in this chapter is for the resistance of channel additive noise.

In the last chapter, Chapter 11, we present some conclusions and propose a few important open problems on MC for ISI channels.

Acknowledgments

Most results described in this book were from my research supported by the Air Force Office of Scientific Research (AFOSR), the National Science Foundation (NSF), and the University of Delaware Research Foundation. I am indebted to Dr. Jon Sjogren at AFOSR and Dr. John Cozzens at NSF for their support of my research projects on modulated coding and filterbank precoding.

I would like to take this opportunity to thank the series editor, Prof. K. J. Ray Liu, for including this book in his Signal Processing and Communications Series. I thank Mr. B. J. Clark, Executive Editor of Marcel Dekker, Inc., for his coordination of the effort, and the Book Editorial Department of Marcel Dekker, Inc., for their editorial help.

I am grateful to Prof. Gonzalo Arce (University of Delaware), Prof. Zhi Ding (University of Iowa), Prof. Yingbo Hua (University of Melbourne), Prof. Lang Tong (Cornell University), Prof. P. P. Vaidyanathan (California Institute of Technology), Prof. Guanghan Xu (University of Texas at Austin), Prof. Zhen Zhang (University of Southern California), and Prof. Michael Zoltowski (Purdue University at West Lafayette) for their valuable discussions and encouragement in my research on modulated coding and filterbank precoding.

I wish to give special thanks to Prof. Hui Liu at University of Washington for collaboration on some of the results included in this book, in particular the PARMC part in Chapter 8.

I am grateful to current and former postdoctoral researchers, Pingyi Fan, Genyuan Wang, and Guangcai Zhou, and graduate students, Weifeng Su, Kai Xiao, Qian Xie, and Yong-Jun Alan Zhang, for their participation and contribution of research results included in this book.

Finally, I would like to thank my wife, Rong Zhang, for her support and understanding during this project and throughout my research.

Xiang-Gen Xia

Contents

Modulated Coding for Intersymbol Interference Channels

Chapter 1

Introduction

Intersymbol interference (ISI) may occur in wireline systems, such as telephone systems; storage systems , such as magnetic recording systems; and wireless systems , such as cellular systems . To improve the performance of a communication system, ISI mitigation is one of the most important tasks, which has been an active research area for several decades. An ISI channel is usually described as

$$y_a(t) = \sum_n x_a(t - \tau_n)h(n) + \eta_a(t), \tag{1.0.1}$$

where $x_a(t)$ and $y_a(t)$ are transmitted and received signals, respectively, $h(n)$ is the ISI channel impulse response, and $\eta_a(t)$ is the additive noise. For a band-limited channel with bandwidth W, the above continuous-time ISI channel can be rewritten as the following discrete linear time invariant (LTI) system

$$y(k) = \sum_n x(k - n)h(n) + \eta(k), \tag{1.0.2}$$

where $x(n) = x_a(nT_s)$, $y(n) = y_a(nT_s)$, and $\eta(n) = \eta_a(nT_s)$ and $T_s \leq 1/(2W)$. Throughout this book, we adopt the ISI channel model (1.0.2) with additive white Gaussian noise (AWGN) $\eta(n)$. The goal of ISI mitigation is to recover the transmitted signal $x(n)$ from the received signal $y(n)$. All ISI mitigation techniques can be categorized into two classes: post equalizations and transmitter assisted equalizations.

1.1 Post Equalizations

In post equalizations, the transmitter does not do anything for the ISI channel and the equalization is purely implemented at the receiver and therefore, one advantage of the post equalization technique is that the transmitter does not need to have the ISI channel information. There have been many post equalization techniques. They are mainly linear equalizers, such as zero-forcing (ZF) equalizers [93] and minimum mean square error (MMSE) equalizers; nonlinear equalizers, such as decision feedback equalizers (DFE) [10, 12, 107]; maximum-likelihood sequence estimation (MLSE) [68]; fractionally spaced equalizers [20, 137, 54]; and blind equalizations/blind system identification [117, 55, 120, 58, 52, 34, 33, 134, 135, 90, 180, 128, 136, 35, 79, 80, 83, 82, 63, 1, 64, 147, 81, 98, 123, 101, 183, 92, 36, 161]. The linear equalizers may enhance the noise and therefore do not perform well for the ISI channels with spectral nulls while the DFE have much better performance but present the difficulty in combining with the existing forward error correction coding. Since this class of equalizations is not the focus of this book, we refer the reader to [76, 108, 127] for more detailed studies on these equalizers.

1.2 Transmitter Assisted Equalizations

In transmitter assisted equalizations, the transmitter does do something to help ISI mitigation, where the transmitter may or may not need the complete ISI channel information. There also have been many transmitter assisted equalization techniques, such as joint convolutional/trellis coded equalization, [11, 7, 187, 22, 182, 28, 29]; Tomlinson-Harashima (TH) precoding [133, 57]; trellis precoding [41, 69]; vector coding [72, 5, 30], and other precoding techniques [74, 155]; prefiltering [48] and partial response signaling (PRS), such as [159, 114, 115]; and OFDM systems [27, 24, 18, 25]. Modulated coding in this book belongs to this class of equalization techniques. Although in OFDM systems the transmitter does not need the ISI channel information, the other transmitter assisted techniques do need the complete ISI channel information. In the joint convolutional/trellis coded equalization, such as [7, 187], and also trellis precoding [41, 69], the coding part is over a finite field and hard to combine with an arbitrary ISI channel although some optimality is possible for some special ISI channels, such as partial response channels in magnetic recording systems. Since TH precoding is one of the earliest and accepted precoding techniques, we next examine it in more detail.

1.2.1 TH Precoding

TH precoding basically erases the ISI channel at the transmitter by using finite information symbol characteristics. A block diagram is shown in Fig.1.1, where $H(z)$ is the z-transform of the ISI channel and the pulse amplitude modulation (PAM) with M symbols is used for the binary-to-complex mapping at the transmitter. The input data symbols $s(k)$ take the symbols of $-M+1, -M+3, ..., -1, 1, 3, ..., M-1$. The precoded symbol $x(k)$ for the transmission is a *real value* in the interval $(-M, M]$:

$$x(k) = s(k) - v(k) + 2Mi(k), \tag{1.2.1}$$

where $i(k)$ is an integer such that $-M < x(k) \leq M$. From (1.2.1), the received signal $y(k)$ with its z-transform $Y(z)$ is

$$Y(z) = S(z) + 2MI(z) + \eta(z), \tag{1.2.2}$$

where $S(z)$ and $I(z)$ are the z-transforms of $s(n)$ and $i(n)$, respectively. After the $2M$ modulo operation at the receiver, the ambiguity part $2MI(z)$ in the received signal is removed but the additive noise $\eta(k)$ is folded by the modulo operation. The final decoded signal is the M PAM demodulated one from $a(k) + \eta_M(k)$ where $\eta_M(k) = \eta(k) \text{mod } 2M$. In other words, the AWGN after the TH precoding and the decoding is folded into $(-M, M]$, which may affect the decoding performance when M is not large. Therefore, when the channel signal-to-noise (SNR) ratio is low and small PAM is used, the TH precoding may not perform well, although the TH precoding and the DFE techniques may approach the ISI capacity at high channel SNR [107].

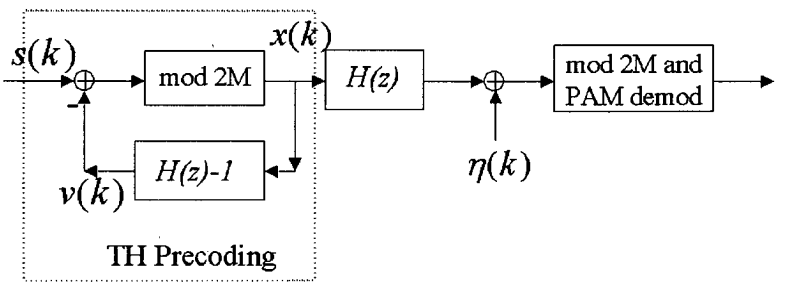

Figure 1.1: TH precoding.

The TH precoding and other prefiltering do not introduce redundancy to transmitted signals, except in the case of vector coding [72, 5] where zeros

are inserted between the blocks of the information symbols such that there is no ISI between blocks. What we want to especially point out here is that the PRS and the prefiltering [159, 114, 115, 48], which has no redundancy introduced, are LTI filtering over the complex field.

1.2.2 Modulated Coding and Vector Coding

Modulated coding (MC) recently studied in [165, 164, 170, 178, 167, 168, 45, 166, 44, 176, 179, 185, 89, 88, 171, 186, 163, 172] is an error correction coding (ECC), in particular a convolutional coding, defined on the real/complex field. In comparison with the current coded modulation scheme for ECC over a finite field, an MC has the encoding scheme shown in Fig.1.2 over the complex field. Since the arithmetic operations of an ISI channel are also over the complex field, an MC can be naturally combined with an ISI channel. The combination provides convenience in the MC design. Different from the TH precoding, an MC adds redundancy at the transmitter and it does not have the modulo operation. MC is a generalization of the PRS and the prefiltering by adding redundancy to the transmitter and a generalization of the vector coding studied by Kasturia, Aslanis, and Cioffi in [72] and Cioffi and Forney [30] and the block-based transmission studied by Al-Dhahir and Cioffi in [5] and the OFDM by considering general convolutional codes rather than only the block codes. Furthermore, the vector coding and block based transmission are designed independently with the input signal constellation, which only belongs to case (i.2) of the MC of this book as mentioned in the Preface. We will show that some small size MC with simple structure over an ISI channel may provide a better performance than the uncoded ISI-free AWGN channel, in other words, the achievable data rates may be better than the capacity of the ISI-free AWGN channel at low channel SNR. Note that in the vector coding and the block based transmission studied, for example, in [72, 5, 30], the water-pouring input signal spectrum and the infinite block size are needed to achieve the ISI channel capacity, which may be complicated in practical implementations, in particular, when the channel SNR is not fixed and further conventional ECC, such as turbo codes, are used before the vector coding. The MC designs introduced in this book do not depend on the channel SNR. More comparisons between the block-based approach and the MC approach are given in Section 4.3.

There are two main different families of MC. One family of MC consists of MC that are designed when an ISI channel is known at the transmitter and the receiver [165, 164, 170, 178, 167, 168, 45, 166, 44, 176, 179, 185]. For this family of MC, the coding performance is the key. For this family MC,

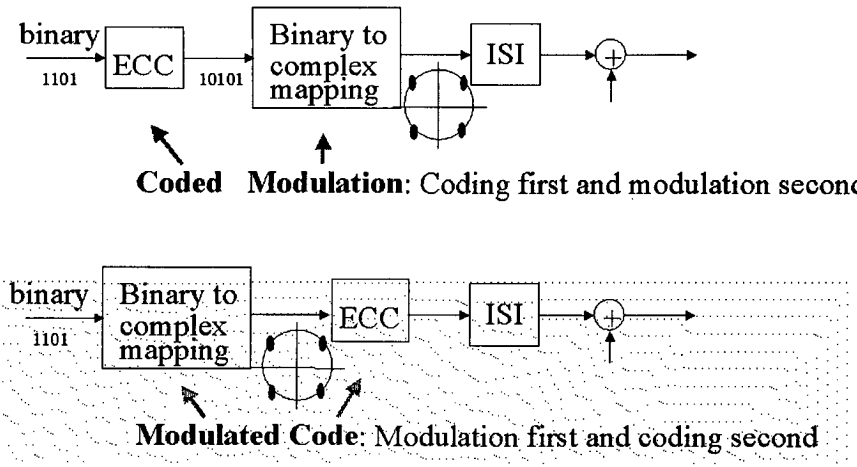

Figure 1.2: Modulated coding vs. coded modulation.

there are two main types of MC designs. One kind of optimal MC design is the optimal MC design that depends on the input signal constellations [178, 170, 166, 44] and the other is the MC design that is independent of the input signal constellations [72, 5, 167, 168, 176, 179, 185]. The other family of MC consists of MC that are designed when an ISI channel is not known at the transmitter or the receiver, which are called polynomial ambiguity resistant MC (PARMC) [89, 88, 171, 186, 163, 172]. Using PARMC the receiver is able to blindly identify the transmitted signal. For this family of MC, the unknown channel information is the key. We shall see later that PARMC is necessary and sufficient for an MC at the transmitter for the blind identification.

In some literature, see for example [165, 89, 88, 171, 163, 172, 53, 118, 77, 97], instead of using "MC" the name "filterbank precoding" is used,.

1.3 Information Rates and Capacity of an ISI Channel with AWGN

We now describe the information rates and the capacity of the ISI channel (1.0.2) with AWGN. Using the water-pouring method, the capacity, $C(E_s)$,

of channel (1.0.2), see for example [59, 21], is

$$C(E_s) = \sup_x I(x,y) = \frac{1}{4\pi}\int_{-\pi}^{\pi} \max\left\{0, \log_2\left[\frac{2K_s|H(e^{j\theta})|^2}{N_0}\right]\right\} d\theta, \quad (1.3.1)$$

where

$$E_s = \frac{1}{2\pi}\int_{-\pi}^{\pi} \max\left\{0, K_s - \frac{N_0}{2}|H(e^{j\theta})|^{-2}\right\} d\theta, \quad (1.3.2)$$

where $I(x,y)$ is the mutual information of the channel (1.0.2) with input x, $K_s > 0$ is a constant parameter and $H(z)$ is the z transform of $h(k)$. Note that in the above capacity formula, the input x may have any distribution. When the input x is restricted to an i.i.d. source, the maximum mutual information is called the information rate, see for example [59, 21, 122, 121]. The *information rate*, $C_{i.i.d.}(E_s)$, of channel (1.0.2), see [59], is

$$C_{i.i.d.} = \sup_{i.i.d.\ x} I(x,y) = \frac{1}{4\pi}\int_{-\pi}^{\pi} \log_2\left[1 + 2\frac{E_s}{N_0}|H(e^{j\theta})|^2\right] d\theta, \quad (1.3.3)$$

which is achieved when the input x is an i.i.d. Gaussian process. The above information rate determines an achievable reliable information rate when the standard random coding technique, such as the existing ECC defined on finite fields, is used. The information rate is also called, for example in [121], *information capacity*. Although the capacity (1.3.1) can be achieved by the standard water-pouring method, the implementation of the filter to shape the optimal water-pouring spectrum is not simple.

When the ISI channel $H(z) = 1$, i.e., ISI-free, the above information rate and capacity formulas are the same, i.e., the capacity of the AWGN channel:

$$C_{AWGN}(E_s) = \frac{1}{2}\log_2\left[1 + \frac{2E_s}{N_0}\right]. \quad (1.3.4)$$

As an example, let us consider the ISI channel with $h(0) = h(1) = 0.7071$. The capacity and the information rates of this channel are plotted in Fig.1.3 and the details are described in the following chapters, in particular Chapters 4 and 5. One can see that the achievable data rate of the MC for this channel is even better than the capacity of the AWGN channel at channel SNR $E_b/N_0 = -1.15$dB, where E_b is the energy per bit. As we shall see later, the MC used in Fig.1.3 is simple and has small size, which means that it does not have the practical implementation problem.

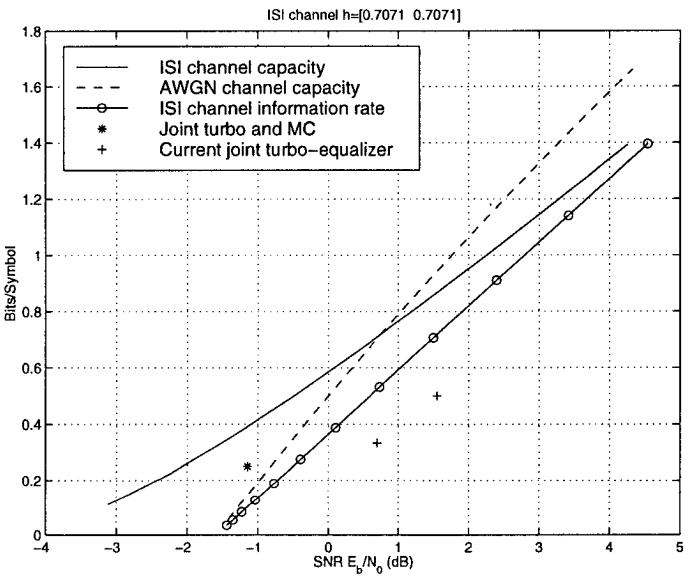

Figure 1.3: ISI channel capacity and information rates.

1.4 Some Notations

Throughout this book, the following notations are used. We use boldfaced capital English letters, $\mathbf{X}(z)$, $\mathbf{Y}(z)$, ..., to denote polynomial matrices/vectors, italic capital English letters, $X(n)$, $Y(n)$,..., to denote constant matrices and vectors that are formed from the scalar sequences $x(n), y(n), ...$, after the serial to parallel conversion unless specified otherwise, and lowercase italic English letters to denote scalar values, $x(n)$, $y(n)$, ... Since we deal with error correction codes defined over the complex field, instead of using D we use z^{-1} as the delay variable. The D transforms become the z transforms.

$\|\cdot\|_F$ indicates the Frobenius norm of a matrix, i.e. $\|A\|_F = \sqrt{\sum_{ij} |a_{ij}|^2}$, where $A = (a_{ij})$. Here, the Frobenius norm of the polynomial matrix in z, for instance $\|\mathbf{G}(z)\|_F$, is defined as the square root of the summation of the Frobenius norms squared of all the coefficient matrices, i.e. $\left(\sum_i \|G_i\|_F^2\right)^{1/2}$, where $\mathbf{G}(z) = \sum_i G_i z^{-i}$.

The symbol $A^\dagger$ denotes the complex-conjugate transpose of a matrix or vector A and A^T denotes the transpose of A.

$f|g$ means f divides g, and

$$Q(x) = \frac{1}{\sqrt{2\pi}} \int_x^\infty e^{-t^2/2} dt.$$

Chapter 2

Modulated Codes: Fundamentals and Coding Gain

In this chapter, we introduce modulated codes (MC) and some of their properties. We also introduce their coding gain concepts in AWGN and ISI channels compared to the uncoded AWGN channel. We show that an MC does not have any coding gain in an AWGN channel and for any finite tap ISI channel there exists an MC with coding gain compared to the uncoded AWGN channel. The results in this chapter are summarized from [165, 164, 170, 178, 166, 44].

2.1 Modulated Codes

An (N, K) *modulated code* (MC) encoder or generator matrix is an N by K polynomial matrix

$$\mathbf{G}(z) = \begin{bmatrix} g_{11}(z) & \cdots & g_{1K}(z) \\ \vdots & \vdots & \vdots \\ g_{N1}(z) & \cdots & g_{NK}(z) \end{bmatrix} = \sum_{l=0}^{Q_G} G(l) z^{-l}, \tag{2.1.1}$$

where $g_{nk}(z)$ is a polynomial of z^{-1} with complex-valued coefficients, $G(l)$ is an $N \times K$ constant matrix with complex entries, and Q_G is a non-negative integer. The rate of the MC is K/N. The constraint length ν of an (N, K)

MC is defined the same as the conventional convolutional codes, i.e.,

$$\nu = \nu_1 + \cdots + \nu_K, \tag{2.1.2}$$

where ν_k is the highest degree of polynomials $g_{1k}(z)$, ..., $g_{Nk}(z)$ of z^{-1} for each fixed k with $k = 1, 2, ..., K$. If an MC generator matrix $\mathbf{G}(z)$ is a constant matrix, it is called a *block MC.*

Let $s(n)$ be a binary information sequence and $x(n)$ be the complex symbol sequence after the binary-to-complex symbol mapping of $s(n)$. Let $X(n)$ be the K by 1 vector sequence of $x(n)$ after the serial to parallel conversion. Their z transforms are $\mathbf{x}(z)$ and $\mathbf{X}(z)$, respectively. Then the encoding of an MC is

$$\mathbf{Y}(z) = \mathbf{G}(z)\mathbf{X}(z), \tag{2.1.3}$$

where $\mathbf{Y}(z)$ is the z transform of the encoded N by 1 vector sequence $Y(n)$. Similar to convolutional codes over a finite field, see for example [86], there is a trellis diagram associated with an MC encoding in (2.1.3). Let M denote the number of the complex symbols of the complex information sequence $x(n)$. Then the trellis diagram has M^ν states and there are M^K branches entering each state and M^K branches leaving each state. Notice that the PRS studied in [159, 114, 115, 113] and the prefiltering studied in [48] corresponds to the special case of MC when $K = N = 1$ in (2.1.1).

The decoding of an MC at the receiver can be achieved either by the maximum likelihood (ML) decoding, such as the Viterbi algorithm, or other suboptimal decoding algorithms, such as the joint MMSE [77] decoding or the joint DFE decoding that we shall see later.

Since, in the encoding of an MC, the coded signal mean power may be different from the information signal mean power. For convenience, an MC is normalized such that the mean power of the encoded signal $y(n)$ is the same as the one of the information sequence $x(n)$. This can be achieved by normalizing the magnitude squared sum of all the coefficients of all the polynomials $g_{n1}(z)$, $g_{n2}(z)$,..., $g_{nK}(z)$ in $\mathbf{G}(z)$ as follows. Let

$$g_{nk}(z) = \sum_l g_{nk}(l) z^{-l}, \quad 1 \le n \le N, 1 \le k \le K. \tag{2.1.4}$$

Then,

$$\sum_{n=1}^{N} \sum_{k=1}^{K} \sum_l |g_{nk}(l)|^2 = N. \tag{2.1.5}$$

If an MC $\mathbf{G}(z)$ satisfies (2.1.5), it is called a *normalized* MC.

A special MC encoding is the spreading in the spread spectrum system, which corresponds to a block $(N,1)$ MC $G = (g_1, \cdots, g_N)^T$ with $g_i \in \{1,-1\}$ and N is the spreading length. Such a case was also studied in [160] using the "wavelet" terminology. A coherent code division multiple access (CDMA) system of K users corresponds to a block (N,K) MC $G = (g_{ij})$ with $g_{ij} \in \{1,-1\}$.

Another special MC encoding is the encoding of the OFDM systems, as we shall see in Section 7.1, which corresponds to a block $(N+\Gamma,N)$ MC $G = [G_1, G_2]^T$ where G_1 is the N-point DFT matrix, G_2 is the submatrix of the first Γ columns of G_1, and Γ is the cyclic prefix length. The vector precoding studied in [72, 30] is also the block MC coding here.

Since the arithmetic operations of the MC encoding and an ISI channel are the same, an MC can be easily combined with an ISI channel, as we shall see later, which is the main motivation of the study of this book. Before going to the ISI channel, we first study an MC in an AWGN channel.

2.2 Coding Gain in AWGN Channel

For a normalized MC $\mathbf{G}(z)$, its *free distance* is defined as the minimum Euclidean distance between two different encoded sequences $y_1(n)$ and $y_2(n)$ in (2.1.3). Therefore, compared with an uncoded system in an AWGN channel, the *coding gain* of a rate K/N MC with its free distance d_{free} in an AWGN channel is

$$\gamma = \frac{d_{free}^2 K}{d_{min}^2 N}, \tag{2.2.1}$$

where d_{min} is the minimum distance between the complex symbols of the information sequence $x(n)$. When binary phase shift key (BPSK) $\{1,-1\}$ signaling is used in the binary-to-complex symbol mapping, the coding gain in (2.2.1) becomes

$$\gamma = \frac{d_{free}^2 K}{4N}. \tag{2.2.2}$$

Lemma 2.1 *A modulated code does not have any coding gain in an AWGN channel.*

Proof. For a general quadrature amplitude modulation (QAM) signal constellation, we may pick up two signal points with the shortest distance, i.e., d_{min}, which is reduced to the BPSK case. Therefore, we only need to prove the case when the BPSK symbols $\{1,-1\}$, i.e., $x(n) \in \{1,-1\}$, and

a normalized MC $\mathbf{G}(z)$ are used. In this case, we only need to prove that the free distance d_{free} of $\mathbf{G}(z)$ satisfies

$$d_{free}^2 \leq \frac{4N}{K}. \tag{2.2.3}$$

Let $X_1(n)$ and $X_2(n)$ be two K by 1 information vector sequences with all components either 1 or -1, and $Y_1(n)$ and $Y_2(n)$ be their corresponding encoded N by 1 vector sequences, i.e.,

$$\mathbf{Y}_i(z) = \mathbf{G}(z)\mathbf{X}_i(z), \quad i = 1, 2.$$

Let $U(n) = X_1(n) - X_2(n)$ and $W(n) = Y_1(n) - Y_2(n)$. Then

$$\mathbf{W}(z) = \mathbf{G}(z)\mathbf{U}(z). \tag{2.2.4}$$

By doing so, the distance between any pair of the MC encoded sequences $Y(n)$ becomes the norm of the corresponding $W(n)$. This implies that the free distance d_{free} is the minimum norm of all possible non-zero vectors $W(n)$. The minimum norm of all possible non-zero vectors $W(n)$ corresponding to all possible $U(n)$ is always less than or equal to the minimum one of any subset $\mathcal{S}$ of the set $\mathcal{A}$ of all the possible non-zero vectors $W(n)$. Therefore, the free distance d_{free} is always less than or equal to the mean norm of all vectors in any subset $\mathcal{S}$ of $\mathcal{A}$. In the following, we want to construct a special subset $\mathcal{S}$ such that the mean norm of all the vectors in $\mathcal{S}$ is exactly $4N/K$, which, therefore, proves the lemma.

Since $X_i(n)$ may take any value in $\{1, -1\}$, the sequence $U(n)$ may take any value in the set $\{0, 2, -2\}$. Let $\mathbf{W}(z) = (\mathbf{w}_1(z), \mathbf{w}_2(z), \cdots, \mathbf{w}_N(z))^T$ and $\mathbf{U}(z) = (\mathbf{u}_1(z), \mathbf{u}_2(z), \cdots, \mathbf{u}_K(z))^T$. Then,

$$\mathbf{w}_n(z) = \sum_{k=1}^{K} g_{nk}(z)\mathbf{u}_k(z).$$

Let l_k be positive integers such that each two polynomials $g_{nk_1}(z)z^{-l_{k_1}}$ and $g_{nk_2}(z)z^{-l_{k_2}}$ for $k_1 \neq k_2$ do not have any common terms of z^{-l} for any $1 \leq n \leq N$. For $1 \leq k \leq K$, let

$$\mathbf{u}_k(z) = \begin{cases} \pm 2z^{-l_k}, & \text{with probability } \frac{1}{K}, \\ 0, & \text{with probability } \frac{K-1}{K}. \end{cases} \tag{2.2.5}$$

We now let the subset $\mathcal{S}$ consist of all vectors $W(n)$ corresponding to all the above input vectors $U(n)$ in (2.2.5). Then, the mean norm of all the vectors in $\mathcal{S}$ can be calculated as

$$E\left(\sum_l |w_n(l)|^2\right) = \sum_{k=1}^{K}\sum_l |g_{nk}(l)|^2 E(|u_k(l)|^2) = \frac{4}{K}.$$

Thus, the mean norm is

$$E\left(\sum_{n=1}^{N}\sum_{l}|w_n(l)|^2\right) = \frac{4N}{K}.$$

This proves the lemma. ■

As a remark, when there is no data rate expansion (LTI filtering) and $N = K = 1$ in an MC, the result in the above lemma was obtained in [159, 115, 113]. When we only consider the ISI channel without coding at the transmitter, the following corollary is implied from Lemma 2.1 by treating a normalized ISI channel $H(z)$ as a normalized $(1,1)$ MC.

Corollary 2.1 *The free distance of the received signals through a normalized ISI channel is always upper bounded by* d_{min}.

From the proof of Lemma 2.1, the following corollary for a general MC is not hard to see.

Corollary 2.2 *For an* (N,K) *MC* $\mathbf{G}(z)$, *let* P_y *be the mean power of the coded sequence* $y(n)$. *The free distance of the encoded sequences is upper bounded by*

$$d_{free}^2 \leq \frac{d_{min}^2 P_y N}{K}.$$

Although an MC does not provide any coding gain in an AWGN channel, it may be different in an ISI channel.

2.3 MC Combined with an ISI Channel

Let $H(z)$ be the z transform of an ISI channel with finite taps $h(n)$ and

$$\sum_{n}|h(n)|^2 = 1, \tag{2.3.1}$$

and $\mathbf{G}(z)$ be a normalized MC used at the transmitter. Then, the combination shown in Fig.2.1 of the MC $\mathbf{G}(z)$ and the ISI channel $H(z)$ becomes another MC $\mathbf{C}(z)$:

$$\mathbf{C}(z) = \mathbf{H}(z)\mathbf{G}(z), \tag{2.3.2}$$

where $\mathbf{H}(z)$ is the following N by N pseudo-circulant polynomial matrix (see [100, 142]):

$$\mathbf{H}(z) = \begin{bmatrix} H_0(z) & z^{-1}H_{N-1}(z) & \cdots & z^{-1}H_1(z) \\ H_1(z) & H_0(z) & \cdots & z^{-1}H_2(z) \\ \vdots & \vdots & \vdots & \vdots \\ H_{N-2}(z) & H_{N-3}(z) & \cdots & z^{-1}H_{N-1}(z) \\ H_{N-1}(z) & H_{N-2}(z) & \cdots & H_0(z) \end{bmatrix}, \tag{2.3.3}$$

where $H_n(z)$ is the nth polyphase component of $H(z)$

$$H_n(z) = \sum_l h(Nl+n)z^{-l}, \quad 0 \le n \le N-1, \tag{2.3.4}$$

and

$$H(z) = \sum_{n=0}^{N-1} H_n(z^N)z^{-n}. \tag{2.3.5}$$

Let $Y(n)$ be the received N by 1 vector sequence with its z transform $\mathbf{Y}(z)$. Then,

$$\mathbf{Y}(z) = \mathbf{C}(z)\mathbf{X}(z) = \mathbf{H}(z)\mathbf{G}(z)\mathbf{X}(z). \tag{2.3.6}$$

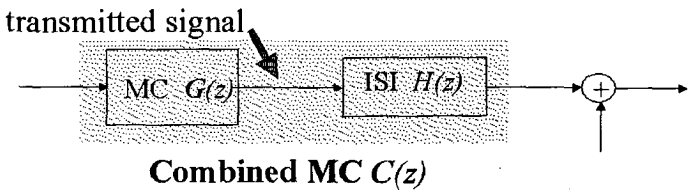

Figure 2.1: The combined MC.

When the ISI channel $H(z)$ is known, the combined MC $\mathbf{C}(z)$ is known. The simplest equalizer at the receiver is the inverse of the combined $\mathbf{C}(z)$. Then, a natural question is when there is an FIR inverse of the combined MC $\mathbf{C}(z)$, i.e., when there is a polynomial matrix $\mathbf{D}(z) = (d_{ij}(z))$ with all FIR components $d_{ij}(z)$ such that $\mathbf{D}(z)\mathbf{C}(z) = I_K$. The following results [165] answer this question.

Let $\mathbf{W}_N$ be the $N \times N$ DFT matrix, i.e., $\mathbf{W}_N \triangleq (W_N^{jk})_{0 \le j,k \le N-1}$, where $W_N = e^{-2\pi\sqrt{-1}/N}$. Let $\Lambda(z)$ be the diagonal matrix

$$\Lambda(z) \triangleq \mathrm{diag}\left(1, z^{-1}, \cdots, z^{-N+1}\right).$$

From (2.3.3)-(2.3.5), it is not hard to see

$$(H(z), z^{-1}H(z), \cdots, z^{-N+1}H(z)) = (1, z^{-1}, \cdots, z^{-N+1})\mathbf{H}(z^N).$$

Replacing z by zW_N^l for $l = 0, 1, ..., N-1$ in the above equality, we have the following $N \times N$ matrix multiplications

$$\hat{\mathbf{H}}(z) = \mathbf{W}_N^* \Lambda(z) \mathbf{H}(z^N), \tag{2.3.7}$$

where

$$\hat{\mathbf{H}}(z) \triangleq \begin{bmatrix} H(z) & z^{-1}H(z) & \cdots & z^{-N+1}H(z) \\ H(zW_N) & z^{-1}W_N^{-1}H(zW_N) & \cdots & z^{-N+1}W_N^{-N+1}H(zW_N) \\ \vdots & \vdots & & \vdots \\ H(zW_N^{N-1}) & z^{-1}W_N^{(-1)(N-1)}H(zW_N^{N-1}) & \cdots & z^{-N+1}W_N^{(-N+1)(N-1)}H(zW_N^{N-1}) \end{bmatrix} \tag{2.3.8}$$

Let $\mathbf{V}(z)$ be the following diagonal matrix

$$\mathbf{V}(z) \triangleq \text{diag}(H(z), H(zW_N), \cdots, H(zW_N^{N-1})). \tag{2.3.9}$$

Then the matrix $\hat{\mathbf{H}}(z)$ in (2.3.8) can be rewritten as

$$\hat{\mathbf{H}}(z) = \mathbf{V}(z)\mathbf{W}_N^* \Lambda(z).$$

This completes the following diagonalization of $\mathbf{H}(z^N)$ by combining (2.3.7):

$$\mathbf{H}(z^N) = (\mathbf{W}_N^* \Lambda(z))^{-1} \mathbf{V}(z) \mathbf{W}_N^* \Lambda(z). \tag{2.3.10}$$

Since the combined MC $\mathbf{C}(z) = \mathbf{H}(z)\mathbf{G}(z)$ has an FIR inverse is equivalent to $\mathbf{C}(z^N) = \mathbf{H}(z^N)\mathbf{G}(z^N)$ has an FIR inverse, we, thus, consider $\mathbf{H}(z^N)\mathbf{G}(z^N)$. By (2.3.10),

$$\mathbf{H}(z^N)\mathbf{G}(z^N) = (\mathbf{W}_N^* \Lambda(z))^{-1} \mathbf{V}(z) \mathbf{W}_N^* \Lambda(z) \mathbf{G}(z^N). \tag{2.3.11}$$

It is clear that $(\mathbf{W}_N^* \Lambda(z))^{-1} = \Lambda(z^{-1})\mathbf{W}_N$. Let

$$\hat{\mathbf{G}}(z) \triangleq \mathbf{W}_N^* \Lambda(z) \mathbf{G}(z^N).$$

Then, $\mathbf{H}(z)\mathbf{G}(z)$ has an FIR inverse is equivalent to $\mathbf{V}(z)\hat{\mathbf{G}}(z)$ has an FIR inverse. Notice that the size of the matrix $\mathbf{V}(z)\hat{\mathbf{G}}(z)$ is $N \times K$.

On the other hand, $\mathbf{V}(z)\hat{\mathbf{G}}(z)$ has an FIR inverse is equivalent to the greatest common divisor (gcd) of all determinants of all $K \times K$ submatrices of the $N \times K$ matrix $\mathbf{V}(z)\hat{\mathbf{G}}(z)$ is cz^{-d} for a non-zero constant c and an integer d, see, for example, [71, 142]. Since $\mathbf{V}(z)$ is diagonal and of the form (2.3.9), the above condition can be simplified further as follows.

Without loss of the generality, we assume

$$H(z) = \sum_{k=0}^{\Gamma-1} h(k)z^{-k},$$

where $h(0) \neq 0$, $h(\Gamma - 1) \neq 0$ and $\Gamma \geq 1$. Let S denote the set of all zeros of the polynomial $H(z)$ of z^{-1}: $S \triangleq \{z_1, z_2, ..., z_{\Gamma-1}\}$ with $H(z_l) = 0$ where z_l, $1 \leq l \leq \Gamma - 1$, may not be necessarily distinct. For a constant c, let $cS \triangleq \{cz_1, cz_2, ..., cz_{\Gamma-1}\}$, a rotated version of S.

Theorem 2.1 *There exists an (N, K) MC such that the combined MC $\mathbf{C}(z)$ has an FIR inverse if and only if*

$$\bigcap_{0 \leq l_1 < l_2 < \cdots < l_K \leq N-1} (S_{l_1} \cup S_{l_2} \cup \cdots \cup S_{l_K}) = \phi, \tag{2.3.12}$$

where $S_{l_k} = W_N^{l_k} S$, $k = 1, 2, ..., K$.

Theorem 2.1 tells us that there exists an MC such that the combined MC has an FIR ideal linear equalization if and only if the intersection of the unions of any K sets of all N rotated ones of the zero set S with angles $l2\pi/N$, $l = 0, 1, ..., N-1$, of the ISI transfer function $H(z)$ is empty. When $K = N$, the intersection in (2.3.12) contains at least S which is not empty. This implies that, when $K = N$ the combined MC $\mathbf{C}(z)$ for an MC does not have an FIR inverse. This is not surprising because an MC with $N = K$ does not add any redundancy in the transmission.

Proof. We first prove the "necessary part." Assume the set

$$\bigcap_{0 \leq l_1 < l_2 < \cdots < l_K \leq N-1} (S_{l_1} \cup S_{l_2} \cup \cdots \cup S_{l_K}) \neq \phi.$$

This implies that the polynomials $\prod_{k=1}^{K} H(W_N^{l_k} z)$ for all possible $0 \leq l_1 < l_2 < \cdots < l_K \leq N - 1$ have at least a common zero z_0. In another words, they have a common factor $z^{-1} - z_0^{-1}$. By the form of $\mathbf{V}(z)\hat{\mathbf{G}}(z)$ and the diagonality of $\mathbf{V}(z)$, the polynomial $\prod_{k=1}^{K} H(W_N^{l_k} z)$ is a factor of

the determinant of the submatrix of $\mathbf{V}(z)\hat{\mathbf{G}}(z)$ at the rows $l_1, l_2, ..., l_K$. When $l_1, l_2, ..., l_K$ run over all possible $0 \leq l_1 < l_2 < \cdots < l_K \leq N-1$, the corresponding submatrices run over all possible $K \times K$ submatrices of $\mathbf{V}(z)\hat{\mathbf{G}}(z)$. Therefore, all determinants of all $K \times K$ submatrices of $\mathbf{V}(z)\hat{\mathbf{G}}(z)$ have at least a common factor $z^{-1} - z_0^{-1}$ no matter what $\hat{\mathbf{G}}(z)$ is. This proves that $\mathbf{V}(z)\hat{\mathbf{G}}(z)$ does not have an FIR inverse.

Let us prove the "sufficient part." Assume (2.3.12) is true. We construct

$$\mathbf{G}(z) = \begin{bmatrix} I_K \\ \mathbf{0}_{(N-K)\times K} \end{bmatrix}, \tag{2.3.13}$$

where $\mathbf{0}_{(N-K)\times K}$ is the all zero $(N-K) \times K$ matrix. Then,

$$\begin{aligned} \hat{\mathbf{G}}(z) &= \mathbf{W}_N^* \Lambda(z) \mathbf{G}(z^N) = \mathbf{W}_N^* \mathrm{diag}(1, z^{-1}, \cdots, z^{-K+1}) \\ &= \left(z^{-k} W_N^{-jk} \right)_{0 \leq j \leq N-1, 0 \leq k \leq K-1}. \end{aligned}$$

It is not hard to see that the determinant of the $l_1, l_2, ..., l_K$ row submatrix of $\mathbf{V}(z)\hat{\mathbf{G}}(z)$ is

$$c_{l_1 l_2 \cdots l_K} \prod_{j=1}^{K} H(z W_N^{l_j}) z^{-(1+2+\cdots+K-1)}, \tag{2.3.14}$$

where $0 \leq l_1 < l_2 < \cdots < l_K \leq N-1$ and $c_{l_1 l_2 \cdots l_K}$ is the Vandermonde's determinant of a $K \times K$ submatrix of the following $N \times K$ matrix

$$\left(W_N^{-jk} \right)_{0 \leq j \leq N-1, 0 \leq k \leq K-1},$$

which is a non-zero constant. By (2.3.12), the greatest common divisor of all polynomials in (2.3.14) is cz^{-d} for a nonzero constant c and an integer d. This proves that the matrix $\mathbf{V}(z)\hat{\mathbf{G}}(z)$ has an FIR inverse and therefore completes the proof. ■

By the fact that

$$\begin{aligned} &\bigcap_{0 \leq l_1 < l_2 < \cdots < l_{K-1} \leq N-1} (S_{l_1} \cup S_{l_2} \cup \cdots \cup S_{l_{K-1}}) \\ &\subset \bigcap_{0 \leq l_1 < l_2 < \cdots < l_K \leq N-1} (S_{l_1} \cup S_{l_2} \cup \cdots \cup S_{l_K}), \end{aligned}$$

we have the following immediate corollary.

Corollary 2.3 *If there exists an (N, K) MC such that the combined MC $\mathbf{C}(z)$ has an FIR inverse, then there also exists an $(N, K-1)$ MC such that the combined MC $\mathbf{C}(z)$ has an FIR inverse.*

Corollary 2.3 is not surprising. It is because, if an MC with less redundancy can be used to eliminate an ISI, then an MC with more redundancy can be used to eliminate the ISI too. The proof of Theorem 2.1 also suggests a way to construct an MC to eliminate $H(z)$. When $H(z)$ satisfies the condition in Theorem 2.1, the MC in (2.3.13) can be used to eliminate the ISI. This MC basically adds $N-K$ zeroes for each set of K consecutive symbols (or samples). It is certainly not necessary, as long as the $N \times K$ polynomial matrix $\mathbf{V}(z)\hat{\mathbf{G}}(z)$ has an FIR inverse. Using this MC the combined MC becomes

$$\hat{\mathbf{H}}(z)\mathbf{G}(z) = \mathbf{F}_K(z) \triangleq$$

$$\begin{bmatrix} H_0(z) & z^{-1}H_{N-1}(z) & \cdots & z^{-1}H_{N-K+1}(z) \\ H_1(z) & H_0(z) & \cdots & z^{-1}H_{N-K+2}(z) \\ \cdot & \cdot & \cdots & \cdot \\ \cdot & \cdot & \cdots & \cdot \\ \cdot & \cdot & \cdots & \cdot \\ H_{K-1}(z) & H_{K-2}(z) & \cdots & H_0(z) \\ \cdot & \cdot & \cdots & \cdot \\ \cdot & \cdot & \cdots & \cdot \\ \cdot & \cdot & \cdots & \cdot \\ H_{N-1}(z) & H_{N-2}(z) & \cdots & H_{N-K}(z) \end{bmatrix}. \tag{2.3.15}$$

By the proof of Theorem 2.1, when the condition (2.3.12) on $H(z)$ is satisfied, polynomial matrix $\mathbf{F}_K(z)$ in (2.3.15) has an FIR inverse.

Using Theorem 2.1 and Corollary 2.3, we have

Corollary 2.4 *The $N \times K$ matrix $\mathbf{F}_K(z)$ in (2.3.15) with $0 < K \leq N$ has an FIR inverse if and only if the condition (2.3.12) is satisfied. If $\mathbf{F}_K(z)$ has an FIR inverse, then $\mathbf{F}_{K-1}(z)$ has an FIR inverse too for $K > 1$.*

We now consider two special cases. The first case is when $K = 1$. In this case, the condition (2.3.12) becomes

$$\bigcap_{0 \leq l \leq N-1} S_l = \phi. \tag{2.3.16}$$

By Theorem 2.1 and Corollary 2.4, we have the following result.

Corollary 2.5 *There exists an $(N,1)$ MC such that the combined MC has an FIR inverse if and only if*

$$gcd\{H(z), H(zW_N), ..., H(zW_N^{N-1})\} = c_1 z^{-d_1},$$

if and only if

$$gcd\{H_0(z), H_1(z), ..., H_{N-1}(z)\} = c_2 z^{-d_2},$$

where c_1 and c_2 are two non-zero constants, and d_1 and d_2 are two integers.

The result in Corollary 2.5 coincides with the known result for fractionally spaced equalizers or multiple receive antenna systems [134, 135], i.e., there are no zeros of $H(z)$ equispaced on a circle with angle $2\pi/N$ separated one zero from another. From Theorem 2.1 and Corollary 2.5, we immediately have the following consequence.

Corollary 2.6 *For any finite tap ISI transfer function $H(z)$, not identically zero, there always exists an (N,K) MC such that the combined MC has an FIR inverse, where N and K may not be fixed.*

An (N,K) MC at the transmitter expands the data rate by N/K times. For a given N, the smallest data rate expansion is $N/(N-1)$, i.e., $K = N-1$. We next want to study this case.

Theorem 2.2 *There exists an $(N,N-1)$ MC such that the combined MC with a finite tape ISI channel $H(z)$ has an FIR inverse if and only if $S_l \cap S_k = \phi$, i.e., polynomials $H(zW_N^l)$ and $H(zW_N^k)$ are coprime, for $0 \le l \ne k \le N-1$.*

Proof. This theorem can be proved by the following set equation:

$$\bigcap_{0\le l_1<l_2<\cdots<l_{N-1}\le N-1} (\cup_{k=1}^{N-1} S_{l_k}) = \bigcap_{l_0=0}^{N-1} (\cup_{l\ne l_0} S_l) = \bigcup_{l\ne k} (S_l \cap S_k).$$

■

Let us consider the case when the ISI transfer function $H(z) = a + z^{-1}$ with $|a| = 1$, i.e., the first order case. In this case, the zero set $S = \{-1/a\}$. For a general N, $S_l = \{-W_N^l/a\}$, $l = 0, 1, ..., N-1$. Clearly, $S_l \cap S_k = \phi$ since $W_N^l \ne W_N^k$ when $0 \le l \ne k \le N-1$. By Theorem 2.2 and Corollary 2.3, we proved the following result.

Corollary 2.7 *Assume the ISI transfer function $H(z) = a + z^{-1}$ with $|a| = 1$. Then, for any integers $0 < K < N$ and the (N,K) MC in (2.3.13) the combined MC always has an FIR inverse, i.e., the MC coded system has an ideal FIR linear equalizer.*

Corollary 2.7 implies that any ϵ (> 0) amount of data rate increasing in the MC coding may eliminate the ISI generated from any first order ISI channel. This is because for any $\epsilon > 0$ there exists a positive integer N such that $0 < 1 - (N-1)/N < \epsilon$. We then use the $(N, N-1)$ MC in (2.3.13). The results in this section were summarized from [165].

2.4 Coding Gain in ISI Channels

The previous section tells us when the combined MC has an FIR linear equalizer without considering the input symbol characteristics. However, in a communication system, what is more important is the distance property of the combined MC given a certain set of input symbols, such as BPSK symbols. To do so, we introduce the coding gain concept of the combined MC.

Although the encoding at the transmitter is based on the normalized MC $\mathbf{G}(z)$, the decoding is based on the combined MC $\mathbf{C}(z)$ in (2.3.2), where $\mathbf{G}(z)$ is in the ISI channel while $\mathbf{C}(z)$ is in the AWGN channel. We assume that the joint maximum-likelihood decoding of the channel decoding and the equalization is used, i.e., the Viterbi decoding algorithm is used for the MC $\mathbf{C}(z)$ at the receiver. For the Viterbi algorithm, we referred the reader to [119]. *The coding gain γ_{ISI} of the MC $\mathbf{G}(z)$ at the transmitter in the ISI channel is defined as the coding gain of the combined MC $\mathbf{C}(z)$ in the AWGN channel*, i.e.,

$$\gamma_{ISI} = \frac{d^2_{free,\mathbf{C}}}{d^2_{min}} \frac{K}{N}, \tag{2.4.1}$$

where $d_{free,\mathbf{C}}$ is the free distance of the combined MC $\mathbf{C}(z)$. When the ISI channel is fixed, the ML decoding performance of the uncoded ISI channel is always not as good as the one of the uncoded AWGN channel, which is from Lemma 2.1 and Corollary 2.1. This implies that the above coding gain γ_{ISI} is a portion of the real coding gain compared to the uncoded ISI channel, i.e., the real coding gain is the sum of γ_{ISI} (dB) and the difference (dB) between the uncoded ISI and AWGN channels, as shown in Fig.2.2.

By normalization, the mean power of the transmitted signal $y(n)$ is the same as the one of the information signal $x(n)$. An important observation is that the mean power of the received signal $q(n)$ may be different. It turns out that, by properly choosing an MC $\mathbf{G}(z)$, the mean power of the received signal $q(n)$ after the ISI channel may be greater than the information signal mean power. The following lemma gives an upper bound on the mean power of the received signal after an ISI channel.

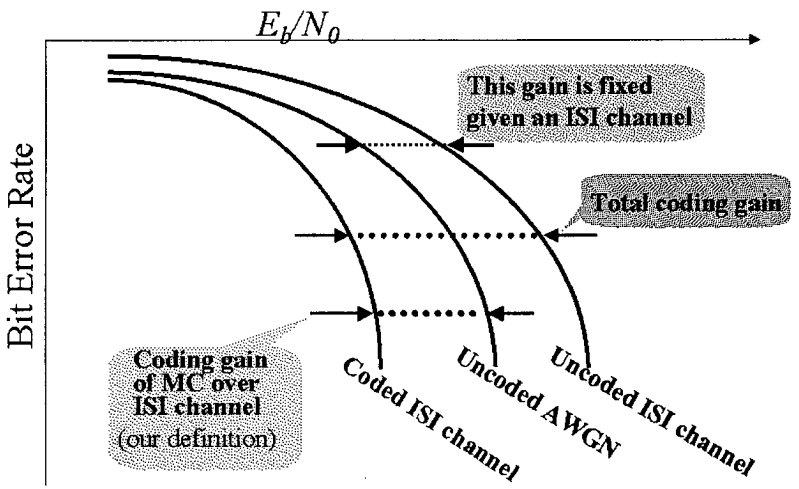

Figure 2.2: Coding gain definition of an MC in an ISI channel.

Lemma 2.2 *Let $H(z)$ be an ISI channel with Γ non-zero taps. Then, the mean power P_q of the received signal $q(n)$ through an MC coded ISI channel is upper bounded by*

$$P_q \leq \Gamma P_x, \tag{2.4.2}$$

where P_x is the mean power of the information sequence $x(n)$.

Proof. Let $y(n)$ be the encoded sequence of the normalized MC. Without loss of generality, we assume that $h(n)$, $n = 0, 1, ..., \Gamma - 1$, are the Γ non-zeros taps of the ISI channel. Then,

$$P_q = E\left|\sum_{n=0}^{\Gamma-1} h(n)y(k-n)\right|^2 \leq \sum_{n=0}^{\Gamma-1} |h(n)|^2 \sum_{n=0}^{\Gamma-1} E|y(k-n)|^2$$

$$= \sum_{n=0}^{\Gamma-1} E|x(k-n)|^2 = \Gamma P_x.$$

■

From Corollary 2.2 and Lemma 2.2, the following upper bounds for the free distance of the received sequences and the coding gain are straightforward.

Corollary 2.8 *Let $H(z)$ be an ISI channel with Γ non-zero taps. Let $\mathbf{G}(z)$ be a normalized (N, K) MC. Then, the free distance of the received sequences after the ISI channel is upper bounded by*

$$d^2_{free,\mathbf{C}} \leq \frac{d^2_{min}\Gamma N}{K}, \tag{2.4.3}$$

and therefore, the coding gain γ_{ISI} is upper bounded by Γ, i.e., $\gamma_{ISI} \leq \Gamma$.

From the above lemma, we may see that, although an MC does not have any coding gain in an AWGN channel, it may have a coding gain in an ISI channel. It is because of the possibility of the increase of the free distance after an ISI channel due to the possibility of the increase of the mean power after an ISI channel when a normalized MC is properly designed. However, it should be pointed out that the mean power increase is not sufficient for the free distance increase. In our recent work [166], it has been proved that for any given ISI channel with finite taps, there always exists an MC such that the coding gain exists compared to the uncoded AWGN channel.

Theorem 2.3 *For any ISI channel $h(n)$, $0 \leq n \leq \Gamma - 1$, with $\Gamma > 1$ and $h(0) \neq 0$, $h(\Gamma - 1) \neq 0$, there exists a normalized modulated code $\mathbf{G}(z)$ that has a coding gain in the ISI channel compared to the uncoded AWGN channel, i.e., $\gamma_{ISI} > 1$.*

Proof. Since the MC encoding is a linear matrix and vector multiplication over the complex domain, without loss of generality, we only consider BPSK signal constellation, i.e., $x(n) = \pm 1$, and all the ISI channel coefficients and MC code coefficients are real-valued. The complex-valued coefficients can be treated similarly. Consider a rate $1/\Gamma$, i.e., $K = 1$ and $N = \Gamma$, normalized block modulated code, i.e.,

$$\mathbf{G}(z) = \begin{bmatrix} g_0 \\ g_1 \\ \vdots \\ g_{\Gamma-1} \end{bmatrix}, \quad \text{and} \quad g_n = \pm 1, \; n = 0, 1, ..., \Gamma - 1. \tag{2.4.4}$$

In this case,

$$\mathbf{H}(z) = \begin{bmatrix} h(0) & h(\Gamma-1)z^{-1} & \cdots & h(1)z^{-1} \\ h(1) & h(0) & \cdots & h(2)z^{-1} \\ \vdots & \vdots & \vdots & \vdots \\ h(\Gamma-1) & h(\Gamma-2) & \cdots & h(0) \end{bmatrix},$$

and the combined MC is

$$\mathbf{C}(z) = \begin{bmatrix} c_{0,0} \\ c_{0,1} \\ \vdots \\ c_{0,\Gamma-1} \end{bmatrix} + \begin{bmatrix} c_{1,0} \\ c_{1,1} \\ \vdots \\ c_{1,\Gamma-1} \end{bmatrix} z^{-1},$$

where

$$\begin{aligned} c_{0,k} &= \sum_{i=0}^{k} h(k-i)g_i, \quad k = 0, 1, ..., \Gamma-1 \\ c_{1,k} &= \sum_{j=0}^{\Gamma-2-k} h(\Gamma-1-j)g_{k+1+j}, \quad k = 0, 1, ..., \Gamma-2 \\ c_{1,\Gamma-1} &= 0. \end{aligned}$$

By considering the input difference sequences $x_1(n) - x_2(n)$ as $(0, \pm 2)$ and $(\pm 2, 0)$, it is not hard to see that the free distance, $d_{free,\mathbf{C}}$, for the MC $\mathbf{C}(z)$ is

$$d^2_{free,\mathbf{C}} = 4 \sum_{k=0}^{\Gamma-1} \left(|c_{0,k}|^2 + |c_{1,k}|^2 \right).$$

In order to prove that there exists an MC $\mathbf{G}(z)$ in (2.4.4) such that the coding gain $\gamma_{ISI} > 1$ for the combined MC $\mathbf{C}(z)$, from (2.4.1) and $d_{min} = 2$ in this case we only need to show that there exists an MC $\mathbf{G}(z)$ in (2.4.4) such that the free distance $d^2_{free,\mathbf{C}} > 4N = 4\Gamma$. From $g_n = \pm 1$, we have

$$d^2_{free,\mathbf{C}} = 4\Gamma + 8d,$$

where

$$d \triangleq \sum_{k=0}^{\Gamma-1} \left[\sum_{i_1=0}^{k} \sum_{i_2=i_1+1}^{k} h(k-i_1)h(k-i_2)g_{i_1}g_{i_2} \right.$$

$$\left. + \sum_{j_1=0}^{\Gamma-2-k} \sum_{j_2=j_1+1}^{\Gamma-2-k} h(\Gamma-1-j_1)h(\Gamma-1-j_2)g_{k+1+j_1}g_{k+1+j_2} \right].$$

By rearranging the above summation, we have

$$d = \sum_{i=0}^{\Gamma-2} g_i \left[\sum_{j=1}^{\Gamma-1-i} g_{i+j} \sum_{k=0}^{\Gamma-1-j} h(k)h(j+k) \right].$$

To prove $d^2_{free,\mathbf{C}} > 4\Gamma$ for a proper choice of g_n, we only need to show $d > 0$ for a proper choice of g_n. Let

$$\tau_0 \triangleq \min\left\{ j:\ 0 \le j \le \Gamma - 1 \text{ and } \sum_{k=0}^{\Gamma-1-j} h(k)h(j+k) \neq 0 \right\}.$$

Since $h(0)h(\Gamma-1) \neq 0$, we have $1 \le \tau_0 \le \Gamma - 1$. Let

$$d_i = \sum_{j=1}^{\Gamma-1-i} g_{i+j} \sum_{k=0}^{\Gamma-1-j} h(k)h(j+k).$$

Then,

$$d_{\Gamma-1-\tau_0} = g_{\Gamma-1} \sum_{k=0}^{\Gamma-1-\tau_0} h(k)h(\tau_0+k) \neq 0.$$

Let $g_{\Gamma-1} = 1$ and for $0 \le i \le \Gamma - 2$ define g_i for the index i from $\Gamma - 2$ to 0 as follows

$$g_i = \begin{cases} \text{sign}(d_i), & \text{if } d_i \neq 0, \\ 1, & \text{if } d_i = 0. \end{cases}$$

Thus,

$$d = \sum_{i=0}^{\Gamma-2} g_i d_i \ge |d_{\tau_0}| > 0.$$

This proves the theorem. ■

This result is contrary to the one obtained in Said [113] and Wong and Anderson [159], where they showed that any PRS, i.e., an MC with $N = K = 1$ (no data rate expansion), does not provide any coding/distance gain compared to the uncoded AWGN channel no matter whether it is in an ISI or ISI-free channel. It should be pointed out that the goal in [159, 115, 113] was the bandwidth efficiency while they wanted to have the distance loosing as less as possible, which is different from the one here. Although the purpose of the study in [48] is the same as the one of MC here, it corresponds only to the case when $K = N = 1$ and there is no coding gain compared to the uncoded AWGN channel. From Lemma 2.1 and Corollary 2.2, it is not hard to see that the coding gain implies the SNR gain at the receiver.

The above proof is a constructive proof. We next present another proof that is helpful in the next section.

Proof. We only need to prove that there exists a normalized $\mathbf{G}(z)$ such that the squared free distance of the combined MC $\mathbf{C}(z)$ is greater than 4Γ.

Let $\mathbf{H}(z)$ be a Γ by Γ pseudo-circulant polynomial matrix as defined in (2.3.3) and the normalized MC $\mathbf{G}(z)$ be a Γ by 1 constant matrix. In this case, the matrices $\mathbf{H}(z)$ and $\mathbf{G}(z)$ can be written as

$$\mathbf{H}(z) = \begin{bmatrix} h(0) & 0 & 0 & \cdots & 0 & 0 \\ h(1) & h(0) & 0 & \cdots & 0 & 0 \\ \vdots & \vdots & \vdots & \vdots & \vdots & \vdots \\ h(\Gamma-2) & h(\Gamma-3) & h(\Gamma-4) & \cdots & h(0) & 0 \\ h(\Gamma-1) & h(\Gamma-2) & h(\Gamma-3) & \cdots & h(1) & h(0) \end{bmatrix}$$

$$+z^{-1}\begin{bmatrix} 0 & h(\Gamma-1) & h(\Gamma-2) & \cdots & h(2) & h(1) \\ 0 & 0 & h(\Gamma-1) & \cdots & h(3) & h(2) \\ \vdots & \vdots & \vdots & \vdots & \vdots & \vdots \\ 0 & 0 & 0 & \cdots & 0 & h(\Gamma-1) \\ 0 & 0 & 0 & \cdots & 0 & 0 \end{bmatrix}, \tag{2.4.5}$$

and

$$\mathbf{G}(z) = G = [g_0\ g_1 \cdots g_{\Gamma-1}]^T, \tag{2.4.6}$$

where ^{T} denotes the matrix transpose.

The squared free distance of the received signal sequence after the ISI channel can be written as:

$$\frac{d^2_{free,\mathbf{C}}}{4} = \sum_{i=0}^{\Gamma-1}\left(\left|\sum_{k=0}^{i} h(k)g_{i-k}\right|^2 + \left|\sum_{j=i+1}^{\Gamma-1} h(\Gamma+i-j)g_j\right|^2\right). \tag{2.4.7}$$

We now only choose values of $g_i, 0 \le i \le \Gamma-1$, in the set $\{1,-1\}$ independently. Assume the probabilities of g_i choosing symbols 1 and -1 are 1/2. Then, for fixed variables g_0 and $g_{\Gamma-1}$, the conditional mean of $d^2_{free,\mathbf{C}}$ given g_0 and $g_{\Gamma-1}$ is obtained as follows:

$$E\left\{\frac{d^2_{free,\mathbf{C}}}{4}\middle| g_0, g_{\Gamma-1}\right\} = \Gamma + 2h(0)h(\Gamma-1)g_0g_{\Gamma-1}, \tag{2.4.8}$$

where the means of other products g_ig_j, $i \neq j$, are zero due to their symmetry properties around zero. It is easy to show that, when we choose g_0 and $g_{\Gamma-1}$ as

$$\text{sign}(g_0g_{\Gamma-1}) = \text{sign}(h_0h_{\Gamma-1}), \tag{2.4.9}$$

the corresponding conditional mean of $d^2_{free,\mathbf{C}}$ is greater than 4Γ. This indicates that there exists an MC G with entries of $\{-1, 1\}$ such that the $d^2_{free,\mathbf{C}}$ of the MC $\mathbf{C}(z)$ is greater than 4Γ. ■

2.5 More Results on Coding Gain

In this section, we investigate the existence of rate $2/\Gamma$ MC having coding gain over a given ISI channel with Γ taps. We also study some upper and lower bounds of the coding gain. The results in this section are summarized from [44].

2.5.1 Existence of Rate $2/\Gamma$ MC with Coding Gain

We first present some results on the MC existence of rate $2/\Gamma$ with coding gain for an ISI channel $h_n = h(n)$, where the new notation h_n is used to simplify the equations.

Theorem 2.4 *Let $H(z)$ be an ISI channel with $\Gamma > 1$ taps and the BPSK be used for the information sequence $x(n)$. If $0 < |h_0 h_{\Gamma-1}| < 1/2$, then, there exists a rate $2/\Gamma$ block MC $\mathbf{G}(z)$ with coding gain compared to the uncoded AWGN channel.*

Proof. We only need to prove that there exists a normalized $\mathbf{G}(z)$ such that the squared free distance of the combined MC $\mathbf{C}(z)$ after the ISI channel is greater than 2Γ.

Consider the following rate $2/\Gamma$ MC

$$\begin{aligned} \mathbf{G}(z) &= (G_0, G_1), \\ G_0^T &= (g_0\ g_1 \cdots\ g_{\Gamma-1}), \\ G_1^T &= (\bar{g}_0 \bar{g}_1\ \cdots\ \bar{g}_{\Gamma-1}). \end{aligned}$$

By using the trellis diagram, the free distance of the received signal sequences after the ISI channel is as follows

$$\frac{d^2_{free,\mathbf{C}}}{4} = \min\{\Delta_1, \Delta_2, \Delta_3, \Delta_4\},$$

where

$$\Delta_1 = \sum_{i=0}^{\Gamma-1} \left(\left| \sum_{k=0}^{i} h_k g_{i-k} \right|^2 + \left| \sum_{j=i+1}^{\Gamma-1} h_{\Gamma+i-j} g_j \right|^2 \right), \quad (2.5.1)$$

$$\Delta_2 = \sum_{i=0}^{\Gamma-1} \left(\left| \sum_{k=0}^{i} h_k \bar{g}_{i-k} \right|^2 + \left| \sum_{j=i+1}^{\Gamma-1} h_{\Gamma+i-j} \bar{g}_j \right|^2 \right), \quad (2.5.2)$$

$$\Delta_3 = \sum_{i=0}^{\Gamma-1} \left(\left| \sum_{k=0}^{i} h_k (g_{i-k} + \bar{g}_{i-k}) \right|^2 + \left| \sum_{j=i+1}^{\Gamma-1} h_{\Gamma+i-j} (g_j + \bar{g}_j) \right|^2 \right), \quad (2.5.3)$$

$$\Delta_4 = \sum_{i=0}^{\Gamma-1} \left(\left| \sum_{k=0}^{i} h_k (g_{i-k} - \bar{g}_{i-k}) \right|^2 + \left| \sum_{j=i+1}^{\Gamma-1} h_{\Gamma+i-j} (g_j - \bar{g}_j) \right|^2 \right). \quad (2.5.4)$$

In order to simplify our analysis, we select the parameters $g_i, \bar{g}_i, 0 < i < \Gamma - 1$, as zeros and $g_0, \bar{g}_0, g_{\Gamma-1}, \bar{g}_{\Gamma-1}$ as real numbers with mean zero. Furthermore, consider the following normalized MC:

$$g_0^2 + g_{\Gamma-1}^2 = \frac{\Gamma}{2},$$
$$\bar{g}_0^2 + \bar{g}_{\Gamma-1}^2 = \frac{\Gamma}{2},$$

and the corresponding formulas (2.5.1)-(2.5.4) become

$$\Delta_1 = \frac{\Gamma}{2} + 2h_0 h_{\Gamma-1} g_0 g_{\Gamma-1}, \quad (2.5.5)$$

$$\Delta_2 = \frac{\Gamma}{2} + 2h_0 h_{\Gamma-1} \bar{g}_0 \bar{g}_{\Gamma-1}, \quad (2.5.6)$$

$$\Delta_3 = (g_0 + \bar{g}_0)^2 + (g_{\Gamma-1} + \bar{g}_{\Gamma-1})^2 + 2h_0 h_{\Gamma-1} (g_0 + \bar{g}_0)(g_{\Gamma-1} + \bar{g}_{\Gamma-1}), \quad (2.5.7)$$

$$\Delta_4 = (g_0 - \bar{g}_0)^2 + (g_{\Gamma-1} - \bar{g}_{\Gamma-1})^2 + 2h_0 h_{\Gamma-1} (g_0 - \bar{g}_0)(g_{\Gamma-1} - \bar{g}_{\Gamma-1}). \quad (2.5.8)$$

By (2.5.5)-(2.5.6), it is easy to obtain that, if we choose

$$\text{sign}(g_0 g_{\Gamma-1}) = \text{sign}(\bar{g}_0 \bar{g}_{\Gamma-1}) = \text{sign}(h_0 h_{\Gamma-1}),$$

then we have

$$\begin{aligned} \Delta_1 &= \frac{\Gamma}{2} + 2|h_0 h_{\Gamma-1} g_0 g_{\Gamma-1}| > \frac{\Gamma}{2}, \\ \Delta_2 &= \frac{\Gamma}{2} + 2|h_0 h_{\Gamma-1} \bar{g}_0 \bar{g}_{\Gamma-1}| > \frac{\Gamma}{2}. \end{aligned}$$

In the following, our main focus is on the proof of $\Delta_3 > \frac{\Gamma}{2}$ and $\Delta_4 > \frac{\Gamma}{2}$ for the same values of $g_0, \bar{g}_0, g_{\Gamma-1}, \bar{g}_{\Gamma-1}$. First, let us consider the case when $\text{sign}(h_0 h_{\Gamma-1}) > 0$.

If $\text{sign}(h_0 h_{\Gamma-1}) > 0$, we choose $g_0 > 0, \bar{g}_0 < 0$, then (2.5.7) and (2.5.8) can be rewritten as follows

$$\begin{aligned} \Delta_3 &= \Gamma - 2g_0\sqrt{\frac{\Gamma}{2} - \bar{g}_{\Gamma-1}^2} + 2\bar{g}_{\Gamma-1}\sqrt{\frac{\Gamma}{2} - g_0^2} \\ &\quad + 2h_0 h_{\Gamma-1}\left(g_0 - \sqrt{\frac{\Gamma}{2} - \bar{g}_{\Gamma-1}^2}\right)\left(\sqrt{\frac{\Gamma}{2} - g_0^2} + \bar{g}_{\Gamma-1}\right), \\ \Delta_4 &= \Gamma + 2g_0\sqrt{\frac{\Gamma}{2} - \bar{g}_{\Gamma-1}^2} - 2\bar{g}_{\Gamma-1}\sqrt{\frac{\Gamma}{2} - g_0^2} \\ &\quad + 2h_0 h_{\Gamma-1}\left(g_0 + \sqrt{\frac{\Gamma}{2} - \bar{g}_{\Gamma-1}^2}\right)\left(\sqrt{\frac{\Gamma}{2} - g_0^2} - \bar{g}_{\Gamma-1}\right). \end{aligned}$$

As $g_0 \longrightarrow +0, \bar{g}_{\Gamma-1} \longrightarrow -0$, and combining with the assumption $|h_0 h_{\Gamma-1}| < 1/2$, we have

$$\begin{aligned} \Delta_3 \longrightarrow \Gamma(1 - h_0 h_{\Gamma-1}) &> \frac{\Gamma}{2}, \\ \Delta_4 \longrightarrow \Gamma(1 + h_0 h_{\Gamma-1}) &> \frac{\Gamma}{2}. \end{aligned}$$

Thus, there exist some values of $g_0 > 0, \bar{g}_0 < 0, g_{\Gamma-1} > 0, \bar{g}_{\Gamma-1} < 0$ such that $\Delta_i > \frac{\Gamma}{2}$ for i=1,2,3,4.

The case when $\text{sign}(h_0 h_{\Gamma-1}) < 0$ can be similarly proved. ■

Theorem 2.4 indicates that there exists a rate $2/\Gamma$ MC code having coding gain over ISI channels except the worst case when $|h_0 h_{\Gamma-1}| = 1/2$ and $h_2 = \cdots = h_{\Gamma-2} = 0$.

Theorem 2.5 *Let $H(z) = h_0 + h_1 z^{-1} + \cdots h_\Gamma z^{-\Gamma}$ be an ISI channel with $\Gamma + 1$ taps, $\Gamma > 0$ and the BPSK be used for the information sequence*

$x(n)$. If $0 < |h_0 h_\Gamma| < 1/2$, then, there exists a rate $1/\Gamma$ normalized MC $\mathbf{G}(z) = G_0 + G_1 z^{-1}$ with coding gain compared to the uncoded AWGN channel, where G_0, G_1 are constant $\Gamma \times 1$ vectors.

Proof. It is easy to obtain that

$$\mathbf{H}(z) = H_0 + z^{-1} H_1,$$

where H_0, H_1 are the following Γ by Γ constant matrices

$$H_0 = \begin{bmatrix} h_0 & 0 & 0 & \cdots & 0 & 0 \\ h_1 & h_0 & 0 & \cdots & 0 & 0 \\ \vdots & \vdots & \vdots & \vdots & \vdots & \vdots \\ h_{\Gamma-2} & h_{\Gamma-3} & h_{\Gamma-4} & \cdots & h_0 & 0 \\ h_{\Gamma-1} & h_{\Gamma-2} & h_{\Gamma-3} & \cdots & h_1 & h_0 \end{bmatrix}, \tag{2.5.9}$$

and

$$H_1 = \begin{bmatrix} h_\Gamma & h_{\Gamma-1} & h_{\Gamma-2} & \cdots & h_2 & h_1 \\ 0 & h_\Gamma & h_{\Gamma-1} & \cdots & h_3 & h_2 \\ \vdots & \vdots & \vdots & \vdots & \vdots & \vdots \\ 0 & 0 & 0 & \cdots & h_\Gamma & h_{\Gamma-1} \\ 0 & 0 & 0 & \cdots & 0 & h_\Gamma \end{bmatrix}. \tag{2.5.10}$$

Thus, the combination of the MC $\mathbf{G}(z)$ and the ISI channel $\mathbf{H}(z)$ becomes

$$\mathbf{C}(z) = \mathbf{H}(z)\mathbf{G}(z) = H_0 G_0 + (H_0 G_1 + H_1 G_0) z^{-1} + H_1 G_1 z^{-2}. \tag{2.5.11}$$

By observing the trellis diagram of $\mathbf{C}(z)$, if we choose the all zero path as the reference, we find that there are only three different error paths which may reach the free distance. The squared free distance between the received signal sequences is

$$\frac{d^2_{free,\mathbf{C}}}{4} = \min\{\Delta_0, \Delta_1, \Delta_2\},$$

where Δ_0, Δ_1, and Δ_2 are the squared distances between the three paths and the all zero path, respectively. They can be calculated as

$$\begin{aligned}
\Delta_0 &= \sum_{i=0}^{\Gamma-1}\left(\left|\sum_{k=0}^{i} h_k g_{i-k}\right|^2 + \left|\sum_{k=0}^{i} h_k \bar{g}_{i-k} + \sum_{j=i}^{\Gamma-1} h_{\Gamma+i-j} g_j\right|^2 \right. \\
&\quad \left. + \left|\sum_{j=i}^{\Gamma-1} h_{\Gamma+i-j}\bar{g}_j\right|^2\right), \\
\Delta_1 &= \sum_{i=0}^{\Gamma-1}\left(\left|\sum_{k=0}^{i} h_k g_{i-k}\right|^2 + \left|\sum_{k=0}^{i} h_k (g_{i-k}+\bar{g}_{i-k}) + \sum_{j=i}^{\Gamma-1} h_{\Gamma+i-j} g_j\right|^2 \right. \\
&\quad \left. + \left|\sum_{k=0}^{i} h_k \bar{g}_{i-k} + \sum_{j=i}^{\Gamma-1} h_{\Gamma+i-j}(g_j+\bar{g}_j)\right|^2 + \left|\sum_{j=i}^{\Gamma-1} h_{\Gamma+i-j}\bar{g}_j\right|^2\right), \\
\Delta_2 &= \sum_{i=0}^{\Gamma-1}\left(\left|\sum_{k=0}^{i} h_k g_{i-k}\right|^2 + \left|\sum_{k=0}^{i} h_k (g_{i-k}-\bar{g}_{i-k}) - \sum_{j=i}^{\Gamma-1} h_{\Gamma+i-j} g_j\right|^2 \right. \\
&\quad \left. + \left|\sum_{k=0}^{i} h_k \bar{g}_{i-k} + \sum_{j=i}^{\Gamma-1} h_{\Gamma+i-j}(g_j-\bar{g}_j)\right|^2 + \left|\sum_{j=i}^{\Gamma-1} h_{\Gamma+i-j}\bar{g}_j\right|^2\right).
\end{aligned}$$

Similar to the previous proof, the conditional means of Δ_i for $i = 0,1,2$ given g_0 and $\bar{g}_0$ are as follows

$$\begin{aligned}
E\{\Delta_0|g_0,\bar{g}_0\} &= \Gamma + 2h_0 h_\Gamma g_0 \bar{g}_0, \\
E\{\Delta_1|g_0,\bar{g}_0\} &= 2\Gamma(1-h_0h_\Gamma) + 2(1+2h_0h_\Gamma)g_0\bar{g}_0, \\
E\{\Delta_2|g_0,\bar{g}_0\} &= 2\Gamma(1+h_0h_\Gamma) + 2(-1+2h_0h_\Gamma)g_0\bar{g}_0.
\end{aligned}$$

If we choose $g_0, \bar{g}_0$ such that the following conditions are satisfied:

$$\text{sign}(g_0\bar{g}_0) = \text{sign}(h_0 h_\Gamma),$$

and

$$g_0 \longrightarrow 0 \text{ or } \bar{g}_0 \longrightarrow 0.$$

By combining with the assumption $|h_0 h_\Gamma| < \frac{1}{2}$, we have

$$\begin{aligned} E\{\Delta_0|g_0,\bar{g}_0\} &> \Gamma, \\ E\{\Delta_1|g_0,\bar{g}_0\} &> \Gamma, \\ E\{\Delta_2|g_0,\bar{g}_0\} &> \Gamma. \end{aligned}$$

This indicates $E\{d^2_{free}|g_0,\bar{g}_0\} > 4\Gamma$. Theorem 2.5 is then proved. ■

When $|h_0 h_{\Gamma-1}| = 1/2$, by the normalization condition (2.3.1) it is not hard to see that $h_0 = \pm 1/\sqrt{2}$, $h_{\Gamma-1} = \pm 1/\sqrt{2}$, and $h_2 = \cdots = h_{\Gamma-2} = 0$. The following theorems deal with two tap ISI channels.

Theorem 2.6 *Let $H(z) = h_0 + h_{\Gamma-1} z^{-(\Gamma-1)}$ be the ISI channel with $\Gamma > 1$. There does not exist a rate $1/(\Gamma - i)$, $\Gamma > i \geq 1$, block MC $\mathbf{G}(z) = G$ with coding gain compared to the uncoded AWGN channel.*

Proof. It is easy to show that for any $i, \Gamma - 1 \geq i \geq 1$, there exist two integers S and P satisfying $\Gamma - 1 = P(\Gamma - i) + S$, $\Gamma - 1 \geq P \geq 1$ and $\Gamma - i > S \geq 0$. By using the definition of $d^2_{free,\mathbf{C}}$, we have

$$d^2_{free,\mathbf{C}} \leq 4\Delta_0,$$

where

$$\Delta_0 = h_0^2 \sum_{k=0}^{\Gamma-i-1} g_k^2 + h_{\Gamma-1}^2 \sum_{k=0}^{\Gamma-i-S-1} g_k^2 + h_{\Gamma-1}^2 \sum_{j=\Gamma-i-S}^{\Gamma-i-1} g_j^2.$$

By the normalizations of $\mathbf{G}(z)$ and the ISI channel $h(n)$, we have

$$d^2_{free,\mathbf{C}} \leq 4\Delta_0 = 4(\Gamma - i).$$

Theorem 2.6 is proved. ■

Theorem 2.6 tells that when the ISI channel pulse response has two taps, there does not exist rate $1/(\Gamma - i)$, $1 \leq i \leq \Gamma - 1$, block MC G with coding gain compared to the uncoded ISI channel. The following theorem gives an answer on the existence of rate $2/(\Gamma + 1)$ MC.

Theorem 2.7 *Let $H(z) = h_0 + h_{\Gamma-1} z^{-\Gamma+1}$ be the ISI channel with $\Gamma > 1$. There exists a rate $2/(\Gamma+1)$ block MC $\mathbf{G}(z) = G$ with coding gain compared to the uncoded AWGN channel.*

Proof. Let the normalized MC $\mathbf{G}(z)$ be a $\Gamma + 1$ by 2 constant matrix:

$$\begin{aligned} \mathbf{G}(z) &= (G_0, G_1), \\ G_0^T &= (g_0\ g_1 \cdots\ g_\Gamma), \\ G_1^T &= (\bar{g}_0 \bar{g}_1\ \cdots\ \bar{g}_\Gamma), \end{aligned}$$

such that

$$\sum_{i=0}^{\Gamma} |g_i|^2 = \sum_{i=0}^{\Gamma} |\bar{g}_i|^2 = \frac{\Gamma+1}{2}.$$

The squared free distance of the received signal sequences after the ISI channel is

$$\frac{d^2_{free,\mathbf{C}}}{4} = \min\{\Delta_1, \Delta_2, \Delta_3, \Delta_4\},$$

where

$$\begin{aligned}
\Delta_1 &= (h_0^2 + h_{\Gamma-1}^2)\sum_{i=0}^{\Gamma} g_i^2 + 2h_0h_{\Gamma-1}(g_0g_{\Gamma-1} + g_1g_\Gamma), \\
\Delta_2 &= (h_0^2 + h_{\Gamma-1}^2)\sum_{i=0}^{\Gamma} \bar{g}_i^2 + 2h_0h_{\Gamma-1}(\bar{g}_0\bar{g}_{\Gamma-1} + \bar{g}_1\bar{g}_\Gamma), \\
\Delta_3 &= (h_0^2 + h_{\Gamma-1}^2)\sum_{i=0}^{\Gamma} (g_i + \bar{g}_i)^2 \\
&\quad +2h_0h_{\Gamma-1}\left((g_0 + \bar{g}_0)(g_{\Gamma-1} + \bar{g}_{\Gamma-1}) + (g_1 + \bar{g}_1)(g_\Gamma + \bar{g}_\Gamma)\right), \\
\Delta_4 &= (h_0^2 + h_{\Gamma-1}^2)\sum_{i=0}^{\Gamma} (g_i - \bar{g}_i)^2 \\
&\quad +2h_0h_{\Gamma-1}\left((g_0 - \bar{g}_0)(g_{\Gamma-1} - \bar{g}_{\Gamma-1}) + (g_1 - \bar{g}_1)(g_\Gamma - \bar{g}_\Gamma)\right).
\end{aligned}$$

Given $g_0, g_{\Gamma-1}, \bar{g}_1, \bar{g}_\Gamma$, the conditional means of $\Delta_i, i = 1,2,3,4$ are

$$\begin{aligned}
E\{\Delta_1|g_0, g_{\Gamma-1}, \bar{g}_1, \bar{g}_\Gamma\} &= \frac{\Gamma+1}{2} + 2h_0h_{\Gamma-1}g_0g_{\Gamma-1}, \\
E\{\Delta_2|g_0, g_{\Gamma-1}, \bar{g}_1, \bar{g}_\Gamma\} &= \frac{\Gamma+1}{2} + 2h_0h_{\Gamma-1}\bar{g}_1\bar{g}_\Gamma, \\
E\{\Delta_3|g_0, g_{\gamma-1}, \bar{g}_1, \bar{g}_\Gamma\} &= \Gamma+1 + 2h_0h_{\Gamma-1}(g_0g_{\Gamma-1} + \bar{g}_1\bar{g}_\Gamma), \\
E\{\Delta_4|g_0, g_{\Gamma-1}, \bar{g}_1, \bar{g}_\Gamma\} &= \Gamma+1 + 2h_0h_{\Gamma-1}(g_0g_{\Gamma-1} + \bar{g}_1\bar{g}_\Gamma).
\end{aligned}$$

If we choose $g_0, g_{\Gamma-1}, \bar{g}_1, \bar{g}_\Gamma$ with

$$\text{sign}(g_0g_{\Gamma-1}) = \text{sign}(\bar{g}_1\bar{g}_\Gamma) = \text{sign}(h_0h_{\Gamma-1}),$$

we have

$$\begin{aligned}
E\{\Delta_1|g_0, g_{\Gamma-1}, \bar{g}_1, \bar{g}_\Gamma\} &> \frac{\Gamma+1}{2}, \\
E\{\Delta_2|g_0, g_{\Gamma-1}, \bar{g}_1, \bar{g}_\Gamma\} &> \frac{\Gamma+1}{2}, \\
E\{\Delta_3|g_0, g_{\Gamma-1}, \bar{g}_1, \bar{g}_\Gamma\} &> \Gamma+1, \\
E\{\Delta_4|g_0, g_{\Gamma-1}, \bar{g}_1, \bar{g}_\Gamma\} &> \Gamma+1.
\end{aligned}$$

This indicates that under the same conditions, the conditional mean given $g_0, g_{\Gamma-1}, \bar{g}_1, \bar{g}_\Gamma$ satisfies

$$E\left\{ \frac{d^2_{free,\mathbf{C}}}{4} \middle| g_0, g_{\Gamma-1}, \bar{g}_1, \bar{g}_\Gamma \right\} > \frac{\Gamma+1}{2}.$$

Theorem 2.7 is then proved. ■

Theorem 2.4 tells us the existence of rate $2/\Gamma$ MC with coding gain for all ISI channels except the case when $|h_0 h_{\Gamma-1}| = 1/2$. When $|h_0 h_{\Gamma-1}| = 1/2$, Theorem 2.7 says that there exists a rate $2/(\Gamma+1)$ MC with coding gain, where the rate is slightly decreased. In next section, we study higher rate MC.

2.5.2 Some Sufficient Conditions on the Existence of Higher Rate Block MC with Coding Gain

One can see from Theorem 2.6 that, for a two tap ISI channel, there does not exist a rate $1/N$ with $N = \Gamma - i, i \geq 1$, normalized block MC G having coding gain over the ISI channel. Based on this result, in what follows we choose $N \geq \Gamma$ in the rate K/N MC $\mathbf{G}(z)$. Let $h_n = h(n)$ be the ISI channel impulse response, where h_n has only at most Γ non-zero taps $h_0, h_1, ..., h_{\Gamma-1}$ with $h_0 \neq 0$ and $h_{\Gamma-1} \neq 0$. When $N \geq \Gamma$, the ISI channel pseudo-circulant matrix $\mathbf{H}(z)$ in (2.3.3) becomes $\mathbf{H}(z) = H_0 + H_1 z^{-1}$, where

$$H_0 = \begin{bmatrix} h_0 & 0 & 0 & \cdots & 0 & 0 \\ h_1 & h_0 & 0 & \cdots & 0 & 0 \\ \vdots & \vdots & \vdots & \vdots & \vdots & \vdots \\ h_{N-2} & h_{N-3} & h_{N-4} & \cdots & h_0 & 0 \\ h_{N-1} & h_{N-2} & h_{N-3} & \cdots & h_1 & h_0 \end{bmatrix}, \tag{2.5.12}$$

and

$$H_1 = \begin{bmatrix} 0 & h_{N-1} & h_{N-2} & \cdots & h_2 & h_1 \\ 0 & 0 & h_{N-1} & \cdots & h_3 & h_2 \\ \vdots & \vdots & \vdots & \vdots & \vdots & \vdots \\ 0 & 0 & 0 & \cdots & 0 & h_{N-1} \\ 0 & 0 & 0 & \cdots & 0 & 0 \end{bmatrix}. \tag{2.5.13}$$

Clearly H_0 is invertible. This proves the following lemma.

Lemma 2.3 *Let $\mathbf{H}(z)$ be an ISI channel with $\Gamma > 1$ taps. If $N \geq \Gamma$, then $\mathbf{H}(z) = H_0 + z^{-1} H_1$, and*

$$\bar{R}_H = H_0^\dagger H_0 + H_1^\dagger H_1$$

$$= \begin{bmatrix} 1 & R_1 & R_2 & R_3 & \cdots & R_{N-1} \\ R_1 & 1 & R_1 & R_2 & \cdots & R_{N-2} \\ \cdots & \cdots & \cdots & \cdots & \cdots & \cdots \\ R_{N-2} & R_{N-3} & \cdots & R_1 & 1 & R_1 \\ R_{N-1} & R_{N-2} & R_{N-3} & \cdots & R_1 & 1 \end{bmatrix}, \tag{2.5.14}$$

where, $1 \leq i \leq N-1$,

$$R_i = \sum_{p=0}^{N-1-i} h_p h_{i+p}. \tag{2.5.15}$$

Furthermore, matrix $\bar{R}_H$ *is positive definite.*

From (2.5.15), when $\Gamma < N$, it is clear that $R_i = 0$ for $i = \Gamma, \Gamma+1, \cdots, N-1$. We first study rate $3/N$ MC.

Theorem 2.8 *Let* $H(z)$ *be an ISI channel with* Γ *taps,* $\Gamma \geq 3$, *and the BPSK be used for the information sequence x(n). If* $0 < |R_i| < \frac{1}{2}$ $(1 \leq i < \Gamma - 1)$, *there exists a rate* $3/N$ *block MC with* $N = \Gamma + i$ *such that it has coding gain compared to the uncoded AWGN channel.*

Proof. If we choose a normalized MC $\mathbf{G}(z)$ as an N by K constant matrix $\mathbf{G}(z) = G = (g_{n,k})_{N\times K} = (G_0, G_1, \cdots, G_{K-1})$, where G_i is the i-th column vector of G, then the squared free distance d^2_{free} can be obtained as follows

$$\begin{aligned} \frac{d^2_{free,\mathbf{C}}}{4} &= \min_{U\neq 0} \left\{ (H_0GU)^\dagger (H_0GU) + (H_1GU)^\dagger (H_1GU) \right\} \\ &= \min_{U\neq 0} \left\{ (GU)^\dagger (H_0^\dagger H_0 + H_1^\dagger H_1)(GU) \right\} \\ &= \min_{U\neq 0} \left\{ (GU)^\dagger \bar{R}_H (GU) \right\}, \end{aligned} \tag{2.5.16}$$

where $U = (u_0, u_1, \cdots, u_{K-1})^T$ is a K by 1 vector, whose elements are in the set $\{-1, 0, +1\}$.

When $N = \Gamma + i$ and $K = 3$, we select $g_{0,0}, g_{\Gamma-1,0}, g_{0,1}, g_{\Gamma-1,1}, g_{i,2}, g_{\Gamma+i-1,2}$ as non-zero real random variables with mean zero, and other elements of G as zeroes. Furthermore, we consider the following normalized MC block G,

$$g^2_{0,0} + g^2_{\Gamma-1,0} = \frac{N}{3} = \frac{\Gamma+i}{3}, \tag{2.5.17}$$

$$g^2_{0,1} + g^2_{\Gamma-1,1} = \frac{N}{3} = \frac{\Gamma+i}{3}, \tag{2.5.18}$$

$$g^2_{i,2} + g^2_{\Gamma+i-1,2} = \frac{N}{3} = \frac{\Gamma+i}{3}. \tag{2.5.19}$$

In this case, we have

$$
\begin{aligned}
&(GU)^{\dagger}\bar{R}_H(GU)\\
&= \left(\frac{\Gamma+i}{3} + 2R_{\Gamma-1}g_{0,0}g_{\Gamma-1,0}\right)u_0^2 + \left(\frac{\Gamma+i}{3} + 2R_{\Gamma-1}g_{0,1}g_{\Gamma-1,1}\right)u_1^2\\
&\quad + \left(\frac{\Gamma+i}{3} + 2R_{\Gamma-1}g_{i,2}g_{\Gamma+i-1,2}\right)u_2^2\\
&+2g_{\Gamma-1,0}u_0(R_{\Gamma-1}g_{0,1}u_1 + R_{\Gamma-i-1}g_{i,2}u_2 + g_{\Gamma-1,1}u_1 + R_i g_{\Gamma+i-1,2}u_2)\\
&+2g_{0,1}u_1(g_{0,0}u_0 + R_i g_{i,2}u_2) + 2g_{i,2}u_2(R_i g_{0,0}u_0 + R_{\Gamma-i-1}g_{\Gamma-1,1}u_1)\\
&+2R_{\Gamma-1}g_{0,0}g_{\Gamma-1,1}u_0u_1 + 2R_i g_{\Gamma-1,1}g_{\Gamma+i-1,2}u_1u_2.
\end{aligned}
$$

Let

$$\operatorname{sign}(g_{0,0}g_{\Gamma-1,0}) = \operatorname{sign}(g_{0,1}g_{\Gamma-1,1}) = \operatorname{sign}(g_{i,2}g_{\Gamma+i-1,2}) = \operatorname{sign}(R_{\Gamma-1}),$$

and

$$|g_{\Gamma-1,0}| = |g_{0,1}| = |g_{i,2}| \to 0.$$

In this case, (2.5.16) can be rewritten as

$$
\begin{aligned}
&(GU)^{\dagger}\bar{R}_H(GU)\\
&\approx \left(\frac{\Gamma+i}{3} + 2|R_{\Gamma-1}g_{0,0}g_{\Gamma-1,0}|\right)u_0^2 + \left(\frac{\Gamma+i}{3} + 2|R_{\Gamma-1}g_{0,1}g_{\Gamma-1,1}|\right)u_1^2\\
&\quad + \left(\frac{\Gamma+i}{3} + 2|R_{\Gamma-1}g_{i,2}g_{\Gamma+i-1,2}|\right)u_2^2\\
&+2R_{\Gamma-1}g_{0,0}g_{\Gamma-1,1}u_0u_1 + 2R_i g_{\Gamma-1,1}g_{\Gamma+i-1,2}u_1u_2.
\end{aligned}
$$

The assumption $0 < |R_i|$ implies that there exists an $h_j \neq 0$ for some j with $0 < j < \Gamma - 1$. Thus, by (2.3.1) and (2.5.15), we have

$$|R_{\Gamma-1}| = |h_0 h_{\Gamma-1}| \leq \frac{h_0^2 + h_{\Gamma-1}^2}{2} < \frac{1}{2}. \tag{2.5.20}$$

Therefore, when $|g_{\Gamma-1,0}|$, $|g_{0,1}|$, and $|g_{i,2}|$ are small enough, by (2.3.1), (2.5.17)-(2.5.19) and (2.5.20) and the assumption $|R_i| < 1/2$, we have

$$
\begin{aligned}
&(GU)^{\dagger}\bar{R}_H(GU)\\
&\geq \left(\frac{\Gamma+i}{3} + 2|R_{\Gamma-1}g_{0,0}g_{\Gamma-1,0}|\right)u_0^2 + \left(\frac{\Gamma+i}{3} + 2|R_{\Gamma-1}g_{0,1}g_{\Gamma-1,1}|\right)u_1^2\\
&\quad + \left(\frac{\Gamma+i}{3} + 2|R_{\Gamma-1}g_{i,2}g_{\Gamma+i-1,2}|\right)u_2^2 - \frac{\Gamma+i}{3}|u_0u_1| - \frac{\Gamma+i}{3}|u_1u_2|.
\end{aligned}
$$

From the above inequality, it is easy to show that for any $U \neq 0$,

$$(GU)^\dagger \bar{R}_H(GU) > \frac{\Gamma + i}{3},$$

which implies

$$\frac{d^2_{free,\mathbf{C}}}{4} > \frac{\Gamma + i}{3}.$$

This proves Theorem 2.8. ■

We next study rate $4/N$ MC.

Theorem 2.9 *Let $H(z)$ be an ISI channel with Γ taps, $\Gamma \geq 4$, and the BPSK be used for the information sequence $x(n)$. If $\max(|R_i|, |R_{\Gamma-i}|) < \frac{1}{2}$ for some $i \geq 2$, then there exists a rate $4/N$ block MC with $N = \Gamma + i + 1$ such that it has coding gain compared to the uncoded AWGN channel.*

Proof. Let G be an N by 4 constant matrix. By using (2.5.16), we have

$$\frac{d^2_{free,\mathbf{C}}}{4} = \min_{U \neq 0} \left\{ (GU)^\dagger \bar{R}_H(GU) \right\},$$

where $U^T = (u_0, u_1, u_2, u_3)$ and $u_i, i = 0, 1, 2, 3$, are in the set $\{-1, 0, 1\}$.

Select $g_{0,0}, g_{\Gamma-1,0}, g_{1,1}, g_{\Gamma,1}, g_{i,2}, g_{\Gamma+i-1,2}, g_{i+1,3}, g_{\Gamma+i,3}$ as non-zero real numbers with mean zero and other elements of G as zeroes. Furthermore, the following normalized MC G are considered,

$$\begin{aligned}
g^2_{0,0} + g^2_{\Gamma-1,0} &= \frac{N}{4} = \frac{\Gamma + i + 1}{4}, \\
g^2_{1,1} + g^2_{\Gamma,1} &= \frac{N}{4} = \frac{\Gamma + i + 1}{4}, \\
g^2_{i,2} + g^2_{\Gamma+i-1,2} &= \frac{N}{4} = \frac{\Gamma + i + 1}{4}, \\
g^2_{i+1,3} + g^2_{\Gamma+i,3} &= \frac{N}{4} = \frac{\Gamma + i + 1}{4}.
\end{aligned}$$

Let

$$\begin{aligned}
&\operatorname{sign}(g_{0,0} g_{\Gamma-1,0}) = \operatorname{sign}(g_{1,1} g_{\Gamma,1}) \\
&= \operatorname{sign}(g_{i,2} g_{\Gamma+i-1,2}) = \operatorname{sign}(g_{i+1,3} g_{\Gamma+i,3}) = \operatorname{sign}(R_{\Gamma-1}),
\end{aligned}$$

and

$$|g_{\Gamma-1,0}| = |g_{1,1}| = |g_{\Gamma+i,2}| = |g_{i+1,3}| \to 0.$$

We have

$$(GU)^\dagger \bar{R}_H(GU)$$

$$\approx \left(\frac{\Gamma+i+1}{4} + 2|R_{\Gamma-1}g_{0,0}g_{\Gamma-1,0}|\right) u_0^2$$
$$+ \left(\frac{\Gamma+i+1}{4} + 2|R_{\Gamma-1}g_{1,1}g_{\Gamma,1}|\right) u_1^2$$
$$+ \left(\frac{\Gamma+i+1}{4} + 2|R_{\Gamma-1}g_{i,2}g_{\Gamma+i-1,2}|\right) u_2^2$$
$$+ \left(\frac{\Gamma+i+1}{4} + 2|R_{\Gamma-1}g_{i+1,3}g_{\Gamma+i,3}|\right) u_3^2$$
$$+2R_i g_{0,0}g_{i,2}u_0u_2 + 2R_{\Gamma-i}g_{i,2}g_{\Gamma-1,1}u_1u_2 + 2R_i g_{\Gamma,1}g_{\Gamma+i,3}u_1u_3.$$

From the assumption $\max(|R_i|, |R_{\Gamma-i}|) < \frac{1}{2}$, similar to the proof of Theorem 2.8 we have

$$(GU)^\dagger \bar{R}_H(GU)$$
$$\geq \left(\frac{\Gamma+i+1}{4} + 2|R_{\Gamma-1}g_{0,0}g_{\Gamma-1,0}|\right) u_0^2 + \left(\frac{\Gamma+i+1}{4} + 2|R_{\Gamma-1}g_{1,1}g_{\Gamma,1}|\right) u_1^2$$
$$+ \left(\frac{\Gamma+i+1}{4} + 2|R_{\Gamma-1}g_{i,2}g_{\Gamma+i-1,2}|\right) u_2^2$$
$$+ \left(\frac{\Gamma+i+1}{4} + 2|R_{\Gamma-1}g_{i+1,3}g_{\Gamma+i,3}|\right) u_3^2$$
$$-\frac{\Gamma+i+1}{4}|u_0u_2| - \frac{\Gamma+i+1}{4}|u_1u_2| - \frac{\Gamma+i+1}{4}|u_1u_3|,$$

and for any $U \neq 0$,

$$(GU)^\dagger \bar{R}_H(GU) > \frac{\Gamma+i+1}{4}.$$

This proves Theorem 2.9. ■

By using the above two theorems, the following corollary is straightforward.

Corollary 2.9 *(i) If $\Gamma = 3$ and $0 < |R_1| < \frac{1}{2}$, then there exists a rate 3/5 normalized MC with coding gain compared to the uncoded AWGN channel.*

(ii) If $\Gamma = 4$ and $|R_2| < \frac{1}{2}$, then there exists a rate 4/7 normalized MC with coding gain compared to the uncoded AWGN channel.

The next result is for two tap ISI channels.

Theorem 2.10 *Let $H(z) = h_0 + h_{\Gamma-1}z^{-\Gamma+1}$ with $\Gamma > 1$. Let the BPSK be used for the information sequence $x(n)$. There exists a rate Γ/N with $N = 2\Gamma - 1$ block MC with coding gain compared to the uncoded AWGN channel.*

Proof. Let G be an N by Γ constant matrix with $N = 2\Gamma - 1$. By using (2.5.16), we have

$$\frac{d^2_{free,\mathbf{C}}}{4} = \min_{U\neq 0}\left\{(GU)^\dagger \bar{R}_H(GU)\right\},$$

where $U^T = (u_0, u_1, \cdots, u_{\Gamma-1})$ and $u_i, i = 0, 1, \cdots, \Gamma - 1$, are in the set $\{-1, 0, 1\}$.

We select

$$g_{0,0}, g_{\Gamma-1,0}, g_{1,1}, g_{\Gamma,1}, \cdots, g_{i,i}, g_{\Gamma+i-1,i}, \cdots, g_{\Gamma-1,\Gamma-1}, g_{2\Gamma-2,\Gamma-1}$$

as non-zero real numbers with mean zero and other elements of G as zeroes. Furthermore, we consider the following normalized MC G: for $0 \leq i \leq \Gamma-1$,

$$g^2_{i,i} + g^2_{\Gamma+i-1,i} = \frac{N}{\Gamma}.$$

Let

$$\text{sign}(g_{i,i}g_{\Gamma+i-1,i}) = \text{sign}(R_{\Gamma-1}),$$

and

$$|g_{\Gamma-1,0}| = |g_{\Gamma-1,\Gamma-1}| \to 0.$$

Then,

$$(GU)^\dagger \bar{R}_H(GU) \approx \sum_{i=0}^{\Gamma-1}\left(\frac{N}{\Gamma} + 2|R_{\Gamma-1}g_{i,i}g_{\Gamma+i-1,i}|u_i^2\right).$$

Similar to before, for any $U \neq 0$, we have

$$(GU)^\dagger \bar{R}_H(GU) > \frac{N}{\Gamma}.$$

This proves Theorem 2.10. ■

This theorem tells us that when the ISI channel length is 2, there exists a rate 2/3 normalized block MC having coding gain. When Γ is large, there exists a rate higher than 1/2 normalized block MC with coding gain compared to the uncoded AWGN channel.

2.5.3 A Method on the Rate Estimation of MC with Coding Gain

In this section, we want to estimate a rate r given an ISI channel such that there exists a rate r MC with coding gain compared to the uncoded AWGN channel. To do so, let us first see two lemmas.

Lemma 2.4 *For $\bar{R}_H$ defined in (2.5.14), its maximum eigenvalue $\lambda_{\max}$ satisfies $\lambda_{\max} > 1$.*

Proof. From Lemma 1, we know that $\bar{R}_H$ is a positive definite matrix. This means that all the eigenvalues of $\bar{R}_H$ are positive. By using the matrix trace result, we have

$$\sum_{i=1}^{N} \lambda_i = N. \tag{2.5.21}$$

Assume the maximum eigenvalue of $\bar{R}_H$ is not greater than 1. Then (2.5.21) implies that $\lambda_i = 1$ for $1 \leq i \leq N$, i.e., $\bar{R}_H = I_N$. This implies $R_{\Gamma-1} = h_0 h_{\Gamma-1} = 0$, which contradicts with the assumption $h_0 \neq 0$ and $h_{\Gamma-1} \neq 0$. The lemma is proved. ■

Lemma 2.5 *If $p_1, p_2, \cdots, p_N$ are N positive numbers, and satisfy*

$$\sum_{i=1}^{N} p_i = N,$$

then,

$$\sum_{i=1}^{N} \frac{1}{p_i} \geq N.$$

We now have the following sufficient condition in terms of the eigenvalues of the matrix $\bar{R}_H$ in (2.5.14).

Theorem 2.11 *For $\bar{R}_H$ defined in (2.5.14), let its eigenvalues be arranged in the decreasing order, $\lambda_1 \geq \lambda_2 \geq \cdots \geq \lambda_N > 0$. If*

$$\frac{1}{\lambda_1} + \frac{1}{\lambda_2} + \cdots + \frac{1}{\lambda_p} < p$$

is satisfied for a positive integer p, then there exists a rate p/N block MC with coding gain compared to the uncoded AWGN channel.

Proof. Since $\bar{R}_H$ is a positive definite matrix, there exists an N by N unitary matrix V such that

$$V^{\dagger}\bar{R}_H V = \Lambda = diag(\lambda_1, \lambda_2, \cdots, \lambda_N).$$

Define

$$W = VG = (w_{i,j})_{N\times p}.$$

Clearly,

$$\sum_{i,j} w_{i,j}^2 = \sum_{i,j} g_{i,j}^2, \tag{2.5.22}$$

and,

$$(GU)^{\dagger}\bar{R}_H(GU) = (WU)^{\dagger}\Lambda(WU).$$

If the matrix W is selected as $W^T = (diag(w_{1,1}, w_{2,2}, \cdots, w_{p,p}), \mathbf{0_{p\times(N-p)}})$, the above formula becomes

$$(GU)^{\dagger}\bar{R}_H(GU) = (WU)^{\dagger}\Lambda(WU) = \sum_{i=1}^{p} \lambda_i w_{i,i}^2 u_i^2. \tag{2.5.23}$$

For $i = 1, 2, ..., p$, let

$$w_{i,i}^2 = \left(\frac{1}{\lambda_i} + \delta_i\right)\frac{N}{p}, \tag{2.5.24}$$

where $\delta_i > 0$ is chosen to satisfy the following condition

$$\sum_{i=1}^{p} \delta_i = p - \sum_{i=1}^{p} \frac{1}{\lambda_i} > 0. \tag{2.5.25}$$

The equalities (2.5.22), (2.5.24) and (2.5.25) ensure that

$$\sum_{i,j} g_{i,j}^2 = N,$$

i.e., the MC G is normalized. From (2.5.23) and (2.5.24), it is not hard to see that

$$\frac{d_{free,\mathbf{C}}^2}{4} = \min_{U\neq 0}(GU)^{\dagger}\bar{R}_H(GU) > \frac{N}{p}.$$

This proves Theorem 2.11. ■

From the above proof, we can similarly prove the following result.

Theorem 2.12 *For $\bar{R}_H$ defined in (2.5.14), let its eigenvalues be arranged in the decreasing order, $\lambda_1 \geq \lambda_2 \geq \cdots \geq \lambda_N > 0$. If*

$$\frac{1}{\lambda_1} + \frac{1}{\lambda_2} + \cdots + \frac{1}{\lambda_p} < p$$

is satisfied for a positive integer p, then there exists a rate $1/N, 2/N, \cdots, p/N$ block MC with coding gain compared to the uncoded AWGN channel.

Using Lemma 2.4 and Theorem 2.11 we can see that, when $N = \Gamma$, there always exists a rate $1/\Gamma$ MC having coding gain over the ISI channel, which coincides with the one in Theorem 2.3.

Let us consider an application of Theorem 2.11 to two tap ISI channels.

Corollary 2.10 *Let $H(z) = h_0 + h_{\Gamma-1} z^{-\Gamma+1}$ with $\Gamma > 1$. There exists a rate $(\Gamma - 1)/\Gamma$ block MC with coding gain compared to the uncoded AWGN channel.*

Proof. When $N = \Gamma$, the eigenvalues of $\bar{R}_H$ are $\lambda_1 = 1 + |h_0 h_{\Gamma-1}|$, $\lambda_2 = \cdots = \lambda_{N-1} = 1$, and $\lambda_N = 1 - |h_0 h_{\Gamma-1}|$. By using Theorem 2.11 and take $p = N - 1$, Corollary 2.10 is proved. ■

We next want to use the results in Theorems 2.11-2.12 to simulate the probabilities of the existence of rate r block MC with coding gain for a given ISI channel for different r. The ISI channels are assumed to have independent real coefficients and the same Gaussian distributions.

The following two tables show the existence probabilities for two different cases on the rates of MC having coding gain. In Table 2.1, the length of ISI channel is chosen to be the same as the row number of the block MC $\mathbf{G}(z) = G$, i.e., $N = \Gamma$. In Table 2.2, the row number of the block MC $\mathbf{G}(z) = G$ is chosen as $N = 2\Gamma - 1$.

Since the conditions in Theorems 2.11-2.12 are only sufficient conditions on the existence, the simulation results presented in Tables 2.1-2.2 are the lower bounds on the existence probabilities of a block MC. By observing the results in Tables 2.1-2.2, we find that there exists a rate higher than 1/2 MC having coding gain for most of the ISI channels with finite lengths.

Table 2.1: Lower bounds of the existence probabilities of MC with coding gain compared to the uncoded AWGN channel, where $N = \Gamma$.

N = 4	Rate	1/4	2/4	3/4					
Existence Prob.		1.0	1.0	0.638515					
N=5	Rate	1/5	2/5	3/5	4/5				
Existence Prob.		1.0	1.0	0.98775	0.40855				
N = 6	Rate	1/6	2/6	3/6	4/6	5/6			
Existence Prob.		1.0	1.0	1.0	0.9749	0.3156			
N = 7	Rate	1/7	2/7	3/7	4/7	5/7	6/7		
Existence Prob.		1.0	1.0	1.0	0.9975	0.9269	0.3389		
N = 8	Rate	1/8	2/8	3/8	4/8	5/8	6/8	7/8	
Existence Prob.		1.0	1.0	1.0	0.9997	0.9942	0.9125	0.3798	
N = 9	Rate	1/9	2/9	3/9	4/9	5/9	6/9	7/9	8/9
Existence Prob.		1.0	1.0	1.0	0.999955	0.9995	0.9910	0.8665	0.4155

Table 2.2: Lower bounds of the existence probabilities of MC with coding gain compared to the uncoded AWGN channel, where $N = 2\Gamma - 1$.

N = 7	Rate	1/7	2/7	3/7	4/7	5/7	6/7				
Existence Prob.		1.0	1.0	1.0	0.999	0.9478	0.31145				
N=9	Rate	1/9	2/9	3/9	4/9	5/9	6/9	7/9	8/9		
Existence Prob.		1.0	1.0	1.0	1.0	0.9968	0.9837	0.8347	0.37155		
N = 11	Rate	1/11	2/11	3/11	4/11	5/11	6/11	7/11	8/11	9/11	10/11
Existence Prob.		1.0	1.0	1.0	1.0	1.0	0.9993	0.9945	0.9582	0.7682	0.3509
N = 13	Rate	1/13	2/13	3/13	4/13	5/13	6/13				
Existence Prob.		1.0	1.0	1.0	1.0	1.0	0.9999				
N = 13	Rate	7/13	8/13	9/13	10/13	11/13	12/13				
Existence Prob.		0.9997	0.9987	0.9889	0.9308	0.6972	0.32355				
N = 15	Rate	1/15	2/15	3/15	4/15	5/15	6/15	7/15			
Existence Prob.		1.0	1.0	1.0	1.0	1.0	0.99995	0.99995			
N = 15	Rate	8/15	9/15	10/15	11/15	12/15	13/15	14/15			
Existence Prob.		0.99995	0.9995	0.9966	0.9819	0.8999	0.6388	0.293			
N = 17	Rate	1/17	2/17	3/17	4/17	5/17	6/17	7/17	8/17		
Existence Prob.		1.0	1.0	1.0	1.0	1.0	1.0	1.0	1.0		
N = 17	Rate	9/17	10/17	11/17	12/17	13/17	14/17	15/17	16/17		
Existence Prob.		1.0	0.9999	0.9989	0.9938	0.9713	0.8598	0.5902	0.27195		

2.5.4 Lower and Upper Bounds on the Coding Gain

In Corollary 2.8, an upper bound of the coding gain of an MC over a given ISI channel has been given, which is the length of the ISI channel and independent of the coefficients of the ISI channel. The upper bound may not be tight enough in some cases. In this section, we first present some new upper bounds of the coding gain of some special MC. In particular, we discuss the case of the ISI channel with two taps. We then present a lower bound of the coding gain of the optimal rate $1/\Gamma$ MC, where Γ is the length of the ISI channel and the optimality means the maximal free distance.

Theorem 2.13 *Let $\mathbf{H}(z) = H_0 + z^{-1}H_1$ be an ISI channel with H_0 and H_1 as in (2.5.9)-(2.5.10) and the BPSK be used for the information sequence $x(n)$. Let $\mathbf{G}(z) = G_0 + z^{-1}G_1 + \cdots + z^{-P}G_P$, where G_p for $p = 0, 1, \cdots, P$ are N by K constant matrices, be a rate K/N normalized MC with $N = \Gamma$. Then, the coding gain γ_{ISI} of the MC $\mathbf{G}(z)$ compared to the uncoded AWGN channel is upper bounded by:*

$\gamma_{ISI} \leq \lambda_{\max}(H_0^\dagger H_0 + H_1^\dagger H_1)$, *if* $\mathbf{G}(z) = G_0$;

$\gamma_{ISI} \leq \max\{\lambda_{\max}(2H_0^\dagger H_0 + H_1^\dagger H_1), \lambda_{\max}(H_0^\dagger H_0 + 2H_1^\dagger H_1)\}$, *if* $\mathbf{G}(z) = G_0 + z^{-1}G_1$;

$\gamma_{ISI} \leq 2\lambda_{\max}(H_0^\dagger H_0 + H_1^\dagger H_1)$, *otherwise,*

where $\dagger$ denotes the complex conjugate transpose, and $\lambda_{max}(A)$ denotes the maximum eigenvalue of matrix A.

Proof. According to the trellis diagram and the randomness of the information vector sequence, we choose the correct path as all-zero path, and the input signal vector sequence with length $P+2$ as $(1,1,1,\cdots,1)^T$, $(1,1,1,\cdots,1)^T$, $\cdots$, $(1,1,1,\cdots,1)^T$, the corresponding error path as $(1,0,0,\cdots,0) \rightarrow (0,1,0,\cdots,0) \rightarrow (0,0,1,0,\cdots,0) \rightarrow \cdots, \rightarrow (0,0,0,\cdots,0,1)$ and the other input signal vector sequence as $(1,1,\cdots,-1,\cdots,1)^T$ (note that the signal vector has only one entry of -1 in its k-th component) , $(1,1,1,\cdots,1)^T$, $\cdots$, $(1,1,1,\cdots,1)^T$. In this case, we know that the distance Δ_k between the two input signal vector sequences is equal to 4 and the corresponding distance between the combined MC output sequences is as follows:

$$\Delta_k = G_0^{k\dagger} H_0^\dagger H_0 G_0^k +$$

$$\sum_{p=1}^{P} \{H_0 G_p^k + H_1 G_{p-1}^k\}^\dagger \{H_0 G_p^k + H_1 G_{p-1}^k\} + G_P^{k\dagger} H_1^\dagger H_1 G_P^k,$$

where G_p^k denotes the k-th column vector of matrix G_p. As we know, the free distance of the combined MC should be equal to or less than Δ_k for

all $k = 1, 2, \cdots, K$. Thus, we have

$$\frac{d^2_{free,\mathbf{C}}}{4} \leq \min_k \Delta_k \leq \frac{\sum_{k=1}^{K} \Delta_k}{K}. \tag{2.5.26}$$

First, let us consider the case of $\mathbf{G}(z) = G_0$. In this case, (2.5.26) becomes

$$\frac{d^2_{free,\mathbf{C}}}{4} \leq \frac{\sum_{k=1}^{K} G_0^{k\dagger}\{H_0^\dagger H_0 + H_1^\dagger H_1\}G_0^k}{K}.$$

By the normalization property of $\mathbf{G}(z)$ it is easy to see that

$$\frac{d^2_{free,\mathbf{C}}}{4} \leq \lambda_{\max}(H_0^\dagger H_0 + H_1^\dagger H_1)\frac{N}{K}.$$

By using the coding gain definition in (2.4.1), the conclusion is obtained.

When $\mathbf{G}(z) = G_0 + z^{-1}G_1$, by using the triangular inequality, we have

$$\frac{d^2_{free,\mathbf{C}}}{4} \leq \frac{\sum_{k=1}^{K} G_0^{k\dagger}\{2H_0^\dagger H_0 + H_1^\dagger H_1\}G_0^k + G_1^{k\dagger}\{H_0^\dagger H_0 + 2H_1^\dagger H_1\}G_1^k}{K}.$$

Using the same method, the above formula becomes

$$\begin{aligned}
\frac{d^2_{free,\mathbf{C}}}{4} &\leq \lambda_{\max}(2H_0^\dagger H_0 + H_1^\dagger H_1)\frac{\sum_{k=1}^{K} G_0^{k\dagger}G_0^k}{K} \\
&\quad + \lambda_{\max}(H_0^\dagger H_0 + 2H_1^\dagger H_1)\frac{\sum_{k=1}^{K} G_1^{1\dagger}G_1^1}{K} \\
&\leq \max\left\{\lambda_{\max}(2H_0^\dagger H_0 + H_1^\dagger H_1), \lambda_{\max}(H_0^\dagger H_0 + 2H_1^\dagger H_1)\right\} \\
&\quad \cdot \frac{\sum_{k=1}^{K}(G_0^{k\dagger}G_0^k + G_1^{k\dagger}G_1^k)}{K} \\
&\leq \max\left\{\lambda_{\max}(2H_0^\dagger H_0 + H_1^\dagger H_1), \lambda_{\max}(H_0^\dagger H_0 + 2H_1^\dagger H_1)\right\}\frac{N}{K}.
\end{aligned}$$

The last part of Theorem 2.13 can be similarly proved. ■

By using the above result, the following corollary can be obtained directly.

Corollary 2.11 *let $H(z) = h_0 + h_{\Gamma-1}z^{-(\Gamma-1)}$ be the ISI channel with $\Gamma > 1$, and the BPSK be used for the information sequence $x(n)$. Then, the coding gain γ_{ISI} of a rate K/Γ MC $\mathbf{G}(z)$ is upper bounded by*

$$\gamma_{ISI} \leq \begin{cases} 1 + |h_0 h_{\Gamma-1}| \leq 1.5, & \text{if } \mathbf{G}(z) = G_0, \\ \frac{3+h_0^2+\sqrt{(1-h_0^2)(1+15h_0^2)}}{2} \leq 2.8, & \text{if } \mathbf{G}(z) = G_0 + z^{-1}G_1, \\ 2\{1 + |h_0 h_{\Gamma-1}|\} \leq 3, & \text{otherwise}, \end{cases} \tag{2.5.27}$$

and the coding gain γ of a rate $K/(\Gamma-1)$ MC $\mathbf{G}(z)$ is upper bounded by

$$\gamma_{ISI} \leq \begin{cases} 1, & \text{if } \mathbf{G}(z) = G_0, \\ \max\{1+h_0^2, 1+h_{\Gamma-1}^2\} < 2, & \text{if } \mathbf{G}(z) = G_0 + z^{-1}G_1, \\ 2, & \text{otherwise.} \end{cases} \tag{2.5.28}$$

This corollary shows that, when the ISI channel has two taps h_0 and $h_{\Gamma-1}$: if $\Gamma = 2$, then the new upper bound is looser than the one, 2, in Corollary 2.8; if $\Gamma = 3$, the new upper bound is the same as the one in Corollary 2.8; if $\Gamma > 3$, the new upper bound is tighter than the one in Corollary 2.8.

As an application of Corollary 2.11, we let $H(z) = h_0 + h_{\Gamma-1}z^{-(\Gamma-1)}$ be the ISI channel with $\Gamma > 1$, and the BPSK be used for the information sequence $x(n)$. The coding gain of rate $1/(\Gamma-1)$ MC is upper bounded by (2.5.28), which implies that there does not exist rate $1/(\Gamma-1)$ block MC having coding gain over the above ISI channel, which coincides with the result in Theorem 2.6.

In the following, we will present a lower bound of the coding gain of the optimal MC over a given ISI channel.

Theorem 2.14 *Let $H(z)$ be an ISI channel with Γ taps with $\Gamma > 1$, and $h_0 \neq 0$ and $h_{\Gamma-1} \neq 0$, and the BPSK be used for the information sequence $x(n)$. Then, the coding gain $\gamma_{ISI,opt}$ of the optimal rate $1/\Gamma$ MC over the ISI channel is lower bounded by*

$$\gamma_{ISI,opt} \geq \max_{s=1,2,\cdots,\Gamma-1} \{1 + \left| \sum_{i=0}^{\Gamma-s-1} h_i h_{i+s} \right|\}. \tag{2.5.29}$$

Proof. Let $\mathbf{G}(z)$ be Γ by 1 constant matrix. The free distance of the received signal sequence after the ISI channel is given by

$$\frac{d_{free,\mathbf{C}}^2}{4} = \sum_{i=0}^{\Gamma-1} \left| \sum_{k=0}^{i} h_k g_{i-k} \right|^2 + \left| \sum_{j=i+1}^{\Gamma-1} h_{\Gamma+i-j} g_j \right|^2.$$

Then it is not hard to see that

$$E\left\{ \frac{d_{free,\mathbf{C}}^2}{4} \middle| g_0, g_s \right\} = \Gamma + 2\left(\sum_{i=0}^{\Gamma-s-1} h_i h_{i+s} \right) g_0 g_s.$$

Without loss of generality, we only consider normalized MC $\mathbf{G}(z)$. In this case,

$$\sum_{i=0}^{\Gamma-1} g_i^2 = \Gamma.$$

Choose g_0 and g_s satisfying the following conditions

$$\text{sign}(g_0 g_s) = \text{sign}\left(\sum_{i=0}^{\Gamma-s-1} h_i h_{i+s}\right), \quad |g_0 g_s| = \frac{\Gamma}{2}.$$

Thus,

$$E\left\{\frac{d^2_{free,\mathbf{C}}}{4}\middle| g_0, g_s\right\} = \Gamma\left(1 + \left|\sum_{i=0}^{\Gamma-s-1} h_i h_{i+s}\right|\right).$$

This indicates that, for all $\Gamma - 1 \geq s \geq 1$, the free distance of the optimal normalized MC over the given ISI channel satisfies

$$\left.\frac{d^2_{free,\mathbf{C}}}{4}\right|_{opt} \geq \Gamma \max_{s=1,2,\cdots,\Gamma-1}\left(1 + \left|\sum_{i=0}^{\Gamma-s-1} h_i h_{i+s}\right|\right).$$

By using the coding gain definition in (2.4.1), (2.5.29) is proved. ■

We next want to see some examples.

Example 1: Let the ISI channel be

$$h = [\frac{1}{\sqrt{2}}, -\frac{1}{\sqrt{2}}].$$

In this case, the lower bound of the coding gain in (2.5.29) of the optimal rate 1/2 MC is 1.5. The upper bounds of the coding gain in Corollary 1 and Γ of the rate K/Γ MC in Theorem 2.3 are

$$1.5 \leq \gamma_{ISI,opt} \leq \begin{cases} 1.5, & \text{if } \mathbf{G}(z) = G_0, \\ 2, & \text{otherwise.} \end{cases}$$

Example 2: Let the ISI channel be

$$h = [0.5, -0.5, 0.5, -0.5].$$

In this case, the lower and upper bounds of the coding gain of the optimal rate 1/4 MC code are

$$1.75 \leq \gamma_{ISI,opt} \leq \begin{cases} 2.7748, & \text{if } \mathbf{G}(z) = G_0, \\ 4, & \text{otherwise.} \end{cases}$$

Example 3: Let the ISI channel be N taps, and the channel response be

$$h = [\frac{1}{\sqrt{N}}, \frac{1}{\sqrt{N}}, \frac{1}{\sqrt{N}}, \cdots, \frac{1}{\sqrt{N}}].$$

In this case, the lower bound of the coding gain of the optimal rate $1/N$ MC code is

$$\gamma_{ISI,opt} \geq 1 + \frac{N-1}{N} \to 2 = 3\text{dB}, \quad \text{as } N \to \infty.$$

Chapter 3

Joint Maximum-Likelihood Encoding and Decoding

In this chapter, we study the maximum-likelihood MC encoding and decoding combined with an ISI channel. We first present the performance analysis by using the union bound, which is determined by the distance spectrum of the combined MC. We then present an algorithm to calculate the distance spectrum by introducing the error-pattern trellis due to the simple MC encoding operations. We also present an algorithm to find the optimal MC given an ISI channel such that the free distance of the combined MC is the maximal. In this chapter, the results in [178] are summarized.

3.1 Performance Analysis of MC

We now present the performance analysis of MC coded ISI channel using the maximum-likelihood sequence estimation (MLSE) when the ISI channel is known at the receiver. Since the combination of an MC and an ISI channel is an MC in the AWGN channel, to study the performance, we only need to study it in the AWGN channel. The encoder for an MC is a finite state machine (FSM), whose transitions are determined by the input data sequence. The decoder attempts to retrace the path, i.e., the state sequence, which the encoder has taken. An error will be made if the decoder follows a path that does not coincide with the one taken by the encoder. An important performance measure is the *error event probability*, which is

similar to the one for trellis codes, for example [119].

Let us first review the performance bounds for trellis codes. Fig.3.1 shows a correct path (solid line) and a set of possible error paths (dotted lines) in a trellis. The code length is l (l time units), and the code is always assumed to start at the all-zero state and terminate also at the all-zero state. The error event probability, $\overline{P}_e$, is an averaged probability of error paths per time unit. The average is taken over all possible correct paths. Thus, $\overline{P}_e$ is bounded by the following union bound

$$\overline{P}_e \leq \sum_c p(c) P\left(\bigcup_i e_i | c\right) \tag{3.1.1}$$

where $p(c)$ is the probability that the encoder chooses path c, and e_i is the ith error path departing from the correct path c in a time unit.

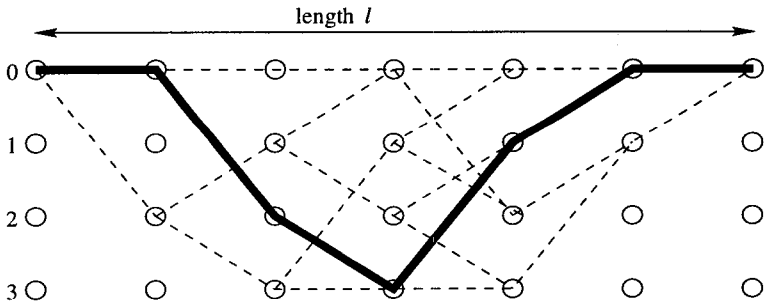

Figure 3.1: The correct path and a set of possible error paths.

The upper bound of the error probability is evaluated in [119, 17]. Let $\mathcal{D}$ denote the set of all possible squared Euclidean distances between the signals on two different paths in the trellis code. We count how often each of the distances d occurs, and denote A_{d^2} the average number of times the distance d occurs, which is named the *average multiplicity* of d. The error probability is upper bounded by

$$\overline{P}_e \leq \sum_{d^2 \in \mathcal{D}} A_{d^2} Q\left(\sqrt{d^2 \frac{RE_b}{2N_0}}\right) \tag{3.1.2}$$

where $R = K/N$ is the code rate, E_b is the energy per information bit, and N_0 is the one-sided noise power spectral density. The smallest d found in the trellis is called the *free Euclidean distance*, d_{free}, or *free distance* for short.

The information bit error probability (BER) associated with the code can also be similarly treated. Each error event $c \to e_i$ will cause a certain number of information bit errors. We count the averaged number of information bit errors, B_{d^2}, on all error paths with distance d. The average is taken over all possible correct paths c. If A_{d^2} in equation (3.1.2) is replaced by B_{d^2}, we obtain a bound on the information bit errors per time unit. Since an (N, K) trellis code processes K information bits per time unit, the average bit error probability is bounded by (see [119]),

$$\overline{P}_b \leq \sum_{d^2 \in \mathcal{D}} \frac{1}{K} B_{d^2} Q\left(\sqrt{d^2 \frac{RE_b}{2N_0}}\right). \tag{3.1.3}$$

The infinite set of triplets $\{d^2, A_{d^2}, B_{d^2}\}$ is called the *distance spectrum* of the trellis code. Each triplet $\{d^2, A_{d^2}, B_{d^2}\}$ in the distance spectrum is called a *spectrum line.*

The lower bound of the error probability is determined by d^2_{free} [17],

$$\begin{aligned} \overline{P}_e &\geq A_{d^2_{free}} Q\left(\sqrt{d^2_{free} \frac{RE_b}{2N_0}}\right), \\ \overline{P}_b &\geq \frac{1}{K} B_{d^2_{free}} Q\left(\sqrt{d^2_{free} \frac{RE_b}{2N_0}}\right). \end{aligned}$$

Algorithms have been presented for computing the distance spectrum,

$$\{d^2, A_{d^2}, B_{d^2}\},$$

for trellis coded modulation (TCM) with some special properties, such as the quasiregularity in [112].

Since MC are also trellis codes with Euclidean distances, the above performance bounds apply directly to MC. In a time unit, K symbols are input to an MC encoder, i.e., $Klog_2M$ bits. The bounds of bit error probability for MC are

$$\overline{P}_b \leq \sum_{d^2 \in \mathcal{D}} \frac{1}{Klog_2M} B_{d^2} Q\left(\sqrt{d^2 \frac{RE_b}{2N_0}}\right), \tag{3.1.4}$$

$$\overline{P}_b \geq \frac{1}{Klog_2M} B_{d^2_{free}} Q\left(\sqrt{d^2_{free} \frac{RE_b}{2N_0}}\right). \tag{3.1.5}$$

A method to compute the distance spectrum for an MC is presented in the following section.

3.2 A Method for Computing the Distance Spectrum of Modulated Codes

Let us first review the method for distance spectrum computation for trellis codes. It has been mentioned in [9, 112] that distance spectrum of a trellis code can be computed from a trellis error diagram, which corresponds to the error-pattern trellis for an MC later. However, there are two main reasons that finite-field-defined trellis codes (e.g., TCM) usually do not use the trellis error diagram in distance spectrum computation. First, for regular trellis codes, the set of distances of incorrect paths from a correct path does not depend on the correct path, and hence the distance spectrum can be calculated by assuming that a specific information sequence, e.g., the all-zero information sequence, was sent [138, 67]. Therefore, the distance spectrum can be computed from the trellis code's own trellis and it is not necessary to build a trellis error diagram. Second, for non-regular trellis codes, e.g., quasiregular trellis codes, all correct paths do not contribute the same to the distances. Thus, we have to consider all correct paths to compute a precise distance spectrum. A solution is to build trellis error diagrams. However, due to the nonlinear binary-to-complex mapping, there is no unique trellis error diagram from which a precise distance spectrum can be computed. In other words, a set of trellis error diagrams have to be built and the distances must be averaged over all these diagrams, which may be too complicated in practice. As an approximation approach, Rouanne [112] has shown that the worst case distance spectrum of quasiregular codes can be computed by first assuming that the all-zero information sequence was sent, and then following the method for regular trellis codes. The BER bound computed from the worst case distance spectrum is clearly a looser upper bound than the one in equation (3.1.3).

We note that an MC is a nonlinear code, i.e., the sum of any two codewords may not be a codeword. A consequence of the nonlinearity is that there does not exist any all-zero path in an MC trellis. Furthermore, correct paths give different contributions to the distances (see details in Section 3.2.1). Thus, trellis error diagrams must be built to compute the precise distance spectrum. Although an MC is nonlinear in terms of finite symbol input information sequences, i.e., the codewords, it is linear when all the input sequences are treated as arbitrary complex-valued, i.e., the MC encoding operation is the complex matrix-vector multiplication. This special property of an MC implies that the distances can be computed from a unique trellis error diagram, the *error-pattern trellis*, by applying the generator matrix $\mathbf{G}(z)$ directly to the *error sequences* along the paths in the trellis. The error-pattern trellis represents the multiplicity A_{d^2} and

B_{d^2} averaged over all correct paths in the MC trellis. Thus, the precise distance spectrum can be obtained by using some searching algorithms on the error-pattern trellis, e.g., the bidirectional stack algorithm [112, 67], and the tight BER upper bound in equation (3.1.4) can be computed. In the next subsection, we present a method to build up such an error-pattern trellis.

3.2.1 Error-Pattern Trellis

First, let us define an error-pattern trellis. The difference between any two information symbols (with total M symbols) is called an *error symbol*. Let M_e denote the number of all different error symbols including error symbol "0". In each time unit n, K symbols are input to the MC encoder with a generator matrix $\mathbf{G}(z)$. These K symbols are called an *input vector*, i.e., $X(n)$. There are M^K different possible input vectors. The difference between two input vectors, $U(n) \triangleq X_1(n) - X_2(n)$, is defined as a *branch error pattern*. The number of all possible branch error patterns is M_e^K. The *error-pattern trellis* associated with the MC $\mathbf{G}(z)$ (or simply error-pattern trellis) is defined as the trellis with K error symbols as the input and $\mathbf{G}(z)$ as the generator matrix. Note that the number of states of the error-pattern trellis is M_e^ν, while the one of the original MC trellis is M^ν, where ν is the constraint length of the MC. For each state in the error-pattern trellis, there are M_e^K branches entering it and also M_e^K branches leaving it.

Let us see the following example. We assume an MC with $K = 2, N = 4$, constraint length $\nu = 2$ and the generator matrix $\mathbf{G}(z)$ as follows:

$$\mathbf{G}(z) = \begin{bmatrix} -0.4695 & 0.1720 \\ -0.4044 & 0.6677 \\ 1.0321 & 0.2742 \\ 1.0840 & -1.1829 \end{bmatrix} + z^{-1} \begin{bmatrix} -0.3806 & -0.9119 \\ -0.6796 & 0.5152 \\ -0.1820 & 0.4657 \\ 0 & 0 \end{bmatrix}. \quad (3.2.1)$$

BPSK signal set $\{1, -1\}$ is used as the information symbols. Fig.3.2 shows the trellis of the code $\mathbf{G}(z)$. There are four branches leaving each state and another four entering it. If binary "0" mapped to BPSK symbol "1" and binary "1" mapped to "-1", the four branches leaving each state correspond to input symbol vectors {1,1},{1,-1},{-1,1},{-1-1}, respectively. If these four input vectors occur at the encoder with equal probability $1/S$, where $S = M^K$ is the number of input vectors, any path with length l in the trellis occurs with a probability of $1/S^l$. In this example, $S = 4$.

Given the generator matrix $\mathbf{G}(z)$, if two different input vector sequences are $\{X_1(n)\}_{n=0}^{l}$ and $\{X_2(n)\}_{n=0}^{l}$ and their output vector sequences are

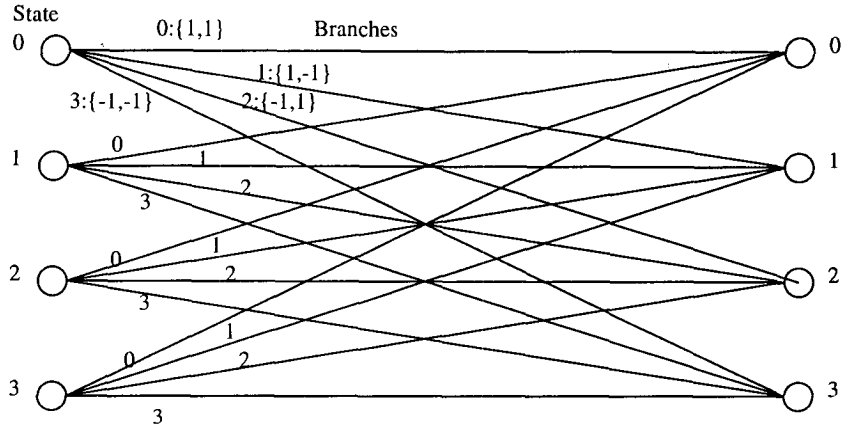

Figure 3.2: The trellis of a modulated code.

$\{Y_1(n)\}_{n=0}^{l}$ and $\{Y_2(n)\}_{n=0}^{l}$, respectively, due to the linearity of the MC encoding operation, the distance between the two output sequences, $d(Y_1, Y_2)$, is determined only by $\{U(n)\}_{n=0}^{l} = \{X_1(n) - X_2(n)\}_{n=0}^{l}$ (see (2.2.4)). Therefore, by exploring all the possible patterns of $U(n)$, the distance set can be determined.

We form the branch error patterns by computing all possible values of $U(n) = X_1(n) - X_2(n)$. Table 3.1 shows the possible branch error patterns. There are total $M_e = 3$ error symbols: $\{0, 2, -2\}$, and they form $M_e^K = 9$ branch error patterns. One can see that the error pattens in Table 3.1 occur with different frequencies. Some patterns are more likely to occur, and some patterns are less likely. We name the frequencies of these occurrences the *weights*, a, of the error patterns, as listed in Table 3.2. Table 3.2 also lists the number, b, of information bit errors associated with each branch error pattern. Similar tables for other signal alphabets can be found in [75].

Table 3.1: Possible branch error patterns.

error input vector $X_2(n)$	correct input vector $X_1(n)$			
	1, 1	1, -1	-1, 1	-1, -1
1, 1	0, 0	0, -2	-2, 0	-2, -2
1, -1	0, 2	0, 0	-2, 2	-2, 0
-1, 1	2, 0	2, -2	0, 0	0, -2
-1, -1	2, 2	2, 0	0, 2	0, 0

Table 3.2: Weights and bit-error numbers of error patterns.

branch error pattern	weight (a)	bit-error number (b)
0, 0	4	0
0, 2	2	1
2, 0	2	1
0, -2	2	1
-2, 0	2	1
2, 2	1	2
2, -2	1	2
-2, 2	1	2
-2, -2	1	2

Note that, for a particular correct path c, only some of the error patterns in Table 3.1 may occur. For example, if we consider a correct path with input $x(n) = (1, 1, 1, 1, \ldots)$, only the branch error patterns in the second column of Table 3.1 occur. In order to obtain the complete distance spectrum, we must consider all correct paths in the trellis. Therefore, we label the error-pattern trellis with the weight a's and bit-error numbers b's listed in Table 3.1.

Fig.3.3 shows the error-pattern trellis. The state number is $M_e^{\nu} = 9$, state 0 conrresponds to the error symbols {0,0} in memory, state 1 to {0,2}, state 2 to {0,-2} and so on. Fig.3.3 only shows 9 branches, but actually for each state, there are $M_e^K = 9$ branches leaving it and 9 branches entering it.

The branches are labelled with their branch error patterns (taken as input vectors), as well as their weight a's and bit-error numbers b's as (a, b). A path p in the error-pattern trellis is called an *absolute error path.* When applying generator matrix $\mathbf{G}(z)$ to the input sequence on such a path p, as shown in equation (2.2.4), we obtain a distance triplet of $\{d^2, A_{d^2}^p, B_{d^2}^p\}$ (superscript p denotes path p). The computation of $\{A_{d^2}^p, B_{d^2}^p\}$ is straightforward [108, 112, 115]. The number $A_{d^2}^p$ is the product of the l weights a_i, $i = 1, 2, \ldots, l$, along the l branches of the path p and then divided by S^l, and $B_{d^2}^p$ is $A_{d^2}^p$ times the sum of the l bit-error numbers b_i, $i = 1, 2, \ldots, l$,

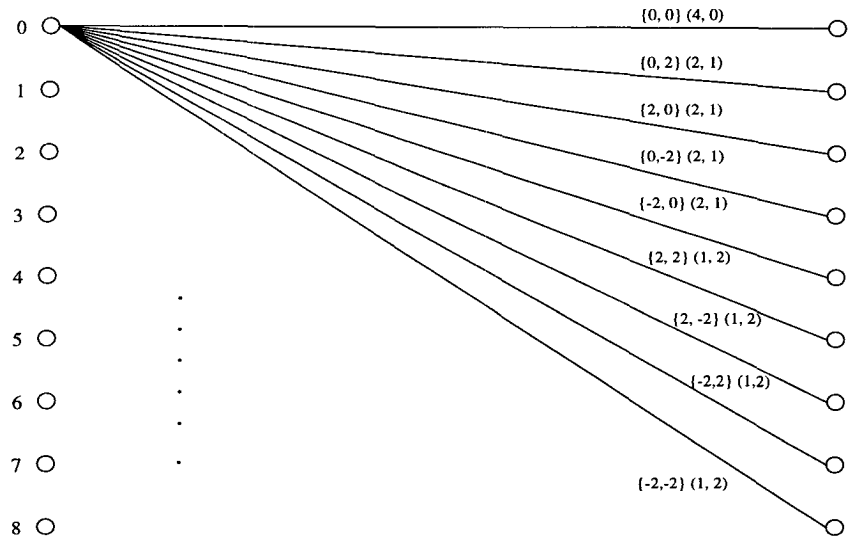

Figure 3.3: The error-pattern trellis.

along its l branches, i.e.,

$$A_{d^2}^p = \frac{1}{S^l} \prod_{i=1}^{l} a_i, \tag{3.2.2}$$

$$B_{d^2}^p = A_{d^2}^p \sum_{i=1}^{l} b_i. \tag{3.2.3}$$

From the definition of an error-pattern trellis, it is not hard to see the following Lemma.

Lemma 3.1 *An absolute error path in an error-pattern trellis can be decomposed into $\prod_{i=1}^{l} a_i$ different pairs of correct paths c and error paths e. All of the pairs in the decomposition have the same Euclidean distance and the same number of bit errors.*

The possibility of each correct path is $1/S^l$. Therefore, the absolute error path p contributes $A_{d^2}^p = \frac{1}{S^l} \prod_{i=1}^{l} a_i$ to the multiplicity of the distance d. For example, the absolute error path with input $(U(n)) = (\{2,0\}, \{-2,-2\})$ can be decomposed into 2 pairs of correct paths and error paths: a correct path with input

$$(X(n)) = (\{1,1\}, \{-1,-1\})$$

and an error path with input

$$(\hat{X}(n)) = (\{-1, 1\}, \{1, 1\}),$$

or a correct path with

$$(X(n)) = (\{1, -1\}, \{-1, -1\})$$

and an error path with

$$(\hat{X}(n)) = (\{-1, -1\}, \{1, 1\}).$$

The number $B_{d^2}^p$, following its definition, is the averaged bit-error number of the $\prod_{i=1}^{l} a_i$ pairs over all possible correct paths. Since each pair occurs with the probability of $1/S^l$ and has the bit-error number of $\sum_{i=1}^{l} b_i$, the averaged value is

$$B_{d^2}^p = \sum_{m=1}^{P_{total}} \frac{1}{S^l} \sum_{i=1}^{l} b_i = \prod_{i=1}^{l} a_i \frac{1}{S^l} \sum_{i=1}^{l} b_i \tag{3.2.4}$$

$$= A_{d^2}^p \sum_{i=1}^{l} b_i \tag{3.2.5}$$

$$= A_{d^2}^p \; b^p, \tag{3.2.6}$$

where P_{total} is the total number of pairs decomposed from an absolute error path, and b^p is the bit-error number of each pair, or the bit-error number along the absolute error path p, i.e.,

$$P_{total} = \prod_{i=1}^{l} a_i, \tag{3.2.7}$$

$$b^p = \sum_{i=1}^{l} b_i. \tag{3.2.8}$$

3.2.2 Distance Spectrum and Bidirectional Searching Algorithm

With the error-pattern trellis, the distance spectrum $\{d^2, A_{d^2}, B_{d^2}\}$ for an MC can be easily computed by following the bidirectional stack algorithm, which was presented in [112, 67] for quasiregular trellis code. The detailed bidirectional distance spectrum calculation algorithm is as follows.

The searching algorithm on an MC error-pattern trellis is based on a bidirectional stack algorithm for TCM in [112]. The algorithm extends paths forward and backward along the error-pattern trellis simultaneously.

A *forward path* leaves the all-zero state in the forward direction and reaches a non-zero state. A *backward path* leaves the all-zero state in the backward direction and reaches a non-zero state. Once a path has remerged with the all-zero path, it is discarded. If a forward path and a backward path reach the same state, we say that the forward path merges with the backward path, or a merger occurs, and a distance d occurs.

A path is determined by the following information.

- fw: forward or bw: backward – direction
- s – terminal state
- l – length
- d – distance
- A – multiplicity
- B – number of bit errors.

The *terminal state* s is the last state reached by a path of *length* l (l branches from the all-zero state for an *fw* path, or l branches to the all-zero state for a *bw* path). A is the product of the weights a_i, $i = 1, 2, \ldots, l$ along l branches, i.e., $A = \prod_{i=1}^{l} a_i$. B is the sum of bit-error numbers b_i, $i = 1, 2, \ldots, l$ along l branches, i.e., $B = \sum_{i=1}^{l} b_i$. The squared distance d^2 is computed by:

1. applying $\mathbf{G}(z)$ to the input sequence $(U(n))$ on the path, and obtaining the output sequence $(W(n)) =$

$$(\{w_1(1), w_2(1), \ldots, w_N(1)\}, \{w_1(2), w_2(2), \ldots, w_N(2)\}, \ldots,$$
$$\{w_1(l), w_2(l), \ldots, w_N(l)\}).$$

2. letting $d^2 = \sum_{i=1}^{l} \sum_{n=1}^{N} w_n^2(i)$.

Two paths are *identical* if and only if they have the same direction, terminal state s, length l and distance d. *Two stacks* are used for storing the information of paths, one for each direction. Each entry in the stack contains a path with all its information. All paths are ordered from the stack top by the order of increasing distances. So the top path in the stack is the most likely to give the free distance. We also have a table that stores the temporary spectrum lines $\{d^2, A_{d^2}, B_{d^2}\}$ by the order of increasing distances.

The algorithm is described as the following steps.

1. Load the forward and backward stacks with the origin node $s = 0$, with squared distance $d^2 = 0$, length $l = 0$, and $A = 1$, $B = 0$.

2. Extend the top path in forward stack by computing its M_e^K successors. For each successor, if it reaches all-zero state, it is discarded; otherwise, compute its l, d^2, A and B. If the top path has l_t, d_t^2, A_t and B_t, then the squared distance d^2, the length l, the multiplicity A and the bit-error number B of a successor are

$$l = l_t + 1, \tag{3.2.9}$$

$$d^2 = d_t^2 + \sum_{n=1}^{N} v_l^2(n), \tag{3.2.10}$$

$$A = A_t \times a_l, \tag{3.2.11}$$

$$B = B_t + b_l, \tag{3.2.12}$$

where $\{v_l(1), v_l(2), \ldots, v_l(N)\}$, a_l and b_l are, respectively, the output symbols, weight and bit-error number on the lth branch of the successor.

3. Delete the top path from the stack.

4. For each successor, check its information with the paths in forward and backward stacks. Three situations may occur as follows.

   (a) The successor is not identical to any forward path. Then, create a new entry in the forward stack to store the successor as a new path and its information.

   (b) The successor is identical to a forward path. Then, update the information of the identical path by

$$A_{new} = A_{old} + A \tag{3.2.13}$$

$$B_{new} = \frac{A_{old} \times B_{old} + A \times B}{A_{old} + A} \tag{3.2.14}$$

   where A_{old}, B_{old} are the old information of the identical path in the forward stack, and A_{new}, B_{new} are the updated information in the stack, respectively. Note that although the paths are identical (same direction, s, l and d^2), they may have different multiplicity and bit-error number. So B is the number of bit errors averaged over the total multiplicities of all identical paths.

   (c) The state s is the terminal state of one or more backward paths in the backward stack. Thus, the successor is merged with these

backward paths, and one or more distance pairs are achieved. Let d^2_{fw}, l_{fw}, A_{fw} and B_{fw} denote the squared distance, the length, the multiplicity and the bit-error number computed in step (b) of the successor, and d^2_{bw}, l_{bw}, A_{bw} and B_{bw} denote the ones in the backward stack of a backward path that merges with the successor, respectively. Thus, the squared distance, d^2_{merger}, the length, l_{merger}, the multiplicity, A_{merger}, and the bit-error number, B_{merger}, of the merger are computed by

$$d^2_{merger} = d^2_{fw} + d^2_{bw} \tag{3.2.15}$$

$$l_{merger} = l_{fw} + l_{bw} \tag{3.2.16}$$

$$A_{merger} = A_{fw} \times A_{bw} \tag{3.2.17}$$

$$B_{merger} = B_{fw} + B_{bw} \tag{3.2.18}$$

Following equations (3.2.2)-(3.2.8) and Lemma 3.1 in Section 3.2.1, the multiplicity and bit-error number, denoted by

$$A(d^2_{merger}) \text{ and } B(d^2_{merger}),$$

respectively, are what the merger contributes to the spectrum line for the squared distance $d^2 = d^2_{merger}$. They can be computed via

$$A(d^2_{merger}) = \frac{A_{merger}}{S^{l_{merger}}}, \tag{3.2.19}$$

$$B(d^2_{merger}) = B_{merger} \times A(d^2_{merger}). \tag{3.2.20}$$

If an entry with squared distance $d^2 = d^2_{merger}$ has existed in the table of the temporary spectrum lines, we increase the values of its multiplicity and bit-error number, $\{A_{d^2}, B_{d^2}\}$, by

$$\{A(d^2_{merger}), B(d^2_{merger})\};$$

If an entry with such a distance has not existed, we create a new entry of $\{d^2_{merger}, A(d^2_{merger}), B(d^2_{merger})\}$ in the table.

5. Rearrange the forward stack and the table of the spectrum lines in the order of increasing distance.

6. Output all the spectrum lines in the table whose distances are smaller than the sum of the minimum forward and backward distances. These spectrum lines are "mature" since their values of $\{A_{d^2}, B_{d^2}\}$ will not be increased any more. After the output, these spectrum lines are erased from the table of the temporary spectrum lines.

7. Change to the backward direction and repeat steps 2–6: extending the top backward path by its M_e^K successors, check their merging information etc. Keep on changing the directions and repeating steps 2–6 until the desired number of spectral lines have been output, then stop.

Fig.3.4 shows the distance spectrum (the first 50 spectral lines) of the MC $\mathbf{G}(z)$ in the example. In this case, d_{free}^2 is 13.0555. Fig.3.5 shows a comparison of the computer simulation results we performed with the performance bounds computed from the spectra of the MC $\mathbf{G}(z)$. An AWGN channel is used.

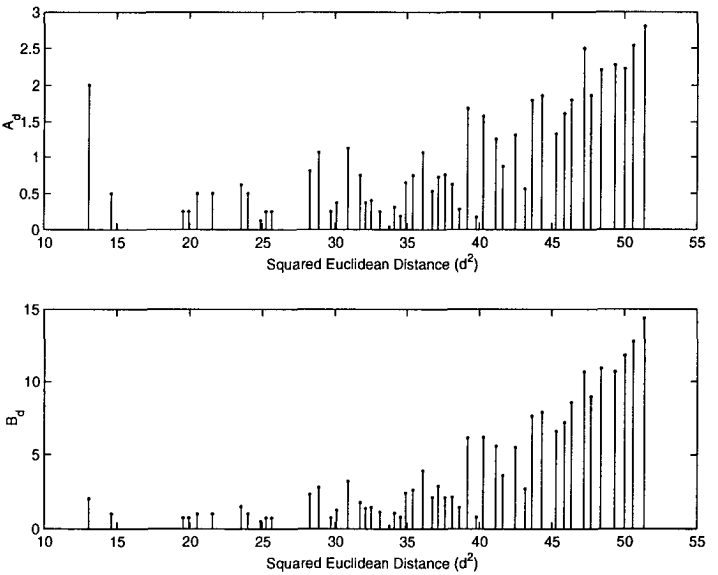

Figure 3.4: Distance spectrum of the MC $\mathbf{G}(z)$.

3.3 Simulation Examples

In this section, we study the optimal modulated codes searched for the ISI channel

$$h = [0.5000, 0.5000, -0.5000, -0.5000].$$

It should be emphasized that the ISI channel can be arbitrary and the above example is purely for convenience. Due to the high complexity in

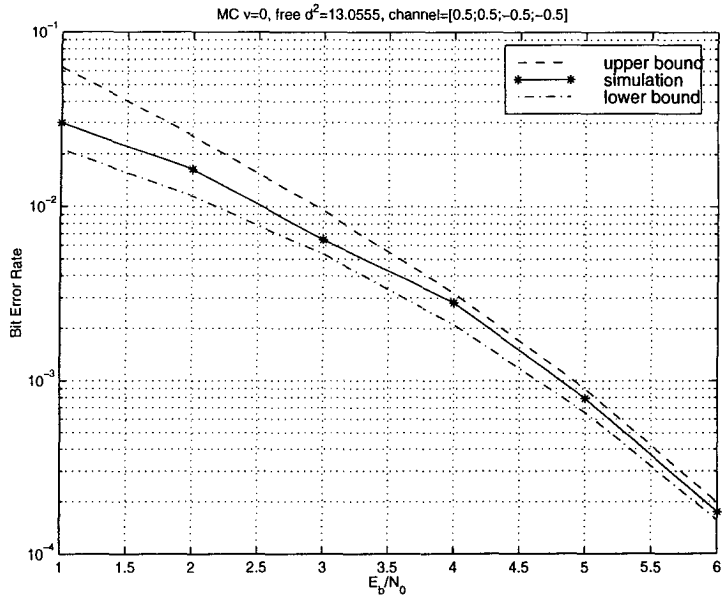

Figure 3.5: BER of the MC $\mathbf{G}(z)$ on AWGN.

searching for good MC with long constraint lengths, we only consider MC with the constraint lengths of $\nu = 0, 1$, respectively. The distance spectrum, simulated BER performances and BER bounds are also shown. The performance comparison with the optimal binary convolutional code on the same channel is presented.

Let $\mathbf{C}(z)$ with $K = 2$ and $N = 4$ be the combined generator matrix as shown in (2.3.2) of an MC $\mathbf{G}(z)$ and the channel h. The generator matrix $\mathbf{C}(z)$ produces another MC. The performance of the MC $\mathbf{G}(z)$ with the ISI channel is the same as the performance of the MC $\mathbf{C}(z)$ with an AWGN channel, and thus is lower bounded by the free distance of the MC $\mathbf{C}(z)$. Therefore, we search for an optimal matrix $\mathbf{G}(z)$ that maximizes the free distance of the corresponding $\mathbf{C}(z)$. Random searching[1] is performed, and suboptimal matrices $\mathbf{G}(z)$ for the ISI channel with constraint lengths $\nu = 0, 1$ are as follows. The combined matrices $\mathbf{C}(z)$ associated with $\mathbf{G}(z)$ and their free distances are also shown below.

[1] An optimal MC searching algorihtm will be presented later.

The case of $\nu = 0$, i.e., block MC:

$$\mathbf{G}_0(z) = \begin{bmatrix} -0.9390 & 0.3440 \\ 0.1302 & 0.9915 \\ 0.9951 & -0.0990 \\ 0.3641 & -0.9314 \end{bmatrix},$$

$$\mathbf{C}_0(z) = \begin{bmatrix} -0.4695 & 0.1720 \\ -0.4044 & 0.6677 \\ 1.0321 & 0.2742 \\ 1.0840 & -1.1829 \end{bmatrix} + z^{-1} \begin{bmatrix} -0.3806 & -0.9119 \\ -0.6796 & 0.5152 \\ -0.1820 & 0.4657 \\ 0 & 0 \end{bmatrix},$$

$$d^2_{free}(\mathbf{C_0}) = 13.0555.$$

The coding gain in this case is

$$\gamma_{ISI,0} = \frac{13.055}{8} = 2.127\text{dB}.$$

The case of $\nu = 1$:

$$\mathbf{G}_1(z) = \begin{bmatrix} 0.0432 & 0.7248 \\ -0.2061 & 0.9041 \\ -0.1953 & -0.6854 \\ 0.8042 & -0.5756 \end{bmatrix} + z^{-1} \begin{bmatrix} 0.6876 & 0 \\ -0.3742 & 0 \\ -0.7015 & 0 \\ -0.1481 & 0 \end{bmatrix},$$

$$\mathbf{C}_1(z) = \begin{bmatrix} 0.0216 & 0.3624 \\ -0.0814 & 0.8145 \\ -0.2223 & -0.2530 \\ 0.3859 & -1.4450 \end{bmatrix} + z^{-1} \begin{bmatrix} 0.9466 & -0.3972 \\ -0.1478 & 0.6305 \\ -1.2838 & 0.2878 \\ -0.5815 & 0 \end{bmatrix}$$

$$+ z^{-2} \begin{bmatrix} 0.4638 & 0 \\ 0.4248 & 0 \\ 0.0740 & 0 \\ 0 & 0 \end{bmatrix},$$

$$d^2_{free}(\mathbf{C_1}) = 14.0422.$$

The coding gain in this case is

$$\gamma_{ISI,1} = \frac{14.0422}{8} = 2.4435\text{dB}.$$

Note that the above codes $\mathbf{C}_i(z)$ are obtained by numerous computer searches, which may not be the optimal ones for the channel h as we will see later. The distance spectrum of the combined code $\mathbf{C}_0(z)$ is the same one as shown in Fig.3.4. Its BER performance and bounds are also shown

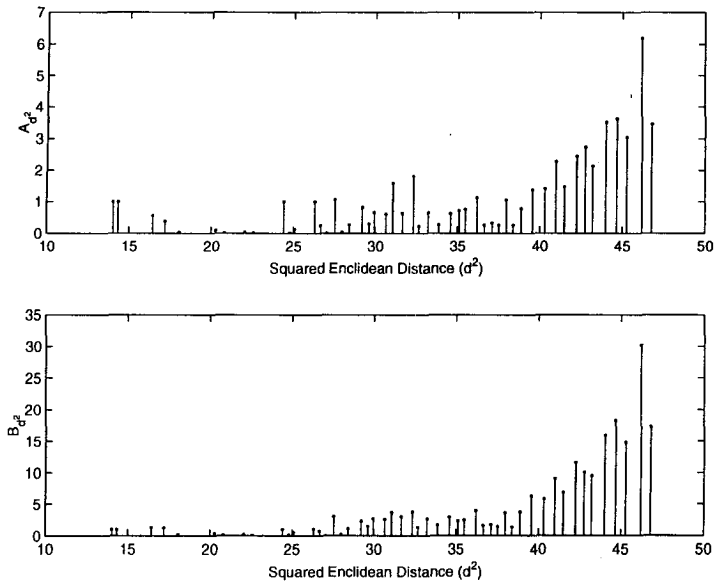

Figure 3.6: Distance spectrum of the MC $\mathbf{C}_1(z)$.

in Fig.3.5. The distance spectrum, BER performance and bounds of the code $\mathbf{C}_1(z)$ are shown in Fig.3.6 and Fig.3.7, respectively.

The optimal binary convolutional codes (CC) with $K = 2$ and $N = 4$ for the ISI channel h with constraint length $\nu = 0$ or 1 are also searched by maximizing the free distance of the combined codes of the CC and the ISI channel. The BPSK symbols $\{1, -1\}$ are used after the CC. The optimal CC we obtained after searching and the maximum free distances of their combined codes are listed below. Their BER performances are compared with the optimal MC in Fig.3.8. The figure also shows the performances of uncoded BPSK on an AWGN channel and the rate 1/2 CC on the ISI channel with the following generator matrix $\mathbf{G}_3(\mathrm{D})$. The CC $\mathbf{G}_3(D)$ has constraint length $\nu = 3$ and its free distance is optimal for an AWGN channel. In the above simulations, all the decoding algorithms are the joint maximum likelihood decoding MC or CC with the ISI channel. In Fig.3.8, the BER vs. E_b/N_0 curves are shown for uncoded BPSK on AWGN channel marked by dashed line; the channel independent CC $\mathbf{G}_3(D)$ marked by $\times$; the optimal binary CC $\mathbf{G}_0(D)$ marked by $\circ$; optimal binary CC $\mathbf{G}_1(D)$ marked by $*$; the MC $\mathbf{G}_0(z)$ marked by $\triangle$; and the MC $\mathbf{G}_1(z)$ marked by $\square$.

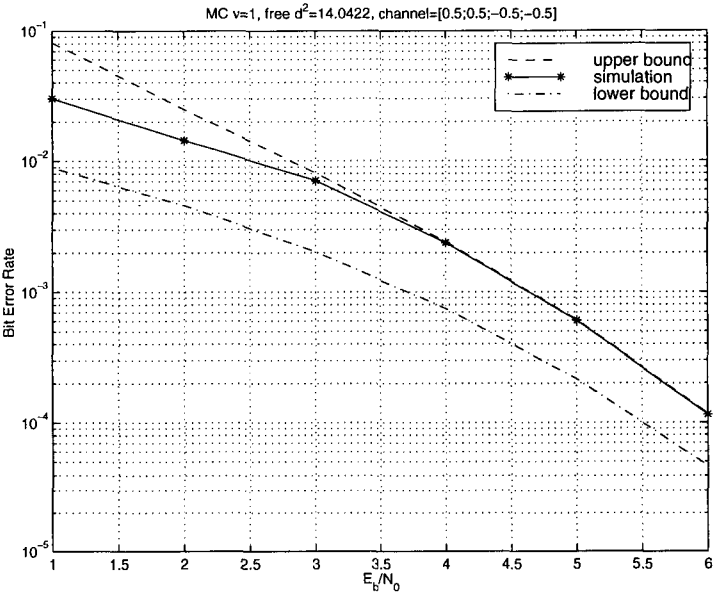

Figure 3.7: BER performance of the MC $\mathbf{C}_1(z)$.

$$
\begin{aligned}
\mathbf{G}_0(D) &= \begin{bmatrix} 1 & 1 \\ 0 & 1 \\ 1 & 0 \\ 1 & 0 \end{bmatrix}, \\
d^2_{free}(\mathbf{C}_0) &= 6.0000, \\
\mathbf{G}_1(D) &= \begin{bmatrix} 1 & 0 \\ 1 & 0 \\ 0 & 1 \\ 0 & 1 \end{bmatrix} + D \begin{bmatrix} 0 & 0 \\ 1 & 0 \\ 0 & 0 \\ 0 & 0 \end{bmatrix}, \\
d^2_{free}(\mathbf{C}_1) &= 10,
\end{aligned}
$$

$$
\mathbf{G}_3(D) = \begin{bmatrix} 1 \\ 1 \end{bmatrix} + D \begin{bmatrix} 1 \\ 1 \end{bmatrix} + D^2 \begin{bmatrix} 0 \\ 1 \end{bmatrix} + D^3 \begin{bmatrix} 1 \\ 1 \end{bmatrix}
$$

where D denotes the delay variable.

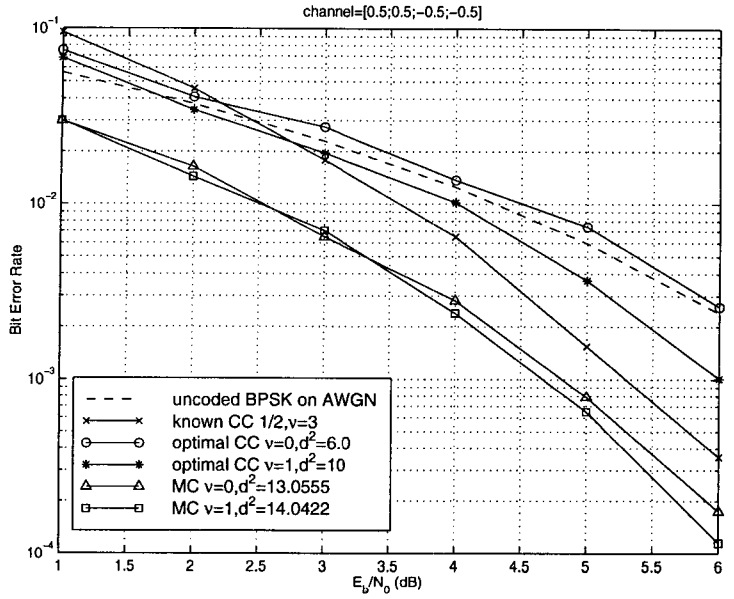

Figure 3.8: BER performance comparison of MC and CC codes on the ISI channel.

3.4 An Algorithm for Searching the Optimal MC Given an ISI Channel

In the previous section, we presented an efficient algorithm to calculate the distance spectrum for a combined MC $\mathbf{C}(z)$. In this section, we present an efficient algorithm to search the optimal MC $\mathbf{G}(z)$ of a given size for a given ISI channel such that the free distance of the combined MC $\mathbf{C}(z)$ is maximal. For convenience, in this section all coefficients are considered real valued.

In what follows, the ISI channel $H(z)$ of $\Gamma+1$ taps is fixed and the size of the combined MC is also fixed, where an (N, K) MC encoder $\mathbf{G}(z)$ of order Q_G is used and the constraint length ν of the combined $\mathbf{C}(z)$ is thus fixed to

$$\nu = \nu_1 K, \quad \text{where } \nu_1 = \lceil \frac{\Gamma}{N} \rceil + Q_G. \tag{3.4.1}$$

In other words, the error-pattern trellis diagram is fixed, i.e., the input patterns are fixed while the outputs on the trellis depend on a particular

MC encoder $\mathbf{G}(z)$. For a given $\mathbf{G}(z)$, the bidirectional searching algorithm presented in Section 3.2 is used to find the free distance $d_{free,\mathbf{C}}$ of $\mathbf{C}(z)$, which is the minimal norm among the output sequences of all the nonzero paths in the error-pattern trellis. Since the MC encoding is over the real field, the norms of the output sequences on the paths can be calculated as follows.

Similar to Section 3.2, $\{U(n)\}$ denotes a difference sequence of two different input signal sequences $\{X_1(n)\}$ and $\{X_2(n)\}$, which corresponds to a path or input sequence in the error-pattern trellis. The norm of the output sequence $\{W(n)\}$ on this path is

$$\sqrt{\sum_n \|W(n)\|^2} = \|\mathbf{W}(z)\|_F = \|\mathbf{C}(z)\mathbf{U}(z)\|_F, \tag{3.4.2}$$

where $\mathbf{W}(z) = \mathbf{C}(z)\mathbf{U}(z)$. Therefore,

$$d^2_{free,\mathbf{C}} = \min_{U\neq 0} \sum_n \|W(n)\|^2 = \min_{U\neq 0} \|\mathbf{C}(z)\mathbf{U}(z)\|^2_F. \tag{3.4.3}$$

We next want to express the output sequence norm in (3.4.2) in terms of the coefficients in an MC encoder $\mathbf{G}(z)$ and an input path $\{U(n)\}$. For convenience, let us first consider it in the z-transform domain.

Let $\mathbf{G}(z) = (g_{ij}(z))$ and $\mathbf{g}_i(z) = [g_{i1}(z), \cdots, g_{iK}(z)]^T$. Then,

$$\mathbf{W}(z) = \mathbf{H}(z) \begin{bmatrix} (\mathbf{U}(z))^T & 0 & \cdots & 0 \\ 0 & (\mathbf{U}(z))^T & \cdots & 0 \\ \cdots & \cdots & \cdots & \cdots \\ 0 & 0 & \cdots & (\mathbf{U}(z))^T \end{bmatrix} \begin{bmatrix} \mathbf{g}_1(z) \\ \mathbf{g}_2(z) \\ \vdots \\ \mathbf{g}_N(z) \end{bmatrix}. \tag{3.4.4}$$

Let $\mathcal{W} = [\cdots, W^T(n-1), W^T(n), \cdots]^T$ be the sequence vector of the output $\mathbf{W}(z)$ with the input $\mathbf{U}(z)$. Then equation (3.4.4) tells us that

$$\mathcal{W} = \mathcal{A}(U)\mathcal{G}, \tag{3.4.5}$$

where $\mathcal{G}$ is a $(KN(Q_G+1))\times 1$ column vector formed from all the coefficients of total number $KN(Q_G+1)$ of $\mathbf{g}_i(z)$ since each $g_{ij}(z)$ has order/degree Q_G, and $\mathcal{A}(U)$ is a constant matrix formed from the coefficients of $\mathbf{H}(z)$ and $\mathbf{U}(z)$. Therefore, the squared norm of the output sequence $\{W(n)\}$ is

$$\|\mathcal{W}\|^2 = \mathcal{G}^T\mathcal{A}^T(U)\mathcal{A}(U)\mathcal{G}, \tag{3.4.6}$$

which is a quadratic form of $\mathcal{G}$. If a path or an input sequence $\{U(n)\}$ repeats a non-all-zero state, i.e., there exists $n_2 \neq n_1$ such that

$$s = [U^T(n_2+1), \cdots, U^T(n_2+\nu_1)] = [U^T(n_1+1), \cdots, U^T(n_1+\nu_1)] \neq \mathbf{0}, \tag{3.4.7}$$

then there always exists another shorter path $\{U_1(n)\}$ such that the norm of its corresponding path output sequence $\{W_1(n)\}$ is the same or smaller, where $\{U_1(n)\}$ is simply obtained by cutting the segment between the same state. This means that the path $\{U(n)\}$ can be ignored or deleted in the free distance calculation. Therefore, to consider the free distance all the paths that have repeated non-all-zero states can be excluded. The *length* of a path $\{U(n)\}$ is defined as $l = n_2 - n_1$, where $U(n)$ for $n \leq n_1$ and $n \geq n_2$ are the all-zero state, i.e., $U(n) = 0$ for $n < n_1 + \nu_1$ and $n > n_2 - \nu_1$, and it does not reach the all-zero state in the middle, i.e.,

$$[U^T(n+1), \cdots, U^T(n+\nu_1)] \neq \mathbf{0}, \quad \text{for} \quad n_1 \leq n < n_2 - \nu_1.$$

Let $\mathcal{P}$ denote all the paths $\{U(n)\}$ of length $M_e^\nu + 1$, where ν is the constraint length of the error-pattern trellis and defined in (3.4.1). Clearly, the set $\mathcal{P}$ has a finite number of paths. Note that there are total M_e^ν states and each state has M_e^K paths joining in and M_e^K paths going out. By the above non-repeating state argument we have

$$d^2_{free,\mathbf{C}} = \min_{0 \neq U \in \mathcal{P}} \sum_n \|W(n)\|^2 = \min_{0 \neq U \in \mathcal{P}} \mathcal{G}^T \mathcal{A}^T(U)\mathcal{A}(U)\mathcal{G}. \tag{3.4.8}$$

Therefore, the optimal (N, K) MC $\mathbf{G}_{opt}(z)$ of order Q_G with the coefficient vector $\mathcal{G}_{opt}$ is

$$\mathcal{G}_{opt} = \arg \max_{\mathcal{G}} \{ \min_{0 \neq U \in \mathcal{P}} \mathcal{G}^T \mathcal{A}^T(U)\mathcal{A}(U)\mathcal{G} : \ \|\mathcal{G}\|^2 = N \}, \tag{3.4.9}$$

where $\|\mathcal{G}\|^2 = N$ is the normalization condition of an MC. When $K = N = 1$, this problem has been considered in [48, 115]. Usually the number of paths in the set $\mathcal{P}$ is large and the optimization problem in (3.4.9) is too expensive to solve. We present the following efficient algorithm proposed in [115].

Algorithm

Step 1: Choose a subset $\mathcal{P}_0$ with a few number of paths of $\mathcal{P}$.

Step 2: Solve the following optimization problem:

$$\mathcal{G}_{opt,0} = \arg \max_{\mathcal{G}} \{ \min_{0 \neq U \in \mathcal{P}_0} \mathcal{G}^T \mathcal{A}^T(U)\mathcal{A}(U)\mathcal{G} : \ \|\mathcal{G}\|^2 = N \}. \tag{3.4.10}$$

Step 3: Find the free distance $d_{free,\mathbf{C}}$ of the combined MC $\mathbf{C}(z)$ using the above MC $\mathcal{G}_{opt,0}$ and a shortest path $U_0 \in \mathcal{P}$ that reaches this free distance.

Step 4: If $U_0 \in \mathcal{P}_0$, stop. Otherwise, add this path to the subset: $\mathcal{P}_0 = \mathcal{P}_0 \cup \{U_0\}$ and go to step 2.

Since the free distance is always reached in $\mathcal{P}$ and $\mathcal{P}$ has only finite elements, the above algorithm always stops in finite steps. Furthermore, it is not hard to see that the solution from the above algorithm is always the optimal MC $\mathbf{G}_{opt}(z)$. As a remark, the initial path subset $\mathcal{P}_0$ in step 1 usually takes the first few shortest paths in the error-pattern trellis. Similar to what was mentioned in [115], this algorithm works very efficiently from our numerical examples.

Example 1:

Consider the ISI channel $h = [0.5, 0.5, -0.5, -0.5]$ in Section 3.3. The optimal block $(4, 2)$ MC is

$$\mathbf{G}_{opt}(z) = \begin{bmatrix} -0.4641 & 0.8875 \\ -0.9982 & -0.0240 \\ -0.0240 & -0.9982 \\ 0.8875 & -0.4641 \end{bmatrix}.$$

The squared free distance of the combined MC is $d^2_{free,\mathbf{C}} = 13.2547$. It has coding gain 2.19 dB compared to the uncoded AWGN channel, which is slightly better than the one in Section 3.3 with the same constraint length.

The optimal $(4, 2)$ MC of constraint length 2 is

$$\mathbf{G}_{opt}(z) = \begin{bmatrix} 0.3716 & -0.1667 \\ -0.0287 & -0.6248 \\ -0.7245 & -0.2528 \\ -0.3990 & 0.7082 \end{bmatrix} + z^{-1} \begin{bmatrix} 0.6264 & 0.7712 \\ 0.7041 & -0.1469 \\ -0.1660 & -0.6064 \\ -0.4914 & -0.2283 \end{bmatrix}.$$

The squared free distance of the combined MC is $d^2_{free,\mathbf{C}} = 16.4367$. It has the coding gain is 3.13dB compared to the uncoded AWGN channel.

Notice that the upper bound of the coding gain of an MC for this channel compared to the uncoded AWGN channel is 6dB.

Example 2:

Consider the ISI channel $[1/\sqrt{2}, 1/\sqrt{2}]$. The optimal $(2, 1)$ MC of constraint length 0 is

$$\mathbf{G}_{opt}(z) = \begin{bmatrix} 1 \\ 1 \end{bmatrix}.$$

The squared free distance of the combined MC is $d^2_{free,\mathbf{C}} = 12$ and the coding gain compared to the uncoded AWGN channel is 1.76dB.

The optimal $(2,1)$ MC of constraint length 1 is

$$\mathbf{G}_{opt}(z) = \begin{bmatrix} 0.5055 \\ 0.8629 \end{bmatrix} + z^{-1} \begin{bmatrix} 0.8629 \\ 0.5054 \end{bmatrix}.$$

The squared free distance of the combined MC is $d^2_{free,\mathbf{C}} = 14.4671$ and the coding gain compared to the uncoded AWGN channel is 2.57dB.

The optimal $(3,2)$ MC of constraint length 0 is

$$\mathbf{G}_{opt}(z) = \begin{bmatrix} 1.0105 & 0.0326 \\ 0.6913 & -0.6914 \\ -0.0327 & -1.0104 \end{bmatrix}.$$

The squared free distance of the combined MC is $d^2_{free,\mathbf{C}} = 8.704$ and the coding gain compared to the uncoded AWGN channel is 1.62dB.

The optimal $(3,2)$ MC of constraint length 2 is

$$\mathbf{G}_{opt}(z) = \begin{bmatrix} -0.0353 & -0.4874 \\ 0.3175 & -0.7121 \\ 0.7598 & -0.3851 \end{bmatrix} + z^{-1} \begin{bmatrix} 0.7834 & 0.2469 \\ 0.3700 & 0.6290 \\ 0.0041 & 0.4694 \end{bmatrix}.$$

The squared free distance of the combined MC is $d^2_{free,\mathbf{C}} = 10.187$ and the coding gain compared to the uncoded AWGN channel is 2.3dB.

Notice that the upper bound of the coding gain of an MC for this channel compared to the uncoded AWGN channel is 3dB.

Chapter 4

Modulated Code Coded Decision Feedback Equalizer

In the previous chapter, we studied the joint maximum-likelihood MC encoding and decoding, where the input signal constellation is fully used. Its complexity is, however, high when the ISI channel length, or the MC size, or the signal constellation size is large. In this chapter, we study a suboptimal encoding and decoding method, namely joint decision feedback equalizations, where the input signal constellation can be arbitrary. The results in this chapter are summarized from [168, 167, 179, 185].

In this chapter, we first introduce MC coded zero-forcing (ZF) decision feedback equalizer (DFE) and its performance analysis and the optimal MC design. We then generalize it to the minimum mean square error (MMSE) DFE (MMSE-DFE), which may perform better than the ZF-DFE for some ISI channels. In the third section, we introduce another optimal MC design such that an ISI channel becomes an ISI-free AWGN channel. Notice that all the MC designs in this chapter are input symbol independent.

4.1 MC Coded Zero-Forcing DFE

In this section, we study the MC coded ZF-DFE studied in [167]. The block diagram for the MC coded ZF-DFE is shown in Fig.4.1, where I_K is the K by K identity matrix, and the K by 1 vector decision takes the best K by 1 vector of all the possible K by 1 information symbol vectors, and η is

the channel additive white Gaussian noise with zero mean and the variance $\sigma_\eta^2 = N_0/2$.

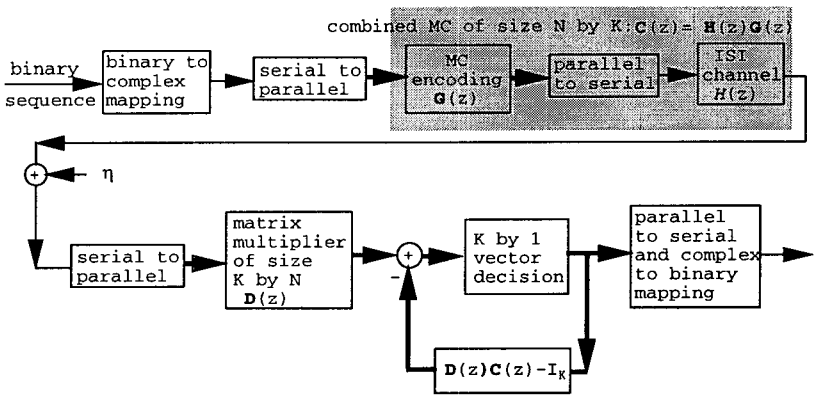

Figure 4.1: MC coded zero-forcing decision feedback equalizer.

The role of the matrix multiplier $\mathbf{D}(z)$ at the receiver in Fig.4.1 for the MC coded ZF-DFE is to convert the nonsquare matrix polynomial $\mathbf{C}(z)$ of the combined MC into a square matrix polynomial so that the DFE can be implemented as shown in Fig.4.1. It is usually the case that the higher the order of the ISI channel to equalize is, the worse the DFE performance is. To make the order of the overall ISI system $\mathbf{F}(z)$ with the matrix multiplier as low as possible, where

$$\mathbf{F}(z) \triangleq \mathbf{D}(z)\mathbf{C}(z) = \mathbf{D}(z)\mathbf{H}(z)\mathbf{G}(z), \tag{4.1.1}$$

and $\mathbf{H}(z)$ is from (2.3.3), the matrix multiplier $\mathbf{D}(z)$ simply takes a K by N constant matrix. It also suggests that the MC $\mathbf{G}(z)$ takes a block code, i.e., $\mathbf{G}(z)$ is an N by K constant matrix. We next want to study the MC design rule for the ZF-DFE. Consider an N by K block MC $\mathbf{G}(z) = G$ and a constant K by N matrix multiplier $\mathbf{D}(z) = E$. The combined MC becomes

$$\mathbf{C}(z) = H(0)G + H(1)Gz^{-1} + \cdots + H(P)Gz^{-P}, \tag{4.1.2}$$

where $\mathbf{H}(z) = \sum_{p=0}^{P} H(p)z^{-p}$ for some $P \geq 0$ and

$$H(0) = \begin{bmatrix} h(0) & 0 & \cdots & 0 \\ h(1) & h(0) & \cdots & 0 \\ \vdots & \vdots & \vdots & \vdots \\ h(N-1) & h(N-2) & \cdots & h(0) \end{bmatrix}, \tag{4.1.3}$$

which is nonsingular when $h(0) \neq 0$. From the feedback loop in the ZF-DFE in Fig.4.1, we want to have $EH(0)G = I_K$, i.e., the feedback does not depend on the current vector. Therefore, the matrix multiplier $\mathbf{D}(z) = E$ is the right inverse (pseudo inverse), $(H(0)G)^{-1}$, of the N by K constant matrix $H(0)G$.

4.1.1 Performance Analysis

Since the matrix multiplier $\mathbf{D}(z) = E$ is implemented at the receiver, the channel additive noise η is also multiplied by the matrix E. Let $E = (e_{ij})_{K\times N}$. Then the mean power of the multiplied noise $\tilde{\eta}$ of η is

$$\sigma_{\tilde{\eta}}^2 = \frac{\sum_{i=1}^{K}\sum_{j=1}^{N}|e_{ij}|^2}{K}\sigma_{\eta}^2 = \frac{\sum_{i=1}^{K}\sum_{j=1}^{N}|e_{ij}|^2}{2K}N_0. \tag{4.1.4}$$

By the normalization condition of the MC G, the mean transmitted signal power is still σ_x^2. Similar to the conventional ZF-DFE for invertible ISI channel, see, for example, [68], the signal-to-noise ratio (SNR) after the MC coded ZF-DFE for the invertible $\mathbf{C}(z)$ is

$$\text{SNR} = \frac{\sigma_x^2}{\sigma_{\tilde{\eta}}^2} = \frac{2K\sigma_x^2}{\sum_{i=1}^{K}\sum_{j=1}^{N}|e_{ij}|^2 N_0}. \tag{4.1.5}$$

Based on this SNR analysis at the receiver, to maximize the SNR we have the following **optimal MC design rule**:

$$\min_{G} \sum_{i=1}^{K}\sum_{j=1}^{N}|e_{ij}|^2 \quad \text{under the condition} \quad EH(0)G = I_K, \tag{4.1.6}$$

where the MC G satisfies the normalization condition

$$\sum_{i=1}^{N}\sum_{j=1}^{K}|g_{ij}|^2 = N. \tag{4.1.7}$$

Let the singular value decomposition (SVD) of the matrix $H(0)G$ be

$$U_l V U_r = H(0)G, \tag{4.1.8}$$

where U_l and U_r are $N \times N$ and $K \times K$ unitary matrices, respectively, and

$$V = \begin{bmatrix} \mathrm{diag}(\lambda_1, \cdots, \lambda_K) \\ 0_{(N-K)\times K} \end{bmatrix}, \tag{4.1.9}$$

and λ_i for $i = 1, 2, ..., K$ are the singular values of the matrix $H(0)G$. Then the matrix multiplier E should be

$$\mathbf{D}(z) = E = U_r^\dagger V^{-1} U_l^\dagger, \tag{4.1.10}$$

where † denotes the conjugate transpose and

$$V^{-1} = (\mathrm{diag}(1/\lambda_1, \cdots, 1/\lambda_K), 0_{K\times(N-K)}). \tag{4.1.11}$$

Thus, the total energy of the matrix E is

$$\sum_{i=1}^{K}\sum_{j=1}^{N} |e_{ij}|^2 = \sum_{i=1}^{K} \frac{1}{\lambda_i^2}. \tag{4.1.12}$$

Therefore, using the elementary inequality on the right hand side of (4.1.12) we have

$$\sum_{i=1}^{K}\sum_{j=1}^{N} |e_{ij}|^2 \geq K \left(\prod_{i=1}^{K} \frac{1}{\lambda_i^2} \right)^{1/K}, \tag{4.1.13}$$

where the equality (the minimum) is reached if and only if

$$\lambda_1 = \lambda_2 = \cdots = \lambda_K = \lambda. \tag{4.1.14}$$

The optimality condition (4.1.14) is the one to design the MC G that whitens the matrix $H(0)$ generated from the ISI channel. In the next subsection, we propose a method to design such MC G given an $H(0)$.

We now study the error probability for the MC coded ZF-DFE in Fig.4.1. Let us consider the vector decision block in Fig.4.1. For a general MC G at the transmitter and the matrix multiplier E with the form in (4.1.10), each $K \times 1$ multiplied noise vector $\tilde{\eta}$ for a fixed time may be colored when $K > 1$. In this case, the vector decision is necessary for the optimal detection. If the MC G whitens $H(0)$, i.e., the condition (4.1.14) holds, then it is not hard to see that each $K \times 1$ multiplied noise vector $\tilde{\eta}$

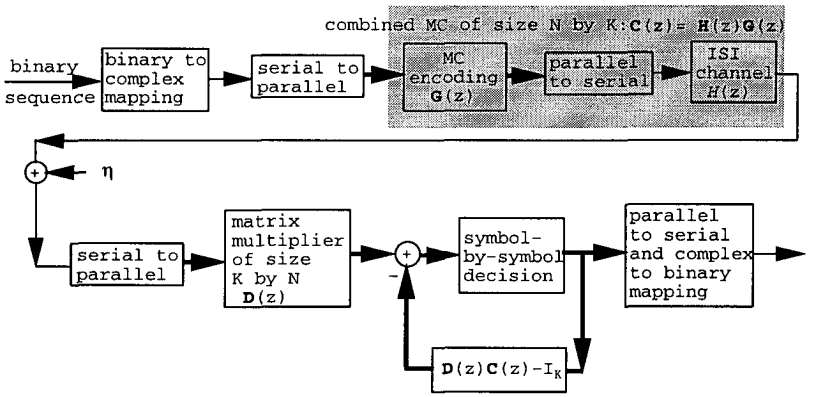

Figure 4.2: MC coded zero-forcing decision feedback equalizer with optimal MC.

for a fixed time is white too. Thus, the vector decision in Fig.4.1 can be reduced to the symbol-by-symbol detection as shown in Fig.4.2.

Assume that the condition (4.1.14) for the MC encoding holds, which is always possible to design as we shall see later. In this case,

$$\sum_{i=1}^{N}\sum_{j=1}^{K}|e_{ij}|^2 = \frac{K}{\lambda^2}.$$

Let $P_s(\gamma_s)$ denote the symbol error probability at the symbol SNR γ_s for the binary-to-complex symbol mapping used at the transmitter in Fig.4.1. For convenience, in what follows we only consider the BPSK binary-to-complex symbol mapping. In this case, the symbol error probability is $P_s(\gamma_s) = Q(\sqrt{2\gamma_s})$, where γ_s is the SNR before the decision block in Fig.4.1. Using the SNR (4.1.5), the corresponding γ_s is

$$\gamma_s = \frac{\sigma_x^2}{2\sigma_{\tilde{\eta}}^2} = \frac{K\sigma_x^2}{\sum_{i=1}^{K}\sum_{j=1}^{N}|e_{ij}|^2 N_0} = \frac{\lambda^2\sigma_x^2}{N_0} = \frac{\lambda^2 K}{N}\frac{E_b}{N_0}. \tag{4.1.15}$$

Then, the bit error rate (BER) for the MC coded ZF-DFE at the E_b/N_0 is

$$\text{BER} = P_s(\gamma_s) = Q\left(\sqrt{2\frac{E_b}{N_0}\gamma}\right), \tag{4.1.16}$$

where γ is the **coding gain** as follows, which is based on the joint ZF-DFE

decoding and compared to the uncoded BPSK in AWGN channel:

$$\gamma = \frac{\lambda^2 K}{N}, \tag{4.1.17}$$

where λ is defined in (4.1.14).

4.1.2 The Optimal MC Design

In this subsection, we present the optimal MC design such that the optimality condition (4.1.14) is satisfied.

Let the singular value decomposition of the $N \times N$ matrix $H(0)$ be defined in (4.1.3) as

$$H(0) = W_l \Lambda W_r, \tag{4.1.18}$$

where W_l and W_r are two $N \times N$ unitary matrices and

$$\Lambda = \text{diag}(\xi_1, \cdots, \xi_N), \tag{4.1.19}$$

where $\xi_1 \geq \cdots \geq \xi_N \geq 0$ are the N singular values of $H(0)$. Since $H(0)$ is nonsingular, we have

$$\xi_1 \geq \cdots \geq \xi_N > 0. \tag{4.1.20}$$

Thus, using the singular value decomposition (4.1.8) for $H(0)G$ we have

$$W_l^\dagger U_l V = \Lambda W_r G U_r^\dagger.$$

Let

$$\bar{G} = W_r G U_r^\dagger \quad \text{and} \quad U = W_l^\dagger U_l. \tag{4.1.21}$$

Then

$$\Lambda^{-1} U V = \bar{G}. \tag{4.1.22}$$

It is not hard to see that $\bar{G}$ is normalized if and only if G is normalized. Let the $N \times N$ unitary matrix $U = (u_{ij})_{N \times N}$ and the MC $\bar{G} = (\bar{g}_{ij})_{N \times K}$. The normalization condition on $\bar{G}$ becomes

$$\sum_{i=1}^{N} \sum_{j=1}^{K} |\bar{g}_{ij}|^2 = \sum_{i=1}^{N} \sum_{j=1}^{K} \frac{\lambda_j^2}{\xi_i^2} |u_{ij}|^2 = N. \tag{4.1.23}$$

The optimality condition (4.1.14) implies that

$$\sum_{i=1}^{N} \frac{1}{\xi_i^2} \sum_{j=1}^{K} |u_{ij}|^2 = \frac{N}{\lambda^2}. \tag{4.1.24}$$

From the coding gain formula (4.1.17), the larger λ is, the more the coding gain is. Therefore, from (4.1.24) the optimal normalized MC $\bar{G}$ is obtained by optimally designing the unitary matrix U such that the left hand side of (4.1.24) is minimal. By the unitariness of the matrix U, there are at most $N - K$ many α_i that are zero, where

$$\alpha_i = \sum_{j=1}^{K} |u_{ij}|^2.$$

Using the monotonic order property (4.1.20) of ξ_i, the minimum of the left hand side of (4.1.24) is reached when

$$\alpha_i = \sum_{j=1}^{K} |u_{ij}|^2 = 0 \quad \text{for } i = K+1, K+2, ..., N.$$

Thus, the optimal unitary matrix U has the following form

$$U = \begin{bmatrix} U_{11} & 0 \\ 0 & U_{22} \end{bmatrix}, \tag{4.1.25}$$

where U_{11} and U_{22} are arbitrary $K \times K$ and $(N-K) \times (N-K)$ unitary matrices, respectively. In this case,

$$\sum_{j=1}^{K} |u_{ij}|^2 = 1, \quad i = 1, 2, ..., K. \tag{4.1.26}$$

Thus, we can solve for the optimal λ^2 given K and N from (4.1.24)

$$\lambda^2 = \frac{N}{\sum_{i=1}^{K} \xi_i^{-2}}, \tag{4.1.27}$$

where ξ_i, $i = 1, 2, ..., K$, are the first K largest singular values of $H(0)$. Going back to (4.1.18)-(4.1.22), the optimal normalized MC G is

$$G_{opt} = W_r^{\dagger} \bar{G} U_r = W_r^{\dagger} \Lambda^{-1} U \begin{bmatrix} \lambda I_K \\ 0_{(N-K)\times K} \end{bmatrix} U_r, \tag{4.1.28}$$

where U_r is an arbitrary $K \times K$ unitary matrix, U is defined in (4.1.25), W_r is the $N \times N$ unitary matrix defined in (4.1.18), Λ is the diagonal matrix defined in (4.1.19), and λ is defined in (4.1.27). This concludes the following result.

Theorem 4.1 *Given an ISI channel $H(z)$, the optimal normalized (N, K) modulated code G for the MC coded zero-forcing decision feedback equalizer in Fig.4.1 is given in (4.1.28).*

Using the optimal λ in (4.1.27) and the optimal coding gain formula in (4.1.17) for the BPSK signaling, we have the following **optimal coding gain** using the optimal (N, K) MC G_{opt} in (4.1.28) for a given channel:

$$\gamma_{ZF-DFE} = \frac{K}{\sum_{i=1}^{K} \xi_i^{-2}}, \tag{4.1.29}$$

where ξ_i, $i = 1, 2, ..., K$, are the first K largest singular values of $H(0)$.

Notice that the sum of all squared singular values ξ_i of $H(0)$ is equal to the sum of all the squared coefficients in $H(0)$, i.e., from (4.1.3),

$$\sum_{i=1}^{N} \xi_i^2 = \sum_{i=1}^{N} i \cdot |h(N-i)|^2. \tag{4.1.30}$$

Clearly, when

$$\sum_{i=1}^{K} \xi_i^{-2} < K, \tag{4.1.31}$$

a coding gain for the MC coded ZF-DFE is achieved. In particular, when $K = 1$ and the largest singular value ξ_1 of the matrix $H(0)$ is greater than 1, a coding gain for the MC coded ZF-DFE is achieved.

4.1.3 Some Simulation Results

In this section, we want to present some simulation results to illustrate the theory for the optimal MC design for the MC coded ZF-DFE developed in the previous sections. We only consider low channel SNR and the BPSK signaling.

Three ISI channels are tested. Channel A: $[1/\sqrt{2}, 1/\sqrt{2}]$; Channel B: $[\sqrt{2/3}, \sqrt{1/3}]$; Channel C: [0.815, −0.407, −0.407]. Channel A and Channel C are spectral null while Channel B is none spectral null. BPSK signaling is used for all the following simulations.

We compare four equalization techniques, namely (i) conventional convolutionally coded and uncoded ZF-DFE; (ii) conventional convolutionally coded and uncoded TH precoding; (iii) MC coded ZF-DFE; and (iv) MC coded joint MLSE. Theoretical BER vs. E_b/N_0 curves for BPSK in AWGN channel and the MC coded ZF-DFE with BPSK signaling are also compared with the simulation results. In (i), the CC decoding and the ZF-DFE are separated, i.e., the ZF-DFE is implemented first and then the CC Viterbi decoding is implemented. The ZF-DFE structure in (i) is the same as the one in the MC coded case. As a remark, we have not implemented more sophisticated DFE algorithms, such as [42, 40], which is because a) we only use the BPSK signaling and b) these algorithms can also be used in the proposed MC coded ZF-DFE. In (ii), the CC and the TH precoding are separately implemented.

In all the following optimal normalized MC G_{ZF-DFE} in (4.1.28), the unitary matrices U and U_r are set to the identity matrices. In the following conventional convolutionally coded ZF-DFE and the TH precoding methods, the rate 1/2 and constraint length 2 with the optimal $d_{free} = 5$ convolutional code, i.e., the convolutional code $(2, 1, 2)$, is used. Since the data rate in the MC coded ZF-DFE is 1/2, we do not implement the comparisons with the TCM where the data rates for the TCM are not below 1. The combined TCM and DFE can be found in, for example, [23].

Channel A: $[1/\sqrt{2}, 1/\sqrt{2}]$.

This is a spectral null channel. We first consider the case when $K = 1$ and $N = 2$ in the MC G. In this case, the optimal MC in (4.1.28) is

$$G_{opt} = \begin{bmatrix} 1.2030 \\ 0.7435 \end{bmatrix}. \tag{4.1.32}$$

The largest singular value of $H(0)$ is $\xi_1 = 1.1441$ and the optimal coding gain in (4.1.29) for the MC coded ZF-DFE is $\gamma_{ZF-DFE} = 1.17$dB. For the MC in (4.1.32), the squared free Euclidean distance of the combined MC with the ISI Channel A is $d^2_{free} = 11.58$. Thus, the coding gain in (2.4.1) of the joint MLSE method is $\gamma_{ISI} = 1.6$dB. It is 0.16dB less than the optimal block $(2, 1)$ MC obtained in Section 3.4 based on the optimal design based on the joint MLSE for the BPSK signaling. However, the above optimal ZF-DFE design does not depend on the signal constellation.

In Fig.4.3, the BERs vs. E_b/N_0 for the conventional uncoded ZF-DFE are plotted with the solid line marked by o; the BERs vs. E_b/N_0 for the convolutionally coded ZF-DFE are plotted with the solid line marked by □; the BERs vs. E_b/N_0 for the uncoded TH precoding are plotted with the

solid line marked by Δ; the BERs vs. E_b/N_0 for the convolutionally coded TH precoding are plotted with the solid line marked by $*$; and the BERs vs. E_b/N_0 for the MC coded ZF-DFE with the above optimal MC code in (4.1.32) are plotted by the solid line. The theoretical BERs vs. E_b/N_0 for uncoded BPSK in the AWGN channel are plotted with the dashed line. The BERs vs. E_b/N_0 of the joint MLSE for the MC in (4.1.32) and Channel A are plotted with the solid line marked by $+$.

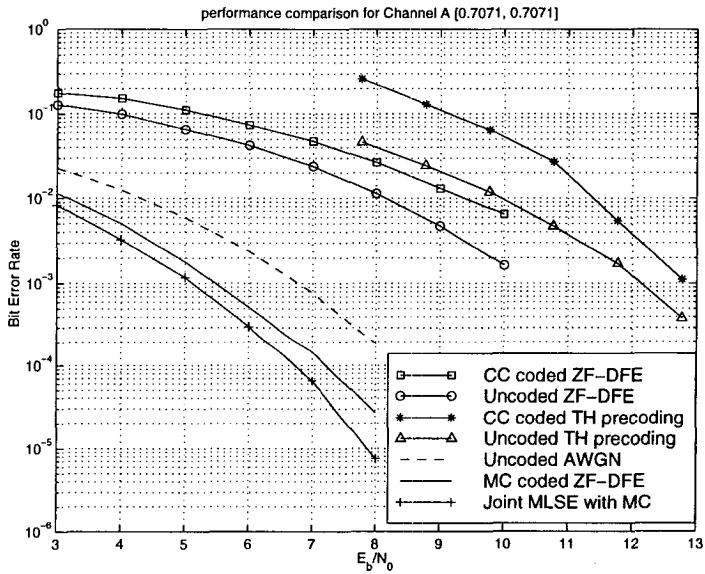

Figure 4.3: Performance comparison for different equalization methods: Channel A and MC code rate 1/2.

We then consider the case when $K = 2$ and $N = 3$ in the MC G. In this case, the optimal MC in (4.1.28) is

$$G_{opt} = \begin{bmatrix} 0.5825 & -1.0497 \\ 0.7264 & 0.4671 \\ 0.3233 & 0.8418 \end{bmatrix}. \tag{4.1.33}$$

The first two largest singular values of $H(0)$ are $\xi_1 = 1.2742$ and $\xi_2 = 0.8817$ and the optimal coding gain in (4.1.29) for the MC coded ZF-DFE is $\gamma_{ZF-DFE} = 0.22$dB. For the MC in (4.1.33), the squared free Euclidean distance of the combined MC $\mathbf{C}(z)$ with the ISI Channel A is $d^2_{free} = 6.52$.

Thus, the coding gain in (2.4.1) of the joint MLSE method is $\gamma_{ISI} = 0.36$dB. It is 1.26dB less than the optimal block $(3,2)$ MC obtained in Section 3.4 based on the optimal design based on the joint MLSE for the BPSK signaling.

In Fig.4.4, we compare the performances of the optimal rate $1/2$ and rate $2/3$ normalized MC in (4.1.32) and (4.1.33), respectively, with both theoretical and simulation results. The BERs vs. E_b/N_0 for the rate $1/2$ in (4.1.32) are plotted with the solid line marked by o and the corresponding theoretical performance is plotted with the dashdot line. The BERs vs. E_b/N_0 for the rate $2/3$ in (4.1.33) are plotted with the solid line marked by $+$ and the corresponding theoretical performance is plotted with the solid line marked by x. The uncoded BPSK in the AWGN is plotted with the dashed line. The BERs vs. E_b/N_0 for the joint MLSE of the rate $2/3$ MC in (4.1.33) and Channel A are plotted with the solid line marked by $\square$. In Fig.4.4, we also compare the performances of the MC $G = [1,1]^T$, which is plotted by the solid line marked by $*$.

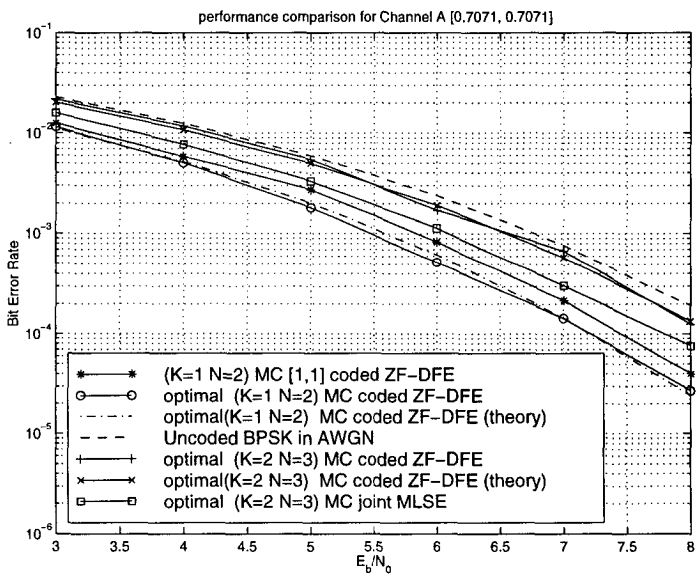

Figure 4.4: Performance comparison for different rate and different normalized MC: Channel A.

Channel B: $[\sqrt{2/3}, \sqrt{1/3}]$.

This is a none spectral null channel. Similar to before, we first consider the case when $K = 1$ and $N = 2$ in the MC G. In this case, the optimal MC in (4.1.28) is

$$G_{opt} = \begin{bmatrix} 1.1547 \\ 0.8165 \end{bmatrix}. \tag{4.1.34}$$

The largest singular value of $H(0)$ is $\xi_1 = 1.1547$ and the optimal coding gain in (4.1.29) for the MC coded ZF-DFE is $\gamma_{ZF-DFE} = 1.25$dB. For the MC in (4.1.34), the squared free Euclidean distance of the combined MC with the ISI channel Channel B is $d^2_{free} = 11.56$. Thus, the coding gain in (2.4.1) of the joint MLSE method is $\gamma_{ISI} = 1.6$dB. Similar to Channel A and the results shown in Fig.4.3, the simulation results for Channel B in this case are shown in Fig.4.5.

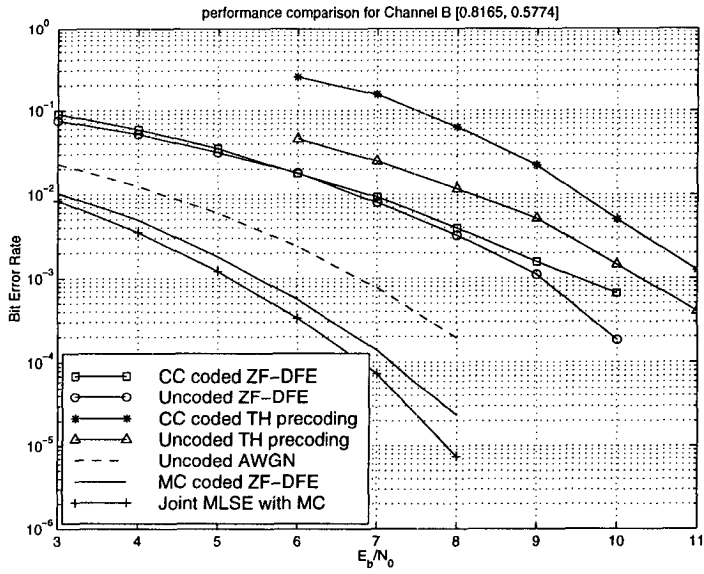

Figure 4.5: Performance comparison for different equalization methods: Channel B and MC code rate 1/2.

We then consider the case when $K = 2$ and $N = 3$ in the MC G. In

this case, the optimal MC in (4.1.28) is

$$G_{opt} = \begin{bmatrix} 0.5811 & -1.0170 \\ 0.7452 & 0.3385 \\ 0.3746 & 0.9043 \end{bmatrix}. \tag{4.1.35}$$

The first two largest singular values of $H(0)$ are $\xi_1 = 1.2667$ and $\xi_2 = 0.9182$ and the optimal coding gain in (4.1.29) for the MC coded ZF-DFE is $\gamma_{ZF-DFE} = 0.44$dB. For the MC in (4.1.35), the squared free Euclidean distance of the combined MC $\mathbf{C}(z)$ with the ISI Channel A is $d^2_{free} = 6.82$. Thus, the coding gain in (2.4.1) of the joint MLSE method is $\gamma_{ISI} = 0.56$dB. Similar to Channel A and the results shown in Fig.4.4, the simulation and the theoretical results for Channel B in this case are shown in Fig.4.6.

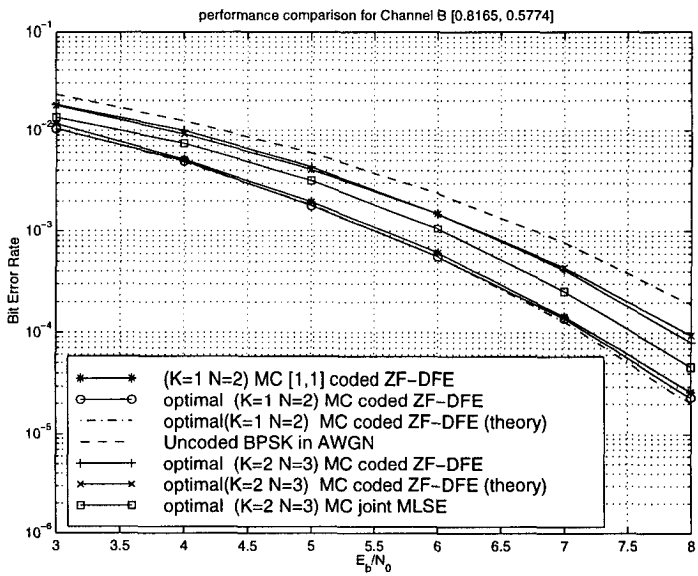

Figure 4.6: Performance comparison for different rate and different normalized MC: Channel B.

Channel C: $[0.815, -0.407, -0.407]$.

This is another spectral null channel. In this case, we only consider the case when $K = 1$ and $N = 2$ in the MC G. In this case, the optimal MC

in (4.1.28) is

$$G_{opt} = \begin{bmatrix} 1.1146 \\ -0.8705 \end{bmatrix}. \tag{4.1.36}$$

The largest singular value of $H(0)$ is $\xi_1 = 1.0435$ and the optimal coding gain in (4.1.29) for the MC coded ZF-DFE is $\gamma_{ZF-DFE} = 0.37$dB. For the MC in (4.1.36), the squared free Euclidean distance of the combined MC with the ISI Channel B is $d^2_{free} = 9.2535$. Thus, the coding gain in (2.4.1) of the joint MLSE method is $\gamma_{ISI} = 0.63$dB. It is interesting to note that the decrease of the coding gain for the MC coded ZF-DFE is due to the increase of the ISI channel length. For the ZF-DFE, the performance is usually better for shorter ISI channels, which can be seen from the following simulation results. Fig.4.7 is similar to Fig.4.3 except that, in Fig.4.7, the theoretical performance for the MC coded ZF-DFE with the optimal rate 1/2 MC in (4.1.36) is plotted with the dashdot line.

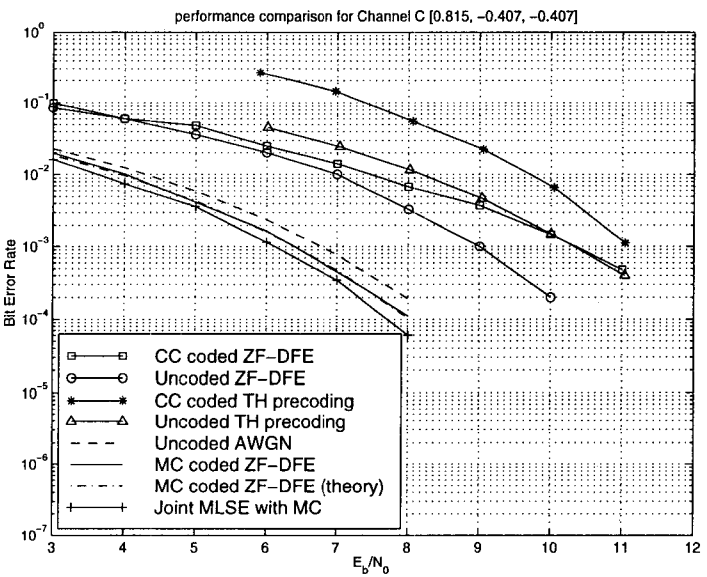

Figure 4.7: Performance comparison for different equalization methods: Channel C and MC code rate 1/2.

From all the above simulation and theoretical results, one can see that the CC coded ZF-DFE and the TH precoding are even worse than the ones

of the corresponding uncoded systems. We think that the reason is because the CC decoding is separated from the equalization. After the equalization the noise is no longer AWGN, which degrades the CC performance because the CC with rate 1/2 and constraint length 2 is optimal in terms of the AWGN channel. One can also see that the simulation and theoretical results for the MC coded ZF-DFE almost coincide.

It is known that in the TH precoding, [133, 57], the modulo operation of $2M$ is used, where M is the number of levels in the PAM signaling at the transmitter. Due to the modulo operation at the receiver, the performance is degraded by the size M is small, such as 2 in the BPSK case here.

4.2 MC Coded Minimum Mean Square Error DFE

In the previous section, we studied the MC coded ZF-DFE and its performance is determined by matrix $H(0)$ in (4.1.3) from the ISI channel. This matrix, however, may have small eigenvalues for some channels where $h(0)$ is small. In this section, we want to develop a general minimum mean square error DFE (MMSE-DFE) for the MC coded ISI channel obtained in [179]. Voois [153] presented the optimal decision-delay for a conventional MMSE-DFE, see for example [116, 43, 28, 29, 4, 6], and derived the optimal scalar filter coefficients. Unlike the scalar coefficients in [153], the filter coefficients in this section are either vectors or matrices. We want to extend Voois's derivation from scalars to vectors/matrices. The results in this section are from [179].

4.2.1 Optimal Decision-Delay and Coefficients of an MC Coded MMSE-DFE

The channel in this section means the combined channel, $\mathbf{C}(z)$, of an (N, K) MC $\mathbf{G}(z)$ and an ISI channel $\mathbf{H}(z)$, unless otherwise specified. The block diagrams of the MMSE-DFE are shown in Fig.4.8 and Fig.4.9.

Let $\mathbf{W}$ denote the L_f-tap *feedforward vector*

$$\mathbf{W} = [W_0 \; W_1 \; \cdots \; W_{L_f-1}]^T,$$

where each W_i is a $K \times N$ matrix.

Let $\mathbf{B}$ denote the L_b-tap *feedback vector*

$$\mathbf{B} = [B_1 \; B_2 \; \cdots \; B_{L_b}]^T.$$

where each B_i is a $K \times K$ matrix.

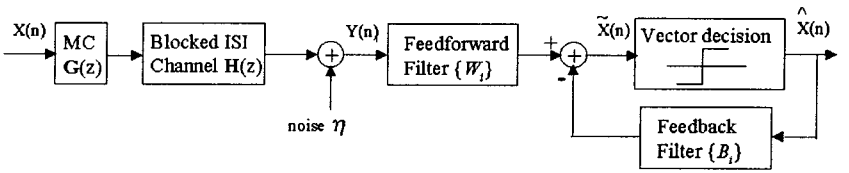

Figure 4.8: An MC coded MMSE-DFE.

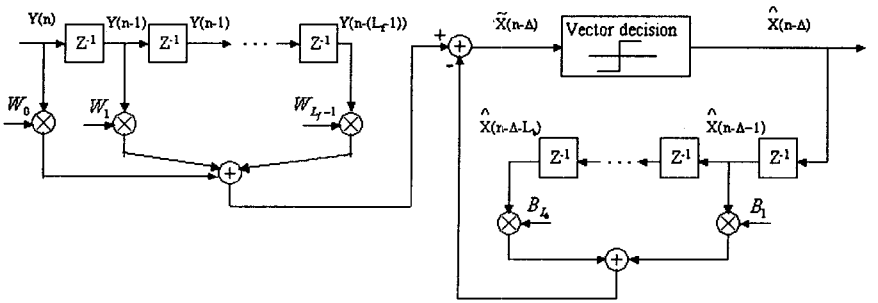

Figure 4.9: The structure of DFE.

Let $\mathbf{X}$ denote the *channel input vector*

$$\mathbf{X} = [X(n)\ X(n-1)\ \cdots\ X(n-(L_f-1)-P)]^T.$$

where each $X(n-i)$ is a $K \times 1$ vector, and P is the highest order of the polynomial matrix $\mathbf{C}(z)$ (the combined channel matrix).

Let $\mathbf{Y}$ denote the *channel output vector*

$$\mathbf{Y} = [Y(n)\ Y(n-1)\ \cdots\ Y(n-(L_f-1))]^T,$$

where each $Y(n-i)$ is an $N \times 1$ vector.

Let η denote the *noise vector*

$$\eta = [\eta(n)\ \eta(n-1)\ \cdots\ \eta(n-(L_f-1))]^T.$$

where each $\eta(n-i)$ is an $N \times 1$ vector of Gaussian noise with zero-mean and variance

$$R_{\eta\eta} = \mathrm{diag}(\sigma_\eta^2, \cdots, \sigma_\eta^2).$$

Let $\hat{X}(n)$ denote the output signal after the decision.

Let $\mathcal{C}$ denote the following block Toeplitz *channel matrix*

$$\mathcal{C} = \begin{bmatrix} C(0) & \cdots & C(P) & 0 & \cdots & \cdots & 0 \\ 0 & C(0) & \cdots & C(P) & \cdots & \cdots & 0 \\ \vdots & \vdots & \vdots & \vdots & \vdots & \vdots & \vdots \\ 0 & 0 & \cdots & 0 & C(0) & \cdots & C(P) \end{bmatrix}. \tag{4.2.1}$$

We have

$$\mathbf{Y} = \mathcal{C}\mathbf{X} + \eta.$$

The autocorrelation and the crosscorrelation of $\mathbf{X}$ and $\mathbf{Y}$ are

$$\begin{aligned} R_{\mathbf{XX}} &= E(\mathbf{X}\mathbf{X}^\dagger) \\ R_{\mathbf{XY}} &= R_{\mathbf{XX}}\mathcal{C}^\dagger \\ R_{\mathbf{YY}} &= \mathcal{C}R_{\mathbf{XX}}\mathcal{C}^\dagger + R_{\eta\eta}. \end{aligned}$$

For an (N, K) block MC G, a given feedforward filter length L_f and a given feedback filter length L_b, the **error vector** between the DFE estimate $\tilde{X}(n-\Delta)$ and the input $X(n-\Delta)$ is expressed as

$$\begin{aligned} e(n) &= X(n-\Delta) - \tilde{X}(n-\Delta) \\ &= X(n-\Delta) - \left(\mathbf{W}^T\mathbf{Y} - \sum_{i=1}^{L_b} B_i\hat{X}(n-\Delta-i)\right) \end{aligned}$$

We assume that all feedback vectors are correct, i.e., $\hat{X}(n) = X(n)$ for any n. Thus,

$$\begin{aligned} e(n) &= X(n-\Delta) - \left(\mathbf{W}^T\mathbf{Y} - \sum_{i=1}^{L_b} B_i X(n-\Delta-i) \right) \\ &= \tilde{\mathbf{B}}^T\mathbf{X} - \mathbf{W}^T\mathbf{Y} \end{aligned}$$

where $\tilde{\mathbf{B}}$ is the *extended feedback vector* as follows

$$\tilde{\mathbf{B}} = [0_{K\times(K\Delta)}\ I_K\ \mathbf{B}^T\ 0_{K\times J}]^T, \tag{4.2.2}$$

where

$$J = K(P + (L_f - 1) - L_b - \Delta).$$

Note that the optimal length of the feedback filter is $L_b = P + (L_f - 1) - \Delta$, and any longer filter does not perform better due to the finite length of the channel. So we assume $L_b \leq P + (L_f - 1) - \Delta$.

The mean-square-error (MSE) σ_e^2 is

$$\begin{aligned} \sigma_e^2 &= E(e(n)^\dagger e(n)) && (4.2.3) \\ &= E((\tilde{\mathbf{B}}^T\mathbf{X} - \mathbf{W}^T\mathbf{Y})^\dagger(\tilde{\mathbf{B}}^T\mathbf{X} - \mathbf{W}^T\mathbf{Y})) && (4.2.4) \\ &= \text{trace}(\mathbf{W}^T R_{\mathbf{YY}}\mathbf{W}^* + \tilde{\mathbf{B}}^T R_{\mathbf{XX}}\tilde{\mathbf{B}}^* \\ &\quad -\tilde{\mathbf{B}}^T R_{\mathbf{XY}}\mathbf{W}^* - \mathbf{W}^T R_{\mathbf{XY}}^\dagger \tilde{\mathbf{B}}^*). && (4.2.5) \end{aligned}$$

Let

$$f(\mathbf{W}) \triangleq \mathbf{W}^T R_{\mathbf{YY}}\mathbf{W}^* + \tilde{\mathbf{B}}^T R_{\mathbf{XX}}\tilde{\mathbf{B}}^* - \tilde{\mathbf{B}}^T R_{\mathbf{XY}}\mathbf{W}^* - \mathbf{W}^T R_{\mathbf{XY}}^\dagger \tilde{\mathbf{B}}^*. \tag{4.2.6}$$

Then, the MSE is minimized when

$$\frac{\partial(\text{trace}(f(\mathbf{W})))}{\partial \mathbf{W}} = 0,$$

which is equivalent to

$$\text{trace}\left(\frac{\partial f(\mathbf{W})}{\partial \mathbf{W}}\right) = 0 \tag{4.2.7}$$

Eqn. (4.2.7) is satisfied when

$$\frac{\partial f(\mathbf{W})}{\partial \mathbf{W}} = 0.$$

For a given $\mathbf{B}$, the MMSE solution is

$$\mathbf{W}^T = \tilde{\mathbf{B}}^T R_{\mathbf{XY}} R_{\mathbf{YY}}^{-1}. \tag{4.2.8}$$

The corresponding MSE is

$$\sigma_e^2 = \text{trace}(\tilde{\mathbf{B}}^T R_{\mathbf{X|Y}} \tilde{\mathbf{B}}^*), \tag{4.2.9}$$

where

$$R_{\mathbf{X|Y}} = R_{\mathbf{XX}} - R_{\mathbf{XY}} R_{\mathbf{YY}}^{-1} R_{\mathbf{XY}}^{\dagger}.$$

We next want to find the optimal feedback vector $\mathbf{B}$. Recall the form of $\tilde{\mathbf{B}}$ in Eqn. (4.2.2). The MSE in Eqn. (4.2.9) can be reduced to

$$\sigma_e^2 = \text{trace}\left([I_K \ \mathbf{B}^T] \, Q(\Delta, L_b) \begin{bmatrix} I_K \\ \mathbf{B}^* \end{bmatrix} \right), \tag{4.2.10}$$

where $Q(\Delta, L_b)$ is the $K(L_b+1) \times K(L_b+1)$ subblock of matrix $R_{\mathbf{X|Y}}$, as follows

$$Q(\Delta, L_b) = S R_{\mathbf{X|Y}} S^T,$$

where

$$S = \begin{bmatrix} 0_{K(L_b+1)\times\Delta} & I_{K(L_b+1)\times K(L_b+1)} & 0_{K(L_b+1)\times J} \end{bmatrix}. \tag{4.2.11}$$

We further partition $Q(\Delta, L_b)$ as

$$Q(\Delta, L_b) = \begin{bmatrix} A_{K\times K} & q^{\dagger} \\ q & \mathcal{P} \end{bmatrix}.$$

Then Eqn. (4.2.10) is further reduced to (note that $\mathcal{P} = \mathcal{P}^{\dagger}$ due to the Hermitian property of matrix $Q(\Delta, L_b)$)

$$\sigma_E^2 = \text{trace}(A_{K\times K} - q^{\dagger}\mathcal{P}^{-1}q) + (\mathbf{B}^* + \mathcal{P}^{-1}q)^{\dagger} \, \mathcal{P} \, (\mathbf{B}^* + \mathcal{P}^{-1}q)).$$

Note that, matrix $(\mathbf{B}^* + \mathcal{P}^{-1}q)^{\dagger} \, \mathcal{P} \, (\mathbf{B}^* + \mathcal{P}^{-1}q)$ is non-negative definite. Thus, the optimal feedback vector that minimizes the σ_e^2 is [153]

$$\mathbf{B} = -(\mathcal{P}^{-1}q)^*, \tag{4.2.12}$$

and the minimum MSE (MMSE) is

$$\sigma_{e,min}^2 = \text{trace}(A_{K\times K} - q^{\dagger}\mathcal{P}^{-1}q). \tag{4.2.13}$$

We note that[153], the decision-delay Δ determines the position of $Q(\Delta, L_b)$ in $R_{\mathbf{X|Y}}$. The decision-delay Δ can vary from 0 to P. Therefore, we compute the MMSE for each value of decision-delay from 0 to P, and choose the optimal decision-delay Δ which yields the least MMSE [153].

4.2.2 Optimal Block MC for MC Coded MMSE-DFE

In Section 4.1, the optimal MC G for the ZF-DFE is based on the singular decomposition of the matrix $H(0)$. This is, however, not necessarily the best block MC for the MMSE-DFE.

For an MC coded MMSE-DFE, we design a block MC G based on the singular decomposition of each constant coefficient matrix $H(i)$, $0 \leq i \leq P_1$ of the blocked channel $\mathbf{H}(z)$ in (2.3.3):

$$H(i) = W_l(i)V(i)W_r(i) \tag{4.2.14}$$

$$V(i) = \text{diag}(\xi_1(i), \cdots, \xi_N(i)), \tag{4.2.15}$$

where P_1 is assumed the order of $\mathbf{H}(z)$. Following Eqns. (4.1.18)-(4.1.28), we compute a block MC G_i for each $H(i)$, $0 \leq i \leq P_1$,

$$G_i = W_r(i)^\dagger (V(i))^{-1} U \begin{bmatrix} \lambda(i) I_K \\ 0_{(N-K)\times K} \end{bmatrix} U_r(i), \ 0 \leq i \leq P_1 \tag{4.2.16}$$

where

$$\lambda^2(i) = \frac{N}{\sum_{k=1}^{K} (\xi_k(i))^{-2}}. \tag{4.2.17}$$

Then following Eqns. (4.2.8)-(4.2.13), we compute the MMSE-DFE coefficients (feedforward $\mathbf{W}$ and feedback $\mathbf{B}$) and its MMSE for each G_i, $0 \leq i \leq P_1$:

$$\sigma^2_{e,min}(G_i) = \text{trace}(A(G_i)_{K\times K} - (q(G_i))^\dagger (\mathcal{P}(G_i))^{-1} q(G_i)), \ 0 \leq i \leq P_1,$$

where $A(G_i)$ and $q(G_i)$ are the corresponding A and q in (4.2.13) with respect to MC G_i. We choose MC G_i that yields the least MMSE among all G_i, $0 \leq i \leq P_1$:

$$G_{opt} = \arg\{\min_{0\leq i\leq P_1} (\sigma^2_{e,min}(G_i))\}. \tag{4.2.18}$$

It is clear that the above MC coded MMSE-DFE with the above MC G_{opt} performs at least as well as the ZF-DFE one. The performance of the MMSE-DFE over the ZF-DFE is, however, channel dependent. Examples and simulation results are given in the following section.

4.2.3 Simulation Results

In this section, we simulate the MC coded MMSE-DFE on some ISI channels using $(2, 1)$ MC.

Channel D

Channel D is $h = \{-0.4083, 0.8165, -0.4083\}$. The blocked 2×2 channel matrix $\mathbf{H}(z)$ is

$$\mathbf{H}(z) = \begin{bmatrix} -0.4083 & 0 \\ 0.8165 & -0.4083 \end{bmatrix} + z^{-1} \begin{bmatrix} -0.4083 & 0.8165 \\ 0 & -0.4083 \end{bmatrix}.$$

In this case, $P_1 = 1$ and

$$H(0) = \begin{bmatrix} -0.4083 & 0 \\ 0.8165 & -0.4083 \end{bmatrix},$$

and

$$H(1) = \begin{bmatrix} -0.4083 & 0.8165 \\ 0 & -0.4083 \end{bmatrix}.$$

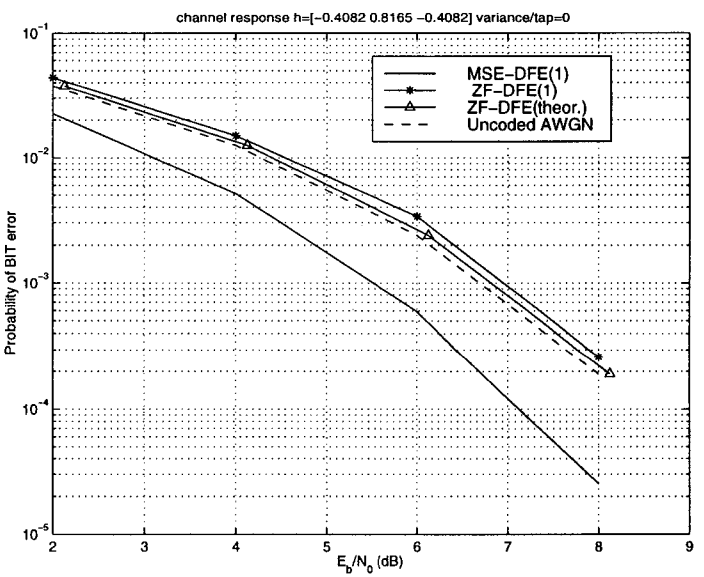

Figure 4.10: BER performance on Channel D.

Feedforward filter length $L_f = 2$ and feedback filter length $L_b = 1$ are sufficient for this channel. The MSE of the ZF-DFE is 0.0051. The minimum MSE of the MMSE-DFE is 0.0038, which is achieved when the MMSE-DFE is designed based on the channel matrix $H(0)$ and the decision-delay $\Delta = 1$.

The BER curves of the MMSE-DFE and the ZF-DFE are shown in Fig.4.10. The theoretical BER of the ZF-DFE and the BER of uncoded BPSK on the AWGN channel are also shown in Fig.4.10. One can see that the MC coded ZF-DFE has no coding gain, while the MC coded MMSE-DFE can achieve more than 1dB coding gain, compared to the uncoded BPSK in the AWGN channel.

Channel E

Channel E is $h = \{0.2271, 0.4602, 0.6883, 0.4602, 0.2271\}$. The blocked ISI channel matrix $\mathbf{H}(z)$ is

$$\mathbf{H}(z) = \begin{bmatrix} 0.2270 & 0 \\ 0.4601 & 0.2270 \end{bmatrix} + z^{-1} \begin{bmatrix} 0.6881 & 0.4601 \\ 0.4601 & 0.6881 \end{bmatrix} + z^{-2} \begin{bmatrix} 0.2270 & 0.4601 \\ 0 & 0.2270 \end{bmatrix}. \quad (4.2.19)$$

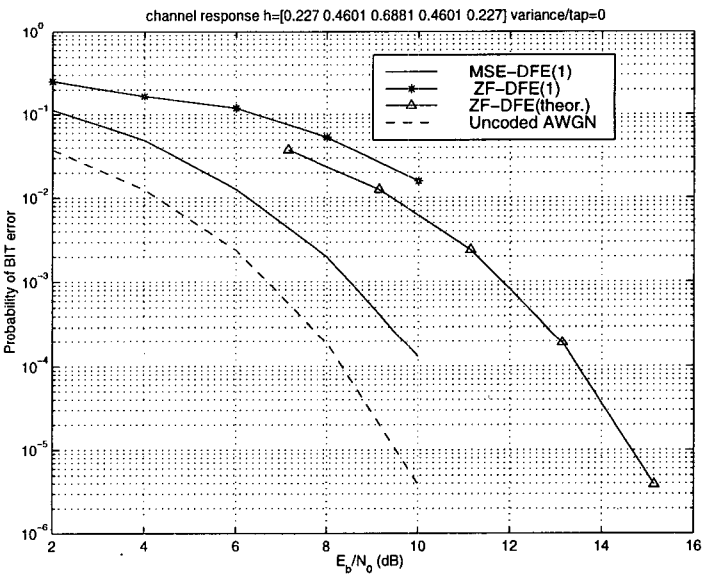

Figure 4.11: BER performance on Channel E.

The matrix $H(0)$ has singular values of $\xi_1 = 0.5532$ and $\xi_2 = 0.0931$.

Following Eqn. (4.1.29), the coding gain for the ZF-DFE is $\gamma_{ZF-DFE} = -5.14$ dB, which is negative compared to the uncoded AWGN channel.

For the MC coded MMSE-DFE, feedforward filter length $L_f = 3$ and feedback filter length $L_b = 2$ are sufficient for this channel. The MSE is minimized when the MC is designed based on the matrix $H(1)$ and the decision-delay of the DFE $\Delta = 2$.

The BER performance of both the MMSE-DFE and the ZF-DFE are plotted in Fig.4.11. Compared to the uncoded BPSK on the AWGN channel, neither MC coded MMSE-DFE nor MC coded ZF-DFE has coding gain. However, MC coded MMSE-DFE performs more than 3 dB better than the ZF-DFE does.

Channel F

Channel F is $h = \{0.8165, 0.5774\}$. For this channel, both MC coded MMSE-DFE and MC coded ZF-DFE achieve more than 1dB coding gain compared to the uncoded AWGN channel and their performances are almost the same as shown in Fig.4.12.

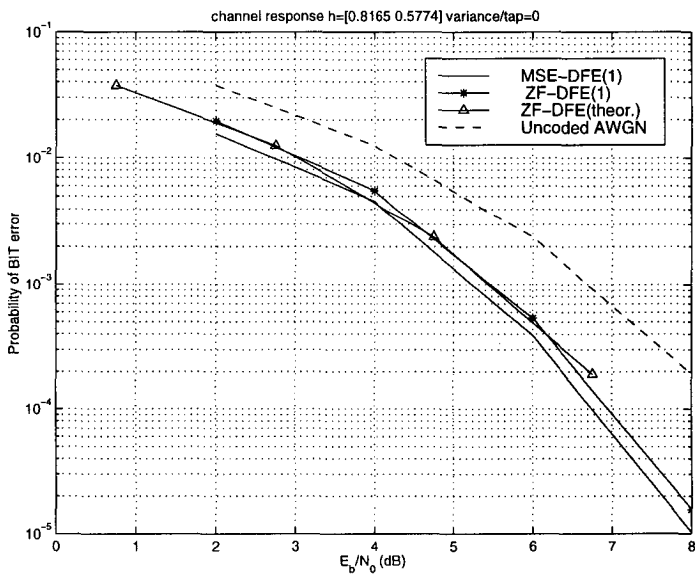

Figure 4.12: BER performance on Channel F.

4.3 An Optimal MC Design Converting ISI Channel into ISI-Free Channel

The block-based transmission techniques, or block MC, in [72, 5] and the MC coded ZF-DFE and MMSE-DFE in Section 4.1 and 4.2 assume no inter-block interference (IBI) either explicitly or implicitly: the IBI is eliminated by inserting zeros in each block in the vector-based precoding in [72, 5] and the IBI is assumed to be eliminated completely by the DFE in the MC coded ZF-DFE and the MMSE-DFE.

In this section, a different MC design is proposed by taking the complete blocked channel matrix into account, rather than considering only single coefficient matrix $H(0)$ of the blocked channel matrix $\mathbf{H}(z)$. The results in this section are from [185]. The new MC design optimally converts an ISI channel with AWGN into an ISI-free AWGN channel and the data rate expansion may provide the coding gain compared to the uncoded AWGN channel in some cases. Since most of the existing error correction coding (ECC) techniques are good for AWGN channels, the MC design in this paper is particularly useful when any further ECC is applied before the MC encoding, such as turbo coding.

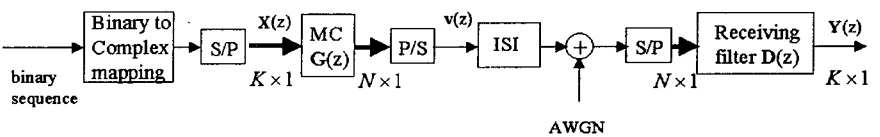

Figure 4.13: MC coded system.

Although the globally optimal MC design of the proposed approach is hard to implement in practice, the simplified sub-optimal MC design performs well. Experimental results show its performance advantage over the previous MC design.

In this section, we are interested in the communication system shown in Fig.4.13, where $\mathbf{G}(z)$ is a modulated encoder and $\mathbf{D}(z)$ is a receiving filter. The transmitted and received symbols are grouped into equal-size blocks.

The receiving filter $\mathbf{D}(z)$ is usually required at the channel output in order to recover the K by 1 signal vector $\mathbf{X}(z)$ as the same in Section 4.1. Then the combination of the MC $\mathbf{G}(z)$, the filter $\mathbf{D}(z)$ and the ISI channel $\mathbf{H}(z)$ becomes:

$$\mathbf{Y}(z) = \mathbf{D}(z)(\mathbf{H}(z)\mathbf{G}(z)\mathbf{X}(z) + \eta(z)) \tag{4.3.1}$$

where the signal is the following K by 1 vector

$$\mathbf{Y}_s(z) = \mathbf{D}(z)\mathbf{H}(z)\mathbf{G}(z)\mathbf{X}(z), \tag{4.3.2}$$

and the noise is the following K by 1 vector

$$\mathbf{Y}_n(z) = \mathbf{D}(z)\eta(z). \tag{4.3.3}$$

In what follows, we impose the following condition on the MC design

$$\mathbf{D}(z)\mathbf{H}(z)\mathbf{G}(z) = I_K, \tag{4.3.4}$$

which ensures that the filtered output is ISI free. Another advantage of such design will be seen later.

As a remark, in the maximum-likelihood MC decoding studied in Section 3.1 the receiving filter $\mathbf{D}(z)$ is not used while the decoding complexity may be high, in particular when the input signal constellation has a large size.

4.3.1 An Optimal Modulated Code Design

The objective of an optimal modulated code design is to design $\mathbf{G}(z)$ and $\mathbf{D}(z)$ such that it is optimal based on a given criterion. In what follows, we use the criterion of maximizing the output SNR normalized to the mean transmission power per information symbol in the following sense:

$$\max_{\mathbf{D}(z)\mathbf{H}(z)\mathbf{G}(z)=I_K} \frac{SNR_Y}{E(|v|^2)N/K}, \tag{4.3.5}$$

where SNR_Y is the SNR in (4.3.1), i.e.,

$$SNR_Y = \frac{E\{|Y_s|^2\}}{E\{|Y_n|^2\}}, \tag{4.3.6}$$

and $E(|v|^2)$ is the mean transmission power. Assume that the mean signal power before the MC encoding is E_x and the variance of the AWGN is $\sigma_\eta^2 = N_0/2$. Then,

$$E\{|Y_s|^2\} = \frac{\|\mathbf{D}(z)\mathbf{H}(z)\mathbf{G}(z)\|_F^2}{K} E_x,$$

and

$$E\{|Y_n|^2\} = \frac{\|\mathbf{D}(z)\|_F^2}{K} \frac{N_0}{2}.$$

Meanwhile, the mean transmission power is

$$E(|v|^2) = \frac{E_x \|\mathbf{G}(z)\|_F^2}{N}.$$

To normalize the mean transmission power such that it is the same as E_x, the following condition is always imposed on an MC $\mathbf{G}(z)$ from now on:

$$\|\mathbf{G}(z)\|_F^2 = N. \tag{4.3.7}$$

By noticing that, when $\mathbf{D}(z)\mathbf{H}(z)\mathbf{G}(z) = I_K$,

$$\|\mathbf{D}(z)\mathbf{H}(z)\mathbf{G}(z)\|_F^2 = K,$$

the criterion (4.3.5) can be rewritten

$$\max_{\mathbf{D}(z)\mathbf{H}(z)\mathbf{G}(z)=I_K} \gamma(\mathbf{G}(z)) = \max_{\mathbf{D}(z)\mathbf{H}(z)\mathbf{G}(z)=I_K} \frac{K^2}{N\|\mathbf{D}(z)\|_F^2}, \tag{4.3.8}$$

where

$$\gamma(\mathbf{G}(z)) \triangleq \frac{K^2}{N\|\mathbf{D}(z)\|_F^2}$$

can be viewed as the **coding gain** compared to the uncoded AWGN channel.

Regardless whether the channel matrix $\mathbf{H}(z)$ comes from blocking a linear time invariant channel $H(z)$ or not, if the channel matrix $\mathbf{H}(z)$ is a constant matrix, i.e., $\mathbf{H}(z) = H_0$, the optimal solution of (4.3.8) is the one that whitens the channel H_0, see Section 4.1.

Lemma 4.1 *When $\mathbf{H}(z) = H_0$, a constant matrix, the solution of (4.3.8) is*

$$G_{opt} = \frac{1}{\lambda} V_0^H \cdot \begin{bmatrix} diag(\lambda_1^{-1}, \cdots, \lambda_K^{-1}) \\ 0_{(N-K)\times K} \end{bmatrix}, \tag{4.3.9}$$

$$D_{opt} = \lambda \cdot I_{K\times N} \cdot U_0^H \tag{4.3.10}$$

where U_0, V_0, and Λ_0 are the singular value decomposition of H_0, i.e. $H_0 = U_0\Lambda_0 V_0$, U_0 and V_0 are two $N\times N$ unitary matrices, $\Lambda_0 = diag(\lambda_1, \lambda_2, \cdots, \lambda_N)$ with $\lambda_1 \geq \lambda_2 \geq \cdots \geq \lambda_N \geq 0$, and

$$\lambda = \sqrt{\sum_{k=1}^{K} \lambda_k^{-2}}. \tag{4.3.11}$$

When $\mathbf{H}(z)$ is not a constant matrix, which is always the case when the ISI channel $H(z)$ has more than one tap, similar result still holds as follows.

Theorem 4.2 *For a general channel matrix* $\mathbf{H}(z)$*, the optimal solution of (4.3.8) is*

$$\mathbf{G}_{opt}(e^{j\omega}) = \frac{1}{\lambda(e^{j\omega})}(\mathbf{V}(e^{j\omega}))^H \begin{bmatrix} diag(\lambda_1^{-1}(e^{j\omega}), \cdots, \lambda_K^{-1}(e^{j\omega})) \\ 0_{(N-K)\times K} \end{bmatrix}, \tag{4.3.12}$$

$$\mathbf{D}_{opt}(e^{j\omega}) = \lambda(e^{j\omega}) I_{K\times N}(\mathbf{U}(e^{-j\omega}))^H, \tag{4.3.13}$$

where $\mathbf{U}(e^{j\omega})$*,* $\Lambda(e^{j\omega})$*, and* $\mathbf{V}(e^{\omega})$ *are the singular value decomposition of* $\mathbf{H}(e^{j\omega})$ *for each* ω*, i.e.,*

$$\mathbf{H}(e^{j\omega}) = \mathbf{U}(e^{j\omega})\Lambda(e^{j\omega})\mathbf{V}(e^{\omega}), \tag{4.3.14}$$

where $\mathbf{U}(e^{j\omega})$ *and* $\mathbf{V}(e^{\omega})$ *are two unitary matrices and*

$$\Lambda(e^{j\omega}) = diag(\lambda_1(e^{j\omega}), \lambda_2(e^{j\omega}), \cdots, \lambda_N(e^{j\omega}))$$

with $\lambda_1(e^{j\omega}) \geq \lambda_2(e^{j\omega}) \geq \cdots \geq \lambda_N(e^{j\omega}) \geq 0$ *for each* $\omega \in [0, 2\pi)$*, and*

$$\lambda(e^{j\omega}) = \sqrt{\sum_{k=1}^{K} (\lambda_k(e^{j\omega}))^{-2}}. \tag{4.3.15}$$

From this theorem, one can see that the received signal after the above optimal receiving filter $\mathbf{D}(e^{j\omega})$ is

$$r(n) = x(n) + \xi(n), \tag{4.3.16}$$

where $\xi(n)$ is an AWGN with mean 0 and variance

$$\sigma_\xi^2 = \frac{\sigma_\eta^2}{\gamma(\mathbf{G}_{opt}(z))},$$

which is because $U(e^{-j\omega})$ is unitary in the receiving filter. In other words, the ISI channel $H(z)$ after the optimal MC and the opitmal receiving filter in Fig.4.13 becomes an ISI-free AWGN channel. When $\gamma(\mathbf{G}_{opt}(z)) > 1$, then a coding gain is achieved compared to the uncoded AWGN channel.

From (4.3.12)-(4.3.15), one can see that, for an arbitrary $\mathbf{H}(z)$, the above optimal MC $\mathbf{G}_{opt}(z)$ and the optimal receiving filter $\mathbf{D}_{opt}$ may not have finite impulse responses (FIR), which may cause the implementation problem at both the transmitter and the receiver. We next want to introduce a suboptimal MC design method.

4.3.2 A Sub-optimal Modulated Code Design

There are two ways to simplify the transmitter and the receiver implementations. One way is to only consider the constant matrix part $H(0)$ of the channel matrix $\mathbf{H}(z)$ for the optimal transmitter and receiver design, which was basically used in Section 4.1. This method may not perform well. As an example, let the ISI channel be

$$h = [0.099\ 0.225\ 0.456\ 0.681\ 0.456\ 0.225\ 0.099].$$

Fig.4.14(a) shows the BER performance of constant MC with the $(5,3)$ MC coded ZF-DFE design in Section 4.1.

The other way is to only consider the receiving filter $\mathbf{D}(z)$ to be a constant matrix D. This method simplifies the receiver. In what follows, we will focus on this method. The problem can then be described as follows:

$$\max_{D\mathbf{H}(z)\mathbf{G}(z)=I_K} \gamma(\mathbf{G}(z)) = \max_{D\mathbf{H}(z)\mathbf{G}(z)=I_K} \frac{K^2}{N\,\|D\|_F^2}, \tag{4.3.17}$$

where D are $K \times N$ constant matrices.

There are **two issues** associated with this optimization problem:

(i) The existence of D and polynomial matrix (FIR) $\mathbf{G}(z)$ such that

$$D\mathbf{H}(z)\mathbf{G}(z) = I_K.$$

(ii) The optimal D and $\mathbf{G}(z)$ under the existence.

We study these two issues next.

The FIR Solution Existence

To study this issue, let us first consider a special case when $D = I_{K\times N}$. In this case, the equation

$$D\mathbf{H}(z)\mathbf{G}(z) = I_K$$

becomes

$$I_{K\times N}\mathbf{H}(z)\mathbf{G}(z) = I_K$$

or its transpose

$$\mathbf{G}^T(z)\mathbf{H}^T(z)I_{N\times K} = I_K.$$

The existence of FIR $\mathbf{G}(z)$ thus becomes the existence of the FIR inverse of the polynomial matrix $\mathbf{H}^T(z)I_{N\times K}$, or the existence of the FIR inverse of the ISI channel $H(z)$ using the MC $I_{N\times K}$, which is reduced to the same case studied in Section 2.3. When D is an arbitrary $K \times N$ constant matrix, we have the following existence result.

Theorem 4.3 *For an arbitrary $K \times N$ constant matrix D and an arbitrary finite tap ISI $\mathbf{h}(z)$, there almost surely exists an FIR $N \times K$ polynomial matrix $\mathbf{G}(z)$ such that $D\mathbf{H}(z)\mathbf{G}(z) = I_K$, where $\mathbf{H}(z)$ is the blocked version of $\mathbf{h}(z)$.*

Proof. Similar to the derivation of Theorem 2.1, the existence of the right FIR inverse of $D\mathbf{H}(z)$ is equivalent to the one of $D\mathbf{H}(z^N)$. So, we next only consider $D\mathbf{H}(z^N)$. Using (2.3.10) and absorbing $\mathbf{W}_N^*\Lambda(z)$ into $\mathbf{G}(z)$, the existence of the right FIR inverse of $D\mathbf{H}(z)$ is equivalent to the one of

$$\mathbf{Q}(z) \triangleq D\Lambda^{-1}(z)\mathbf{W}_N\mathbf{V}(z),$$

which is equivalent to the greatest common divisor (gcd) of the determinants of all the $K \times K$ minors of $K \times N$ polynomial matrix $\mathbf{Q}(z)$ to be dz^{n_0} for some non-zero constant d and an integer n_0. Let $\mathbf{Q}_1(z) = D\Lambda^{-1}(z)\mathbf{W}_N$. Due to the diagonal forms of $\mathbf{V}(z)$ and $\Lambda^{-1}(z)$, it is not hard to see that the determinant of the K by K submatrix of $\mathbf{Q}(z)$ at its columns $1 \le l_1 < l_2 < \cdots < l_K \le N$ is

$$c_{l_1 l_2 \cdots l_K} z^{-d_{l_1,l_2\cdots l_K}} \prod_{k=1}^{K} H(zW_N^{l_k}) \tag{4.3.18}$$

where $c_{l_1 l_2 \cdots l_K}$ is a constant and $c_{l_1 l_2 \cdots l_K} z^{-d_{l_1 l_2 \cdots l_K}}$ is the determinant of the K by K submatrix of $\mathbf{Q}_1(z)$ at its columns $1 \le l_1 < l_2 < \cdots < l_K \le N$.

Notice that, when $D = I_{K\times N}$, the above $c_{l_1 l_2 \cdots l_K}$ is the Vandermonde's determinant of a $K \times K$ submatrix of the first K rows of the DFT matrix, which is always nonzero. As long as none of the constants $c_{l_1 l_2 \cdots l_K}$ is zero, the condition (2.3.12) is sufficient for the existence, which holds almost surely for an arbitrarily given polynomial $H(z)$. By noticing the form of $\mathbf{Q}_1(z)$, it is not hard to see that, for an arbitrarily given D, it is almost surely that none of the constants $c_{l_1 l_2 \cdots l_K}$ is zero. This proves Theorem 4.3. ■

From the above proof, one can see that it is similar but more general to the proof of Theorem 2.1 in Section 2.3.

The Optimal Solution

We next want to present the optimal solution of the optimization problem (4.3.17).

Theorem 4.4 *For a finite tap ISI channel $H(z)$ with its blocked version*

$$\mathbf{H}(z) = H(0) + H(1)z^{-1} + \cdots + H(P)z^{-P},$$

let its SVD be $\mathbf{H}(z) = \mathbf{U}(z)\Lambda(z)\mathbf{V}(z)$ *for each complex* $z \neq 0$ *including* $z = \infty$. *If all the components in matrix* $\mathbf{U}(z)$ *are analytic for* $|z| > r$ *for some* $0 < r < 1$, *then the optimal constant receiving* $K \times N$ *filter matrix* D *and the optimal FIR* $N \times K$ *modulated code* $\mathbf{G}(z)$ *based on the criterion (4.3.17) are given by*

$$D_{opt} = \lambda I_{K\times N}(U_0)^\dagger, \tag{4.3.19}$$

$$\mathbf{G}_{opt}(z) = \frac{1}{\lambda}\ arg\ min\left\{\|\mathbf{G}(z)\|_F :\ \frac{1}{\lambda}D_{opt}\mathbf{H}(z)\mathbf{G}(z) = I_K\right\} \tag{4.3.20}$$

where λ *is a scaling factor such that* $\|\mathbf{G}_{opt}(z)\|_F^2 = N$ *and* U_0 *is the left unitary matrix in the SVD of* $H(0)$, *i.e,* $H(0) = U_0\Lambda_0 V_0$.

Proof. From Theorem 4.2, regardless of a scaling factor, the optimal receiving filter $\mathbf{D}(e^{j\omega})$ in the frequency domain is $\bar{\mathbf{D}}(e^{j\omega}) = I_{K\times N}(\mathbf{U}(e^{j\omega}))^\dagger$. As long as the receiving filter is given, the optimal MC $\mathbf{G}(z)$ is the minimum norm solution of the equation $\bar{\mathbf{D}}(z)\mathbf{H}(z)\mathbf{G}(z) = I_K$. Since we are only interested in a constant receiving filter D, the optimal constant receiving filter $\bar{D}$ should be the constant projection of the above $\bar{\mathbf{D}}(e^{j\omega})$ in the finite energy signal space L^2.

By the condition that $\mathbf{U}(z)$ is analytic for $|z| > r$ for some constant $r < 1$, it can be expanded as follows

$$\mathbf{U}(z) = \sum_{n=0}^{\infty} U_n z^{-n},\ \ |z| > r. \tag{4.3.21}$$

By replacing z with $e^{j\omega}$, (4.3.21) becomes

$$\mathbf{U}(e^{j\omega}) = \sum_{n=0}^{\infty} U_n e^{-nj\omega}, \tag{4.3.22}$$

which is the Fourier expansion of $\mathbf{U}(e^{j\omega})$. The constant projection of $\mathbf{U}(e^{j\omega})$ is, thus, U_0. Therefore, the optimal constant approximation of $\bar{\mathbf{D}}(e^{j\omega})$ is $\bar{D} = I_{K\times N}(U_0)^\dagger$. We next want to show that U_0 can be obtained from the SVD of H_0.

Let $z = \infty$ in (4.3.21), we have $\mathbf{U}(z)|_{z=\infty} = U_0$. On the other hand,

$$\mathbf{H}(z)|_{z=\infty} = \mathbf{U}(z)|_{z=\infty}\Lambda(z)|_{z=\infty}\mathbf{V}(z)|_{z=\infty}.$$

While $\mathbf{H}(z)|_{z=\infty} = H(0)$, it implies that the SVD of $H(0)$ is

$$H(0) = U_0\Lambda(z)|_{z=\infty}\mathbf{V}(\mathbf{z})|_{z=\infty}.$$

This proves Theorem 4.4. ■

The analyticity condition of $\mathbf{U}(z)$ in the above theorem is more general than the one of FIR $\mathbf{U}(z)$. However, it is still not easy to check and is rather a theoretical result. On the other hand, this theorem explains the optimality of the MC design from some theoretical perspectives. For more about the analyticity condition, see [111]. This theorem also suggests that the optimal D_{opt} and $\mathbf{G}_{opt}(z)$ can be obtained as follows:

Algorithm

Step 1: Do singular value decomposition of the constant matrix $H(0)$ of $\mathbf{H}(z)$ as $H(0) = U_0\Lambda_0 V_0$ with $\Lambda_0 = \text{diag}(\lambda_1, \cdots, \lambda_N)$ and $\lambda_1 \geq \cdots \geq \lambda_N \geq 0$.

Step 2: Let $\bar{D} = I_{K\times N}(U_0)^\dagger$.

Step 3: Find the minimum norm solution of $\mathbf{G}(z)$ from the equation

$$\bar{D}\mathbf{H}(z)\mathbf{G}(z) = I_K$$

as

$$\bar{\mathbf{G}}(z) = \arg\min\{\|\mathbf{G}(z)\|_F : \ \bar{D}\mathbf{H}(z)\mathbf{G}(z) = I_K\}.$$

Step 4: The optimal MC is

$$\mathbf{G}_{opt}(z) = \frac{\sqrt{N}}{\|\bar{\mathbf{G}}(z)\|_F}\bar{\mathbf{G}}(z). \tag{4.3.23}$$

Step 5: The optimal constant receiving filter matrix is

$$D_{opt} = \frac{\|\bar{\mathbf{G}}(z)\|_F}{\sqrt{N}}\bar{D}. \tag{4.3.24}$$

When the optimal constant projection $\bar{D}$ is obtained, the minimum norm solution of $\mathbf{G}(z)$ in Step 3 is the pseudo-inverse of the linear equations

$$\bar{D}\mathbf{H}(z)\mathbf{G}(z) = I_K$$

of the variables in matrices $G(n)$ in $\mathbf{G}(z) = \sum_n G(n)z^{-n}$. As long as the order of the channel matrix $\mathbf{H}(z)$ is known, the maximal order of the MC $\mathbf{G}(z)$ can be estimated. In our following simulations, the estimated order of $\mathbf{G}(z)$ is the McMillan degree [142] of $\mathbf{H}(z)$.

An important remark is that, although the optimal receiving filter D is based on the constant matrix $H(0)$ of the channel matrix $\mathbf{H}(z)$ for the sake of the receiving filter simplicity, the optimal MC $\mathbf{G}(z)$ at the transmitter is

based on the whole polynomial matrix $\mathbf{H}(z)$. This is a difference between the study in this section and the ones in Section 4.1 and [72, 5]. A difference of the above MC design and the MC coded MMSE-DFE design in Section 4.2 will be explained later.

4.3.3 Delayed Design

The above design can be generalized as follows, if we add a delay z^{-d} into (4.3.4), the optimal design problem in (4.3.17) becomes

$$\max_{D\mathbf{H}(z)\mathbf{G}(z)=z^{-d}I_K} \gamma(\mathbf{G}(z)) = \max_{D\mathbf{H}(z)\mathbf{G}(z)=z^{-d}I_{K\times K}} \frac{K^2}{N\,\|D\|_F^2}. \qquad (4.3.25)$$

For some cases, such delayed MC design performs better. With some minor modification, the optimal solution can be obtained in a similar way as before.

4.3.4 Some Simulation Results

In this section, we will verify the performance of the proposed polynomial MC design via simulations, and compare it with the constant block channel matrix based MC design. Ccomparisons are also made with the TH precoding and the MSE-DFE equalizer. In all the simulations, we assume the input signals are i.i.d. random sequences with zero mean.

New Sub-optimal MC Design vs. Constant MC Design

We first compare the performance of the sub-optimal MC design with the constant channel matrix based design techniques in Section 4.1 and [72, 5, 30]. Without loss of generality, the optimal constant MC ZF-DFE design in Section 4.1 is compared, where the constant channel matrix is equivalent to the one in [72, 5, 30] if L (number of channel taps) zeroes are inserted after each block.

The ISI channel h = [0.099 0.225 0.456 0.681 0.456 0.225 0.099] is tested. The input i.i.d. signals are chosen from binary set $\{-1, +1\}$ and $(5, 3)$ MC are used. The theoretical coding gain (assume no error in DFE) of the optimal constant MC with ZF-DFE design, is: -25dB, while the coding gain of the sub-optimal MC design (with delay $d = 1$), is -14.2dB. Fig.4.14(a) shows their BER simulated performance.

Next, we examine the asymptotic performance of the sub-optimal MC design. Table 4.1 shows the coding gains (losses) of rate 2/3 MC design on

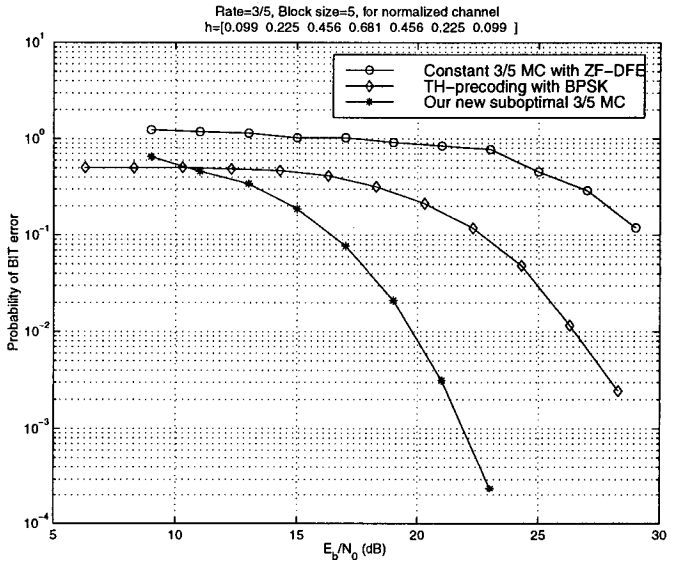

(a)

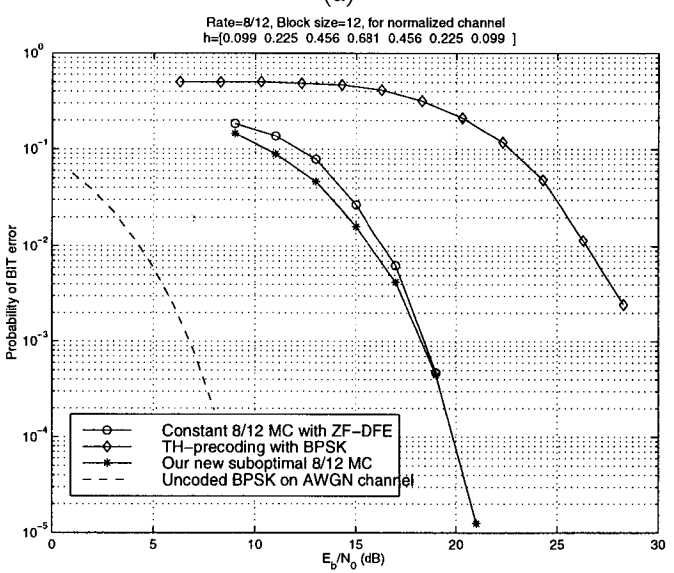

(b)

Figure 4.14: Bit error rate performance of the constant MC with ZF-DFE and our sub-optimal MC.

the above ISI channel, where the coding gain/loss is compared to the ideal AWGN channel.

Table 4.1: Coding gains for different block size.

Block size (N)	Coding gain (theory) of MC with ZF-DFE (dB)	Coding gain of sub-optimal MC (dB)
3	-22.3230	-18.0145 (d=1)
6	-23.9676	-13.4890 (d=1)
9	-13.4793	-12.1571 (d=1)
12	-11.2472	-11.5629
18	-10.1252	-10.2951
∞	-9.20	-9.20

Note: The first three block sizes 3,6 and 9, and the delayed sub-optimal MC design are used with $d = 1$ in (4.3.25). The infinite block size coding gain here is obtained by using sufficient large block size (N=1000). See also [5] for the calculation of the optimal coding gain of infinite block size. The results in the second column in Table 4.1 also apply to the vector coding [72, 30] as we explained before.

As we observed from Table 4.1, the coding gain/loss of both MC design approaches asymptotically to the same optimal value as the block size increases. The reader may notice that there is a small difference between the theoretical coding gain of the constant MC and that of the sub-optimal MC, when the block size is larger than 12 in Table 4.1. The theoretical result on the ZF-DFE is, however, based on the complete cancellation of the IBI from the DFE, which may not be true for spectral null channels, in particular when the channel SNR is not so high, as indicated in Fig.4.14(b).

MC Design vs. TH Precoding

In this subsection, we compare the performances of the MC coding and the TH precoding. The test channel is $h = [0.7071\ 0.7071]$. Two MC designs are tested. One is the simple MC with $\mathbf{D}(z) = D = I_{K\times N}$ in Fig.4.13. In this case, the receiver does not need to implement the filter D and the ISI is completely compensated by the transmitter filter. With this aspect, the MC coding is similar to the TH precoding, where the receiver in the TH precoded system does not need any filter either. Unlike the MC coding, in the TH precoded system, the receiver needs the modulo operation that may degrade the performance when the modulo size is small, such as in the BPSK case. The other MC design is the suboptimal MC design, which

implements the filter D at the receiver. The BER vs. E_b/N_0 curves are shown in Fig.4.15, where the $(4,3)$ and $(4,2)$ MC are used. One can clearly see the improvement over the TH precoding.

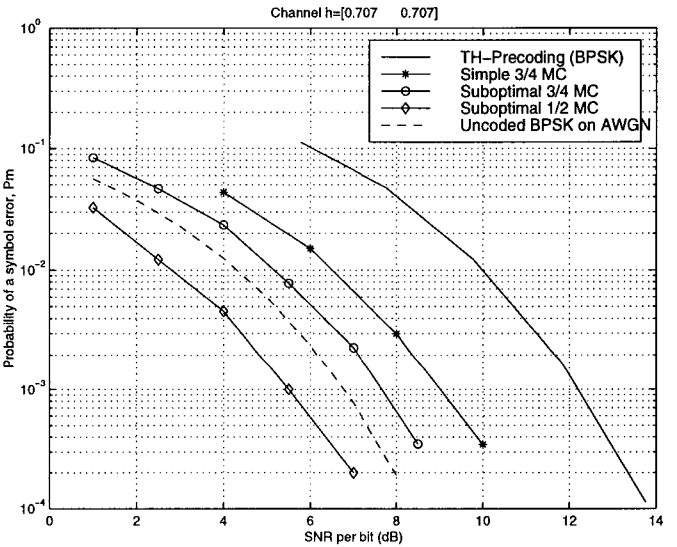

Figure 4.15: Performance comparison of the MC coding and the TH precoding.

Suboptimal MC Design vs. MSE-DFE

We now want to compare the performances between the sub-optimal MC design and the conventional decision feedback equalization (DFE) technique. Consider ISI channel h = [0.417 0.815 0.417] that has severe ISI.

In order to maintain the same data rate for both systems, the binary signal set {-1, +1} is chosen as the input signal sets for the DFE system, and the QPSK signal set {-1,-j,+1,j} is chosen for the 1/2 code rate MC coded system. The block size N for the sub-optimal MC is $N = 10$, i.e., $(10,5)$ MC is used. Fig.4.16 shows their BER performances.

MC Design vs. Turbo-Equalizer

As we explained before, one of the most important advantages of the MC design method proposed in this section is that the MC converts the ISI into the AWGN channel with coding gain compared to the uncoded AWGN

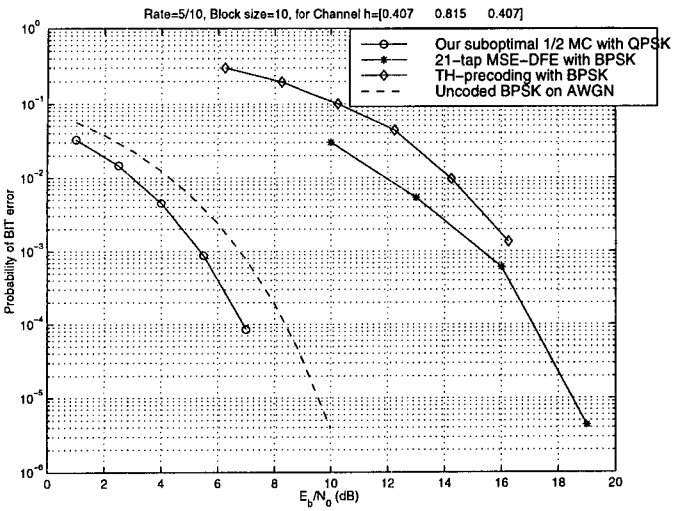

Figure 4.16: Performance comparison of the sub-optimal 1/2 rate MC design of block size 10 and QPSK, and the uncoded MMSE-DFE with 21-taps and BPSK.

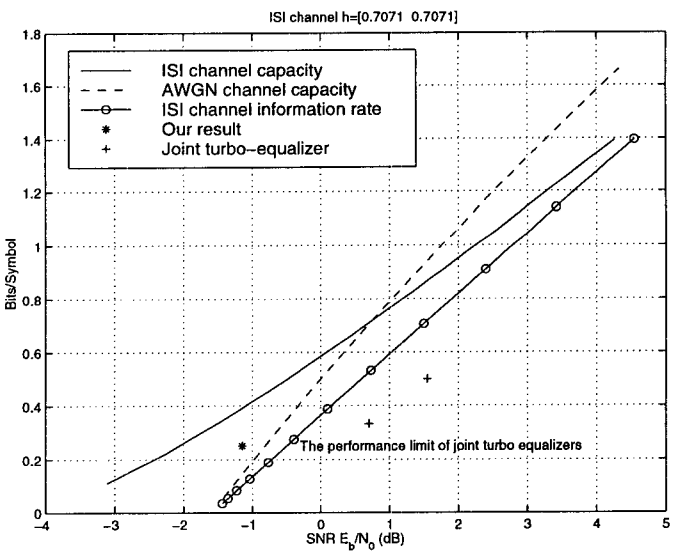

Figure 4.17: Performance comparison with existing turbo-equalizers.

channel if only the first K symbols of each N symbols are maintained at the receiver. This property allows us to add a turbo code before the MC and the BER vs. SNR curves of the turbo code performance over the AWGN channel are then shifted by the coding gain to the left over the ISI channel. This is not achievable for the MC coded ZF-DFE in Section 4.1 and the MMSE-DFE in Section 4.2.

Let us consider the ISI $[0.7071, 0.7071]$. When we choose the MC of size $K = 10$ and $N = 20$, i.e., of rate $1/2$, the suboptimal MC designed from steps 1-5 in Section 4.3.2 has 1.85dB coding gain compared to the uncoded AWGN channel. If the rate $1/2$ turbo code is used before the MC and the turbo decoding is used at the receiver, the performance of the turbo/MC coded ISI channel is shown by $*$ in Fig.4.17, where the turbo code of the BER 10^{-5} at $E_b/N_0 = 0.7$dB is assumed. The current performance limit of the turbo-equalizer (joint turbo and ISI channel equalization) is the information rate curve marked by $\circ$ in Fig.4.17 and the current state of the art turbo-equalizers are marked by $+$, see for example [51, 49]. It is surprising that our result in the ISI channel even outperforms the AWGN channel capacity at $E_b/N_0 = -1.15$dB, which has broken the achievable performance limit of all current joint coded equalization, such as joint turbo-equalizer, i.e., the ISI channel information rate. The above suboptimal $(20, 10)$ MC is listed as follows.

$$\mathbf{G}(z) = \begin{bmatrix}
0.0591 & -0.1181 & 0.1759 & -0.2335 & 0.2885 \\
0.1169 & -0.2249 & 0.3156 & -0.3814 & 0.4163 \\
0.172 & -0.3108 & 0.3898 & -0.3905 & 0.3114 \\
0.223 & -0.368 & 0.3826 & -0.2579 & 0.0318 \\
0.2687 & -0.3909 & 0.296 & -0.0313 & -0.2655 \\
0.3082 & -0.377 & 0.1484 & 0.2072 & -0.4138 \\
0.3406 & -0.328 & -0.0301 & 0.3702 & -0.3309 \\
0.3647 & -0.2488 & -0.2029 & 0.3978 & -0.0637 \\
0.3804 & -0.1463 & -0.3334 & 0.2807 & 0.2392 \\
0.3873 & -0.0299 & -0.3941 & 0.062 & 0.4092 \\
0.3851 & 0.0893 & -0.3732 & -0.1794 & 0.3502 \\
0.3736 & 0.1997 & -0.2753 & -0.3563 & 0.0947 \\
0.3535 & 0.2917 & -0.1201 & -0.4031 & -0.2135 \\
0.3254 & 0.3569 & 0.0608 & -0.3023 & -0.4014 \\
0.2895 & 0.3887 & 0.2288 & -0.0917 & -0.3652 \\
0.2465 & 0.3836 & 0.3483 & 0.1511 & -0.1263 \\
0.1978 & 0.343 & 0.3958 & 0.3392 & 0.1836 \\
0.1451 & 0.2715 & 0.3627 & 0.4058 & 0.3931 \\
0.089 & 0.1749 & 0.2546 & 0.3252 & 0.3838 \\
0.028 & 0.0563 & 0.0853 & 0.1153 & 0.1469
\end{bmatrix}$$

$$
\begin{bmatrix}
-0.3434 & 0.3944 & -0.4453 & 0.4909 & -0.5368 \\
-0.4157 & 0.3774 & -0.3005 & 0.1873 & -0.041 \\
-0.1607 & -0.0338 & 0.2421 & -0.4196 & 0.5337 \\
0.2203 & -0.4103 & 0.4637 & -0.3474 & 0.0817 \\
0.4278 & -0.3581 & 0.0714 & 0.2873 & -0.5275 \\
0.2991 & 0.0688 & -0.4149 & 0.4572 & -0.122 \\
-0.0653 & 0.4237 & -0.3519 & -0.1132 & 0.5182 \\
-0.379 & 0.3354 & 0.1764 & -0.5008 & 0.1615 \\
-0.394 & -0.1031 & 0.4713 & -0.0774 & -0.5059 \\
-0.098 & -0.4332 & 0.1429 & 0.4718 & -0.2 \\
0.275 & -0.3109 & -0.3748 & 0.2571 & 0.4907 \\
0.4306 & 0.1353 & -0.397 & -0.3744 & 0.2374 \\
0.2473 & 0.4404 & 0.1065 & -0.3997 & -0.4727 \\
-0.1296 & 0.2866 & 0.47 & 0.223 & -0.2732 \\
-0.4048 & -0.1668 & 0.2111 & 0.4847 & 0.4522 \\
-0.3626 & -0.4474 & -0.3286 & -0.0395 & 0.3072 \\
-0.0346 & -0.2606 & -0.4334 & -0.5002 & -0.4296 \\
0.3232 & 0.201 & 0.038 & -0.149 & -0.3387 \\
0.4278 & 0.4546 & 0.4619 & 0.4474 & 0.409 \\
0.1805 & 0.2167 & 0.2564 & 0.3006 & 0.3508
\end{bmatrix}
$$

$$
+z^{-1}
\begin{bmatrix}
-0.0054 & -0.011 & -0.0166 & -0.0224 & -0.0286 \\
-0.0038 & -0.0077 & -0.0117 & -0.0158 & -0.0201 \\
0.0012 & 0.0024 & 0.0037 & 0.005 & 0.0064 \\
0.0021 & 0.0043 & 0.0065 & 0.0087 & 0.0111 \\
-0.0007 & -0.0014 & -0.0021 & -0.0029 & -0.0037 \\
-0.0015 & -0.0029 & -0.0044 & -0.006 & -0.0077 \\
0.0006 & 0.0011 & 0.0017 & 0.0023 & 0.0029 \\
0.0011 & 0.0022 & 0.0034 & 0.0046 & 0.0058 \\
-0.0005 & -0.001 & -0.0015 & -0.002 & -0.0026 \\
-0.0009 & -0.0018 & -0.0027 & -0.0037 & -0.0047 \\
0.0005 & 0.001 & 0.0014 & 0.002 & 0.0025 \\
0.0008 & 0.0015 & 0.0023 & 0.0031 & 0.004 \\
-0.0005 & -0.001 & -0.0014 & -0.002 & -0.0025 \\
-0.0007 & -0.0013 & -0.002 & -0.0027 & -0.0034 \\
0.0005 & 0.001 & 0.0015 & 0.002 & 0.0026 \\
0.0006 & 0.0011 & 0.0017 & 0.0023 & 0.003 \\
-0.0005 & -0.0011 & -0.0016 & -0.0022 & -0.0028 \\
-0.0005 & -0.001 & -0.0015 & -0.002 & -0.0026 \\
0.0007 & 0.0014 & 0.0021 & 0.0028 & 0.0036 \\
0 & 0 & 0 & 0 & 0
\end{bmatrix}
$$

$$
\begin{bmatrix}
-0.0351 & -0.0422 & -0.0499 & -0.0585 & -0.0683 \\
-0.0247 & -0.0296 & -0.0351 & -0.0411 & -0.048 \\
0.0079 & 0.0094 & 0.0112 & 0.0131 & 0.0153 \\
0.0137 & 0.0164 & 0.0194 & 0.0228 & 0.0266 \\
-0.0045 & -0.0054 & -0.0064 & -0.0075 & -0.0088 \\
-0.0094 & -0.0113 & -0.0134 & -0.0157 & -0.0183 \\
0.0036 & 0.0043 & 0.0051 & 0.0059 & 0.0069 \\
0.0072 & 0.0086 & 0.0102 & 0.0119 & 0.0139 \\
-0.0032 & -0.0038 & -0.0045 & -0.0053 & -0.0062 \\
-0.0058 & -0.007 & -0.0082 & -0.0097 & -0.0113 \\
0.0031 & 0.0037 & 0.0043 & 0.0051 & 0.006 \\
0.0049 & 0.0059 & 0.0069 & 0.0081 & 0.0095 \\
-0.0031 & -0.0037 & -0.0043 & -0.0051 & -0.006 \\
-0.0042 & -0.0051 & -0.006 & -0.007 & -0.0082 \\
0.0032 & 0.0038 & 0.0045 & 0.0053 & 0.0062 \\
0.0037 & 0.0044 & 0.0052 & 0.0061 & 0.0071 \\
-0.0034 & -0.0041 & -0.0049 & -0.0057 & -0.0067 \\
-0.0032 & -0.0038 & -0.0045 & -0.0053 & -0.0061 \\
0.0044 & 0.0053 & 0.0063 & 0.0074 & 0.0086 \\
0 & 0 & 0 & 0 & 0
\end{bmatrix}
$$

Chapter 5

Capacity and Information Rates for Modulated Code Coded Intersymbol Interference Channels

In Chapter 2, we studied the distance property of the MC coded ISI channel and showed that, for any finite tap ISI channel, there exists an MC with coding gain compared to the uncoded AWGN channel. This tells that using a proper MC at the transmitter and the joint MLSE at the receiver, the BER vs. E_b/N_0 performance of the MC coded ISI channel is better than the one of the uncoded AWGN channel. In this chapter, we want to study the capacity and the information rates of the MC coded discrete-time Gaussian channel with ISI (or ISI channel with AWGN) (1.0.2). We first derive some lower bounds and then prove the existence of MC such that the MC coded ISI channel has larger information rates than the ISI channel itself does at low channel SNR. This suggests a combination of turbo and MC codings for an ISI channel, which is also discussed in this chapter. The results in this chapter are summarized from [45, 184].

5.1 Some Lower Bounds of Capacity and Information Rates

We first derive some lower bounds for the capacity and information rates of an MC coded ISI channel. From (2.3.6), the MC coded system becomes the following multi-input and multi-output (MIMO) system (or multivariate channel):

$$\mathbf{Y}(z) = \mathbf{C}(z)\mathbf{X}(z) + \Xi(z) = \mathbf{H}(z)\mathbf{G}(z)\mathbf{X}(z) + \Xi(z), \tag{5.1.1}$$

where $\Xi(n)$ is an $N \times 1$ vector sequence and all components are i.i.d. Gaussian and is blocked from $\eta(n)$ in (1.0.2). From (5.1.1), one can see that the MC coded system becomes a K-input and N-output system. To study its capacity and information rates, we need the following capacity result for an N-input and N-output multivariate system obtained by Brandenburg and Wyner [21]. Let an N-input and N-output multivariate channel be

$$\mathbf{Y}(z) = \mathbf{P}(z)\mathbf{X}(z) + \Xi(z), \tag{5.1.2}$$

where all components in the noise $\Xi(n)$ are i.i.d. Gaussian and with the same statistics of $\eta(n)$ in (1.0.2). Then, the capacity of the multivariate channel (5.1.2) is

$$C(S,N) = \frac{1}{4\pi}\sum_{k=1}^{N}\int_{-\pi}^{\pi} d\theta \max\left\{0, \log_2 \frac{2\lambda_k(\theta)K_S}{N_0}\right\}, \tag{5.1.3}$$

where

$$\frac{1}{2\pi}\sum_{k=1}^{N}\int_{-\pi}^{\pi} d\theta \max\left\{0, K_S - \frac{N_0}{2}\lambda_k^{-1}(\theta)\right\} = S, \tag{5.1.4}$$

and $\lambda_k(\theta)$, $k = 1, 2, ..., N$, are the N eigenvalues of matrix $\mathbf{P}^{\dagger}(e^{j\theta})\mathbf{P}(e^{j\theta})$ for each θ with $-\pi \le \theta < \pi$, the dagger † denotes the complex conjugate transpose of matrix $\mathbf{P}(e^{j\theta})$, and S denotes the mean norm squared, i.e., $\|X\|^2$, of $N \times 1$ vectors X and is treated as the signal mean power of $N \times 1$ vectors. The information rate of the multivariate channel (5.1.2) can be derived similar to (1.3.3):

$$C_{i.i.d.}(S,N) = \frac{1}{4\pi}\sum_{k=1}^{N}\int_{-\pi}^{\pi} \log_2\left[1 + \frac{2S\lambda_k(\theta)}{NN_0}\right] d\theta, \tag{5.1.5}$$

where $\lambda_k(\theta)$ are the same as in the capacity (5.1.3). Notice that the units of the capacity $C(S,N)$ and the information rates $C_{i.i.d.}(S,N)$ are bits per

vector symbol of size N, i.e., bits per N symbols. The signal mean power S is also the mean power of vectors of size N, i.e., the mean power per N symbols.

With the above results it is not hard to derive some lower bounds for the capacity and the information rates of the MC coded system in (5.1.1). Notice that the MC coded ISI channel in (5.1.1) does not have the same number of inputs and outputs as in the multivariate channel in (5.1.2) studied by Brandenburg and Wyner [21].

For each θ, $-\pi \leq \theta < \pi$, let the singular value decomposition of $\mathbf{C}(e^{j\theta})$ be

$$\mathbf{C}(e^{j\theta}) = \mathbf{H}(e^{j\theta})\mathbf{G}(e^{j\theta}) = \mathbf{U}(e^{j\theta})\Lambda(e^{j\theta})\mathbf{V}(e^{j\theta}), \tag{5.1.6}$$

where $\mathbf{U}(e^{j\theta})$ and $\mathbf{V}(e^{j\theta})$ are $N \times N$ and $K \times K$ unitary matrices and

$$\Lambda(e^{j\theta}) = \begin{bmatrix} \bar{\Lambda}(e^{j\theta}) \\ 0_{(N-K)\times K} \end{bmatrix}, \tag{5.1.7}$$

where

$$\bar{\Lambda}(e^{j\theta}) = \mathrm{diag}(\bar{\lambda}_1(\theta), \cdots, \bar{\lambda}_K(\theta)), \tag{5.1.8}$$

$0_{(N-K)\times K}$ is the $(N-K)$ by K all zero matrix, and $\bar{\lambda}_k(\theta) \geq 0$ are the singular values of $\mathbf{C}(e^{j\theta})$. In what follows, we assume $\bar{\lambda}_k(\theta) > 0$, $1 \leq k \leq K$, which is possible by employing MC even when the ISI channel $H(z)$ has spectral nulls as we have seen in Section 2.3.1. Then, (5.1.1) becomes

$$\mathbf{Y}_1(e^{j\theta}) = \Lambda(e^{j\theta})\mathbf{X}_1(e^{j\theta}) + \Xi_1(e^{j\theta}), \tag{5.1.9}$$

where

$$\mathbf{Y}_1(e^{j\theta}) = \mathbf{U}^\dagger(e^{j\theta})\mathbf{Y}(e^{j\theta}),\ \mathbf{X}_1(e^{j\theta}) = \mathbf{V}(e^{j\theta})\mathbf{X}(e^{j\theta}),$$

$$\Xi_1(e^{j\theta}) = \mathbf{U}^\dagger(e^{j\theta})\Xi(e^{j\theta}). \tag{5.1.10}$$

Since $\mathbf{U}(e^{j\theta})$ and $\mathbf{V}(e^{j\theta})$ are both unitary, the capacity and the information rates of the system (5.1.9) are the same as the ones of the system (5.1.1), i.e.,

$$\sup_{X_1} I(X_1, Y_1) = \sup_{X} I(X, Y), \quad \sup_{i.i.d.\ X_1} I(X_1, Y_1) = \sup_{i.i.d.\ X} I(X, Y). \tag{5.1.11}$$

Let

$$\mathbf{Y}_2(e^{j\theta}) = \bar{\Lambda}(e^{j\theta})\mathbf{X}_1(e^{j\theta}) + \Xi_2(e^{j\theta}), \tag{5.1.12}$$

where $\Xi_2(e^{j\theta})$ only takes the first K rows of $\Xi_1(e^{j\theta})$ and $\bar{\Lambda}(e^{j\theta})$ is defined in (5.1.8). Since the system (5.1.12) is obtained by cutting the last $N-K$ rows from the system (5.1.9), the information is not increased, i.e., from (5.1.11),

$$\sup_{X} I(X,Y) \geq \sup_{X_1} I(X_1,Y_2), \quad \sup_{i.i.d.\ X} I(X,Y) \geq \sup_{i.i.d.\ X_1} I(X_1,Y_2). \quad (5.1.13)$$

Notice that the system (5.1.13) is now a K-input and K-output multivariate system and therefore we may apply the Brandenburg and Wyner's capacity and information rate results (5.1.3) and (5.1.5). Although the MC coded ISI system can be converted to an MIMO system (5.1.1), it is however a single-input single-output (SISO) system. Therefore, the units for vectors in (5.1.3) and (5.1.5) need to be changed to the units for symbols. By doing so, we obtain the following lower bounds for the capacity and the information rates of the MC coded ISI channel. The capacity, $C_{MC}(E_s)$, is lower bounded by

$$C_{MC}(E_s) \geq \frac{1}{4\pi N} \sum_{k=1}^{K} \int_{-\pi}^{\pi} d\theta \max\left\{0, \log_2 \frac{2\lambda_k(\theta) K_S}{N_0}\right\}, \quad (5.1.14)$$

where

$$\frac{1}{2\pi} \sum_{k=1}^{K} \int_{-\pi}^{\pi} d\theta \max\left\{0, K_S - \frac{N_0}{2}\lambda_k^{-1}(\theta)\right\} = KE_s, \quad (5.1.15)$$

and $\lambda_k(\theta)$, $k = 1, 2, ..., K$, are the K eigenvalues of the following matrix

$$\mathbf{C}^{\dagger}(e^{j\theta})\mathbf{C}(e^{j\theta}) = \mathbf{G}^{\dagger}(e^{j\theta})\mathbf{H}^{\dagger}(e^{j\theta})\mathbf{H}(e^{j\theta})\mathbf{G}(e^{j\theta}). \quad (5.1.16)$$

The information rates, $C_{I,MC}(E_s)$, are lower bounded by

$$C_{i.i.d.,MC}(E_s) \geq \frac{1}{4\pi N} \sum_{k=1}^{K} \int_{-\pi}^{\pi} \log_2 \left[1 + \frac{2E_s\lambda_k(\theta)}{N_0}\right] d\theta, \quad (5.1.17)$$

where $\lambda_k(\theta)$ are the same as in the capacity (5.1.14).

Note that the MC encoding causes the rate K/N loss, which has been taken into the account in the above lower bounds. Otherwise, the factor $1/N$ in (5.1.14) and (5.1.17) would be $1/K$.

5.2 MC Existence with Increased Information Rates

With the lower bound (5.1.17) of the information rates of the MC coded ISI channel, in this subsection we want to prove the following existence result

by constructing an MC for an arbitrarily given finite tap ISI channel $H(z)$.

Theorem 5.1 *For any finite tap ISI channel* $H(z) = \sum_{k=0}^{\Gamma-1} h(k)z^{-k}$ *with* $h(0) \neq 0$, $h(\Gamma-1) \neq 0$, *and* $\Gamma > 1$, *there exists an MC such that, when the SNR,* E_s/N_0, *is sufficiently low, the MC coded ISI channels have larger information rates than the original ISI channel, i.e.,*

$$C_{i.i.d.,MC}(E_s) > C_{i.i.d.}(E_s), \quad \textit{when } E_s \textit{ is small,} \tag{5.2.1}$$

where the rate reduction due to the MC encoding has been taken into the account in the MC coded ISI channel.

Proof. Without loss of generality, we may assume that the ISI channel $H(z)$ is normalized as in (2.3.1). Consider $N \times 1$ modulated code $G = [g_1, \cdots, g_N]^T$ with

$$\sum_{k=1}^{N} |g_k|^2 = N, \tag{5.2.2}$$

where $N \geq 2\Gamma - 1$ is chosen. The condition $N \geq 2\Gamma - 1$ will be used later for ensuring the MC existence. In this case, the blocked version in (2.3.3) of the ISI channel $H(z)$ can be written as

$$\mathbf{H}(z) = H(0) + H(1)z^{-1}, \tag{5.2.3}$$

where

$$H(0) =$$

$$\begin{bmatrix} h(0) & 0 & \cdots & 0 & 0 & \cdots & 0 & \cdots & 0 \\ h(1) & h(0) & \cdots & 0 & 0 & \cdots & 0 & \cdots & 0 \\ \vdots & \vdots & \vdots & \vdots & \vdots & \vdots & \vdots & \vdots & \vdots \\ h(\Gamma-1) & h(\Gamma-2) & \cdots & h(0) & 0 & \cdots & 0 & \cdots & 0 \\ 0 & h(\Gamma-1) & \cdots & h(1) & h(0) & \cdots & 0 & \cdots & 0 \\ \vdots & \vdots & \vdots & \vdots & \vdots & \vdots & \vdots & \vdots & \vdots \\ 0 & 0 & \cdots & 0 & 0 & \cdots & h(\Gamma-1) & \cdots & h(0) \end{bmatrix}_{N \times N} \tag{5.2.4}$$

and

$$H(1) =$$

$$\begin{bmatrix} 0 & 0 & \cdots & 0 & h(\Gamma-1) & h(\Gamma-2) & \cdots & h(1) \\ 0 & 0 & \cdots & 0 & 0 & h(\Gamma-1) & \cdots & h(2) \\ \vdots & \vdots & \vdots & \vdots & \vdots & \vdots & \vdots & \vdots \\ 0 & 0 & \cdots & 0 & 0 & 0 & \cdots & h(\Gamma-1) \\ 0 & 0 & \cdots & 0 & 0 & 0 & \cdots & 0 \\ \vdots & \vdots & \vdots & \vdots & \vdots & \vdots & \vdots & \vdots \\ 0 & 0 & \cdots & 0 & 0 & 0 & \cdots & 0 \end{bmatrix}_{N\times N} \tag{5.2.5}$$

Let $g_{N-\Gamma+2} = \cdots = g_N = 0$ in the MC G, i.e.,

$$G = [g_1, \cdots, g_{N-\Gamma+1}, 0, \cdots, 0]^T, \quad \text{and} \quad \sum_{k=1}^{N-\Gamma+1} |g_k|^2 = N. \tag{5.2.6}$$

In this case, it is not hard to see

$$H(1)G = 0. \tag{5.2.7}$$

In the following, we want to apply the information rate lower bound (5.1.17) to prove the existence. To do so, we first need to calculate the eigenvalues of the matrix $\mathbf{C}^\dagger(e^{j\theta})\mathbf{C}(e^{j\theta})$ in (5.1.16). By (5.2.3) and (5.2.7), we have

$$\mathbf{C}^\dagger(e^{j\theta})\mathbf{C}(e^{j\theta})$$

$$= G^\dagger(H^\dagger(0) + H^\dagger(1)e^{-j\theta})(H(0) + H(1)e^{j\theta})G = G^\dagger H^\dagger(0)H(0)G. \tag{5.2.8}$$

Let $H_1(0)$ be the submatrix of the first $N-\Gamma+1$ columns of $H(0)$, i.e., $H(0) = [H_1[0], H_2(0)]$. By the normalization of $H(z)$, i.e.,

$$\sum_{k=0}^{\Gamma-1} |h(k)|^2 = 1.$$

We have

$$H^\dagger(0)H(0) = \begin{bmatrix} H_{11} & H_{12} \\ H_{12}^\dagger & H_{22} \end{bmatrix}, \tag{5.2.9}$$

where H_{11} is the following nonnegative definite matrix

$$H_{11} = H_1^\dagger(0)H_1(0) =$$

$$\begin{bmatrix} 1 & h_{1,2} & \cdots & h_{1,N-\Gamma+1} \\ h_{1,2}^* & 1 & \cdots & h_{2,N-\Gamma} \\ \vdots & \vdots & \vdots & \vdots \\ h_{1,N-\Gamma+1}^* & h_{2,N-\Gamma}^* & \cdots & 1 \end{bmatrix}_{(N-\Gamma+1)\times(N-\Gamma+1)} \tag{5.2.10}$$

Let $G_1 = [g_1, \cdots, g_{N-\Gamma+1}]^T$. Then,

$$\mathbf{C}^\dagger(e^{j\theta})\mathbf{C}(e^{j\theta}) = G^\dagger H^\dagger(0)H(0)G = G_1^\dagger H_{11} G_1. \tag{5.2.11}$$

Let H_{11} have the following diagonalization

$$H_{11} = U^\dagger \Lambda U, \tag{5.2.12}$$

where U is an $(N-\Gamma+1)\times(N-\Gamma+1)$ unitary constant matrix and

$$\Lambda = \mathrm{diag}(\lambda_1, \cdots, \lambda_{N-\Gamma+1})$$

and $\lambda_1 \geq \cdots \geq \lambda_{N-\Gamma+1} \geq 0$ are the eigenvalues of H_{11}. Clearly, by (5.2.10) we have

$$\sum_{k=1}^{N-\Gamma+1} \lambda_k = \mathrm{trace}(H_{11}) = N-\Gamma+1. \tag{5.2.13}$$

We claim that, under the condition on the ISI channel length, $\Gamma > 1$, the following inequality holds:

$$\lambda_{N-\Gamma+1} < 1. \tag{5.2.14}$$

In fact, if $\lambda_{N-\Gamma+1} \geq 1$. By (5.2.13) and $\lambda_1 \geq \cdots \geq \lambda_{N-\Gamma+1} \geq 0$, we have

$$\lambda_1 = \cdots = \lambda_{N-\Gamma+1} = 1.$$

In other words, the matrix H_{11} is the $(N-\Gamma+1)\times(N-\Gamma+1)$ identity matrix $I_{N-\Gamma+1}$, which is not possible when $h(0) \neq 0$, $h_{\Gamma-1} \neq 0$, $\Gamma > 1$, $N \geq 2\Gamma - 1$, and the vector $\{h(k)\}_{k=0}^{\Gamma-1}$ has the unit norm.

By (5.2.13) and (5.2.14), we have

$$\sum_{k=1}^{N-\Gamma} \lambda_k > N-\Gamma. \tag{5.2.15}$$

In other words, if we let

$$\kappa = \frac{\sum_{k=1}^{N-\Gamma} \lambda_k}{N-\Gamma}, \tag{5.2.16}$$

then,

$$\kappa > 1. \tag{5.2.17}$$

We are now ready to design the MC G such that the MC coded ISI channel has larger information rates than the ISI channel itself does. Let

$$F = UG_1 = [f_1, f_2, \cdots, f_{N-\Gamma+1}]^T. \tag{5.2.18}$$

Then, by (5.2.11), (5.2.12), and (5.2.18), we have

$$\mathbf{C}^\dagger(e^{j\theta})\mathbf{C}(e^{j\theta}) = F^\dagger \Lambda F = \sum_{k=1}^{N-\Gamma+1} |f_k|^2 \lambda_k. \tag{5.2.19}$$

Let

$$f_1 = f_2 = \cdots = f_{N-\Gamma} = \sqrt{\frac{N}{N-\Gamma}}, \quad \text{and } f_{N-\Gamma+1} = 0. \tag{5.2.20}$$

Clearly,

$$\sum_{k=1}^{N-\Gamma+1} |f_k|^2 = N.$$

Since U is unitary, by (5.2.18) we have

$$G_1 = U^\dagger F, \quad \text{and} \quad \sum_{k=1}^{N-\Gamma+1} |g_k|^2 = N, \tag{5.2.21}$$

which ensures that the MC G in (5.2.6) is a normalized $N \times 1$ MC. We next want to prove that this MC is what we wanted for the existence proof.

In fact, by (5.2.19), (5.2.20) and (5.2.16), we have

$$\mathbf{C}^\dagger(e^{j\theta})\mathbf{C}(e^{j\theta}) = N\kappa = \lambda(\theta), \tag{5.2.22}$$

where $\lambda(\theta)$ is the only eigenvalue of $\mathbf{C}^\dagger(e^{j\theta})\mathbf{C}(e^{j\theta})$ and it is also θ independent. Using the information rate lower bound (5.1.17) we have

$$C_{I,MC}(E_s) \geq \frac{1}{2N} \log_2 \left[1 + \frac{2E_s}{N_0} N\kappa\right]. \tag{5.2.23}$$

By Jensen's inequality, it is not hard to prove that the capacity of the AWGN channel is greater than or equal to the information rates of any ISI channel with AWGN, i.e.,

$$C_{i.i.d.}(E_s) = \frac{1}{4\pi} \int_{-\pi}^{\pi} \log_2 \left[1 + 2\frac{E_s}{N_0} |H(e^{j\theta})|^2\right] d\theta \leq \frac{1}{2} \log_2 \left[1 + 2\frac{E_s}{N_0}\right]. \tag{5.2.24}$$

Therefore, by (5.2.23) and (5.2.24) we have

$$\frac{C_{i.i.d.,MC}(E_s)}{C_{i.i.d.}(E_s)} \geq \frac{\frac{1}{2N}\log_2\left[1+\frac{2E_s}{N_0}N\kappa\right]}{\frac{1}{2}\log_2\left[1+2\frac{E_s}{N_0}\right]}. \tag{5.2.25}$$

Since the limit of the right-hand side of (5.2.25) is κ when E_s/N_0 goes to 0, i.e.,

$$\frac{\frac{1}{2N}\log_2\left[1+\frac{2E_s}{N_0}N\kappa\right]}{\frac{1}{2}\log_2\left[1+2\frac{E_s}{N_0}\right]} \to \kappa > 1 \quad \text{as} \quad \frac{E_s}{N_0} \to 0. \tag{5.2.26}$$

The inequalities (5.2.25) and (5.2.26), thus, imply that, for any $N \geq 2\Gamma - 1$, there always exists $E > 0$ such that when $E_s/N_0 < E$, we have

$$C_{i.i.d.,MC}(E_s) > C_{i.i.d.}(E_s),$$

which proves Theorem 5.1. ■

The above proof is constructive and the MC to achieve the larger information rates is given in (5.2.6), (5.2.18), (5.2.20), and (5.2.21). From the proof (5.2.14)-(5.2.15), one can see that the ISI provides the information rate gain at low SNR. The inequalities (5.2.23)-(5.2.25) in the above proof also provide the following lower bound of the information rate gain of the MC coded ISI over the ones of the ISI itself.

Corollary 5.1 *For a normalized ISI channel of length Γ with AWGN, the ratio of the information rates of the MC coded ISI channel over the ones of the ISI channel itself is lower bounded by*

$$\frac{C_{i.i.d.,MC}(E_s)}{C_{i.i.d.}(E_s)} \geq \frac{2\pi\log_2\left[1+\frac{2E_s}{N_0}N\kappa\right]}{N\int_{-\pi}^{\pi}\log_2\left[1+2\frac{E_s}{N_0}|H(e^{j\theta})|^2\right]d\theta} \geq \frac{\log_2\left[1+\frac{2E_s}{N_0}N\kappa\right]}{N\log_2\left[1+2\frac{E_s}{N_0}\right]}, \tag{5.2.27}$$

where κ is defined in (5.2.16) and $N \geq 2\Gamma - 1$.

The above lower bound can be evaluated when the ISI channel $H(z)$ is known.

5.3 Numerical Results

In this section, we want to evaluate the capacities (5.1.14) and the information rates (5.1.17) of some MC coded ISI channels and compare them

with the ones of the ISI channels themselves. We consider two different ISI channels:

Channel A: [0.5, 0.5, -0.5, -0.5], which is a spectral null channel;

Channel B: $[\sqrt{2/3}, \sqrt{1/3}] \approx [0.8165, 0.5774]$, which does not have spectral null.

The MC G_A for Channel A is chosen from Section 3.3, which is obtained by using the joint MLSE. The $(4, 2)$ MC G_A is

$$G_A = \begin{bmatrix} -0.9390 & 0.3440 \\ 0.1302 & 0.9915 \\ 0.9951 & -0.0990 \\ 0.3641 & -0.9314 \end{bmatrix} \tag{5.3.1}$$

The coding gain for the MC in (5.3.1) is $\gamma_{ISI} = 2.127$dB compared to the

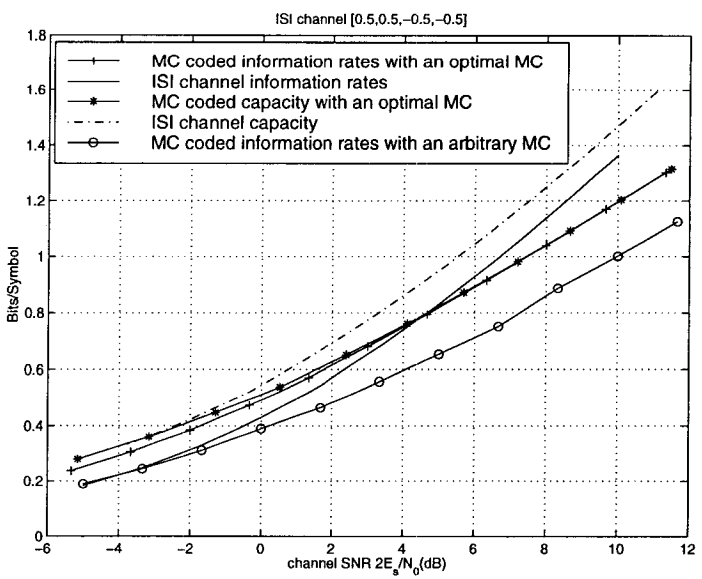

Figure 5.1: Channel A: MC coded and uncoded information rates. The curves for the information rates of the MC coded channels are the lower bounds.

uncoded BPSK over AWGN channel. Fig.5.1 shows the information rates

and the capacities for Channel A. The information rates of Channel A with AWGN and without MC coding are shown by the solid line. The lower bound (5.1.17) of the information rates of the MC coded Channel A with AWGN are marked by +, where the MC in (5.3.1) is used. One can see that the MC coded information rates are above the uncoded information rates when the channel SNR $2E_s/N_0$ are below 4.7dB. The capacity of Channel A with AWGN is shown by the dashdot line and the capacity lower bound (5.1.14) of the MC coded Channel A with AWGN is marked by $*$. Although the capacity and the information rates of the uncoded Channel A have a significant gap when the SNR is below 12dB, their corresponding ones of the MC coded channel are rather close, which is due to that the MC encoding improves the ISI channel condition. The last curve marked by $\circ$ is the lower bound of the information rates of the MC coded Channel A with AWGN and the MC is arbitrarily chosen, which is far below the rest curves.

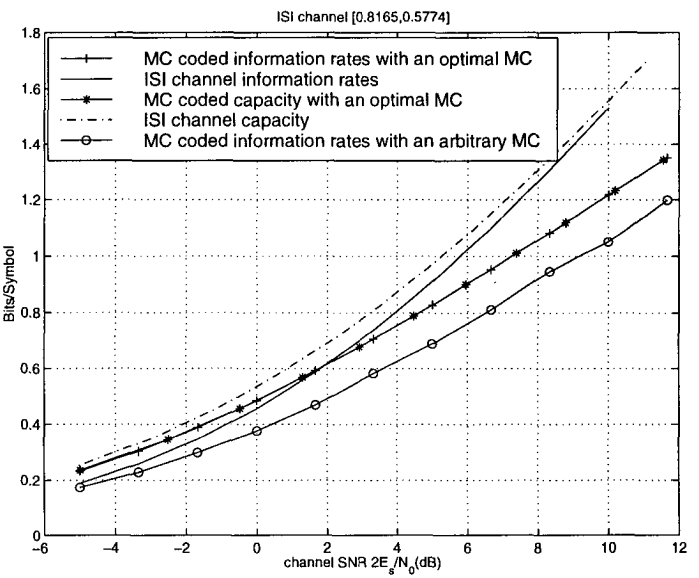

Figure 5.2: Channel B: MC coded and uncoded information rates. The curves for the information rates of the MC coded channels are the lower bounds.

The MC G_B for Channel B is chosen from Section 4.1, which is obtained by using the MC coded ZF-DFE criterion. The $(2,1)$ MC G_B is

$$G_B = \begin{bmatrix} 1.1547 \\ 0.8165 \end{bmatrix}. \tag{5.3.2}$$

The coding gain based on the MC coded ZF-DFE is 1.25dB and the coding gain based on the joint MLSE is $\gamma_{ISI} = 1.6$dB, where both of them are compared to the uncoded BPSK over AWGN channel. Fig.5.2 shows the information rates and the capacities for Channel B. The information rates of Channel B with AWGN and without MC coding are shown by the solid line. The lower bound (5.1.17) of the information rates of the MC coded Channel B with AWGN are marked by $+$, where the MC in (5.3.2) is used. One can see that the MC coded information rates are above the uncoded information rates when the channel SNR $2E_s/N_0$ are below 2dB. The capacity of Channel B with AWGN is shown by the dashdot line and the capacity lower bound (5.1.14) of the MC coded Channel A with AWGN is marked by $*$. Similar to Channel A, the capacity and the information rate lower bounds of the MC coded Channel B almost coincide due to the channel condition improvement of the MC encoding. The last curve marked by $\circ$ is the information rate lower bound of the MC coded Channel B with AWGN and the MC is arbitrarily chosen, which is much worse than the one using the MC (5.3.2) with certain optimality.

The above examples are, by no means, of any special purposes. They are arbitrarily chosen from the previous chapters. From these two examples, one can see that, the worse the ISI channel spectrum is, the better the MC improves the information rates, and the closer the information rate lower bound and the capacity lower bound of the MC coded ISI channel are.

5.4 Combined Turbo and MC Coding

Turbo codes [16, 15, 37] have been used to approach the AWGN channel capacity at relatively low channel SNR. For an ISI channel, joint turbo equalizations have been also studied in for example [39, 110, 50], where the performance is bounded by the ISI channel information rates, i.e., the maximal mutual information when the input is i.i.d. In the meantime, for MC, as we have seen in the previous section, the MC coded ISI channel has higher information rates than the original ISI channel does when the channel SNR is relatively low. This suggests a combination of turbo and MC codings.

In this section, we propose a joint iterative decoding of combined turbo and MC coded ISI channel. In the combined turbo and MC coded ISI sys-

tem, we use the MC to encode the symbols generated from the turbo encoder after multiplexing/interleaving/binary-to-complex-symbol mapping. At the receiver, we combine the soft MC decoder with the turbo decoder through the exchange of two kinds of extrinsic information. Simulation results show that the combination of the turbo and MC encoding/decoding on the ISI channel significantly outperforms the current turbo equalization techniques. Our examples show that the combined system may outperform the capacity of the AWGN channel and the ISI channel information rates at low SNR. The results in this section are from [184].

5.4.1 Joint Turbo and Modulated Code Encoding

The structure of the combination of the turbo code and the MC is illustrated in Fig.5.3, where π_1 and π_2 are two interleavers. The turbo code is similar to the one used in [16], i.e., the parallel concatenated convolutional code (PCCC). The MC can be designed in several ways, for instance, the optimal design in Section 3.4 and the suboptimal designs in Section 4.

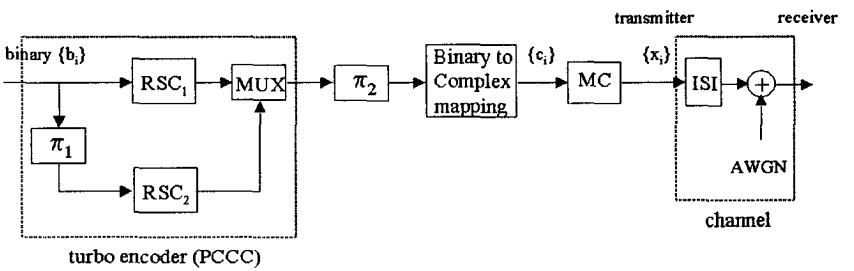

Figure 5.3: The structure of the combination of turbo and modulated encoding.

In Fig.5.3, the information bits $\{b_i\}$ are first encoded by the PCCC turbo encoder, and after multiplexing, interleaving and symbol mapping, the resulted symbols $\{c_i\}$ are then fed into the MC. Finally the coded data $\{x_i\}$ is transmitted over the ISI channel.

5.4.2 Joint Soft Turbo and MC Decoding

The decoding structure is illustrated in Fig.5.4, which consists of three basic soft-in and soft-out (SISO) decoding blocks that originated from the SISO APP module in [14]. The SISO decoding block is a four port

device that accepts two inputs I_u and I_c. The I_u represents the sequence of the probabilities of the input bits (or symbols) $\{u_k\}$ in log domain, i.e., $I_u = \{\log P(u_k)\}_{k=1}^{N}$, where N is the length of the data sequence. I_c represents the sequence of the probabilities of the output bits (or symbols) $\{c_k\}$, i.e., $I_c = \{\log P(c_k)\}_{k=1}^{N}$.

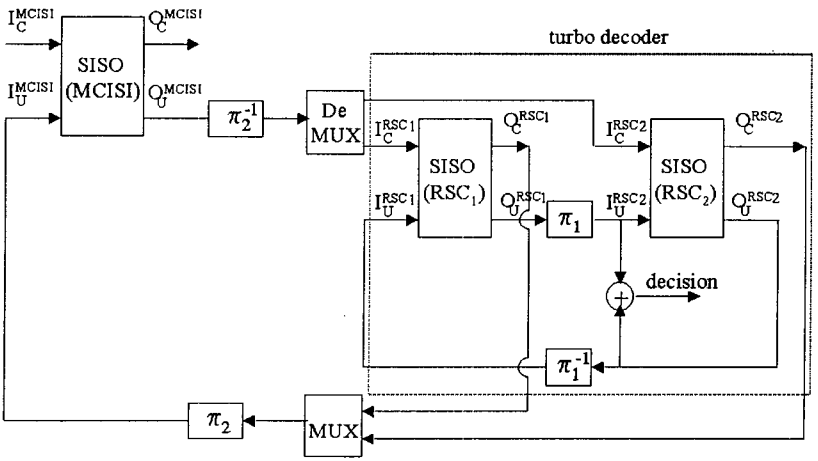

Figure 5.4: The structure of the joint soft turbo decoder and soft modulated code decoder.

Based on the knowledge of the trellis diagram, which can be either of the convolutional code or of the MC coded ISI, the SISO decoder generates two outputs: O_u and O_c, where O_u is the sequence of the new estimated probabilities of the input bits (or symbols) after the decoder excludes the priorly known values I_u, and O_c is the sequence of the new estimated probabilities of the output bits (or symbols) after the decoder excludes the priorly input values I_c, as shown in the following:

$$\begin{aligned} O_u &= \{\log P(u_k|\text{decoding})\}_{k=1}^{N} - I_u \\ O_c &= \{\log P(c_k|\text{decoding})\}_{k=1}^{N} - I_c \end{aligned}$$

Note, O_u and O_c are also viewed as the extrinsic information of the corresponding input and output bits (or symbols) of the code.

In Fig.5.4, the decoding algorithm starts at the MCISI (combined modulated code and ISI) SISO decoding block. The initial value of I_u^{MCISI} is taken as zero, since no prior information about the MC inputs is known in

the beginning. The I_c^{MCISI} is the soft information of the channel output symbols.

Assume that the channel noise is AWGN with variance σ_η. Then, I_c^{MCISI} can be calculated from the received signal $Y = \{y_k\}_{k=1}^N$ as follows:

$$I_c^{MCISI} = \{\log P(c_k|Y)\}_{k=1}^N = \left\{ \frac{-|y_k - c_k|^2}{2\sigma_\eta^2} \right\}_{k=1}^N$$

The output O_u^{MCISI} of the MCISI SISO decoder is then de-interleaved and de-multiplexed into two separate parts: I_c^{RSC1}, I_c^{RSC2}, which are then input into the two constituent SISO decoders of the turbo decoder.

Inside the turbo decoder, it is similar to the decoding algorithm in [16] that the decoded output O_u of either one is interleaved or de-interleaved before entering the other SISO decoder as I_u. The O_u is called the extrinsic information between the two constituent decoders that sustains the iteration of the inner decoding loop in the turbo decoder.

Another extrinsic information, which is different from [16], is the outputs O_c^{RSC1} and O_c^{RSC2} of the turbo decoder that connects the turbo decoder and the SISO MCISI decoding block, and therefore sustains the iteration of the outer decoding loop.

5.4.3 Simulation Results

We now verify the performance of the combined turbo code and MC for ISI channels. The ISI channel [0.7071, 0.7071] is tested. The turbo code we use here is the one from [16] with the interleave length 65536.

First, we use the following optimal $(3, 2)$ MC of constraint length 2 designed using the joint MLSE design of Section 3.4:

$$\mathbf{G}(z) = \begin{bmatrix} -0.0353 & -0.4874 \\ 0.3175 & -0.7121 \\ 0.7598 & -0.3851 \end{bmatrix} + \begin{bmatrix} 0.7834 & 0.2469 \\ 0.3700 & 0.6290 \\ 0.0041 & 0.4694 \end{bmatrix} z^{-1},$$

which has the coding gain 2.3dB compared to the uncoded AWGN channel. In order for the comparison with the same signal rate, the punctured 1/2 rate turbo code and the above rate 2/3 MC are combined, while in turbo equalization the unpunctured 1/3 rate turbo code is used. Therefore, both systems have the same coding rate, 1/3.

Fig.5.5(a) shows the BER vs E_b/N_0 results of the combination of the turbo and MC method and that of the turbo equalization method. It is observed that our new coding scheme has about 0.9dB gain over the turbo equalization method and is also above the ISI information rate.

As another example of MC is the following optimal $(2,1)$ MC of constraint length 3:

$$\mathbf{G}(z) = \begin{bmatrix} 0.2318 \\ 0.6614 \end{bmatrix} + \begin{bmatrix} 0.9290 \\ 0.7463 \end{bmatrix} z^{-1} + \begin{bmatrix} 0.2748 \\ -0.0655 \end{bmatrix} z^{-2} + \begin{bmatrix} -0.0958 \\ -0.0025 \end{bmatrix} z^{-3},$$

which has the coding gain 2.62dB compared to the uncoded AWGN channel. Fig.5.5(b) shows the performance of the combined turbo code and the modulated code method. We notice that the BER reaches 10^{-4} at $E_b/N_0 = -1.15dB$, which is also above the information rate curve of the ISI channel marked by dotted line in Fig.5.6. This information rate, in fact, is the upper limit of the turbo equalization techniques. Surprisingly, this performance is above the AWGN channel capacity.

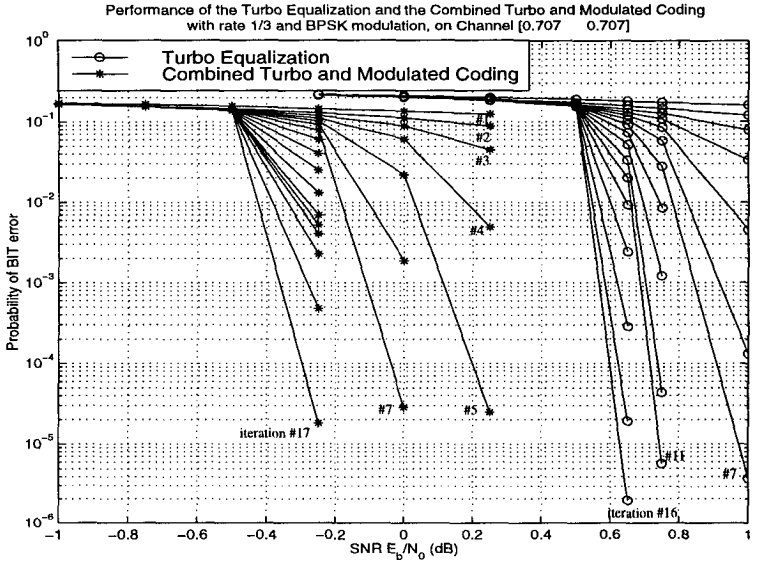

(a)

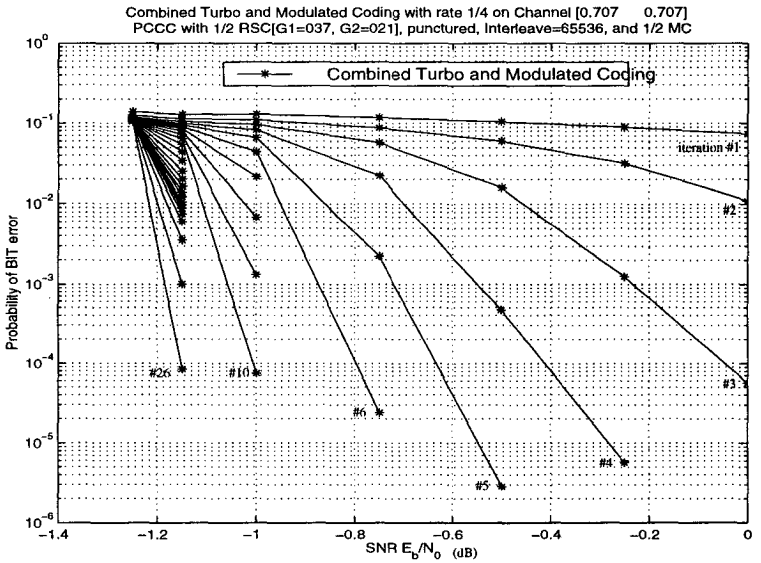

(b)

Figure 5.5: Performance comparison of the combined turbo code and modulated code method and the turbo equalization method on the ISI channel $h = [0.7071\ 0.7071]$: (a) overall code rate 1/3; (b) overall code rate 1/4.

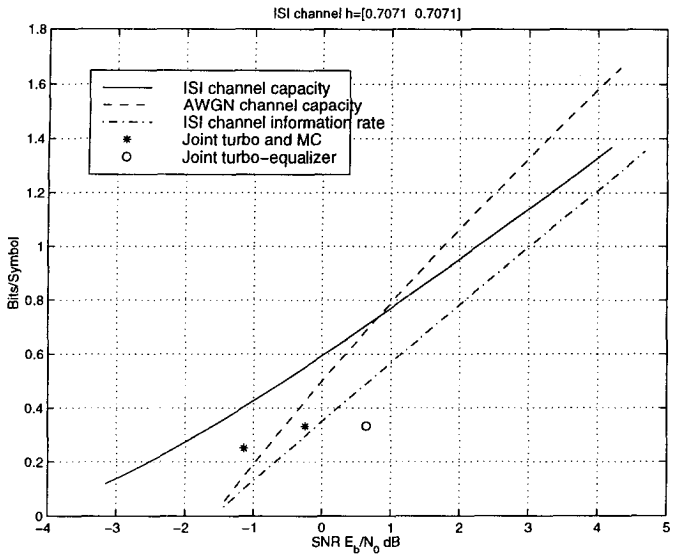

Figure 5.6: Performance of the combined turbo code and modulated code.

Chapter 6

Space-Time Modulated Coding for Memory Channels

Space-time coding for multiple transmit and receive antenna communication systems has recently attracted considerable attention, see for example [158, 157, 132, 70, 131, 130, 129, 8, 19, 60, 62, 61, 65, 66], which is mainly because of the significant capacity increase from diversities. Such studies include, for example, the capacity studies [132, 70, 157], space-time trellis coded modulation (TCM) schemes [131, 130], the combination of the space-time coding and signal processing [131, 130], and differential space-time coding [129, 60, 62, 61, 65, 66]. Most studies for such systems so far are for memoryless channels that may fit slow fading environment well, where all the paths from different transmit and receive antennas are assumed constants and treated as independent random variables. A recent study on multiple transmit and receive antenna systems with memory can be found in [8], where no space-time coding was considered. In this chapter, we are interested in multiple transmit and receive antenna channels with memory, where there are ISI for each pair of transmit and receive antennas. However, we assume that all the ISI channels for all the different pairs are known at both the transmitter and the receiver.

In this chapter, we generalize MC to space-time MC for multiple transmit and receive antenna ISI channels. Similar to the MC for single antenna ISI channels (in previous chapters), the space-time MC can be naturally combined with the multiple antenna channels. We generalize the MC coded

ZF-DFE for single antenna systems studied in Chapter 4 to space-time MC coded multiple antenna systems. By using the capacity formula of the multivariate channel with memory in [21], we first derive lower bounds of the capacities C and the information rates $C_{i.i.d.}$ for the MC coded systems, where $C_{i.i.d.}$ is the i.i.d. information rates when the input is an i.i.d. source, see for example [122, 121]. As a property of the space-time MC, it is proved that for an N transmit and N receive antenna channel $\mathbf{H}(z)$ with memory and AWGN and for any rate r, $0 < r < 1$, there exist rate r MC such that the MC coded systems have larger information rates $C_{i.i.d.}$ than the system itself does, when the channel SNR is relatively low and the channel $\mathbf{H}(z)$ is not paraunitary [142]. Notice that for a channel $\mathbf{H}(z)$, the condition that $\mathbf{H}(z)$ is not paraunitary holds almost surely. Another remark is that, when $N = 1$ this result is more general than the one obtained in Chapter 5 for MC coded single antenna systems, where only rate $1/P$ MC with $P \geq 2\Gamma - 1$ were constructed. The results in this chapter are summarized from [176].

6.1 Channel Model and Space-Time MC

Before going to space-time MC, let us first describe the channel model. Consider an N transmit antenna and M receive antenna channel with finite memory and AWGN, i.e.,

$$r_m(t) = \sum_{n=1}^{N} \sum_{k=0}^{\Gamma-1} h_{m,n}(k) s_n(t-k) + \eta_m(t), \quad 1 \leq m \leq M, \tag{6.1.1}$$

where $s_n(t)$ is the information sequence at the nth transmit antenna, $r_m(t)$ is the received signal at the mth receive antenna, $h_{m,n}(k)$ is the ISI channel finite impulse response of length Γ corresponding to the nth transmit antenna and the mth receive antenna, and $\eta_m(t)$ is the AWGN at the mth receive antenna. Let $H_{m,n}(z)$ denote the z-transform of $h_{m,n}(k)$ in terms of variable k. Let $\mathbf{H}(z)$ denote the following $M \times N$ matrix polynomial

$$\mathbf{H}(z) = (H_{m,n}(z))_{1 \leq m \leq M, 1 \leq n \leq N}. \tag{6.1.2}$$

Then, channel (6.1.1) is an N input and M output system with transfer matrix function $\mathbf{H}(z)$, i.e.,

$$\mathbf{R}(z) = \mathbf{H}(z)\mathbf{S}(z) + \eta(z), \tag{6.1.3}$$

where $\mathbf{R}(z) = (R_1(z), \cdots, R_M(z))^T$, $\mathbf{S}(z) = (S_1(z), \cdots, S_N(z))^T$, and $\eta(z) = (\eta_1(z), \cdots, \eta_M(z))^T$, ^{T} stands for the transpose, and $R_m(z)$, $S_n(z)$ and $\eta_m(z)$ are the z-transforms of $r_m(t)$, $s_n(t)$, and $\eta_m(t)$, respectively.

For convenience, in what follows the above channel transfer matrix function $\mathbf{H}(z)$ is normalized so that the channel itself does not have any gain:

$$\sum_{m=1}^{M}\sum_{n=1}^{N}\sum_{k}|h_{m,n}(k)|^2 = M. \tag{6.1.4}$$

In the following, we want to encode the information sequences $s_n(t)$ by using a space-time MC given the channel $\mathbf{H}(z)$.

A space-time MC for N transmit antennas is an (NP, K) MC, where the nth block of block length P of the MC encoded $NP \times 1$ vector is transmitted at the nth antenna as shown in Fig.6.1.

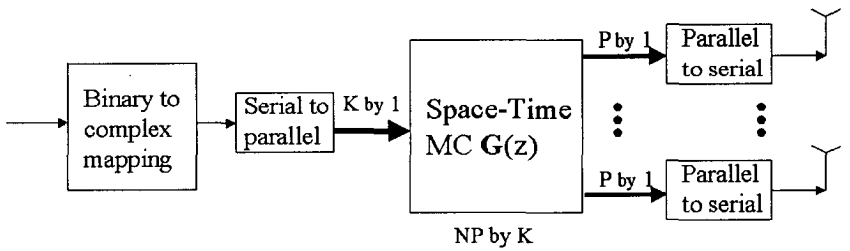

Figure 6.1: Space-time modulated code encoding.

Similar to the combination of an MC and an ISI in the single antenna case (2.3.2)-(2.3.6), which corresponds to $N = 1$ and $L = NP$ here, the space-time MC can be combined with the multiple transmit and receive antenna channel $\mathbf{H}(z)$ in (6.1.2) by blocking it with block size P. The combined MC and channel is

$$\mathcal{C}(z) = \mathcal{H}(z)\mathbf{G}(z), \tag{6.1.5}$$

where $\mathcal{H}(z)$ is the blocked version of $\mathbf{H}(z)$ and has the following pseudo-circulant form, see for example [175],

$$\mathcal{H}(z) = \begin{bmatrix} \mathbf{H}_0(z) & z^{-1}\mathbf{H}_{P-1}(z) & \cdots & z^{-1}\mathbf{H}_1(z) \\ \mathbf{H}_1(z) & \mathbf{H}_0(z) & \cdots & z^{-1}\mathbf{H}_2(z) \\ \vdots & \vdots & \vdots & \vdots \\ \mathbf{H}_{P-2}(z) & \mathbf{H}_{P-3}(z) & \cdots & z^{-1}\mathbf{H}_{P-1}(z) \\ \mathbf{H}_{P-1}(z) & \mathbf{H}_{P-2}(z) & \cdots & \mathbf{H}_0(z) \end{bmatrix}, \tag{6.1.6}$$

where $\mathbf{H}_p(z)$ is the pth polyphase component of $\mathbf{H}(z) = \sum_k H(k)z^{-k}$:

$$\mathbf{H}_p(z) = \sum_l H(Pl+p)z^{-l}, \quad 0 \le p \le P-1.$$

The space-time MC coded system in (6.1.1) and (6.1.3) after the blocking becomes

$$\mathcal{R}(z) = \mathcal{C}(z)\mathbf{X}(z) + \Xi(z), \tag{6.1.7}$$

where the size of $\mathcal{R}(z)$ is $MP \times 1$ and the mth receive antenna receives the mth block of block length P in the vector $\mathcal{R}(z)$, the size of $\mathcal{C}(z)$ is $MP \times K$, the size of $\mathbf{X}(z)$ is $K \times 1$, and the size of $\Xi(z)$ is $MP \times 1$ and it is blocked from $\eta(z)$ in (6.1.3). All the components of $\Xi(z)$ are i.i.d. Gaussian with mean 0 and single-sided power spectral density N_0. Since the rank of $\mathcal{C}(z)$ in (6.1.7) and (6.1.5) is at most $\min\{MP, NP, K\}$, for the decodability of the MC coded system (6.1.7), K has to satisfy the following condition

$$K \le \min\{MP, NP\}. \tag{6.1.8}$$

In the following we shall study the MC coded multi-input and multi-output (MIMO) system (6.1.7) under condition (6.1.8).

6.2 Space-Time MC Coded ZF-DFE

Similar to single antenna MC coded ISI channels, there are several decoding schemes for the space-time MC coded multiple transmit and receive antenna systems discussed in the preceding chapters, such as the MLSE decoding, the MMSE decoding, and the joint ZF-DFE and MMSE-DFE decodings. Different decoding algorithms also give different criterion for the optimal MC design at the transmitter. In this section, we want to study the ZF-DFE decoding and the corresponding optimal space-time MC design. The others can be similarly done.

6.2.1 MC Coded ZF-DFE and Performance Analysis

Consider an N transmit antenna and M receive antenna system with $M \times N$ transfer polynomial matrix $\mathbf{H}(z)$. For a space-time (NP, K) MC $\mathbf{G}(z)$, $K < NP$ is always assumed in what follows. The block diagram for the space-time MC coded ZF-DFE is shown in Fig.6.2, where I_K is the K by K identity matrix, and the K by 1 vector decision takes the best K by 1 vector of all the possible K by 1 information symbol vectors, and η is the channel

additive white Gaussian noise with zero mean and variance $\sigma_\eta^2 = N_0/2$, and $\mathcal{H}(z)$ is the blocked version of $\mathbf{H}(z)$ and has size $MP \times NP$.

The matrix multiplier $\mathcal{D}(z)$ at the receiver in Fig.6.2 for the MC coded ZF-DFE converts the nonsquare polynomial matrix $\mathcal{C}(z)$ of the combination into a square polynomial matrix so that the DFE can be implemented as shown in Fig.6.2. It is usually the case that the higher the order of the ISI channel to equalize is, the worse the DFE performance is. To make the order of the overall system $\mathcal{F}(z)$ after the matrix multiplier as low as possible, where

$$\mathcal{F}(z) \triangleq \mathcal{D}(z)\mathcal{C}(z) = \mathcal{D}(z)\mathcal{H}(z)\mathbf{G}(z), \tag{6.2.1}$$

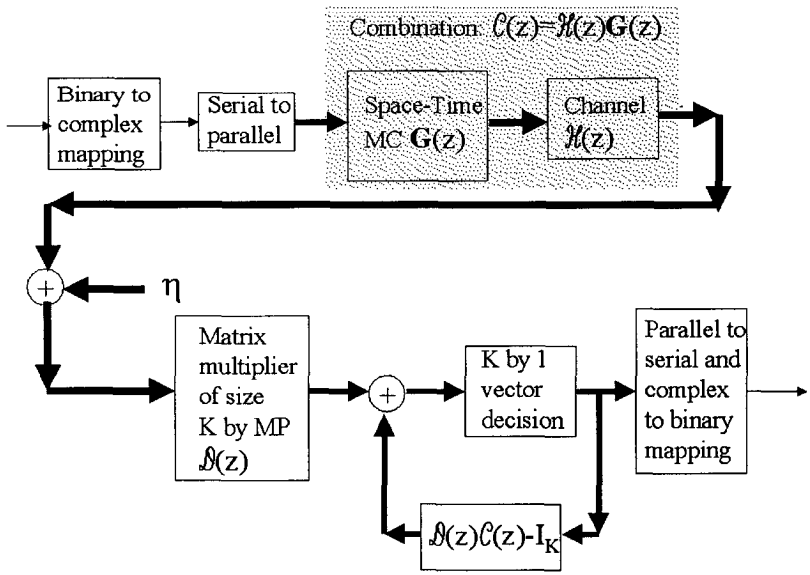

Figure 6.2: Space-time MC coded zero-forcing decision feedback equalizer.

and $\mathcal{H}(z)$ is as (6.1.6), the matrix multiplier $\mathcal{D}(z)$ simply takes a K by MP constant matrix. It also suggests that the MC $\mathbf{G}(z)$ takes a block code, i.e., $\mathbf{G}(z)$ is an MP by K constant matrix. We next want to study the MC design rule for the above ZF-DFE. Consider an NP by K block MC $\mathbf{G}(z) = \mathcal{G}$ and a constant K by NP matrix multiplier $\mathcal{D}(z) = \mathcal{D}$. The combined MC of the channel and the transmitter MC $\mathcal{G}$ becomes

$$\mathcal{C}(z) = \mathcal{H}_0\mathcal{G} + \mathcal{H}_1\mathcal{G}z^{-1} + \cdots + \mathcal{H}_{\Gamma_1}\mathcal{G}z^{-\Gamma_1}, \tag{6.2.2}$$

where $\mathcal{H}(z) = \sum_{k=0}^{\Gamma_1} \mathcal{H}_k z^{-k}$ and

$$\mathcal{H}_0 = \begin{bmatrix} H(0) & 0 & \cdots & 0 \\ H(1) & H(0) & \cdots & 0 \\ \vdots & \vdots & \vdots & \vdots \\ H(P-1) & H(P-2) & \cdots & H(0) \end{bmatrix}_{MP \times NP}, \tag{6.2.3}$$

where $H(0), ..., H(P-1)$ are $M \times N$ constant coefficient matrices in the channel $\mathbf{H}(z) = \sum_{k=0}^{\Gamma-1} H(k) z^{-k}$. From the feedback loop in the ZF-DFE in Fig.6.2, we want to have $\mathcal{D}\mathcal{H}_0\mathcal{G} = I_K$, i.e., the feedback does not depend on the current vector. Therefore, the matrix multiplier $\mathcal{D}(z) = \mathcal{D}$ is the right inverse (pseudo-inverse), $(\mathcal{H}_0\mathcal{G})^{-1}$, of the $MP \times K$ constant matrix $\mathcal{H}_0\mathcal{G}$. This also implies that the MC coded matrix $\mathcal{H}_0\mathcal{G}$ should have full column rank. In other words, the $MP \times NP$ matrix $\mathcal{H}_0$ should have rank at least K. For an arbitrarily given $\mathbf{H}(z)$, the matrix $\mathcal{H}_0$ almost surely has full rank. Without loss of generality, in what follows we always assume that $\mathcal{H}_0$ has full rank. As we shall see later on the MC design, it is only needed that the rank of $\mathcal{H}_0$ is at least K.

After the matrix multiplier of $\mathcal{D}(z) = \mathcal{D} = (d_{ij})_{K \times MP}$ at the receiver, the mean power of the multiplied noise $\tilde{\eta}$ of η becomes

$$\sigma_{\tilde{\eta}}^2 = \frac{\sum_{i=1}^{K} \sum_{j=1}^{MP} |d_{ij}|^2}{K} \sigma_\eta^2 = \frac{\sum_{i=1}^{K} \sum_{j=1}^{MP} |d_{ij}|^2}{2K} N_0. \tag{6.2.4}$$

By the normalization condition of the MC $\mathcal{G}$, the mean transmitted signal power is still σ_x^2. Similar to the conventional ZF-DFE for invertible ISI channel, see, for example, [68], the signal-to-noise ratio (SNR) after the MC coded ZF-DFE for the invertible $\mathcal{C}(z)$ is

$$\text{SNR} = \frac{\sigma_x^2}{\sigma_{\tilde{\eta}}^2} = \frac{2K\sigma_x^2}{\sum_{i=1}^{K} \sum_{j=1}^{MP} |d_{ij}|^2 N_0}. \tag{6.2.5}$$

Based on this SNR analysis at the receiver, to maximize the SNR we have the following **optimal MC design rule**:

$$\min_{\mathcal{G}} \sum_{i=1}^{K} \sum_{j=1}^{MP} |d_{ij}|^2 \quad \text{under the condition} \quad \mathcal{D}\mathcal{H}_0\mathcal{G} = I_K, \tag{6.2.6}$$

where the MC $\mathcal{G} = (g_{ij})$ satisfies the normalization condition

$$\sum_{i=1}^{NP} \sum_{j=1}^{K} |g_{ij}|^2 = NP. \tag{6.2.7}$$

Let the singular value decomposition of the matrix $\mathcal{H}_0\mathcal{G}$ be

$$U_l V U_r = \mathcal{H}_0\mathcal{G}, \tag{6.2.8}$$

where U_l and U_r are $MP \times MP$ and $K \times K$ unitary matrices, respectively, and

$$V = \begin{bmatrix} \text{diag}(\lambda_1, \cdots, \lambda_K) \\ 0_{(MP-K)\times K} \end{bmatrix}, \tag{6.2.9}$$

and λ_i for $i = 1, 2, ..., K$ are the singular values of the matrix $\mathcal{H}_0\mathcal{G}$. Then the matrix multiplier $\mathcal{D}$ is

$$\mathcal{D}(z) = \mathcal{D} = U_r^\dagger V^{-1} U_l^\dagger, \tag{6.2.10}$$

where

$$V^{-1} = (\text{diag}(1/\lambda_1, \cdots, 1/\lambda_K), 0_{K\times(MP-K)}). \tag{6.2.11}$$

Thus, the total energy of the matrix $\mathcal{D}$ is

$$\sum_{i=1}^{K}\sum_{j=1}^{MP} |d_{ij}|^2 = \sum_{i=1}^{K} \frac{1}{\lambda_i^2}. \tag{6.2.12}$$

Therefore, using the elementary inequality on the right hand side of (6.2.12) we have

$$\sum_{i=1}^{K}\sum_{j=1}^{MP} |d_{ij}|^2 \geq K \left(\prod_{i=1}^{K} \frac{1}{\lambda_i^2} \right)^{1/K}, \tag{6.2.13}$$

where the equality (the minimum) is reached if and only if

$$\lambda_1 = \lambda_2 = \cdots = \lambda_K = \lambda. \tag{6.2.14}$$

The optimality condition (6.2.14) is the one to design the MC $\mathcal{G}$ that whitens the matrix $\mathcal{H}_0$ generated from the ISI channel. In the next subsection, we propose a method to design such MC $\mathcal{G}$ given an $\mathcal{H}_0$ in (6.2.3).

We next want to study the performance of the MC coded ZF-DFE in Fig.6.2, i.e., the error probability. Let us consider the vector decision block in Fig.6.2. For a general MC $\mathcal{G}$ at the transmitter and the matrix multiplier $\mathcal{D}$ with the form in (6.2.10), each $K \times 1$ multiplied noise vector $\tilde{\eta}$ for a fixed time may be colored when $K > 1$. In this case, the vector decision is necessary for optimal detection. If the MC $\mathcal{G}$ whitens $\mathcal{H}_0$, i.e., the condition

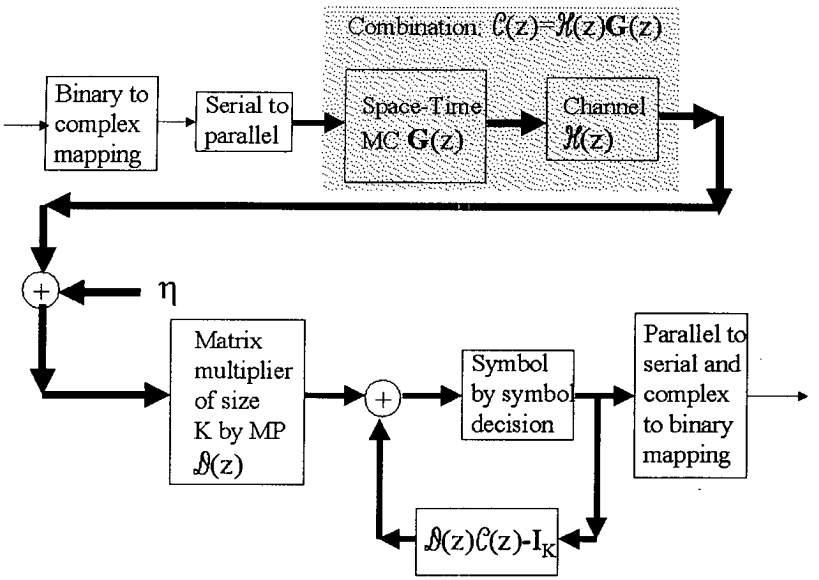

Figure 6.3: Space-time MC coded zero-forcing decision feedback equalizer with optimal MC.

(6.2.14) holds, then it is not hard to see that each $K \times 1$ multiplied noise vector $\tilde{\eta}$ for a fixed time is white too. Thus, the vector decision in Fig.6.2 can be reduced to the symbol-by-symbol detection as shown in Fig.6.3.

Assume that the condition (6.2.14) for the MC encoding holds, which is always possible to design as we shall see later. In this case,

$$\sum_{i=1}^{MP}\sum_{j=1}^{K}|d_{ij}|^2 = \frac{K}{\lambda^2}.$$

Let $P_s(\gamma_s)$ denote the symbol error probability at the symbol SNR γ_s for the binary-to-complex symbol mapping used at the transmitter in Fig.6.2. For convenience, in what follows we only consider the BPSK binary-to-complex symbol mapping. In this case, the symbol error probability is $P_s(\gamma_s) = Q(\sqrt{2\gamma_s})$, where γ_s is the SNR before the decision block in Fig.6.2. Using the SNR (6.2.5), the corresponding γ_s is

$$\gamma_s = \frac{\sigma_x^2}{2\sigma_{\tilde{\eta}}^2} = \frac{K\sigma_x^2}{\sum_{i=1}^{K}\sum_{j=1}^{MP}|d_{ij}|^2 N_0} = \frac{\lambda^2\sigma_x^2}{N_0} = \frac{\lambda^2 K}{NP}\frac{E_b}{N_0}, \qquad (6.2.15)$$

where E_b is the total energy of all the transmit antennas per bit. Then, the bit error rate (BER) for the MC coded ZF-DFE at the E_b/N_0 is

$$\text{BER} = P_s(\gamma_s) = Q\left(\sqrt{2\frac{E_b}{N_0}\gamma}\right), \tag{6.2.16}$$

where γ is the **coding gain** as follows, which is based on the joint ZF-DFE decoding and compared to the uncoded BPSK in AWGN channel:

$$\gamma = \frac{\lambda^2 K}{NP}, \tag{6.2.17}$$

where λ is defined in (6.2.14).

6.2.2 The Optimal Space-Time MC Design

In this subsection, we present the optimal MC design such that the optimality condition (6.2.14) is satisfied. Consider the singular value decomposition of $\mathcal{H}_0^\dagger \mathcal{H}_0$:

$$\mathcal{H}_0^\dagger \mathcal{H}_0 = W^\dagger \Lambda W, \tag{6.2.18}$$

where W is an $NP \times NP$ unitary matrix and

$$\Lambda = \begin{cases} \text{diag}(\xi_1^2, \cdots, \xi_{NP}^2), & \text{when } MP \geq NP, \\ \text{diag}(\xi_1^2, \cdots, \xi_{MP}^2, 0, \cdots, 0), & \text{when } MP < NP, \end{cases} \tag{6.2.19}$$

where

$$\xi_1 \geq \cdots \geq \xi_{\min\{MP,NP\}} > 0, \tag{6.2.20}$$

are the $\min\{NP, MP\}$ singular values of $\mathcal{H}_0$. Using the singular value decomposition (6.2.8) of $\mathcal{H}_0\mathcal{G}$ we have

$$U_r \mathcal{G}^\dagger W^\dagger \Lambda W \mathcal{G} U_r^\dagger = \text{diag}(\lambda_1^2, \cdots, \lambda_K^2).$$

Define

$$\bar{\mathcal{G}} = W\mathcal{G}U_r^\dagger. \tag{6.2.21}$$

Then

$$\bar{\mathcal{G}}^\dagger \Lambda \bar{\mathcal{G}} = \text{diag}(\lambda_1^2, \cdots, \lambda_K^2) \overset{step1}{=} \lambda I_K, \tag{6.2.22}$$

where step 1 is from the optimal criterion (6.2.14). Let

$$\lambda = \frac{NP}{\sum_{i=1}^{K} \xi_i^{-2}}, \tag{6.2.23}$$

and

$$\bar{\mathcal{G}} = \begin{bmatrix} \text{diag}(\lambda/\xi_1, \cdots, \lambda/\xi_K) \\ 0_{(NP-K)\times K} \end{bmatrix}. \tag{6.2.24}$$

By (6.2.23), it is not hard to see that $\bar{\mathcal{G}}$ is normalized. Since both W and U_r are unitary, by (6.2.21) the MC $\mathcal{G}$ is also normalized. Clearly, $\mathcal{G}$ satisfies the optimality condition (6.2.14), which is therefore optimal. Note that only the inverses of the K largest singular values of $\mathcal{H}_0$ are needed, and the rank of $\mathcal{H}_0$ only needs to be K or above.

Going back to (6.2.18)-(6.2.22), the optimal normalized MC $\mathcal{G}$ is

$$\mathcal{G}_{opt} = W^{\dagger} \bar{\mathcal{G}} U_r, \tag{6.2.25}$$

where U_r is an arbitrary $K \times K$ unitary matrix, W is the $NP \times NP$ unitary matrix defined in (6.2.18), and $\bar{\mathcal{G}}$ is defined in (6.2.23)-(6.2.24).

Theorem 6.1 *Given an N transmit and M receive antenna channel $\mathbf{H}(z)$, the optimal normalized (NP, K) modulated code $\mathcal{G}$ for the space-time MC coded zero-forcing decision feedback equalizer in Fig.6.2 is given in (6.2.25).*

Using the optimal λ in (6.2.23) and the optimal coding gain formula in (6.2.17) for the BPSK signaling, we have the following **optimal coding gain** using the optimal (NP, K) MC $\mathcal{G}_{opt}$ in (6.2.25) for a given channel:

$$\gamma_{opt} = \frac{K}{\sum_{i=1}^{K} \xi_i^{-2}}, \tag{6.2.26}$$

where ξ_i, $i = 1, 2, ..., K$, are the first K largest singular values of $\mathcal{H}_0$. One might want to ask when the above coding gain $\gamma_{opt} > 1$. We have the following simple result.

Theorem 6.2 *When $K = 1$ and $P \geq \Gamma$ in the MC $\mathcal{G}_{opt}$ in (6.2.25), if $M > N$, i.e., the number of the receive antennas is greater than the number of the transmit antennas, then the corresponding coding gain $\gamma_{opt} > 1$.*

Proof. To prove this theorem, by (6.2.26) we need to prove that the first singular value ξ_1 of $\mathcal{H}_0$ is greater than 1, i.e., $\xi_1 > 1$. Assume that all

the singular values of $\mathcal{H}_0$ are less than 1. We want to derive a contradiction. Consider the following matrix sequence for $l = 1, 2, ...$:

$$A_l \triangleq \left[\mathcal{H}_0^\dagger \mathcal{H}_0\right]^{2^l}. \tag{6.2.27}$$

By (6.2.18),

$$A_l = W^\dagger \text{diag}(\xi_1^{2^{l+1}}, \cdots, \xi_{NP}^{2^{l+1}}) W. \tag{6.2.28}$$

By the assumption that $\xi_k \leq 1$ for all k, we have

all the magnitudes of the elements in matrix A_l are bounded by NP. (6.2.29)

We now want to see the direct expansion of A_l in (6.2.27). Let

$$H = \sum_{k=0}^{P-1} H^\dagger(k) H(k). \tag{6.2.30}$$

It is not hard to see that the left upper corner $N \times N$ submatrix of A_l is always

$$C_l \triangleq (H)^{2^l} + B_l, \tag{6.2.31}$$

where B_l is a nonnegative definite matrix. Since $P \geq \Gamma$, by the normalization condition in (6.1.4) on $\mathbf{H}(z)$ and the condition $M \geq N$, we have

$$\sum_{n=1}^{N} \lambda_n = \text{trace}(H) = M > N, \tag{6.2.32}$$

where $\lambda_1 \geq \cdots \geq \lambda_N \geq 0$ are the eigenvalues of H. Clearly, $\lambda_1 > 1$ by (6.2.32). Since B_l is nonnegative definite, we have $\text{trace}(B_l) \geq 0$. Therefore,

$$\text{trace}(C_l) = \text{trace}(H^{2^l}) + \text{trace}(B_l) \geq \lambda_1^{2^l} \to \infty, \text{ when } l \to \infty. \tag{6.2.33}$$

This implies that some elements in matrix A_l go to ∞ as l goes to ∞, which contradicts with (6.2.29). This proves Theorem 6.2. ■

Although in Theorem 6.2 the condition $M > N$ is required, the result in Theorem 6.2 still holds when $M = N$ and the channel matrix $\mathbf{H}(z)$ is not paraunitary. Since the proof in this case is notationally tedious, we omit it here. We shall see some numerical simulation results later.

6.3 Capacity and Information Rates of the Space-Time MC Coded MIMO Systems

In this section, we want to study the capacity and information rates of the space-time MC coded channels similar to the one in Chapter 5. The basic idea for the following capacity and information rate study is based on the capacity formula obtained by Brandenburg and Wyner [21] for N-input and N-output systems (or multivariate channels) with memory and AWGN.

6.3.1 Capacity and Information Rates of MIMO Systems without MC Encoding

Let us now study the capacity and information rates of the MIMO system (6.1.3) using the ones in (5.1.3)-(5.1.5) for N input and N output systems derived by Brandenburg and Wyner [21]. To derive the exact capacity and information rates for the system (6.1.3), the difficulty arises from the number N of the inputs may be different from the number M of the outputs. When $M = N$, the above capacity formula (5.1.3) and the information rate formula (5.1.5) can be directly applied by replacing $\mathbf{P}(z)$ with $\mathbf{H}(z)$. By changing the units in (5.1.3) and (5.1.5) from per vectors to per symbols, the capacity and the information rates of an N transmit antenna and N receive antenna system are

$$C(E_s, N) = \frac{1}{4\pi N} \sum_{k=1}^{N} \int_{-\pi}^{\pi} d\theta \max \left\{ 0, \log_2 \frac{2\lambda_k(\theta) K_S}{N_0} \right\}, \tag{6.3.1}$$

where

$$\frac{1}{2\pi} \sum_{k=1}^{N} \int_{-\pi}^{\pi} d\theta \max \left\{ 0, K_S - \frac{N_0}{2} \lambda_k^{-1}(\theta) \right\} = N E_s, \tag{6.3.2}$$

and $\lambda_k(\theta)$, $k = 1, 2, ..., N$, are the N eigenvalues of matrix $\mathbf{H}^{\dagger}(e^{j\theta})\mathbf{H}(e^{j\theta})$ and E_s denotes the mean symbol power. The information rate is

$$C_{i.i.d.}(E_s, N) = \frac{1}{4\pi N} \sum_{k=1}^{N} \int_{-\pi}^{\pi} \log_2 \left[1 + \frac{2E_s \lambda_k(\theta)}{N_0} \right] d\theta, \tag{6.3.3}$$

where $\lambda_k(\theta)$ are the same as in the capacity (6.3.1).

When the number of the receive antennas is not equal to the number of the transmit antennas, i.e., $M \neq N$, we may use the singular value decompositions of the MIMO system $\mathbf{H}(z)$ (6.1.3) and then convert it to

a subsystem with $\min\{M,N\}$ inputs and $\min\{M,N\}$ outputs. By doing so, we have the following lower bound for the capacity and the information rates.

$$C(E_s,N,M) \geq \frac{1}{4\pi \min\{N,M\}} \sum_{k=1}^{\min\{N,M\}} \int_{-\pi}^{\pi} d\theta \max\left\{0, \log_2 \frac{2\lambda_k(\theta)K_S}{N_0}\right\}, \tag{6.3.4}$$

where

$$\frac{1}{2\pi} \sum_{k=1}^{\min\{N,M\}} \int_{-\pi}^{\pi} d\theta \max\left\{0, K_S - \frac{N_0}{2}\lambda_k^{-1}(\theta)\right\} = \min\{N,M\}E_s, \tag{6.3.5}$$

and $\lambda_k(\theta)$, $k = 1,2,...,\min\{N,M\}$, are the $\min\{N,M\}$ squared singular values of matrix $\mathbf{H}(e^{j\theta})$. The information rate is

$$C_{i.i.d.}(E_s,N,M) \geq \frac{1}{4\pi \min\{N,M\}} \sum_{k=1}^{\min\{N,M\}} \int_{-\pi}^{\pi} \log_2\left[1 + \frac{2E_s\lambda_k(\theta)}{N_0}\right] d\theta, \tag{6.3.6}$$

where $\lambda_k(\theta)$ are the same as in the capacity (6.3.4).

6.3.2 Capacity and Information Rates of the Space-Time MC Coded MIMO Systems

We next want to study the capacities and the information rates of the space-time MC coded MIMO systems (6.1.7). It is not hard to see that the MC coded MIMO system (6.1.7) is a K input and MP output system. Based on the decodability condition (6.1.8), there are two cases for the parameters K, NP, MP: **Case (i)** when $K = MP \leq NP$ and **Case (ii)** when $K < MP$ and $K \leq NP$.

We first consider Case (i). Similar to (6.3.1)-(6.3.3), the capacity and the information rates of the space-time MC coded system in (6.1.7) when $K = MP \leq NP$ are

$$C(E_s,K,NP,MP) = \frac{1}{4\pi NP} \sum_{k=1}^{K} \int_{-\pi}^{\pi} d\theta \max\left\{0, \log_2 \frac{2\lambda_k(\theta)K_S}{N_0}\right\}, \tag{6.3.7}$$

where

$$\frac{1}{2\pi} \sum_{k=1}^{K} \int_{-\pi}^{\pi} d\theta \max\left\{0, K_S - \frac{N_0}{2}\lambda_k^{-1}(\theta)\right\} = KE_s, \tag{6.3.8}$$

and $\lambda_k(\theta)$, $k = 1, 2, ..., K$, are the K squared singular values of matrix $\mathcal{C}(e^{j\theta})$ in (6.1.5). The information rate is

$$C_{i.i.d.}(E_s, K, NP, MP) = \frac{1}{4\pi NP} \sum_{k=1}^{K} \int_{-\pi}^{\pi} \log_2 \left[1 + \frac{2E_s \lambda_k(\theta)}{N_0}\right] d\theta, \quad (6.3.9)$$

where $\lambda_k(\theta)$ are the same as in the capacity (6.3.7). Notice that the data rate loss $K/(NP)$ in the above MC encoding has been taken into the account in the above formulas and otherwise the factor $1/(NP)$ in (6.3.7) and (6.3.9) would be $1/K$.

For Case (ii), similar to (6.3.4)-(6.3.6), the capacity and the information rates of the space-time MC coded system in (6.1.7) when $K < MP$ and $K \leq NP$ are lower bounded by

$$C(E_s, K, NP, MP) \geq \frac{1}{4\pi NP} \sum_{k=1}^{K} \int_{-\pi}^{\pi} d\theta \max \left\{0, \log_2 \frac{2\lambda_k(\theta) K_S}{N_0}\right\}, \quad (6.3.10)$$

where

$$\frac{1}{2\pi} \sum_{k=1}^{K} \int_{-\pi}^{\pi} d\theta \max \left\{0, K_S - \frac{N_0}{2} \lambda_k^{-1}(\theta)\right\} = KE_s, \quad (6.3.11)$$

and $\lambda_k(\theta)$, $k = 1, 2, ..., K$, are the K squared singular values of matrix $\mathcal{C}(e^{j\theta})$ in (6.1.5). The information rate is lower bounded by

$$C_{i.i.d.}(E_s, K, NP, MP) \geq \frac{1}{4\pi NP} \sum_{k=1}^{K} \int_{-\pi}^{\pi} \log_2 \left[1 + \frac{2E_s \lambda_k(\theta)}{N_0}\right] d\theta, \quad (6.3.12)$$

where $\lambda_k(\theta)$ are the same as in the capacity (6.3.10).

We next show that there exists space-time MC such that the information rates of the MC coded system in (6.1.7) are larger than the ones of the original system in (6.1.3) when the channel SNR is low and the number of transmit antennas is equal to the number of receive antennas, i.e., $M = N$. When $M \neq N$, similar arguments can be used to show the space-time MC existence with the larger information rate lower bound of the MC coded system over the information rate lower bound of the original system.

Before going to the results, we need to introduce two concepts on $N \times N$ polynomial matrix $\mathbf{H}(z)$. An $N \times N$ polynomial matrix $\mathbf{H}(z)$ is called *paraunitary* if and only if, see [142],

$$\mathbf{H}^{\dagger}(e^{i\theta})\mathbf{H}(e^{i\theta}) = dI_N, \quad -\pi \leq \theta < \pi, \quad (6.3.13)$$

where $d > 0$ is a constant. The above paraunitariness is a generalization of the unitariness for constant matrices. When $N > 1$, an $N \times N$ polynomial matrix $\mathbf{H}(z)$ is almost surely not paraunitary. When $N = 1$, a polynomial is paraunitary if and only if it is a single delay dz^{-k_0}, i.e., no ISI. An $N \times N$ polynomial matrix $\mathbf{H}(z)$ is called *pseudo-paraunitary* if and only if

$$\mathbf{H}(e^{i\theta}) = d(e^{j\theta})\mathbf{U}(e^{j\theta}), \quad -\pi \leq \theta < \pi, \tag{6.3.14}$$

where $d(e^{j\theta})$ is a scalar function of $e^{i\theta}$ and has at least two terms of $e^{jk\theta}$ for different k and $\mathbf{U}(e^{j\theta})$ is an $N \times N$ unitary matrix for any θ. For an $N \times N$ polynomial matrix with $N > 1$, it is almost surely not pseudo-paraunitary. However, for $N = 1$, any polynomial $H(z)$ is pseudo-paraunitary unless it is only a delay, i.e., $H(z) = dz^{-k_0}$, and in this case it is paraunitary.

Lemma 6.1 *If the blocked version $\mathcal{H}(z)$ in (6.1.6) with block size P of an $N \times N$ polynomial matrix $\mathbf{H}(z)$ is pseudo-paraunitary (or paraunitary), then $\mathbf{H}(z)$ is also pseudo-paraunitary (or paraunitary).*

Proof. When $N = 1$, the blocked version $\mathcal{H}(z)$ can be diagonalized as follows, see (2.3.10),

$$\mathcal{H}(z^P) = [W_P^* \mathbf{U}(z)]^\dagger \Lambda(z) W_P^* \mathbf{U}(z), \tag{6.3.15}$$

where $W_P = \frac{1}{\sqrt{P}}(w_P^{pq})_{0 \leq p,q \leq P-1}$, $w_P = \exp(-j2\pi/P)$,

$$\mathbf{U}(z) = \text{diag}(1, z^{-1}, \cdots, z^{-P+1}),$$

and

$$\Lambda(z) = \text{diag}(\mathbf{H}(z), \mathbf{H}(zw_P), \cdots, \mathbf{H}(zw_P^{P-1})). \tag{6.3.16}$$

When $N > 1$, $\mathcal{H}(z^P)$ can be permuted both row-wisely and column-wisely such that each $P \times P$ submatrix of the permuted $\mathcal{H}(z^P)$ is pseudo-circulant and corresponds to the case when $N = 1$. Therefore, the diagonalization (6.3.15) can be used to each $P \times P$ submatrix of the permuted matrix of $\mathcal{H}(z^P)$. Then each diagonalized $P \times P$ submatrix of $\mathcal{H}(z^P)$ is permuted back. Let $\mathcal{P}$ denote the permutation matrix. Then, $\mathcal{H}(z^P)$ has the following diagonalization

$$\mathcal{H}(z^P) = \mathcal{P}^T \text{diag}\left([W_P^* \mathbf{U}(z)]^\dagger, \cdots, [W_P^* \mathbf{U}(z)]^\dagger\right) \mathcal{P}^T \Lambda(z) \mathcal{P}^T$$

$$\text{diag}\left(W_P^* \mathbf{U}(z), \cdots, W_P^* \mathbf{U}(z)\right) \mathcal{P}^T, \tag{6.3.17}$$

where $\Lambda(z)$ has the form (6.3.16). Since all matrices W_P, $\mathbf{U}(z)$, and $\mathcal{P}$ are unitary, by the form of $\Lambda(z)$ in (6.3.16), $\mathcal{H}(z)$ is pseudo-paraunitary (or unitary) implies that $\mathbf{H}(z)$ is also pseudo-paraunitary (or unitary). ■

We are now ready to state and prove the following results.

Theorem 6.3 *Let $\mathbf{H}(z)$ be an $N \times N$ transfer polynomial matrix of an N transmit antenna and N receive antenna system with AWGN. If $\mathbf{H}(z)$ is not pseudo-paraunitary, then for any $1 \leq K < NP$, there exists an (NP, K) space-time MC such that the information rates in (6.3.12) of the MC coded system (6.1.7) are larger than the information rates in (6.3.3) of the original system (6.1.3), when the channel SNR is sufficiently low.*

Proof. For each θ with $-\pi \leq \theta < \pi$, let $\mathcal{H}(e^{j\theta})$ in (6.1.6) have the following singular value decomposition

$$\mathcal{H}(e^{j\theta}) = \mathbf{U}(e^{j\theta})\Lambda(e^{j\theta})\mathbf{V}(e^{j\theta}), \tag{6.3.18}$$

where $\mathbf{U}(e^{j\theta})$ and $\mathbf{V}(e^{j\theta})$ are both unitary and

$$\Lambda(e^{j\theta}) = \text{diag}(\bar{\lambda}_1(\theta), \cdots, \bar{\lambda}_{NP}(\theta))$$

with

$$\bar{\lambda}_1(\theta) \geq \cdots \geq \bar{\lambda}_{NP}(\theta) \geq 0. \tag{6.3.19}$$

By the Parseval's equality, the channel normalization (6.1.4) with $M = N$ and the form (6.1.6) of $\mathcal{H}(z)$,

$$\frac{1}{2\pi}\int_{-\pi}^{\pi}\sum_{k=1}^{NP}\bar{\lambda}_k^2(\theta)d\theta = \frac{1}{2\pi}\int_{-\pi}^{\pi}\text{trace}(\mathcal{H}^\dagger(e^{j\theta})\mathcal{H}(e^{j\theta}))d\theta =$$

$$P\sum_{m=1}^{M}\sum_{n=1}^{N}\sum_{k}|h_{m,n}(k)|^2 = NP. \tag{6.3.20}$$

Let $\bar{\mathbf{G}}(e^{j\theta})$ be the following $NP \times K$ matrix

$$\bar{\mathbf{G}}(e^{j\theta}) = \mathbf{V}^\dagger(e^{j\theta})\begin{bmatrix}\text{diag}(\sqrt{\frac{NP}{K}}, \cdots, \sqrt{\frac{NP}{K}}) \\ 0_{(NP-K)\times K}\end{bmatrix}_{NP\times K} \tag{6.3.21}$$

Then, the K squared singular values of matrix $\mathcal{H}(e^{j\theta})\bar{\mathbf{G}}(e^{j\theta})$ are

$$\bar{\lambda}_k^{(1)}(\theta) = \frac{NP}{K}\bar{\lambda}_k^2(\theta), \ 1 \leq k \leq K. \tag{6.3.22}$$

We claim that, when $\mathbf{H}(z)$ is not pseudo-paraunitary, we have

$$\frac{1}{2\pi}\int_{-\pi}^{\pi}\sum_{k=1}^{K}\bar{\lambda}_k^2(\theta)d\theta > K. \tag{6.3.23}$$

In fact, if

$$\frac{1}{2\pi}\int_{-\pi}^{\pi}\sum_{k=1}^{K}\bar{\lambda}_k^2(\theta)d\theta \leq K, \tag{6.3.24}$$

then, by (6.3.20) and (6.3.19) we have

$$\bar{\lambda}_1(\theta) = \cdots = \bar{\lambda}_{NP}(\theta) = \lambda(\theta), \text{ almost surely.} \tag{6.3.25}$$

By (6.3.18), we know that $\mathcal{H}(z)$ is pseudo-paraunitary. Therefore, by Lemma 6.1 $\mathbf{H}(z)$ is also pseudo-paraunitary, which contradicts the condition in Theorem 6.3.

Let $\lambda_n(\theta)$, $1 \leq n \leq N$, be the N squared singular values of matrix $\mathbf{H}(e^{j\theta})$. By the normalization (6.1.4) of $\mathbf{H}(z)$ and the Parseval's equality, similar to (6.3.20) we have

$$\frac{1}{2\pi}\int_{-\pi}^{\pi}\sum_{n=1}^{N}\lambda_n(\theta)d\theta = N. \tag{6.3.26}$$

Let

$$\bar{\kappa} \triangleq \frac{\int_{-\pi}^{\pi}\sum_{k=1}^{K}\bar{\lambda}_k^{(1)}(\theta)d\theta}{P\int_{-\pi}^{\pi}\sum_{n=1}^{N}\lambda_n(\theta)d\theta}, \tag{6.3.27}$$

which only depends on the channel $\mathbf{H}(z)$. Therefore, by (6.3.22), (6.3.23), and (6.3.26), we have

$$\bar{\kappa} > 1. \tag{6.3.28}$$

If $\mathbf{V}(z)$ in the decomposition (6.3.18) is a polynomial matrix, i.e., each component in $\mathbf{V}(z)$ has only finite terms of z^{-k}, then we claim that the (NP, K) MC $\bar{\mathbf{G}}(z)$ in (6.3.21) is the MC $\mathbf{G}(z)$ we wanted to construct for the proof. We next want to prove this claim. To do so, we consider the ratio $R_I(\gamma)$ of the information rate (6.3.12) for the MC coded system over the information rate (6.3.3) for the original system, where

$$\gamma = \frac{2E_s}{N_0}.$$

By the lower bound in (6.3.12), the ratio $R_I(\gamma)$ is lower bounded by

$$R_I(\gamma) \geq \frac{\int_{-\pi}^{\pi}\sum_{k=1}^{K}\log_2(1+\gamma\bar{\lambda}_k^{(1)}(\theta))d\theta}{P\int_{-\pi}^{\pi}\sum_{n=1}^{N}\log_2(1+\gamma\lambda_n(\theta))d\theta}. \tag{6.3.29}$$

Thus,

$$\begin{aligned}\lim_{\gamma\to 0} R_I(\gamma) &\geq \lim_{\gamma\to 0} \frac{\int_{-\pi}^{\pi}\sum_{k=1}^{K}\log_2(1+\gamma\bar{\lambda}_k^{(1)}(\theta))d\theta}{P\int_{-\pi}^{\pi}\sum_{n=1}^{N}\log_2(1+\gamma\lambda_n(\theta))d\theta} \\ &\overset{step1}{=} \frac{\int_{-\pi}^{\pi}\sum_{k=1}^{K}\bar{\lambda}_k^{(1)}(\theta)d\theta}{P\int_{-\pi}^{\pi}\sum_{n=1}^{N}\lambda_n(\theta)d\theta} \\ &= \bar{\kappa} > 1, \end{aligned} \tag{6.3.30}$$

where step 1 is from the L'Hôpital's rule.

When $\mathbf{V}(z)$ has infinite terms of z^{-k}, it is truncated into a polynomial matrix $\mathbf{V}_1(z)$ in a way that it is close enough to $\mathbf{V}(z)$ and the corresponding MC $\mathbf{G}(z)$ defined similar to $\bar{\mathbf{G}}(z)$ in (6.3.21) by replacing $\mathbf{V}(z)$ with $\mathbf{V}_1(z)$ is also close enough to $\bar{\mathbf{G}}(z)$. Then, the corresponding squared singular values $\lambda_k^{(1)}(\theta)$ of $\mathcal{H}(z)\mathbf{G}(z)$ are also close to $\bar{\lambda}_k^{(1)}(\theta)$ in (6.3.22) such that

$$\kappa \triangleq \frac{\int_{-\pi}^{\pi}\sum_{k=1}^{K}\lambda_k^{(1)}(\theta)d\theta}{P\int_{-\pi}^{\pi}\sum_{n=1}^{N}\lambda_n(\theta)d\theta} \approx \bar{\kappa}, \quad \text{and } \kappa > 1. \tag{6.3.31}$$

With the MC $\mathbf{G}(z)$ defined above, the corresponding information rate ratio $R_I(\gamma)$ is lower bounded by $\kappa > 1$ as the channel SNR γ goes to 0, which is similar to (6.3.29)-(6.3.30).

The above arguments prove that when the channel SNR γ is sufficiently small, the information rates of the MC coded system are larger than the ones of the original system. This proves Theorem 6.3. ■

From Theorem 6.3, it is known that, for almost all N transmit antenna and N receive antenna systems with $N > 1$ and any (NP, K) with $K < NP$, there exists an (NP, K) space-time MC such that the MC coded systems have larger information rates than the ones of the original systems, when the channel SNR are small. Since when $N = 1$, i.e., a single antenna system, the ISI channel $H(z)$ with length $\Gamma > 1$ is always pseudo-paraunitary, Theorem 6.3 does not apply to the case when $N = 1$. In order to include this case, we have the following result.

Theorem 6.4 *Let $\mathbf{H}(z) = \sum_{k=0}^{\Gamma-1} H(k)z^{-k}$ be an $N \times N$ transfer polynomial matrix of an N transmit antenna and N receive antenna system with AWGN. If $\mathbf{H}(z)$ is not paraunitary, then, for any $1 \leq K < NP$ with $P \geq \Gamma$, there exists an (NP, K) space-time MC such that the information rates in (6.3.12) of the MC coded system (6.1.7) are larger than the information rates in (6.3.3) of the original system (6.1.3), when the channel SNR is sufficiently low.*

Proof. By Theorem 6.3, we only need to prove Theorem 6.4 for the case when $\mathbf{H}(z)$ is pseudo-paraunitary. In this case,

$$\mathbf{H}(e^{j\theta}) = d(e^{j\theta})\mathbf{U}(e^{j\theta}),$$

where $d(e^{j\theta})$ is a scalar function of $e^{j\theta}$ and has at least two different terms of $e^{jk\theta}$ and $\mathbf{U}(e^{j\theta})$ is unitary. Since a unitary matrix multiplication does not change the information rates, by absorbing $\mathbf{U}(e^{j\theta})$ into the signal, the system $\mathbf{H}(z)$ is equivalently converted to $d(e^{j\theta})I_N$, which is equivalent to N single antenna systems with the transfer functions $d(e^{j\theta})$. Since $\mathbf{H}(e^{j\theta})$ has length Γ, so does $d(e^{j\theta})$ due to the fact that

$$\mathbf{H}^\dagger(e^{j\theta})\mathbf{H}(e^{j\theta}) = |d(e^{j\theta})|^2 I_N.$$

Therefore, to prove Theorem 6.4 we only need to consider the case of single antenna systems, i.e., $N = 1$, with finite ISI. In this case, everything else but (6.3.23) in the proof of Theorem 6.3 directly applies here. This implies that we only need to prove (6.3.23) under the conditions that the single antenna system transfer function $H(z)$ of length Γ with $\Gamma > 1$, and $P \geq \Gamma$. If (6.3.23) is false, i.e., (6.3.24) holds, then, similarly we have

$$\bar{\lambda}_1(\theta) = \cdots = \bar{\lambda}_P(\theta) = \lambda(\theta), \text{ almost surely.} \tag{6.3.32}$$

Going back to (6.3.18),

$$\mathcal{H}(e^{j\theta}) = \lambda(\theta)\mathbf{U}(e^{j\theta})\mathbf{V}(e^{j\theta}). \tag{6.3.33}$$

Since $\mathcal{H}(e^{j\theta})$ is pseudo-circulant, it has the diagonalization (6.3.15). By combining (6.3.33) and (6.3.15), we have

$$\text{diag}(H(e^{j\theta/P}), H(e^{j\theta/P}w_P), \cdots, H(e^{j\theta/P}w_P^{P-1})) = \lambda(\theta)\mathbf{W}(\theta),$$

where $\mathbf{W}(\theta)$ is unitary. Therefore,

$$|H(e^{j\theta/P}w_P^p)|^2 = \lambda^2(\theta), \quad \text{for } p = 0, 1, ..., P-1. \tag{6.3.34}$$

By expanding (6.3.34) and setting $\theta = 0$, we have

$$\left|\sum_{k=0}^{\Gamma-1} h(k)\exp(jkp/P)\right|^2 = \lambda^2(0), \quad \text{for } p = 0, 1, ..., P-1. \tag{6.3.35}$$

Since $P \geq \Gamma$, (6.3.35) is possible only if the sequence $h(0)$, $h(1)$,...,$h(\Gamma-1)$ has one non-zero element, which contradicts with the condition that $H(z)$ has at least two terms. This proves (6.3.23) and therefore Theorem 6.4 is proved. ■

From the above proof, the following corollary is immediate.

Corollary 6.1 *For a single antenna system with transfer function $H(z)$ of length $\Gamma > 1$ and AWGN, there always exists a rate K/P MC with $1 \leq K < P \geq \Gamma$ such that the MC coded systems have larger information rates than the original system does, when the channel SNR is small.*

The above result is a generalization of the one obtained in Chapter 5, where rate $1/P$ with $P \geq 2\Gamma - 1$ MC were constructed. Examples shall be presented later to illustrate the above results. One thing should be emphasized here is that, in all the above proofs of the information rate increase, the condition $K < NP$, i.e., the data rate increase of the MC encoding, ensures (6.3.23) and therefore $\kappa > 1$ in (6.3.31) or $\bar{\kappa} > 1$ in (6.3.28).

6.4 Numerical Results

In this section, we see some simulation results on both MC coded ZF-DFE and the capacity and the information rates of the MC coded systems and the systems themselves. In the following simulations, the number of transmit and receive antennas are both 2, i.e., $N = M = 2$. The block size in the space-time MC in Fig.6.1 is $P = 3$. The space-time MC code rate is 2/6, i.e., $K = 2$. In this case, the rate for each transmit antenna is 2/3. The BPSK is used for all the simulations and no additional coding is used before the MC encoding.

We consider two different multiple transmit and receive antenna channels with memory and AWGN: Channel A $\mathbf{H}_A(z)$ and Channel B $\mathbf{H}_B(z)$.

Channel A $\mathbf{H}_A(z)$ has length $\Gamma = 3$ and its 3 coefficient matrices are:

$$H(0) = H(1) = H(2) = \begin{bmatrix} 0.4762 & 0.4286 \\ -0.3810 & 0.3333 \end{bmatrix}, \tag{6.4.1}$$

which is a spectral-null channel because $\mathbf{H}_A(z) = (1+z^{-1}+z^{-2})H(0)$. The optimal $(6,2)$ space-time MC $\mathcal{G}_{opt}$ in (6.2.25) for this channel is

$$\mathcal{G}_{opt,A} = \begin{bmatrix} 0.9350 & -0.7529 \\ 0.5778 & 1.2182 \\ 0.7498 & -0.6038 \\ 0.4634 & 0.9769 \\ 0.4161 & -0.3351 \\ 0.2572 & 0.5421 \end{bmatrix}. \tag{6.4.2}$$

The optimal coding gain with this MC is $\gamma_{opt} = 1.96$dB. Fig.6.4 shows the capacities and information rates $C_{i.i.d.}$ of the MC coded/uncoded systems.

The solid line shows the original channel information rates $C_{i.i.d.}$ (6.3.3) with $N = 2$ while the solid line marked by $\square$ shows the lower bound (6.3.12) of the information rates $C_{i.i.d.}$ of the space-time MC coded channel using the optimal MC in (6.4.2). One can see that the information rates $C_{i.i.d.}$ of the MC coded channel are above the ones of the original channel when the channel SNR is below about 2.5dB. The dashed line shows the original channel capacity (6.3.1) while the solid line marked by $*$ shows the capacity lower bound (6.3.10) of the MC coded channel. Fig.6.5 shows the BER performance comparison. The solid line shows the theoretical BER vs. E_b/N_0 curve of the MC coded ZF-DFE and the solid line marked by $\times$ shows the simulation results. The dashed line shows the BER vs. E_b/N_0 curve of the uncoded BPSK over the AWGN channel (i.e., the ideal single antenna channel). One can clearly see the coding gain of the MC. Since the rate for each antenna in this case is 2/3 and all the ISI channels of all transmit and receive antenna pairs are the same, basically $1 + z^{-1} + z^{-2}$, it is possible to compare it with its single antenna system with the ISI channel $0.5774(1 + z^{-1} + z^{-2})$. The rate of the MC for the single antenna system is 2/3 comparing to Channel A. In this case, the optimal coding gain using the ZF-DFE developed in Section 4.1 is -4.20dB, i.e., coding loss. Compared to the coding gain 1.96dB, the MC coded multiple transmit and receive antenna channel significantly outperforms the corresponding single antenna channel.

Channel B $\mathbf{H}_B(z)$ has length $\Gamma = 5$ and its 5 coefficient matrices are:

$$H(0) = \begin{bmatrix} 0.8111 & 0.5469 \\ 0.7117 & 0.6691 \end{bmatrix}, \quad H(1) = \begin{bmatrix} -0.1459 & -0.0136 \\ -0.0880 & -0.0507 \end{bmatrix},$$
$$H(2) = \begin{bmatrix} -0.0183 & -0.1676 \\ -0.1263 & 0.1129 \end{bmatrix}, \quad H(3) = \begin{bmatrix} 0.0154 & -0.0152 \\ -0.0457 & 0.0323 \end{bmatrix},$$
$$H(4) = \begin{bmatrix} -0.0620 & -0.0617 \\ -0.0228 & -0.0970 \end{bmatrix} \tag{6.4.3}$$

This channel is randomly chosen. The optimal $(6, 2)$ space-time MC $\mathcal{G}_{opt}$ in (6.2.25) is

$$\mathcal{G}_{opt,B} = \begin{bmatrix} 0.6276 & -0.9998 \\ 0.4449 & -0.7658 \\ -1.0787 & -0.0931 \\ -0.8155 & 0.0032 \\ 0.5606 & 0.9498 \\ 0.4488 & 0.7529 \end{bmatrix}. \tag{6.4.4}$$

The optimal coding gain with this MC is $\gamma_{opt} = 3.24$dB. Similar to Channel A, Fig.6.6 shows the capacities C and information rates $C_{i.i.d.}$ of the MC

coded/uncoded systems and Fig.6.7 shows the BER performance comparison. From Fig.6.6, one can see that the information rates $C_{i.i.d.}$ of the MC coded channel are above the ones of the original channel when the channel SNR is below about 6dB.

From both Fig.6.4 and Fig.6.6, the capacity lower bound curves almost coincide with the information rate lower bound curves of the MC coded channels. It is, however, not always the case for any MC.

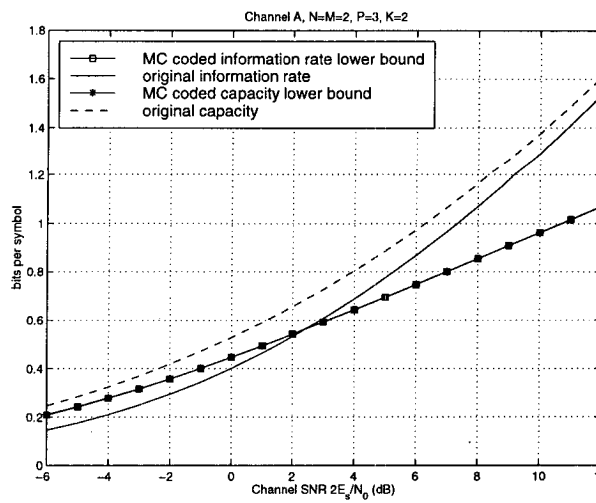

Figure 6.4: Channel A: Capacities C and information rates $C_{i.i.d.}$ for the MC coded and uncoded channels.

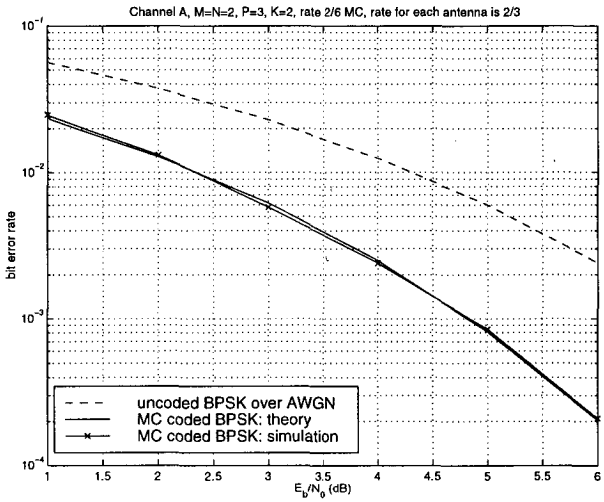

Figure 6.5: Channel A: BER performance for the MC coded channel using the joint ZF-DFE, where the theoretical coding gain is 1.96dB.

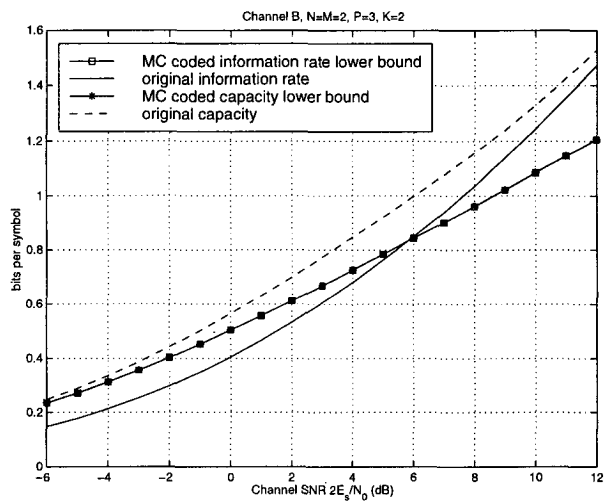

Figure 6.6: Channel B: Capacities C and information rates $C_{i.i.d.}$ for the MC coded and uncoded channels.

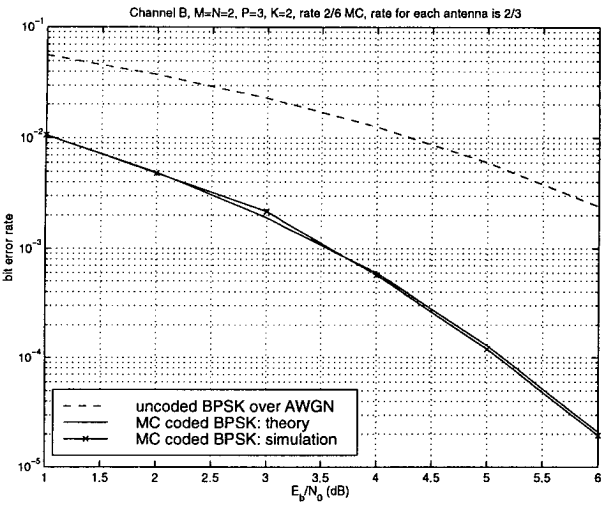

Figure 6.7: Channel B: BER performance for the MC coded channel using the joint ZF-DFE, where the theoretical coding gain is 3.24dB.

Chapter 7

Modulated Code Coded Orthogonal Frequency Division Multiplexing Systems

Orthogonal frequency division multiplexing (OFDM) systems have been widely used in high speed digital wireline communication systems, such as VHDSL and ADSL [25]. One of the main reasons is because OFDM systems convert ISI channels into ISI-free channels by inserting the cyclic prefix as an overhead at the transmitter. For tutorials, see, for example, [18, 189, 3]. Recently, the applications of OFDM systems to high speed digital wireless communication systems have become an active research area. In frequency-selective channels, however, the ISI channel may have spectral nulls, which may degrade the performance of the existing OFDM systems because the Fourier transform of the ISI channel needs to be inverted for each subcarrier at the OFDM system receiver. For this reason, the coded OFDM systems were proposed in, for example, [189, 188, 47], where the conventional trellis coded modulation (TCM) was used in [189, 188], and turbo codes were used in [47]. Another problem with the existing OFDM systems is that when the ISI channel has many taps, the data rate overhead of the cyclic prefix insertion is high.

In this chapter, we first propose an MC coded OFDM system by simply inserting one or more zeroes between each two sets of K consecutive information symbols, which may be independent of the ISI channel. However,

the MC can be general. Notice that, due to the insertion of zeroes, the data rate is expanded in the MC coded OFDM systems. We show that, for spectral null channels the MC coded OFDM systems perform better than the existing OFDM systems do even when the conventional convolutional codes and TCM are used in the OFDM systems, i.e., COFDM systems [189, 188, 47]. The rationale is that the proposed MC coded scheme may be able to remove the spectral nulls of an ISI channel without even knowing the channel information. Furthermore, the proposed MC coded OFDM system does not increase the encoding/decoding complexity as much as the conventional COFDM does, where the Viterbi decoding for the conventional COFDM is needed.

We also propose vector OFDM systems, which are used to reduce the data rate overhead of the prefix insertion. The basic idea for the vector OFDM systems is basically from the above MC coded OFDM systems, where no zeroes are inserted between each two sets of K consecutive information symbols but each K consecutive information symbols are blocked together as a $K \times 1$ vector sequence. Compared to the MC coded OFDM systems, the data rate before the prefix insertion for vector OFDM systems is not changed. When $K \times 1$ vector sequence is processed, the ISI channel can be blocked into a $K \times K$ matrix ISI channel but the length of the matrix ISI channel is only about $1/K$ of the original ISI channel length. The cyclic prefix length for the vector OFDM system only needs to be greater than or equal to the matrix ISI channel length. This implies that the data rate overhead of the original cyclic prefix insertion is reduced by K times for the vector OFDM systems. The bit error rate (BER) performances of the vector and conventional OFDM systems are compared. Our simulation results show that the BER performance of the vector OFDM systems is similar to the conventional OFDM systems. The results in this part are from [169].

We then study the performance of the MC coded OFDM systems in frequency selective multipath Rayleigh fading channels obtained in [154]. Both analytical and simulation results are presented.

7.1 OFDM Systems for ISI Channels

In this section, the conventional OFDM system is presented by including the theoretical bit error rate (BER) performance analysis.

Let $x(n)$ stand for the information symbol sequences after the binary to complex mapping, such as BPSK and QPSK symbol sequences. Let N be the number of carriers in the OFDM system, i.e., the size of the IFFT and FFT in the OFDM system as shown in Fig.7.1 is N. Let the ISI channel

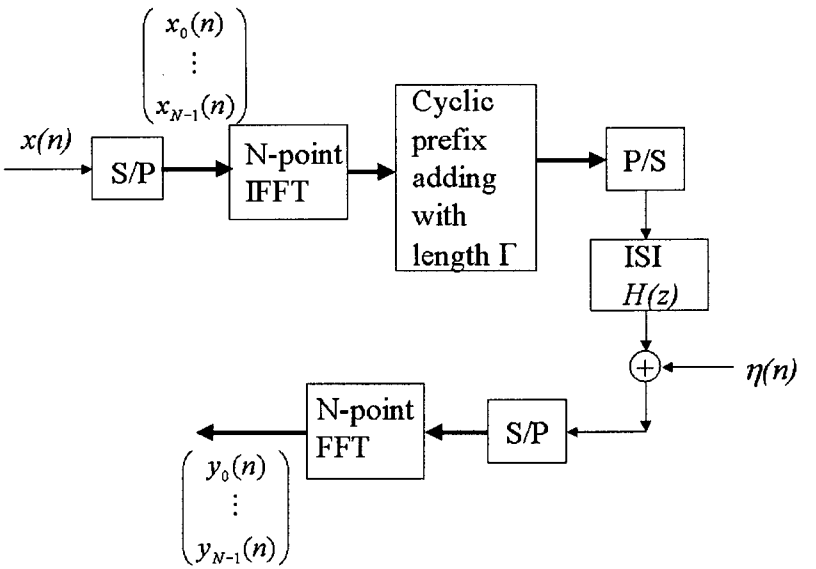

Figure 7.1: Conventional OFDM system.

have the following transfer function

$$H(z) = \sum_{n=0}^{L} h(n) z^{-n}, \tag{7.1.1}$$

where $h(n)$ are the impulse responses of the ISI channel. Let Γ be the cyclic prefix length in the OFDM system as shown in Fig.7.1 and $\Gamma \geq L$ for the purpose of removing the ISI. Let $\eta(n)$ be the AWGN, as shown in Fig.7.1, with mean zero, variance $\sigma_\eta^2 = N_0/2$, and N_0 is the single-sided power spectral density of the noise $\eta(n)$. Let $r(n)$ be the received signal at the receiver and $y(n)$ be the signal after the FFT of the received signal $r(n)$. Then, the relationship between the information symbols $x(n)$ and the signal $y(n)$ can be formulated as

$$y_k(n) = H_k x_k(n) + \xi_k(n), \quad k = 0, 1, ..., N-1, \tag{7.1.2}$$

where $q_k(n)$ denotes the kth subsequence of $q(n)$, i.e.,

$$(q(n))_n = (q_0(n), q_1(n), ..., q_{N-1}(n))_n,$$

and q stands for x, y, and ξ, $\xi(n)$ is the FFT of the noise $\eta(n)$ and therefore has the same statistics as $\eta(n)$, and

$$H_k = H(z)|_{z=\exp(j2\pi k/N)}, \quad k = 0, 1, ..., N-1. \tag{7.1.3}$$

The receiver needs to detect the information sequence $x_k(n)$ from $y_k(n)$ through (7.1.2).

From (7.1.2), one can clearly see that the ISI channel $H(z)$ is converted to N ISI-free subchannels H_k. The *key* for this property to hold is the insertion of the cyclic prefix with length Γ that is greater than or equal to the the number of ISI taps L. Similar properties will be used in the following MC coded OFDM systems in Section 7.2. As mentioned in Section 2.1, the OFDM system itself is actually an MC coded system with the following channel independent block $(N+\Gamma, N)$ MC

$$\mathbf{G}(z) = \begin{bmatrix} \mathbf{W}_N \\ \bar{\mathbf{W}}_N \end{bmatrix},$$

where $\mathbf{W}_N$ is the N-point DFT matrix and $\bar{\mathbf{W}}_N$ is the first Γ row submatrix of $\mathbf{W}_N$ and corresponds to the cyclic prefix.

For the ISI-free system in (7.1.2), the performance analysis of the detection is as follows. Let $P_{ber,x}(E_b/N_0)$ be the bit error rate (BER) for the signal constellation $x(n)$ in the AWGN channel at the SNR E_b/N_0, where E_b is the energy per bit. Then, the BER vs. E_b/N_0 of the OFDM shown in Fig.7.1 is

$$P_e = \frac{1}{N}\sum_{k=0}^{N-1} P_{ber,x}\left(\frac{|H_k|^2 N E_b}{(N+\Gamma)N_0}\right). \tag{7.1.4}$$

For example, when the BPSK for $x(n)$ is used, we have

$$P_{ber,x}(E_b/N_0) = Q\left(\sqrt{\frac{2E_b}{N_0}}\right). \tag{7.1.5}$$

Therefore, the BER vs. E_b/N_0 for the OFDM system is

$$P_e = \frac{1}{N}\sum_{k=0}^{N-1} Q\left(\sqrt{\frac{2|H_k|^2 N E_b}{(N+\Gamma)N_0}}\right). \tag{7.1.6}$$

Numerical examples will be presented in Section 7.3.5.

7.2 General MC Coded OFDM Systems for ISI Channels

We now propose an MC coded OFDM system whose block diagram is shown in Fig.7.2. It is formulated as follows, which is the goal of this section.

Symbol $x(n)$ is as before, i.e., the information sequence after the binary to complex mapping. The information sequence $x(n)$ is blocked into $K \times 1$ vector sequence

$$\bar{x}(n) = (x_0(n), x_1(n), ..., x_{K-1}(n))^T,$$

where $x_k(n) = x(Kn + k)$, $k = 0, 1, ..., K - 1$. Symbol $\mathbf{G}(z)$ is an (M, K) MC.

The MC coded $M \times 1$ vector sequence is denoted by $\tilde{x}(n)$. Let $K \times 1$ polynomial vector $\bar{X}(z)$ and $M \times 1$ polynomial vector $\tilde{X}(z)$ denote the z transforms of vector sequences $\bar{x}(n)$ and $\tilde{x}(n)$, respectively. Then,

$$\tilde{X}(z) = \mathbf{G}(z)\bar{X}(z). \tag{7.2.1}$$

The MC coded $M \times 1$ vector sequence $\tilde{x}(n)$ is *blocked again* into $MN \times 1$ vector sequence

$$\hat{x}(n) = (\tilde{x}_0^T(n), \tilde{x}_1^T(n), ..., \tilde{x}_{N-1}^T(n))^T,$$

where each $\tilde{x}_k(n) = \tilde{x}(Nn+k)$ is already an $M \times 1$ vector for $k = 0, 1, ..., N-1$.

Let $\tilde{z}_l(n)$, $l = 0, 1, ..., N - 1$, be the output of the N-point IFFT of $\tilde{x}_k(n)$, $k = 0, 1, ..., N - 1$, i.e.,

$$\tilde{z}_l(n) = \frac{1}{\sqrt{N}} \sum_{k=0}^{N-1} \tilde{x}_k(n) \exp(j2\pi kl/N), \quad l = 0, 1, ..., N - 1, \tag{7.2.2}$$

which is the N-point IFFT of the individual components of the N vectors $\tilde{x}_k(n)$.

The cyclic prefix in Fig.7.2 is to add the first $\tilde{\Gamma}$ vectors $\tilde{z}_l(n)$, $l = 0, 1, ..., \tilde{\Gamma} - 1$, to the end of the vector sequence $\tilde{z}_l(n)$, $l = 0, 1, ..., N - 1$. In other words, the vector sequence after the cyclic prefix is

$$\hat{z}(n) = (\tilde{z}_0^T(n), \tilde{z}_1^T(n), ..., \tilde{z}_{N-1}^T(n), \tilde{z}_0^T(n), ..., \tilde{z}_{\tilde{\Gamma}-1}^T(n))^T, \tag{7.2.3}$$

which has size $M(N + \tilde{\Gamma}) \times 1$. The cyclic prefix length $\tilde{\Gamma}$ will be determined later for the purpose of removing the ISI of the MC coded OFDM system.

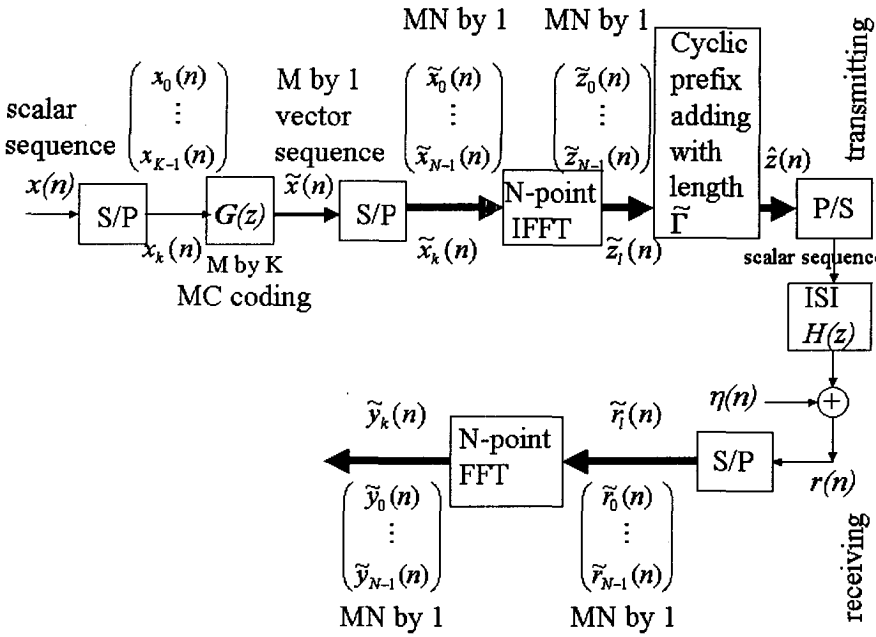

Figure 7.2: MC coded OFDM system.

Notice that each subvector $\tilde{z}_l(n)$ in $\hat{z}(n)$ in (7.2.3) has size $M \times 1$ and the prefix components are also vectors rather than scalars in the conventional OFDM systems as shown in Fig.7.1.

The transmitted scalar sequence in the MC coded OFDM system in Fig.7.2 is $z(n)$ and is obtained by the parallel to serial conversion of the vector sequence $\hat{z}(n)$ in (7.2.3). Notice that the MC coded OFDM system in Fig.7.2 is different from the OFDM systems with antenna diversities, such as [85, 84, 78]. In the MC coded OFDM system in Fig.7.1, there is only *one* transmitting antenna and *one* receiving antenna.

$r(n)$ is the received scalar sequence at the receiver, which is converted to the following $MN \times 1$ vector sequence

$$\hat{r}(n) = (\tilde{r}_0^T(n), \tilde{r}_1^T(n), ..., \tilde{r}_{N-1}^T(n))^T,$$

where each $\tilde{r}_l(n)$ has size $M \times 1$. The output of the N-point FFT of $\hat{r}(n)$

is

$$\tilde{y}_k(n) = \frac{1}{\sqrt{N}} \sum_{l=0}^{N-1} \tilde{r}_l(n) \exp(-j2\pi lk/N), \quad k = 0, 1, ..., N-1, \tag{7.2.4}$$

where the formulation is similar to the N-point IFFT in (7.2.2) and each $\tilde{y}_k(n)$ is an $M \times 1$ vector. In what follows, we derive a similar output and input relationship between $\tilde{y}_k(n)$ and $\tilde{x}_k(n)$ as in (7.1.2) for converting the ISI channel into an ISI-free channel, and also in what follows "ISI-free" means that there is no interference between inter-vectors.

Since a single input and single output (SISO) linear time invariant (LTI) system with transfer function $H(z)$ is equivalent to an M input and M output system by the blocking process with block length M, i.e., the serial to parallel process. The equivalence here means that the M inputs and M outputs are the blocked versions (or serial to parallel conversions) of the single input and single output and vice versa. The equivalent systems are shown in Fig.7.3, where the equivalent multi-input multi-output (MIMO) transfer function matrix $\mathbf{H}(z)$ is the blocked version of $H(z)$ in (2.3.3). If the order of $H(z)$ is L as in (7.1.1), then the order $\tilde{L}$ of the blocked version $\mathbf{H}(z)$ in (2.3.3) of $H(z)$ with block size M is

$$\tilde{L} = \lceil \frac{L}{M} \rceil, \tag{7.2.5}$$

where $\lceil a \rceil$ stands for the smallest integer b such that $b \geq a$. Clearly,

$$\tilde{L} < \frac{L}{M} + 1. \tag{7.2.6}$$

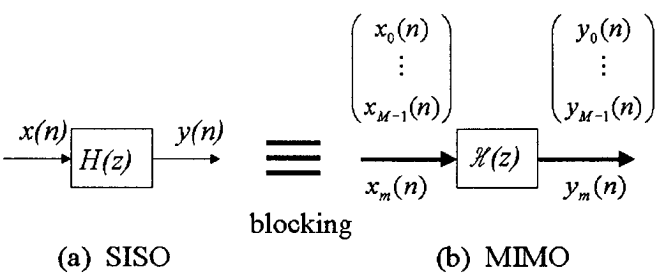

Figure 7.3: Equivalent (a) SISO and (b) MIMO systems.

Using the above equivalence of the SISO and MIMO systems, the MC coded OFDM system in Fig.7.2 is equivalent to the one shown in Fig.7.4. The equivalent MC coded OFDM system in Fig.7.4 is the same as the conventional OFDM system in Fig.7.1 if the scalar sequences $x(n)$ and $y(n)$ are replaced by $M \times 1$ vector sequences $\tilde{x}(n)$ and $\tilde{y}(n)$, respectively. Therefore, similar to (7.1.2) it is not hard to derive the relationship between $\tilde{x}_k(n)$ and $\tilde{y}_k(n)$:

$$\tilde{y}_k(n) = \mathbf{H}_k \tilde{x}_k(n) + \tilde{\xi}_k(n), \quad k = 0, 1, ..., N-1, \tag{7.2.7}$$

under the condition on the cyclic prefix length $\tilde{\Gamma}$ that should be greater than or equal to the order of the MIMO transfer function matrix $\mathbf{H}(z)$ in (2.3.3), i.e.,

$$\tilde{\Gamma} \geq \tilde{L}. \tag{7.2.8}$$

The constant matrices $\mathbf{H}_k$ in (7.2.7) are similar to the constants H_k in (7.1.2) and have the following forms

$$\mathbf{H}_k = \mathbf{H}(z)|_{z=\exp(j2\pi k/N)}, \quad k = 0, 1, ..., N-1. \tag{7.2.9}$$

The additive noise $\tilde{\xi}_k(n)$ in (7.2.7) is the blocked version of $\xi(n)$ and its components have the same power spectral density as $\eta(n)$ does and all components of all the vectors $\tilde{\xi}_k(n)$ are i.i.d. complex Gaussian random variables in general. Notice that in the transmitter and receiver diversity OFDM systems studied by Li et. al. in [84, 78, 85], the input-output relationship has the same form as (7.2.7) where the ISI channel matrix $\mathbf{H}(z)$ may not be necessarily pseudo-circulant.

The conventional OFDM system is the special case of the MC coded OFDM system, if the $M \times 1$ vector sequences $\tilde{x}(n)$ and $\tilde{y}(n)$ are replaced by the scalar sequences $x(n)$ and $y(n)$ and taking the MC $\mathbf{G}(z)$ as constant scalar 1. When the MC $G = I_{M \times M}$, i.e., $M = K$, the MC coded OFDM system is the *vector OFDM system*, where as we can see in (7.2.6) that the prefix length $\tilde{L}$ is reduced by M times compared to the original L. In other words, the vector OFDM system can be used to reduce the overhead of the cyclic prefix insertion of the conventional OFDM system. And in the following, we only consider the special case of the MC coded OFDM system when the MC $\mathbf{G}(z)$ takes the following channel independent $M \times K$ constant matrix

$$\mathbf{G}(z) = G = \begin{bmatrix} I_{K \times K} \\ 0_{(M-K) \times K} \end{bmatrix}, \tag{7.2.10}$$

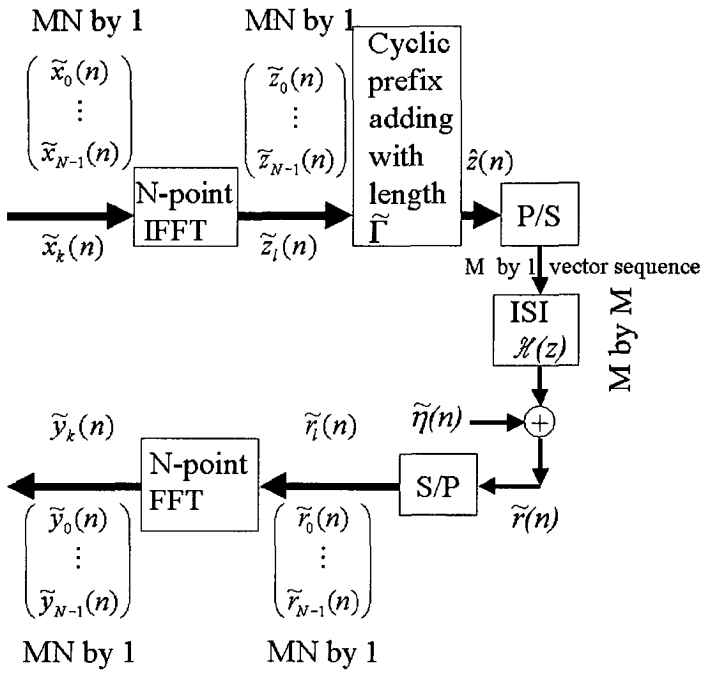

Figure 7.4: An equivalent MC coded OFDM system.

where $M > K$, $I_{K\times K}$ stands for the $K \times K$ identity matrix and $0_{(M-k)\times K}$ stands for the $(M - K) \times K$ all zeroes matrix. The MC (7.2.10) is just inserting $M - K$ zeroes between each two sets of K consecutive information samples. As an example, let us consider the case $M = 3, K = 2$. In each MC coded OFDM block, $KN = 2N$ information symbols $(x_1, x_2, ..., x_{2N})$ are sent. The $2N$ information symbol sequence is filled in a $3 \times N$ matrix:

$$\tilde{X} = \begin{bmatrix} X_1 \\ X_2 \\ 0_{1\times N} \end{bmatrix} = \begin{bmatrix} x_1 & x_3 & \cdots & x_{2N-1} \\ x_2 & x_4 & \cdots & x_{2N} \\ 0 & 0 & \cdots & 0 \end{bmatrix}, \tag{7.2.11}$$

where $X_1 = (x_1, x_3, ..., x_{2N-1})$, $X_2 = (x_2, x_4, ..., x_{2N})$, $0_{1\times N}$ is a row vector of zeroes with length N, and the row direction corresponds to the time index. After the $2N$ information symbols and N zeroes are filled in the $3 \times N$ matrix $\tilde{X}$, N-point inverse discrete Fourier transforms are taken *rowwisely* to the matrix, i.e., $Z_1 = IFFT_N(X_1)$, $Z_2 = IFFT_N(X_2)$. Then the cyclic prefix is added. The signal after the cyclic prefix is transmitted

columnwisely. The $3 \times N$ matrix $\tilde{R}$ is obtained by columnwisely arranging the received symbols $r_n, n = 1, 2, ..., 3N$ at the receiver:

$$\tilde{R} = \begin{bmatrix} R_1 \\ R_2 \\ R_3 \end{bmatrix} = \begin{bmatrix} r_1 & r_4 & \cdots & r_{3N-2} \\ r_2 & r_5 & \cdots & r_{3N-1} \\ r_3 & r_6 & \cdots & r_{3N} \end{bmatrix}. \tag{7.2.12}$$

The N-point discrete Fourier transforms are taken rowwisely to $\tilde{R}$:

$$\tilde{Y} = \begin{bmatrix} Y_1 \\ Y_2 \\ Y_3 \end{bmatrix} \tag{7.2.13}$$

where $Y_1 = FFT(R_1)$, $Y_2 = FFT(R_2)$, and $Y_3 = FFT(R_3)$. The decoding is based on $\tilde{Y}$ as in (7.2.15) in the following. Notice that the MC (7.2.10) is independent of the ISI channel and does not change the signal energy, i.e., the energy of the signal x_n before the MC coding is equal to the energy of the signal $\tilde{x}_n$ after the MC coding.

Another remark we want to make here is that the way to insert zeroes in the above MC coded OFDM system is different from the following one. From (7.2.11), one can see that the zeroes are inserted as a row in a matrix. It is clear that zeroes may be inserted as a column in a matrix as shown in (7.2.14):

$$\mathcal{X} = \begin{bmatrix} x_1 & x_4 & \cdots & x_{n-3} & 0 & x_n & \cdots & x_{3N-5} \\ x_2 & x_5 & \cdots & x_{n-2} & 0 & x_{n+1} & \cdots & x_{3N-4} \\ x_3 & x_6 & \cdots & x_{n-1} & 0 & x_{n+2} & \cdots & x_{3N-3} \end{bmatrix}. \tag{7.2.14}$$

Based on the decoding of the conventional OFDM system, this method of inserting zeroes is equivalent to the one of not sending information at the $(1 + (n-1)/3)$th frequency, i.e., $2\pi(1 + (n-1)/3)/N$, of the ISI channel. Hence, if the ISI channel is known spectral-null at this frequency, there will be no information loss at this frequency. However, the knowledge of the ISI channel at the transmitter is usually not known in wireless applications. This implies that the method of inserting zeroes as in (7.2.14) is not appropriate.

When the MC (7.2.10) is used, equation (7.2.7) becomes

$$\tilde{y}_k(n) = \tilde{\mathbf{H}}_k \bar{x}_k(n) + \tilde{\xi}_k(n), \quad k = 0, 1, ..., N-1, \tag{7.2.15}$$

where for $k = 0, 1, ..., N-1$,

$$\bar{x}_k(n) = \bar{x}(Nn + k) = (x_0(Nn + k), x_1(Nn + k), ..., x_{K-1}(Nn + k))^T \tag{7.2.16}$$

are the original $K \times 1$ information vector sequences and need to be detected from $\tilde{y}_k(n)$, and for each k, $\bar{\mathbf{H}}_k$ denotes the first K column submatrix of $\mathbf{H}_k$ in (7.2.9).

We now have two systems (7.2.7) and (7.2.15) in the OFDM decoding, where the system (7.2.7) is from the OFDM system without adding any redundancy, i.e., no zeroes is inserted, and the system (7.2.15) is from MC coded OFDM system by adding some redundancy, i.e., inserting zeroes. With the same DFT size N, the OFDM system (7.2.7) without adding zeroes is referred as the vector OFDM system, which is basically equivalent to the conventional OFDM system. Clearly the performances of the MC coded and the vector/conventional OFDM systems depend on the singular values of the matrices $\mathbf{H}_k$ in (7.2.7) and the matrices $\bar{\mathbf{H}}_k$ in (7.2.15) because the inversions of these matrices are needed in the decoding in general. The following known result [56] tells us that the singular values of the submatrices $\bar{\mathbf{H}}_k$ in (7.2.15) are always above the ones of $\mathbf{H}_k$ in (7.2.7).

Proposition 7.1 *Let $A = [a_1, \cdots, a_n]$ be a column partitioning of an $m \times n$ matrix A. If $A_r = [a_1, \cdots, a_r]$ denotes the submatrix of the first r columns of A, then, for $r = 1, ..., n-1$,*

$$\sigma_1(A_{r+1}) \geq \sigma_1(A_r) \geq \sigma_2(A_{r+1}) \geq \cdots \geq \sigma_r(A_{r+1}) \geq \sigma_r(A_r) \geq \sigma_{r+1}(A_{r+1}),$$

where $\sigma_i(A_r)$ represents the i-th singular value in the SVD decomposition of A_r.

This result tells us that the singular values of a sub column submatrix of a matrix are always greater than or equal to the matrix itself.

7.3 Channel Independent MC Coded OFDM System for ISI Channels

The goal of this section is to restrict ourselves to a special MC coding scheme that is independent of an ISI channel $H(z)$.

7.3.1 A Special MC

Before going to the details, we first see the rationale. By noticing that the vector sequence $\tilde{x}_k(n)$ in (7.2.7) is the MC coded sequence of the original information sequence $x_k(n)$ in Fig.7.2, there are two methods for detecting the original information sequence $x_k(n)$. One method is to detect $\tilde{x}_k(n)$ first from the ISI-free vector system (7.2.7) and then decode the MC $\mathbf{G}(z)$

for $x_k(n)$. The problem with this method is that, when the ISI channel $H(z)$ is spectral null, the blocked matrix channel $\mathbf{H}(z)$ is also spectral null by the diagonalization of $\mathbf{H}(z^M)$ in (2.3.10). One will see later that the performance of the detection of $\tilde{x}_k(n)$ in (7.2.7) for spectral null ISI channels is too poor that the coding gain of the MC $\mathbf{G}(z)$ is too far away to make it up. This implies that the separate ISI removing and MC decoding may not perform well for spectral null channels, which is similar to the existing COFDM systems.

The other method is the joint ISI removing and MC decoding, i.e., the combination of the MC $\mathbf{G}(z)$ with the vector systems (7.2.7). If the MC $\mathbf{G}(z)$ is not a *constant matrix*, the encoded vector sequence $\tilde{x}_k(n)$ is the convolution of the information vector sequence $x_k(n)$ and the MC impulse response $g(n)$. The convolution and the constant matrix $\mathbf{H}_k$ multiplications in (7.2.7) induces ISI, which may complicate the decoding of the system (7.2.7) and is beyond the scope of this book.

The above arguments suggest that we may want to use a constant $M \times K$ matrix MC $\mathbf{G}(z) = G$. In this case, (7.2.7) becomes

$$\tilde{y}_k(n) = \mathbf{H}_k G \bar{x}_k(n) + \tilde{\xi}_k(n), \quad k = 0, 1, ..., N-1, \tag{7.3.1}$$

where, for $k = 0, 1, ..., N-1$, and

$$\begin{aligned} \bar{x}_k(n) &= \bar{x}(Nn+k) = (x_0(Nn+k), x_1(Nn+k), ..., x_{K-1}(Nn+k))^T \\ &= (x(K(Nn+k)+0), x(K(Nn+k)+1), \\ &\quad ..., x(K(Nn+k)+K-1))^T \end{aligned} \tag{7.3.2}$$

are the original $K \times 1$ information vector sequences and need to be detected from $\tilde{y}_k(n)$. It is clear that one wants to have the singular values of all matrices $\{\mathbf{H}_k G\}_{k=0,1,...,N-1}$ as large as possible for the optimal output SNR. However, since the transmitter usually does not have the channel information $\mathbf{H}_k$, it may not be easy to optimally design the constant MC G in (7.3.1) at the transmitter. The above two arguments suggest the use of the MC in (7.2.10). This MC was used in Section 2.3.1 for converting a spectral null channel into a nonspectral-null matrix channel as long as the M equally spaced rotations of the zero set of $H(z)$ do not intersect each other. Notice that the MC (7.2.10) is independent of the ISI channel and does not change the signal energy, i.e., the energy of the signal $x(n)$ before the MC coding is equal to the energy of the signal $\tilde{x}(n)$ after the MC coding.

As mentioned before, without the data rate expansion, i.e., $M = K$ in (7.2.10), the above system (7.2.15) may not be invertible if the ISI channel $H(z)$ has spectral nulls, i.e., $\mathbf{H}_k$ may not be invertible (may have zero

singular values). We, however, will study this case later for the purpose of reducing the prefix length rather than improving the robustness of the system. With the data rate expansion, i.e., $M > K$, it was proved in Section 2.3.1 that, under a minor condition on the channel as mentioned before, the non-squared matrices $\bar{\mathbf{H}}_k$ are invertible (have all nonzero singular values). Clearly, the performance of the detection of the information symbols $\bar{x}_k(n)$ in (7.2.15) depends on how large the singular values of the $M \times K$ matrices $\bar{\mathbf{H}}_k$ are, i.e., how high the output SNR is. From the above argument, the MC coding is already able to convert systems $\mathbf{H}_k$ with possibly zero singular values into systems $\bar{\mathbf{H}}_k$ with all nonzero singular values. In general, Proposition 7.1 intuitively explains why the MC coding may improve the performance of the OFDM system. We next show a simple example to analytically see how the MC coding improves the performance.

7.3.2 An Example

We now consider a simple example to see how the MC coding works. Let the ISI channel be

$$H(z) = \frac{1}{\sqrt{2}}(1 + z^{-1}).$$

Consider 4 carriers, i.e., $N = 4$, and 1/2 rate MC (7.2.10), i.e., $K = 1$ and $M = 2$. In this case, the MC coding inserts one zero in each two information symbols. According to (2.3.3), the blocked ISI channel with block size 2 is

$$\mathbf{H}(z) = \frac{1}{\sqrt{2}} \begin{bmatrix} 1 & z^{-1} \\ 1 & 1 \end{bmatrix}. \tag{7.3.3}$$

In the conventional OFDM system, the input-output relationship (7.1.2) is

$$y_k(n) = \frac{1}{\sqrt{2}}(1 + \exp(-j2\pi k/4))x_k(n) + \xi_k(n), \quad k = 0, 1, 2, 3, \tag{7.3.4}$$

where

$$H_k = \frac{1 + \exp(-j2\pi k/4)}{\sqrt{2}}$$

or $H_0 = \sqrt{2}$, $H_1 = \frac{1-j}{\sqrt{2}}$, $H_2 = 0$, and $H_3 = \frac{1+j}{\sqrt{2}}$. One can see that the third subcarrier channel in (7.3.4) completely fails. The BER performance of the conventional OFDM system is, thus,

$$P_e \approx \frac{1}{4}\frac{1}{2} = \frac{1}{8}. \tag{7.3.5}$$

For the MC coded OFDM system, the input-output relationship (7.2.15) is

$$\tilde{y}_k(n) = \frac{1}{\sqrt{2}} \begin{bmatrix} 1 \\ 1 \end{bmatrix} x_k(n) + \tilde{\xi}_k(n), \quad k = 0, 1, 2, 3, \tag{7.3.6}$$

where

$$\tilde{\mathbf{H}}_k = \frac{1}{\sqrt{2}} \begin{bmatrix} 1 \\ 1 \end{bmatrix}, \quad k = 0, 1, 2, 3,$$

which have the same singular value 1. (7.3.6) is rewritten as

$$\frac{1}{\sqrt{2}}[1 \;\; 1]\tilde{y}_k(n) = x_k(n) + \tilde{\xi}_k'(n), \tag{7.3.7}$$

where $\tilde{\xi}_k'(n)$ are complex Gaussian random variables with the same statistics as $\tilde{\xi}_k(n)$. In this case, the BER performance of the MC coded OFDM is the same as the uncoded AWGN performance if the additional cyclic prefix is ignored. For example, when BPSK is used, the BER is

$$P_e = Q\left(\sqrt{\frac{2E_b}{N_0}}\right). \tag{7.3.8}$$

As a remark, since the MC (7.2.10) does not increase the signal energy, the bit energy E_b before the prefix insertion does not increase although the data rate is increased. In (7.3.8) the cyclic prefix data expansion is ignored otherwise the E_b/N_0 in (7.3.8) needs to be replaced by

$$\frac{NE_b}{(N+\tilde{\Gamma})N_0} = \frac{4E_b}{5N_0}.$$

Clearly, the BER performance (7.3.8) of the MC coded OFDM system is much better than (7.3.5) of the uncoded OFDM system. One might want to ask us to compare it with the existing COFDM systems as studied in [189, 188, 47]. Since, in the existing COFDM systems, the conventional TCM or other error correction codes are used, the coding gain is limited for a fixed computational load. For example, the coding gain is about 3dB at the BER of 10^{-5} in [189], 6dB at the BER of 10^{-7}, and 7dB at the BER of 10^{-9} in [188], which can not bring the BER (7.3.5) down to (7.3.8). One might also want to compare the data rate with the existing COFDM. To increase the data rate for our MC coded OFDM system, high rate modulation schemes, such as 64QAM or 256QAM, can be used before the MC coded OFDM system. The *key* point here is that the existing COFDM systems do not erase the spectral nulls of the ISI channel while the MC coded

OFDM systems here may do as shown in the above simple example, where the spectral null characteristics play the key role in the performance degradation of an OFDM system. We shall see more complicated and general examples later via computer simulations.

Let us consider the MC (7.2.10) without data rate increase, i.e., $M = K$. In this case, the input-output relationship (7.3.1) for the MC coded OFDM system, which will be called vector OFDM later, becomes

$$\tilde{y}_k(n) = \frac{1}{\sqrt{2}} \begin{bmatrix} 1 & e^{-j2\pi k/4} \\ 1 & 1 \end{bmatrix} \bar{x}_k(n) + \tilde{\xi}_k(n), \quad k = 0, 1, 2, 3, \tag{7.3.9}$$

where

$$\mathbf{H}_k = \frac{1}{\sqrt{2}} \begin{bmatrix} 1 & e^{-j2\pi k/4} \\ 1 & 1 \end{bmatrix}, \quad k = 0, 1, 2, 3,$$

and the singular values of $\mathbf{H}_0$ are $\sqrt{2}$ and 0, which confirms the previous argument, i.e., the zero singular value can not be removed if no data rate expansion is used in the MC coding. In this case, there are equivalently 8 subchannels and one of them fails due to the 0 singular value. Thus, the BER performance is

$$P_e \approx \frac{1}{8}\frac{1}{2} = \frac{1}{16}. \tag{7.3.10}$$

Notice that, even when a subchannel fails, the BER performance (7.3.10) of the vector OFDM system is better than the one (7.3.5) of the conventional OFDM system. This will be seen in Section 7.3.5 from other simulation results for all other examples presented in this paper.

We next derive the analytical BER vs. E_b/N_0 for the MC coded OFDM systems for general ISI channels.

7.3.3 Performance Analysis of MC Coded OFDM Systems for ISI Channels

To study the BER performance of the MC coded OFDM systems proposed in Section 7.3.1, let us go back to the MIMO system (7.2.15), where the components of the vectors $\bar{x}_k(n)$ defined in (7.3.2) are from the original information symbols $x(n)$. We need to estimate $\bar{x}_k(n)$ from $\tilde{y}_k(n)$ through (7.2.15) for each fixed index k. There are different methods for the estimation, such as the maximum-likelihood (ML) estimation and the minimum mean square error (MMSE) estimation. In what follows, for the BER performance analysis we use the MMSE estimation, which is simpler. For the simulations presented in Section 7.3.5, we use the ML estimation for each

fixed index k. Clearly the BER for the MMSE estimation is an upper bound of the BER for the ML estimation when the vector size of $\bar{x}_k(n)$ is greater than 1, i.e., $K > 1$.

The MMSE estimator of $\bar{x}_k(n)$ in (7.2.15) is given by

$$\hat{\bar{x}}_k(n) = (\bar{\mathbf{H}}_k)^+ \tilde{y}_k(n), \quad k = 0, 1, ..., N-1, \tag{7.3.11}$$

where $^+$ stands for the pseudo-inverse, i.e.,

$$(\bar{\mathbf{H}}_k)^+ = \left((\bar{\mathbf{H}}_k^*)^T \bar{\mathbf{H}}_k\right)^{-1} (\bar{\mathbf{H}}_k^*)^T. \tag{7.3.12}$$

The noise of the MMSE estimator $\hat{\bar{x}}_k(n)$ is

$$\hat{\tilde{\xi}}_k(n) = (\bar{\mathbf{H}}_k)^+ \tilde{\xi}_k(n), \tag{7.3.13}$$

whose components are, in general, complex Gaussian random variables. Then, the theoretical BER can be calculated as long as the original binary to complex mapping, number of carriers, N, the ISI channel $H(z)$, and the MC coding rate K/M are given.

For simplicity, let us consider the BPSK signal constellation. In this case, the complex Gaussian random noise are reduced to the real Gaussian random noise by cutting the imaginary part that does not affect the performance. Thus the noise in this case is

$$\mathrm{Re}\left(\hat{\tilde{\xi}}_k(n)\right).$$

Therefore, the BER vs. E_b/N_0 for the MMSE estimator given in (7.3.11) is

$$P_e = \frac{2^{K-1}}{2^K - 1} \frac{1}{N} \sum_{k=0}^{N-1} \left(1 - \frac{1}{(2\pi)^{K/2} (\det M_k)^{1/2}} \int_{-\gamma_b}^{\infty} \cdots \int_{-\gamma_b}^{\infty} \right.$$

$$\left. \exp\left\{-\frac{1}{2} \bar{x}^T M_k^{-1} \bar{x}\right\} dx_1 \cdots dx_K \right), \tag{7.3.14}$$

where the factor $2^{K-1}/(2^K - 1)$ is due to the conversion of the symbol error rate (SER) of $\bar{x}$ to the BER, $\bar{x} = (x_1, \cdots, x_K)$,

$$\gamma_b = \sqrt{\frac{2E_b N}{N_0(N + \tilde{\Gamma})}}, \tag{7.3.15}$$

and

$$M_k = \mathrm{Re}\left((\bar{\mathbf{H}}_k)^+\right) \mathrm{Re}\left((\bar{\mathbf{H}}_k)^+\right)^T + \mathrm{Im}\left((\bar{\mathbf{H}}_k)^+\right) \mathrm{Im}\left((\bar{\mathbf{H}}_k)^+\right)^T. \tag{7.3.16}$$

The overall data rate overhead can be easily calculated as

$$\frac{M(N+\tilde{\Gamma})}{KN} \approx \frac{M(N+\frac{L}{M})}{KN} = \frac{MN+L}{KN}, \tag{7.3.17}$$

where $L+1$ is the length of the ISI channel $H(z)$, and $\approx$ is due to the fact that $\tilde{\Gamma} = \lceil L/M \rceil = L/M$ if L is a multiple of M and $1 + L/M$ otherwise. The uncoded OFDM systems reviewed in Section 7.1 corresponds to the case when $K = M = 1$, in which the data rate overhead for the uncoded OFDM systems is

$$\frac{N+L}{N}. \tag{7.3.18}$$

7.3.4 Vector OFDM Systems

When the ISI channel length $L+1$ in (7.1.1) is large, the cyclic prefix length $\Gamma = L$ in the conventional OFDM systems is large too. As a consequence, the data rate overhead $(N+L)/N$ is high when L is large. In this section, we propose vector OFDM systems that reduce the data rate overhead while the ISI channels are still converted to ISI-free channels.

The vector OFDM systems are the MC coded systems in Fig.7.2 with the special MC $\mathbf{G}(z) = I_{K\times K}$ that basically blocks the input data into $K\times 1$ vectors and the data rate is not changed, i.e., no redundancy is added. In other words, the MC (7.2.10) in the MC coded OFDM systems takes the squared identity matrix, i.e., $M = K$ in (7.2.10). Similar to (7.3.17), the vector cyclic prefix data rate overhead is

$$\frac{K(N\tilde{\Gamma})}{KN} \approx \frac{N+\frac{L}{K}}{N}. \tag{7.3.19}$$

Compared to the data rate overhead $(N+L)/N$ for the conventional OFDM systems, the data rate overhead in the vector OFDM systems is reduced by K times, where K is the vector size.

The receiver is the same as the one for the MC coded OFDM systems in the previous sections with $K = M$. In this case, the ISI-free systems (7.2.15) at the receiver becomes

$$\tilde{y}_k(n) = \mathbf{H}_k \bar{x}_k(n) + \tilde{\xi}_k(n), \quad k = 0, 1, ..., N-1, \tag{7.3.20}$$

where $\mathbf{H}_k$ are defined in (7.2.9) and (2.3.3). As mentioned in the preceding sections, the robustness of the vector OFDM systems to spectral nulls of ISI channels is similar to the one of the conventional uncoded OFDM systems, since no redundancy is inserted in vector OFDM systems. In other words,

the BER performance of the vector OFDM systems is similar to the one for the uncoded OFDM systems. The performance analysis in Section 7.3.3 for the MC coded OFDM systems applies to the vector OFDM systems by replacing $M = K$.

To reduce the cyclic prefix overhead, another simple way is to increase the number N of the subcarriers, i.e., the DFT/IDFT size, in the conventional OFDM system. In the above vector OFDM, the prefix overhead is reduced the same as this simple way but the DFT/IDFT size does not increase.

7.3.5 Numerical Results

In this section, we present numerical results for some theoretical and simulation curves of the BER vs. E_b/N_0. The number of carriers is chosen as 256, i.e., $N = 256$, in all the following numerical examples. Three ISI channels are considered:

Channel A: $h = [0.407,\ 0.815,\ 0.407]$, which is a spectral-null channel;

Channel B: $h = [0.8,\ 0.6]$. Although it does not have spectral-nulls, its Fourier transform values at some frequencies are small and the small values cause the performance of the conventional uncoded OFDM system;

Channel C: $h = [0.0001 + 0.0001j,\ 0.0485 + 0.0194j,\ 0.0573 + 0.0253j,\ 0.0786 + 0.0282j,\ 0.0874 + 0.0447j,\ 0.9222 + 0.3031j,\ 0.1427 + 0.0349j,\ 0.0835 + 0.0157j,\ 0.0621 + 0.0078j,\ 0.0359 + 0.0049j,\ 0.0214 + 0.0019j]$, which does not have spectral null or small Fourier transform values.

Their Fourier power spectrum (dB) are plotted in Fig.7.5. Channel A and Channel C are selected from the examples presented in [127].

For Channel A and Channel B, six curves of the BER vs. E_b/N_0 are plotted in Figs.7.6-7.7, respectively. The theoretical and simulated curves for the uncoded OFDM system with BPSK signaling are marked by $\times$ and $\square$, respectively. The theoretical and simulated curves for the MC coded OFDM system with rate 1/2, i.e., $K = 1$ and $M = 2$, and the BPSK signaling are marked by $+$ and $\circ$, respectively. The simulated curve for the MC coded OFDM svstem with rate 1/2, i.e., $K = 1$ and $M = 2$, and the QPSK signaling is marked by ∇. One can clearly see the improvement of the MC coding. The BER performances of the uncoded and MC coded OFDM systems are incomparable, where, we think, the difference can not be reached by any existing COFDM systems. The QPSK MC coded OFDM system has the same data rate as the uncoded BPSK OFDM system while their performances are much different. The performance improvement can not be achieved by any existing COFDM system using the TCM or even turbo codes.

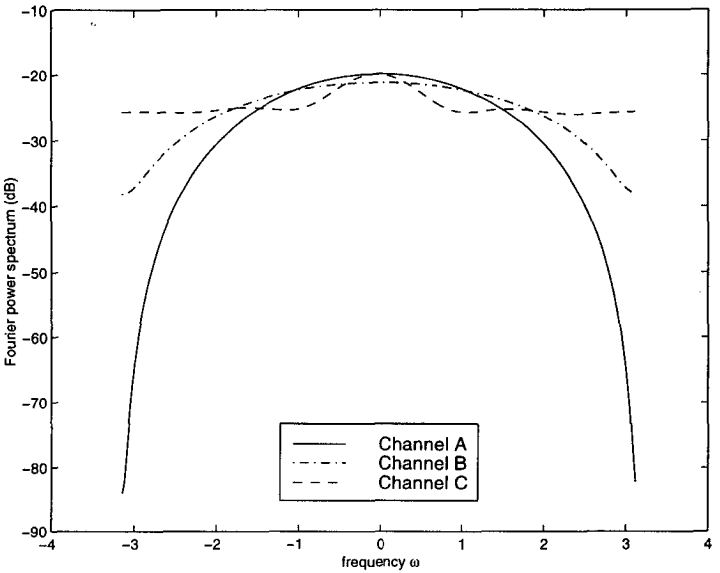

Figure 7.5: Fourier spectrum for three ISI channels.

From Fig.7.5, the nonspectral-null property of Channel B is better than that of Channel A. One can see that the BER performances of all the OFDM systems in Fig.7.7 for Channel B are better than the ones in Fig.7.6 for Channel A.

The curves for the vector OFDM with vector size $K = 2$, i.e., $K = M = 2$ in the MC coded OFDM system are marked by $*$ in Figs.7.6-7.7. One can see that the performance for the vector OFDM system is even better than the one for the uncoded OFDM system for these two channels. The data rate overhead for Channel A is saved by half for the vector OFDM system compared with the conventional OFDM system.

For Channel C, three simulation curves of the BER vs. E_b/N_0 are plotted in Fig.7.8, where the signal constellations are all BPSK. The uncoded conventional OFDM system is marked by $\circ$. The MC coded OFDM system of rate 1/2 with $K = 1$ and $M = 2$ is marked by ∇. The vector OFDM system with vector size 2, i.e., $K = M = 2$, is marked by $+$. Since the ISI channel is not spectral null, the MC coding does not show too much performance advantage. The vector OFDM system, however, still performs better than the conventional OFDM system while the cyclic prefix data rate overhead for the vector OFDM and the conventional OFDM are $(256 + 5)/256$

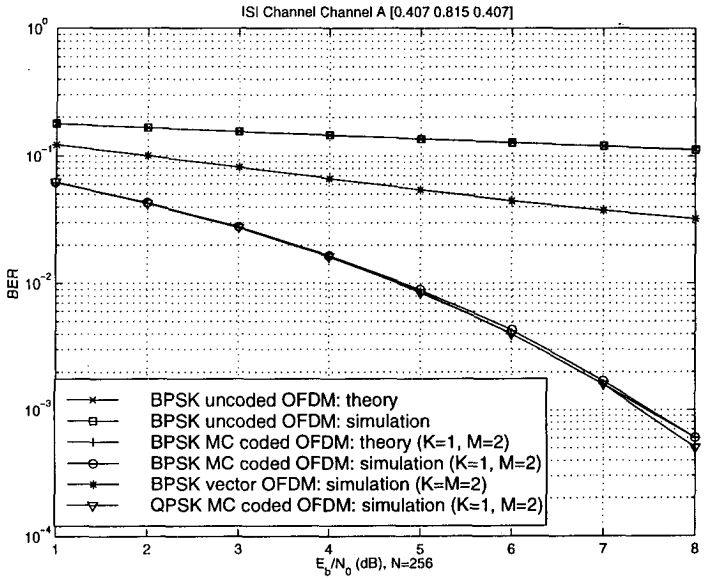

Figure 7.6: Performance comparison of OFDM systems: Channel A.

and $(256 + 10)/256$, respectively. Note that the prefix length of the vector OFDM system is only half of that of the conventional OFDM system.

7.4 Channel Independent MC Coded OFDM System for Frequency-Selective Fading Channels

In the previous sections, we studied the MC coded OFDM systems in time-invariant ISI channels. In this section, we want to study the performance of the MC coded OFDM systems in time-variant ISI channels, i.e., frequency-selective multipath fading channels, modeled as

$$y(n) = \sum_{l=0}^{L-1} h_l(n)x(n-l) + \eta(n), \tag{7.4.1}$$

where $x(n)$ and $y(n)$ are the input and output, respectively, and $\eta(n)$ is the additive noise as before, and L is the number of paths, i.e., the channel

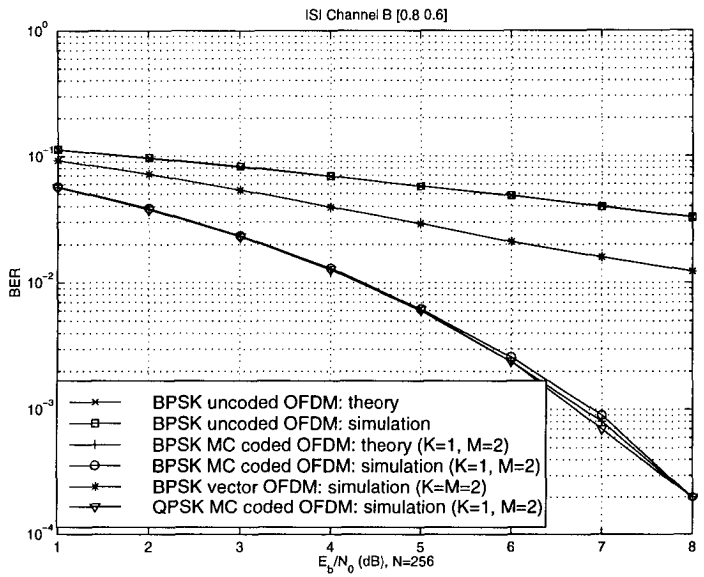

Figure 7.7: Performance comparison of OFDM systems: Channel B.

taps. We assume that the input information symbol sequence $x(n)$ is i.i.d. with mean 0 and variance E_x. We also assume that the multipaths h_l are independent of each other. The main idea of the following study is to approximate the time-variant $h_l(n)$ by using time-invariant paths in each MC coded OFDM block and move the approximation error into the additive noise, where the block length of the MC coded OFDM system in Fig.7.2 is NM, N is the number of subcarriers, i.e., the DFT length, and M is the block/vector length.

7.4.1 Performance Analysis

For convenience, we consider the frequency-selective multipath channel (7.4.1) in the block $n = 1, 2, ..., NM$ and use the center channel value $h_l(\frac{NM}{2})$ as the approximation value of $h_l(n)$, $n = 1, 2, ..., NM$, for each $l = 0, 1, ..., L-1$, and it is also used in the MC coded OFDM system decoding. Then, we have

$$y(n) = \sum_{l=0}^{L-1} h_l(\frac{NM}{2})x(n-l) + \eta_1(n) + \eta(n), \qquad (7.4.2)$$

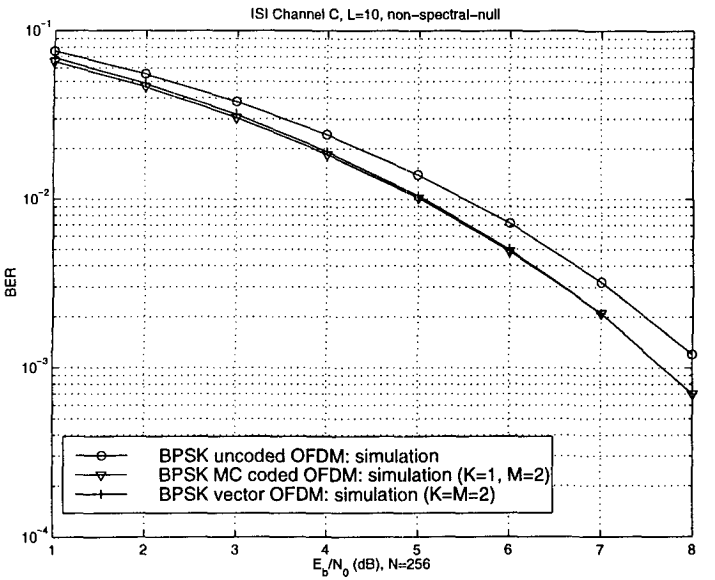

Figure 7.8: Performance comparison of OFDM systems: Channel C.

where

$$\eta_1(n) = \sum_{l=0}^{L-1} \left(h_l(n) - h_l(\frac{NM}{2}) \right) x(n-l) \tag{7.4.3}$$

is the approximation error of the multipath channel and independent of the additive noise $\eta(n)$. Thus, the MC coded OFDM system in the time-variant channel (7.4.1) becomes the one in the time-invariant channel (7.4.2) and at the receiver, the MC coded OFDM system becomes (7.2.15), where the constant matrices $\bar{\mathbf{H}}_k$ are from the time-invariant ISI channel $h_l = h_l(\frac{NM}{2})$, $l = 0, 1, ..., L-1$, and the additive noise is from the original $\eta(n)$ and the approximation error $\eta_1(n)$. Therefore, to study the performance, we only need to study the noise $\eta_1(n) + \eta(n)$ and the singular values of $\bar{\mathbf{H}}_k$ in the linear systems (7.2.15). Let us first study the noise $\eta_1(n)$ in (7.4.3). By the independence of h_l, $l = 0, 1, ..., L-1$, and the i.i.d. property of the input $x(n)$, the correlation function $\eta_1(n)$ is

$$E\left(\eta_1(n)\eta_1^*(n+\tau)\right) =$$

$$E_x\delta(\tau)\sum_{l=0}^{L-1}\left[E\left(h_l(n)h_l^*(n+\tau)\right)+E\left(h_l(\frac{NM}{2})h_l^*(\frac{NM}{2})\right)\right.$$

$$\left.-E\left(h_l(n)h_l^*(\frac{NM}{2})\right)-E\left(h_l(\frac{NM}{2})h_l^*(n+\tau)\right)\right], \tag{7.4.4}$$

where $E(\cdot)$ stands for the expectation. For the Rayleigh fading channels, we have

$$E(h_l(n)h_l^*(n+\tau))=\frac{\Omega_l}{2}J_0(2\pi f_m\tau T_s), \tag{7.4.5}$$

where $J_0(x)$ is the zeroth-order Bessel function of the first kind, T_s is the sampling interval length, $f_m=v/\lambda_c$ is the maximum Doppler shift, v is the velocity of the mobile user, λ_c is the carrier wavelength, and Ω_l is the mean power of the lth path h_l. Thus,

$$E(\eta_1(n)\eta_1^*(n+\tau))=E_x\delta(\tau)\sum_{l=0}^{L-1}\Omega_l\left(J_0(0)-J_0(2\pi f_mT_s(n-\frac{NM}{2}))\right). \tag{7.4.6}$$

Thus, the mean power of η_1 is

$$\sigma_{\eta_1}^2=\frac{\sum_{n=1}^{NM}\sum_{l=0}^{L-1}\Omega_l\left(J_0(0)-J_0(2\pi f_mT_s(n-\frac{NM}{2}))\right)}{NM}, \tag{7.4.7}$$

and the total mean noise power is

$$\sigma_{\eta_1}^2+\sigma_\eta^2. \tag{7.4.8}$$

After the mean noise power is calculated, we now come back to the linear systems (7.2.15) at the receiver with respect to the channel (7.4.2). Using the SVD decomposition of $\bar{\mathbf{H}}_k$, (7.2.15) becomes the following equivalent system:

$$\tilde{y}_k(n)=\Lambda_k(n)V_k(n)\bar{x}_k(n)+\tilde{\xi}_k(n),\quad k=0,1,...,N-1, \tag{7.4.9}$$

where $V_k(n)$ are $K\times K$ unitary matrices, and $\Lambda_k(n)$ are $M\times K$ matrices of the form

$$\Lambda_k(n)=\begin{bmatrix}\text{diag}(\lambda_1,...,\lambda_K)\\ 0_{(M-K)\times K}\end{bmatrix}, \tag{7.4.10}$$

and λ_1, λ_2, ..., λ_K are K nonzero singular values of $\bar{\mathbf{H}}_k$.

For convenience, in what follows we consider BPSK signaling, i.e., $\bar{x}_k(n)$ take binary values. When $K = 1$, the BER of (7.4.9) is

$$P_e = \int Q\left(\sqrt{\frac{\lambda^2 E_b}{\sigma_{\eta_1}^2 + \sigma_\eta^2}}\right) p(\lambda) d\lambda, \tag{7.4.11}$$

where Q stands for the Q function, $E_b = E_x$ is the mean signal power per bit, and $p(\lambda)$ is the probability density function of the singular values λ_k in (7.4.10) and shall be estimated later. By taking the bandwidth expansion of the cyclic prefix insertion into account, the BER of the MC coded OFDM system in Fig.7.2 when $K = 1$, is

$$P_b = \int Q\left(\sqrt{\frac{\lambda^2 E_b N}{(\sigma_{\eta_1}^2 + \sigma_\eta^2)(N + \tilde{\Gamma})}}\right) p(\lambda) d\lambda. \tag{7.4.12}$$

When $K > 1$, although it is hard to have the exact BER expression due to the fact that the K noise components in (7.4.9) after the inversion of the matrix $V_k(n)$ may not be i.i.d., it is not hard to derive its lower and upper bounds as follows. The BER is lower bounded by the BER when all the K noise components in $(V_k(n))^{-1}\tilde{\xi}_k(n)$ are i.i.d., i.e.,

$$P_b \geq \int Q\left(\sqrt{\frac{E_b K N}{\gamma(\sigma_{\eta_1}^2 + \sigma_\eta^2)(N + \tilde{\Gamma})}}\right) p(\gamma) d\gamma, \tag{7.4.13}$$

where γ is determined by the singular values λ_k in (7.4.10) as

$$\gamma = \sum_{k=1}^{K} \frac{1}{\lambda_k^2}, \tag{7.4.14}$$

and $p(\gamma)$ is the probability density function of random variable γ. The BER is upper bounded by the BER when the total noise power of all the components is in one of the K noise components in $(V_k(n))^{-1}\tilde{\xi}_k(n)$, i.e.,

$$P_b \leq \frac{1}{K} \int Q\left(\sqrt{\frac{E_b N}{\gamma(\sigma_{\eta_1}^2 + \sigma_\eta^2)(N + \tilde{\Gamma})}}\right) p(\gamma) d\gamma, \tag{7.4.15}$$

where γ is as in (7.4.14).

We next want to study the probability distribution of the singular values of the $\bar{\mathbf{H}}_k$ in (7.2.15) when $h_l = h_l(\frac{NM}{2})$ and $h_l(n)$ are Rayleigh fading. The distributions of the singular values can be determined as follows, when $K = N$ or $K = 1$.

Theorem 7.1 *The distribution of the singular values of a vector OFDM system, i.e., $K = N$, in frequency-selective multipath Rayleigh fading channels is Rayleigh distribution.*

Proof. The blocked channel $\mathbf{H}(z)$ in Fig.7.4 of $H(z)$ has the diagonalization (2.3.10). By (7.2.9), $\mathbf{H}_k = \mathbf{H}(z)|_{z=\exp(j2\pi k/N)}$, the singular values of $\mathbf{H}_k$ are the magnitudes of $H(zW_M^m)|_{z=\exp(j2\pi k/(MN))}$ for $m = 0, 1, ..., M-1$. Since each coefficient $h_l(\frac{NM}{2})$ in $H(z)$ is complex Gaussian, the random variables $H(zW_M)|_{z=\exp(j2\pi k/(MN))}, k = 0, 1, ..., N-1$ are also complex Gaussian. This proves Theorem 7.1. ■

Notice that when $M = 1$, the vector OFDM is the conventional OFDM and therefore, the singular values of the conventional OFDM systems also have the Rayleigh distribution.

Theorem 7.2 *The distribution of the singular values of an MC coded OFDM system with $K = 1$ in frequency-selective multipath Rayleigh fading channels is Nakagami distribution.*

Proof. From the proof in Theorem 7.1, all components in each matrix $\mathbf{H}_k$ are all complex Gaussian. When $K = 1$, the singular values of $\bar{\mathbf{H}}_k$ are the norms of the the first columns of matrix $\mathbf{H}_k$, which, therefore, has Nakagami distribution. ■

For the MC coded OFDM system in (7.2.15) with a general $K < N$, the distribution of the singular values varies between gamma and Nakagami distributions from our many numerical examples. Some examples are shown in Section 7.4.2 and see Fig.7.9 and Fig.7.10.

Since, the BER bounds in (7.4.13) and (7.4.15) depend on γ in (7.4.14) and its probability density function. It is important to estimate it. Although we are not able to analytically prove any distribution result for $K > 1$, our many numerical results show that it is not hard to see the distribution from the histogram of γ as shown in Fig.7.10(b), where it is a gamma distribution.

7.4.2 Simulation Results

We now present some simulation results on the MC coded OFDM system in Fig.7.2 in frequency-selective Rayleigh fading channels. We consider two ray Rayleigh fading channels with equal power, i.e., $L = 2$ and $\Omega_1 = \Omega_2$. Each Rayleigh fading ray is generated by the Jakes's method [127] with the following parameters: 34 paths with equal strength multipath components, 8 oscillators, carrier frequency $f_c = 850$ MHz, simulation time sample interval length $T_s = 41.667\mu s$. The velocities of users considered are

$v = 4$ km/hour, $v = 40$ km/hour and $v = 100$ km/hour. The corresponding Doppler shifts are 3.15 Hz, 31.48 Hz, and 78.7 Hz, respectively.

We first consider the length of the DFT/IDFT in the MC coded OFDM system to be $N = 64$. The channel independent MC (7.2.10) is used. In order to have the same update time duration length, the DFT/IDFT length in the conventional OFDM system is 192 and thus the channel update time duration length is $192T$ for both the MC coded and the conventional OFDM systems. In the decoding, the channel values $h_0(96)$ and $h_1(96)$ are used. In this simulation, the user moving speeds are 4 km/hour and 40 km/hour.

Let us first see the singular value distributions, which do not depend on a Doppler shift but on the OFDM block size, the MC size, and the DFT/IDFT size. Fig.7.9 (a) and (b) show the singular value histograms of the conventional OFDM systems and the MC coded OFDM systems with $K = 1$ and $M = 2$, respectively. One can see that the singular values of the conventional OFDM systems have the Rayleigh distribution while the ones of the MC coded OFDM systems have the Nakagami distribution as Theorems 1 and 2 claimed. The singular value histogram of the MC coded OFDM system with $K = 2$ and $M = 3$ is shown in Fig.7.10(a) and it is a gamma distribution. The histogram of

$$\gamma = \frac{1}{\lambda_1^2} + \frac{1}{\lambda_2^2}$$

is shown in Fig.7.10(b), which has gamma distribution too, but with different parameters. It is usually the case that, the larger the singular values are, the better the performance of the OFDM system is. From Figs.7.9-7.10, one can see that the singular value mean of the MC coded OFDM systems with $K = 2$ and $M = 3$ is larger than the ones of the conventional and vector OFDM systems, and the one of the MC coded OFDM system with $K = 1$ and $M = 2$ is larger than the one of the MC coded OFDM system with $K = 2$ and $M = 3$.

In the following BER performance simulations, we consider the MC in (7.2.10) with $K = 2$ and $M = 3$, i.e., the MC coding rate is 2/3. We also consider the conventional convolutionally coded (CC) OFDM with CC rate 2/3 and constraint length 2 and 3×2 generator matrix $[1, 1 + D; 1 + D, D; 1, 1]$. The Viterbi decoding algorithm is used after the OFDM decoding in the COFDM. Fig.7.11(a) and (b) show the performance comparisons when the moving speeds are 40 km/hour and 4 km/hour, respectively.

When the user moving speed is 100 km/hour, we consider the total block size 48: the DFT/IDFT size for the MC coded ($K = 2$ and $M = 3$) and the conventional OFDM systems are 16 and 48, respectively. The reason for reducing the size is that when the Doppler shift is large, the channel update

needs to be faster in order to maintain a certain system performance quality. The channel update time duration length in both systems is $48T_s$. The BER performances of the MC coded OFDM and the COFDM are shown in Fig.7.12(a). One can see that the BER performances of the MC coded and the convolutional coded OFDM systems are comparable while the decoding of the MC coded OFDM system is much simpler than the Viterbi decoding in the COFDM. The performances of the MC coded OFDM and the conventional COFDM, however, differ significantly when the spectral-null time-invariant ISI channel is considered as shown in Fig.7.12(b).

As a remark, although we only showed results in Rayleigh fading channels with two equal power rays, similar results hold with more than two rays.

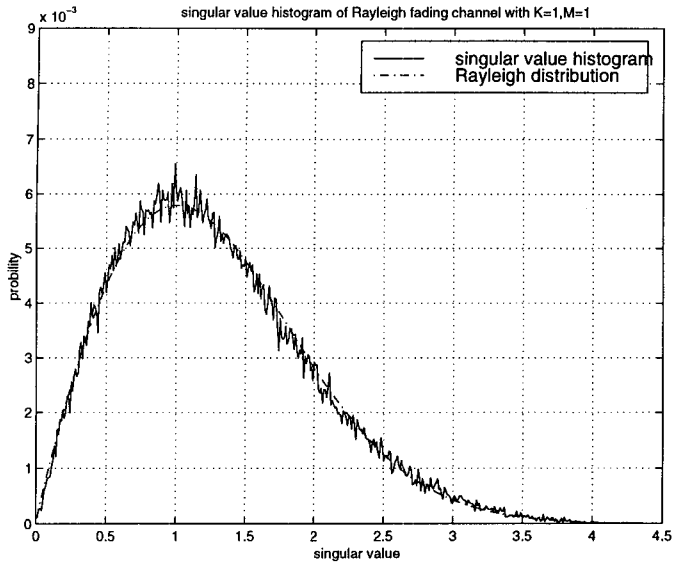

(a)

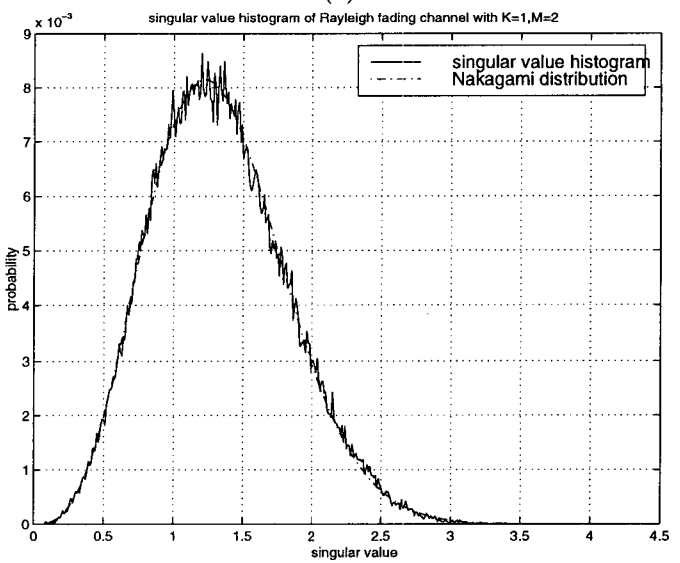

(b)

Figure 7.9: Singular value histograms of the conventional and MC coded OFDM systems in a two ray frequency-selective Rayleigh fading channel: (a) $K = 1$ and $M = 1$; (b) $K = 1$ and $M = 2$.

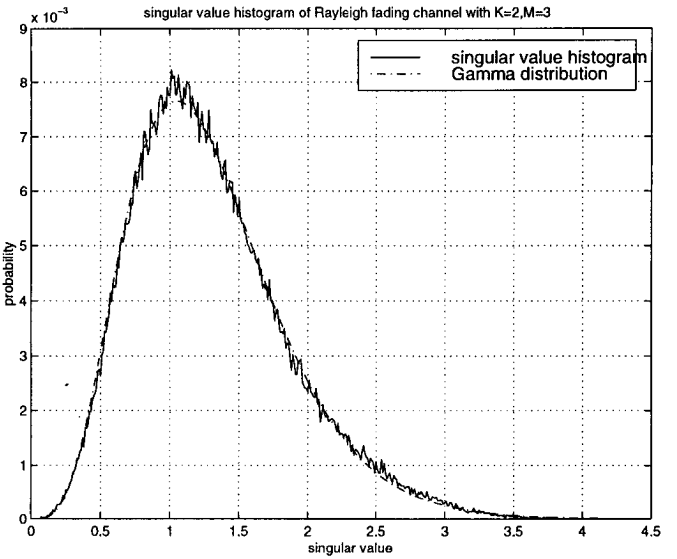

(a)

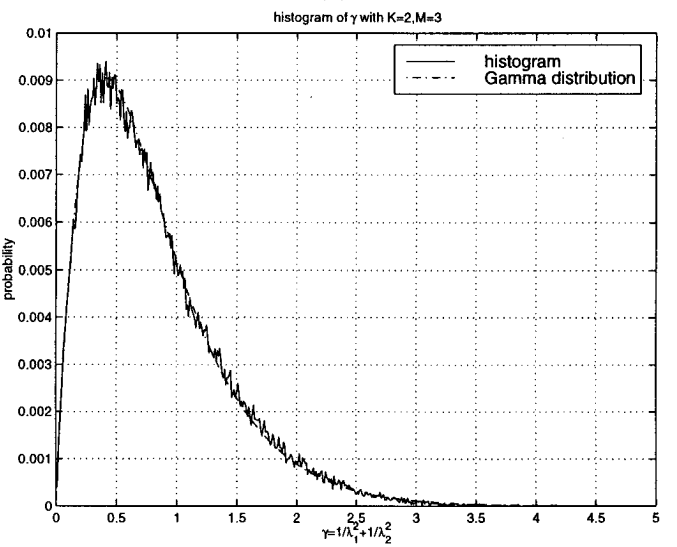

(b)

Figure 7.10: Singular value histograms of MC coded OFDM systems with $K = 2$ and $M = 3$ in a two ray frequency-selective Rayleigh fading channel: (a) singular value historgram; (b) γ histogram.

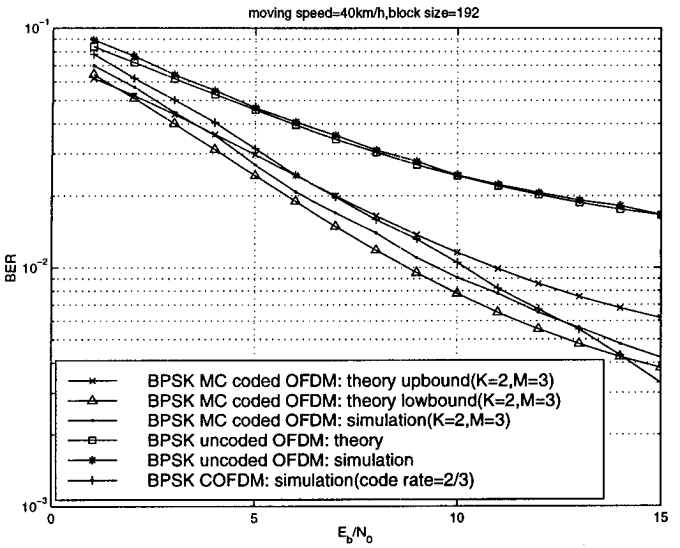

(a)

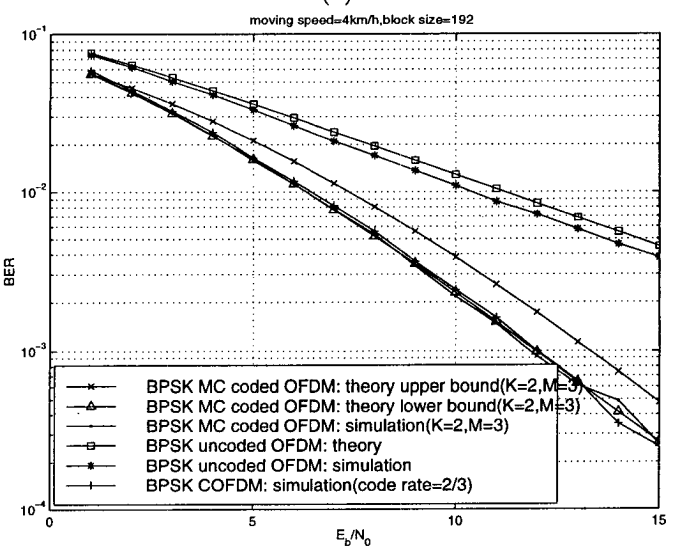

(b)

Figure 7.11: Performance comparison of the conventional OFDM, MC coded OFDM, and COFDM systems in two ray frequency-selective Rayleigh fading channels with moving speed (a) 40km/h and (b) 4km/h.

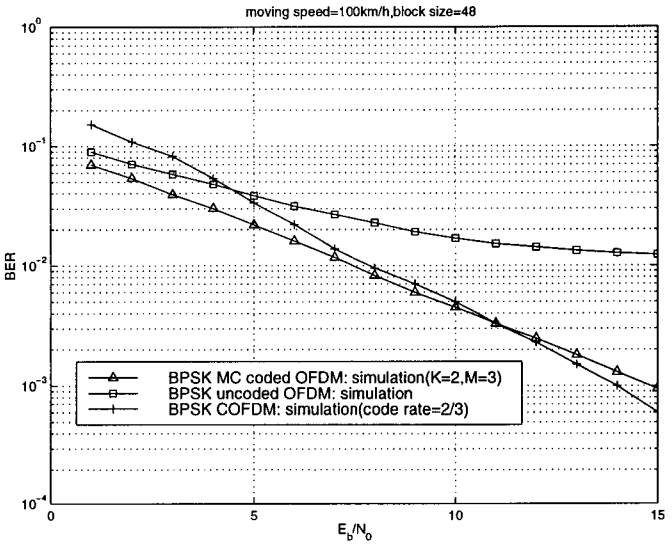

(a)

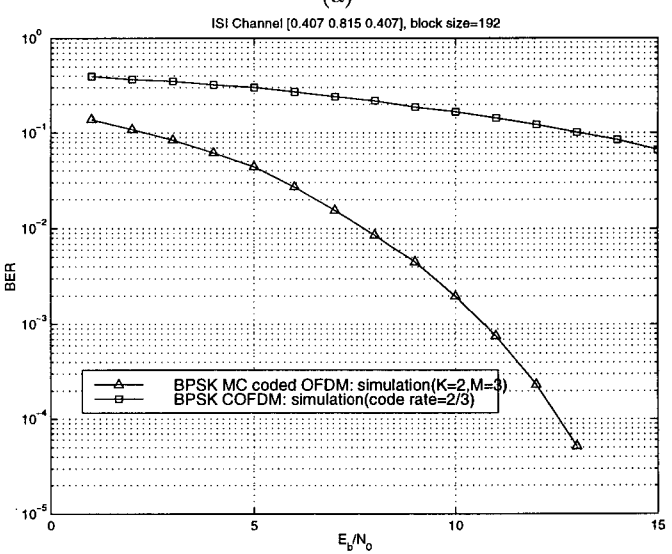

(b)

Figure 7.12: Performance comparison of MC coded OFDM and COFDM systems in (a) two ray frequency-selective Rayleigh fading channels with moving speed 100km/h and (b) spectral-null ISI channel.

Chapter 8

Polynomial Ambiguity Resistant Modulated Codes for Blind ISI Mitigation

In Chapters 2-6, both transmitter and receiver need the ISI channel information for the MC encoding and decoding. In Chapter 7, the transmitter does not need the ISI information but the receiver does. In some applications, however, the ISI channel information may not be available to neither the transmitter nor the receiver. In the following chapters, we study the MC encoding and decoding when the ISI channel is not known at the transmitter or the receiver.

As a part of post equalization techniques, blind equalization attracts much attention lately due to the recent advances in channel identification using output diversities [134, 135, 101]. Spatial diversity (antenna arrays) and temporal diversity (fractional sampling) are the most studied among many others. Many blind identification algorithms exploiting either second order cyclostationary statistics [134, 135, 90, 180, 128, 136, 35, 63, 147, 81, 98, 123, 101, 36] or algebraic structures (often referred to as the deterministic solutions) [90, 180] have been proposed. However, the use of output diversities inevitably multiplies the number of data samples and therefore causes additional computations at the receiver. A new transmitter assisted (MC coded or precoded) blind equalization method has been studied lately in [53, 89, 88, 171, 186, 163, 118, 172]as explained below, where the overall

data rate expansion over the baud rate is not an integer multiple but a fractional number. The filterbank precoding in [165] is generalized to the blind equalization in [53] without much analysis on a precoder. Later, in [118] some precoding analysis in the time domain is introduced. In [89, 88], the concept of *ambiguity resistant* precoders (ARP) is first introduced in the z-transform domain for the blind identification by injecting a minimum amount of *structured* redundancy at the transmitter. The blind equalization problem for both a baud-rate sampled single-receiver system and an undersampled multi-receiver system is addressed in [89, 88] by casting them into a multi-input and multi-output (MIMO) framework with more outputs than inputs. With the existing MIMO identification methods, for example [90, 91, 181, 98, 147], the multi-input signal can be identified up to a nonsingular constant matrix from the multi-output signal. The ambiguity resistant precoders proposed in [89, 88] are capable of removing the constant matrix ambiguity directly from the receiver outputs. These precoders can be thought of as a family of the precoders proposed in [165] with an additional ambiguity resistant capability (by adding memory to the precoding), which is essential to the blind identifiability. In [186, 163, 172], ARP are systematically studied, characterized, and constructed. To resist an ISI channel, an ARP is sufficient. However, in practical communication systems, the additive noise has to be taken into the account. Therefore, a natural question is which ARP is more robust to the additive noise. In [163], such an issue is addressed, where an optimality on ARP is introduced and some optimal ARP are characterized and constructed. In [171], the concept of the ambiguity resistance is generalized from resisting only constant matrices to any FIR polynomial matrices as shown in Fig.8.1, which are called *(strong) polynomial ambiguity resistant* precoders (PARP). Based on the definitions in [171], strong PARP not only resist the ambiguity in the input signals but also in the FIR channel inverse, while regular PARP only resist the ambiguity in the input signal. In [172], such (strong) PARP are characterized and constructed. Since (strong) PARP are also MC, we call them (strong) polynomial ambiguity resistant MC (PARMC) in what follows.

In this chapter, we want to introduce (strong) PARMC and their applications in blind channel identification, which are are summarized from [89, 88, 171]. The theory developed in this chapter applies to not only single antenna systems but also multiple antenna systems as space-time coding. As a remark, a different approach for space-time coding, called *differential space-time coding*, for memoryless multiple antenna channels have been studied in [129, 60, 62, 61, 65, 66], where the channel information is not necessary and the space-time coding is achieved by using unitary constant

matrices. Another approach is reported in [162].

8.1 PARMC: Definitions

A *polynomial matrix* $\mathbf{Q}(z)$ of size $N \times K$ has the following form

$$\mathbf{Q}(z) = \sum_{m=0}^{P} Q(m) z^{-m}, \tag{8.1.1}$$

where $Q(m)$ are $N \times K$ constant matrices. $\mathbf{Q}(z)$ is also referred to as a matrix polynomial in some literature, see for example, [142]. A function matrix $\mathbf{V}(z)$ is a matrix where all entries are functions of z^{-1}. If $Q(P) \neq 0$, the integer P is defined as the *order* of $\mathbf{Q}(z)$. A polynomial matrix $\mathbf{H}(z)$ is *invertible* if it has full rank for some value z, whereas $\mathbf{Q}(z)$ is *irreducible* if it has full rank for all $z \neq 0$ including $z = \infty$. A squared polynomial matrix is *unimodular* if its determinant is a nonzero constant. When $N = K$, $\mathbf{Q}(z)$ is irreducible is equivalent to that $\mathbf{Q}(z)$ is unimodular, i.e, its determinant is a nonzero constant. $\mathbf{Q}(z)$ has FIR inverse if and only if $\mathbf{Q}(z)$ has determinant cz^{-n_0} for some nonzero constant c and integer n_0. $\mathbf{Q}(z)$ is irreducible implies that it has FIR inverse. Clearly, the probability of an $N \times N$ polynomial matrix having FIR inverse is 0. On the other hand, when $N > K$, $\mathbf{Q}(z)$ is irreducible if and only if all the determinants of all the $K \times K$ submatrices of $\mathbf{Q}(z)$ are coprime, which holds with probability 1 for an arbitrarily given $N \times K$ polynomial matrix $\mathbf{Q}(z)$. It is clear that an $N \times K$ irreducible polynomial matrix $\mathbf{Q}(z)$ with $K < N$ has a $K \times N$ irreducible polynomial matrix inverse $\mathbf{Q}^{-1}(z)$, i.e, $\mathbf{Q}^{-1}(z)\mathbf{Q}(z) = I_K$, where $\mathbf{Q}^{-1}(z)$ may not be unique. For more about unimodular and irreducible polynomial matrices, we refer the reader to Kailath [71] and Vaidyanathan [142].

We are now ready to define (strong) polynomial ambiguity resistant MC. First, let us define polynomial ambiguity resistant MC (PARMC).

Definition 8.1 *An $N \times K$ irreducible polynomial matrix $\mathbf{G}(z)$ is rth order polynomial ambiguity resistant (PAR) if the following equation for a $K \times K$ function matrix $\mathbf{V}(z)$ has only trivial solutions of the form $\mathbf{V}(z) = \alpha(z) I_K$ for some nonzero polynomial $\alpha(z)$ of order at most r:*

$$\mathbf{E}(z)\mathbf{G}(z) = \mathbf{G}(z)\mathbf{V}(z), \tag{8.1.2}$$

where $\mathbf{E}(z)$ is an $N \times N$ nonzero polynomial matrix of order at most r. A rth order PAR polynomial matrix is called a rth order polynomial ambiguity resistant modulated code (PARMC).

The above polynomial ambiguity resistant property only requires the uniqueness of the right hand side matrix $\mathbf{V}(z)$ up to a nonzero polynomial. Strong PARMC are defined as follows.

Definition 8.2 *An $N \times K$ irreducible polynomial matrix $\mathbf{G}(z)$ is strong rth order polynomial ambiguity resistant if the following equation for an $N \times N$ nonzero polynomial matrix $\mathbf{E}(z)$ of order at most r and a $K \times K$ function matrix $\mathbf{V}(z)$ have only trivial solutions of the forms $\mathbf{E}(z) = \alpha(z)I_N$ and $\mathbf{V}(z) = \alpha(z)I_K$ for some nonzero polynomial $\alpha(z)$ of order at most r:*

$$\mathbf{E}(z)\mathbf{G}(z) = \mathbf{G}(z)\mathbf{V}(z).$$

A strong rth order PAR polynomial matrix is called a strong rth order PARMC.

The above strong polynomial ambiguity resistant property requires a uniqueness up to a nonzero polynomial not only for the right-hand side matrix $\mathbf{V}(z)$ but also for the left-hand side nonzero polynomial matrix $\mathbf{E}(z)$. Obviously, strong PARMC are PARMC. The ambiguity resistant MC studied in [89, 88] are the strong 0th order PARMC here. It can be easily verified that a (strong) rth order PARMC is also a (strong) $(r-1)$th order PARMC. We will see later in Section 8.3.1 that (i) the input $\mathbf{X}(z)$ is blindly identifiable from the output $\mathbf{Y}(z)$ and the MC $\mathbf{G}(z)$ in the MC coded system in Fig.8.1 *if and only if* the MC $\mathbf{G}(z)$ is PARMC, and (ii) both the input $\mathbf{X}(z)$ and the ISI channel inverse $\mathbf{H}^{-1}(z)$ are blindly identifiable from the output $\mathbf{Y}(z)$ and the MC $\mathbf{G}(z)$ in the MC coded system in Fig.8.1 *if and only if* the MC $\mathbf{G}(z)$ is strong PARMC. A family of *strong* PARMC is first presented in [89, 88, 171] and shall be seen in the following section.

8.2 Basic Properties and a Family of PARMC

We first see some basic properties of PARMC and a family of PARMC. More properties and constructions will be presented later. To do so, let us see the Smith form decomposition of a polynomial matrix. For more details, we refer the reader to [142]. Any $N \times K$ polynomial matrix $\mathbf{H}(z)$

has the following Smith form decomposition

$$\mathbf{H}(z) = \mathbf{W}(z) \begin{bmatrix} \gamma_0(z) & 0 & \cdots & 0 & 0 & \cdots & 0 \\ 0 & \gamma_1(z) & \cdots & 0 & 0 & \cdots & 0 \\ \vdots & \vdots & \vdots & \vdots & \vdots & \vdots & \vdots \\ 0 & 0 & \cdots & \gamma_p(z) & 0 & \cdots & 0 \\ 0 & 0 & \cdots & 0 & 0 & \cdots & 0 \\ \vdots & \vdots & \vdots & \vdots & \vdots & \vdots & \vdots \\ 0 & 0 & \cdots & 0 & 0 & \cdots & 0 \end{bmatrix} \mathbf{U}(z), \quad (8.2.1)$$

where $\mathbf{W}(z)$ and $\mathbf{U}(z)$ are unimodular polynomial matrices with sizes $N \times N$ and $K \times K$, respectively, $\gamma_i(z)$ are polynomials of z^{-1}, $\gamma_i(z)$ divides $\gamma_{i+1}(z)$, for $i = 0, 1, ..., p-2$, i.e.,

$$\gamma_i(z) | \gamma_{i+1}(z), \ i = 0, 1, ..., p-2, \quad (8.2.2)$$

and

$$\gamma_i(z) = \frac{\Delta_{i+1}(z)}{\Delta_i(z)}, \quad (8.2.3)$$

where $\Delta_0(z) = 1$, $\Delta_i(z)$ for $i > 0$ is the greatest common divisor of all the $i \times i$ minors of $\mathbf{H}(z)$. Clearly, if $\mathbf{H}(z)$ is irreducible and $N \geq K$, then

$$\mathbf{H}(z) = \mathbf{W}(z) \begin{bmatrix} I_K \\ 0_{(N-K)\times K} \end{bmatrix} \mathbf{U}(z), \quad (8.2.4)$$

where I_K and $0_{(N-K)\times K}$ are $K \times K$ identity and $(N-K) \times K$ all zero matrices, respectively.

We now want to see some basic properties of PARMC.

Theorem 8.1 *If an $N \times K$ polynomial matrix $\mathbf{G}(z)$ is rth order polynomial ambiguity resistant, then*

(i) there exists no $N \times N$ irreducible (unimodular) polynomial matrix $\mathbf{E}(z)$ of order $r_1 \leq r/N$ and $K \times K$ function matrix $\mathbf{V}(z)$ such that the first column of matrix $\mathbf{E}(z)\mathbf{G}(z)\mathbf{V}(z)$ is $(1, 0, 0, ..., 0)^T$;

(ii) $N > K$;

(iii) the order of $\mathbf{G}(z)$, Q_g, must be greater than r/N.

Proof. We first prove the necessity of condition (i). Assume there are an $N \times N$ irreducible polynomial matrix $\mathbf{E}(z)$ of order $r_1 \leq r/N$ and a $K \times K$ function matrix $\mathbf{V}(z)$ such that the first column in matrix $\mathbf{E}(z)\mathbf{G}(z)\mathbf{V}(z)$ is $(1, 0, 0, ..., 0)^T$, i.e.,

$$\mathbf{E}(z)\mathbf{G}(z)\mathbf{V}(z) = \begin{bmatrix} 1 & * & * & \cdots & * \\ 0 & * & * & \cdots & * \\ \vdots & \vdots & \vdots & & \vdots \\ 0 & * & * & \cdots & * \end{bmatrix}.$$

Then, by doing column elementary operations, all elements in the first row of the above matrix can be reduced to 0 except the first one. More specifically, there exists a unimodular polynomial matrix $\mathbf{V}_1(z)$ such that

$$\mathbf{E}(z)\mathbf{G}(z)\mathbf{V}(z)\mathbf{V}_1(z) = \begin{bmatrix} 1 & 0 & 0 & \cdots & 0 \\ 0 & * & * & \cdots & * \\ \vdots & \vdots & \vdots & & \vdots \\ 0 & * & * & \cdots & * \end{bmatrix}.$$

Define

$$F_l = \text{diag}(2, 1, 1, \cdots, 1)_{N \times N}, \quad \text{and } F_r = \text{diag}(2, 1, 1, \cdots, 1)_{K \times K}.$$

We have

$$F_l\mathbf{E}(z)\mathbf{G}(z)\mathbf{V}(z)\mathbf{V}_1(z)F_r^{-1} = F_l \begin{bmatrix} 1 & 0 & 0 & \cdots & 0 \\ 0 & * & * & \cdots & * \\ \vdots & \vdots & \vdots & & \vdots \\ 0 & * & * & \cdots & * \end{bmatrix} F_r^{-1}$$

$$= \begin{bmatrix} 1 & 0 & 0 & \cdots & 0 \\ 0 & * & * & \cdots & * \\ \vdots & \vdots & \vdots & & \vdots \\ 0 & * & * & \cdots & * \end{bmatrix} = \mathbf{E}(z)\mathbf{G}(z)\mathbf{V}(z)\mathbf{V}_1(z).$$

Upon defining

$$\tilde{\mathbf{E}}(z) = \mathbf{E}^{-1}(z)F_l\mathbf{E}(z), \quad \text{and } \mathbf{X}(z) = \mathbf{V}(z)\mathbf{V}_1(z)F_r\mathbf{V}_1^{-1}(z)\mathbf{V}^{-1}(z), \tag{8.2.5}$$

we are able to establish the following equality,

$$\tilde{\mathbf{E}}(z)\mathbf{G}(z) = \mathbf{G}(z)\mathbf{X}(z). \tag{8.2.6}$$

Since the order of $\mathbf{E}(z)$ is less than or equal to r/N and the order of $\mathbf{E}^{-1}(z)$ is at most $(N-1)r/N$ due to that $\mathbf{E}(z)$ is unimodular (square irreducible), the order of $\tilde{\mathbf{E}}(z)$ is at most r. From (8.2.6), by the assumption that $\mathbf{G}(z)$ is rth order polynomial ambiguity resistant, we have $\mathbf{X}(z) = \alpha(z)I_K$ for some nonzero polynomial $\alpha(z)$ of order at most r. From its definition in (8.2.5), it is clear that $\tilde{\mathbf{E}}(z)$ is also $N \times N$ irreducible because $\mathbf{E}(z)$ and F_l are all irreducible (unimodular). By the condition that $\mathbf{G}(z)$ is irreducible, the left-hand side $\tilde{\mathbf{E}}(z)\mathbf{G}(z)$ is also irreducible. This forces that the polynomial $\alpha(z)$ is a nonzero constant, i.e., $\mathbf{X}(z) = \alpha I_K$. This is, however, impossible by the definition of $\mathbf{X}(z)$, which proves the necessity of condition (i).

We now prove the necessity of condition (ii). When $K \geq N$, using the Smith form decomposition (8.2.4), $\mathbf{G}(z)$ can be decomposed into

$$\mathbf{G}(z) = \mathbf{W}(z)(I_N, 0_{N\times(K-N)})\mathbf{U}(z),$$

where $\mathbf{W}(z)$ and $\mathbf{U}(z)$ are two unimodular polynomial matrices. For any $N \times N$ irreducible polynomial matrix $\mathbf{E}(z)$ ($\mathbf{E} \neq \alpha I_N$ where α is a constant) of order at most r, define

$$\mathbf{V}(z) = \mathbf{U}^{-1}(z) \begin{bmatrix} \mathbf{W}^{-1}(z)\mathbf{E}(z)\mathbf{W}(z) & 0 \\ 0 & I_{K-N} \end{bmatrix} \mathbf{U}(z).$$

Then, $\mathbf{V}(z) \neq \alpha I_K$. But

$$\mathbf{E}(z)\mathbf{G}(z) = \mathbf{G}(z)\mathbf{V}(z),$$

which contradicts with the assumption.

The necessity of condition (iii) follows from condition (i) and the following argument. When $\mathbf{G}(z)$ has its order less than or equal to r/N, its first column can be reduced to $(1, 0, ..., 0)^T$ by using elementary row and column operations, and the product of the row operations has an order less than or equal to r/N. ■

Conditions (i)-(iii) are useful in constructing PARMC. Condition (ii) implies that the bandwidth expansion is needed to resist the polynomial ambiguity. Condition (iii) implies that a constant matrix MC G is not polynomial ambiguity resistant, which proves the following corollary.

Corollary 8.1 *Any block MC is not a PARMC.*

We next present a family of PARMC that was the first family we found in [89, 88, 171].

Theorem 8.2 *The following polynomial matrix* $\mathbf{G}(z)$ *of size* $N \times (N-1)$ *is strong* r*th order polynomial ambiguity resistant:*

$$\mathbf{G}(z) = \begin{bmatrix} 1 & 0 & 0 & \cdots & 0 & 0 \\ z^{-r-1} & 1 & 0 & \cdots & 0 & 0 \\ 0 & z^{-r-1} & 1 & \cdots & 0 & 0 \\ \vdots & \vdots & \vdots & & \vdots & \vdots \\ 0 & 0 & 0 & \cdots & z^{-r-1} & 1 \\ 0 & 0 & 0 & \cdots & 0 & z^{-r-1} \end{bmatrix}_{N\times(N-1)}, \quad (8.2.7)$$

for an integer $r \geq 0$.

Proof. The $\mathbf{G}(z)$ matrix in (8.2.7) is clearly irreducible.
Define

$$\mathbf{G}_l^{-1}(z) =$$

$$\begin{bmatrix} 1 & 0 & 0 \\ -z^{-(r+1)} & 1 & 0 \\ z^{-2(r+1)} & -z^{-(r+1)} & 1 \\ \vdots & \vdots & \vdots \\ (-1)^{N-2}z^{(-N+2)(r+1)} & (-1)^{N-3}z^{(-N+3)(r+1)} & (-1)^{N-4}z^{(-N+4)(r+1)} \end{bmatrix}$$

$$\begin{matrix} \cdots & 0 & 0 & 0 \\ \cdots & 0 & 0 & 0 \\ \cdots & 0 & 0 & 0 \\ & \vdots & \vdots & \vdots \\ \cdots & -z^{-(r+1)} & 1 & 0 \end{matrix}_{(N-1)\times N}$$

It is easy to check that

$$\mathbf{G}_l^{-1}(z)\mathbf{G}(z) = I_{N-1}.$$

Let $\mathbf{E}(z) = (e_{m,n}(z))_{N\times N}$ be an $N \times N$ nonzero polynomial matrix with order at most r such that $\mathbf{E}(z)\mathbf{G}(z) = \mathbf{G}(z)\mathbf{V}(z)$. We want to prove that $\mathbf{E}(z) = \alpha(z)I_N$ for some scalar polynomial $\alpha(z)$. It is not hard to show that $\mathbf{E}(z) = \alpha(z)I_N$ implies $\mathbf{V}(z) = \alpha(z)I_K$.

By the above equations, we have $\mathbf{V}(z) = \mathbf{G}_l^{-1}(z)\mathbf{E}(z)\mathbf{G}(z)$. Note that

$$\mathbf{E}(z)\mathbf{G}(z) =$$

$$\begin{bmatrix} e_{1,1}(z) + e_{1,2}(z)z^{-r-1} & e_{1,2}(z) + e_{1,3}(z)z^{-r-1} \\ e_{2,1}(z) + e_{2,2}(z)z^{-r-1} & e_{2,2}(z) + e_{2,3}(z)z^{-r-1} \\ \vdots & \vdots \\ e_{N,1}(z) + e_{N,2}(z)z^{-r-1} & e_{N,2}(z) + e_{N,3}(z)z^{-r-1} \end{bmatrix}$$

$$\begin{bmatrix} \cdots & e_{1,N-1}(z) + e_{1,N}(z)z^{-r-1} \\ \cdots & e_{2,N-1}(z) + e_{2,N}(z)z^{-r-1} \\ & \vdots \\ \cdots & e_{N,N-1}(z) + e_{N,N}(z)z^{-r-1} \end{bmatrix},$$

and

$$\mathbf{G}(z)\mathbf{G}_l^{-1}(z) =$$

$$\begin{bmatrix} 1 & 0 & \cdots & 0 & 0 \\ 0 & 1 & \cdots & 0 & 0 \\ \vdots & \vdots & & \vdots & \vdots \\ 0 & 0 & \cdots & 1 & 0 \\ (-1)^{N-1}z^{(-N+1)(r+1)} & (-1)^{N-2}z^{(-N+2)(r+1)} & \cdots & z^{-r-1} & 0 \end{bmatrix},$$

we only need to compare the elements in the last row of $\mathbf{E}(z)\mathbf{G}(z)$ and that of $\mathbf{G}(z)\mathbf{V}(z)$. It can be verified that $b_{N,m}(z)$, the mth element of the last row of the matrix $\mathbf{G}(z)\mathbf{V}(z)$, is given by

$$b_{N,m}(z) = (-1)^{N-1}e_{1,m+1}(z)z^{-N(r+1)} + e_{N-1,m}(z)z^{-r-1} +$$

$$+ \sum_{n=2}^{N-1} \left((-1)^{N-n+1}e_{n-1,m}(z) + (-1)^{N-n}e_{n,m+1}(z)\right) z^{(-N+n-1)(r+1)}.$$

From $\mathbf{E}(z)\mathbf{G}(z) = \mathbf{G}(z)\mathbf{V}(z)$, we have

$$b_{N,m}(z) = e_{N,m}(z) + e_{N,m+1}(z)z^{-r-1}.$$

When the orders of all polynomials of $e_{m,n}(z)$ for $1 \leq m, n \leq N$ are less than $r+1$, the above equalities imply the following equations

$$e_{1,m+1}(z) = 0, \quad \text{and } e_{N,m}(z) = 0, \quad \text{for } m = 1, 2, ..., N-1,$$

and

$$e_{n,m}(z) = e_{n+1,m+1}(z), \quad \text{for } m = 1, 2, ..., N-1, n = 1, 2, ..., N-1.$$

It is not hard to see that these equations imply that $e_{m,n}(z) = 0$ for $n \neq m$ and $e_{n,n}(z) = e_{1,1}(z)$ for all n. In other words, we have proved that $\mathbf{E}(z) = \alpha(z)I_N$ for some polynomial $\alpha(z)$. Since $\mathbf{E}(z)$ is nonzero, $\alpha(z)$ is also nonzero. Clearly the order of $\alpha(z)$ is at most r. This proves the theorem. ■

8.3 Applications in Blind Identification

We now discuss the application of PARMC to blind system identification of a multi-input multi-output communication system with ISI/multipath channels.

8.3.1 Blind Identifiability

A general ISI communication system is shown in Fig.8.1, where $\mathbf{X}(z)$ is the input signal of size $K \times K$, $\mathbf{G}(z)$ is the MC of size $N \times K$, $\mathbf{H}(z)$ is an ISI channel transfer matrix of size $M \times N$, $\mathbf{Y}(z)$ is the output signal of size $M \times K$, $K < N < M$, and $\eta(z)$ is the additive noise term of size $M \times K$. Herein, the goal is to identify $\mathbf{X}(z)$ from $\mathbf{Y}(z)$ without knowing the ISI channel characteristics. Note that $\mathbf{G}(z)$ is by design and is thus known to the receiver. The techniques presented here concern the exploitation of the MC structure in removing the unknown channel effects. Notice that the K columns in the input signal $\mathbf{X}(z)$ does not necessarily mean K users or K transmit antennas. For the single user and single transmit antenna case, it simply means that K signals are considered simultaneously.

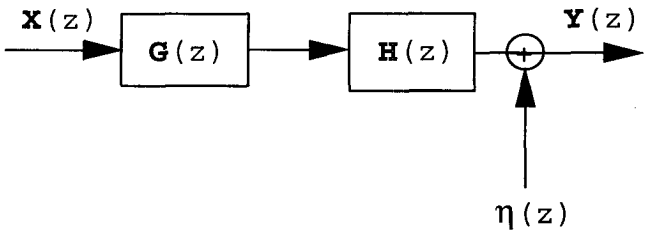

Figure 8.1: A general MC coded system of matrix form.

Since $\mathbf{H}(z)$ is almost surely irreducible, we assume it is irreducible in the remainder of this paper. The irreducibility of $\mathbf{H}(z)$ ensures that its inverse is also a polynomial matrix and thus input can be perfectly recovered from the output using FIR equalizers.

There are essentially two problems to be studied in blind identification. One is on blind identifiability and the other is on blind identification algorithm development. For convenience, we assume a noise-free system and set $\eta(z)$ to be zero. In the case of $K = 1$, the overall system in Fig.8.1 is a single input multiple output (SIMO) system, which has been extensively studied in [134, 135, 90, 180, 128, 136, 35, 63, 147, 81, 98, 123, 101, 36]. Therefore, in the following we only consider the case where $K > 1$. For a

random input $K \times K$ signal $\mathbf{X}(z)$ with $K > 1$, the greatest common divisor (gcd) of all component polynomials of $\mathbf{X}(z)$ is almost surely a nonzero constant and $\mathbf{X}(z)$ is almost surely invertible for a complex value z. Such is assumed throughout our discussions.

We first study the blind identifiability for the input signal. Knowing $\mathbf{Y}(z)$, let $\mathbf{X}_1(z)$ and $\mathbf{H}_1(z)$ be the candidate input and channel, respectively. The gcd of the components of $\mathbf{X}_1(z)$ is assumed to be a nonzero constant, whereas $\mathbf{H}_1(z)$ is an $M \times N$ irreducible polynomial as $\mathbf{H}(z)$. Then, the blind identifiability can be described by the following uniqueness:

$$\mathbf{Y}(z) = \mathbf{H}_1(z)\mathbf{G}(z)\mathbf{X}_1(z) = \mathbf{H}(z)\mathbf{G}(z)\mathbf{X}(z) \text{ implies } \mathbf{X}_1(z) = \alpha\mathbf{X}(z), \tag{8.3.1}$$

for some nonzero α. The uniqueness (8.3.1) implies that the input signal $\mathbf{X}(z)$ can be uniquely determined up to a scale from the output signal $\mathbf{Y}(z)$ and the known MC $\mathbf{G}(z)$. In other words, the input signal $\mathbf{X}(z)$ can be blindly identified. It should be noticed that without the MC $\mathbf{G}(z)$ in Fig.8.1, the input signal $\mathbf{X}(z)$ can only be blindly identified up to a $K \times K$ nonsingle constant matrix $\mathbf{T}$ ambiguity by using MIMO blind identification techniques [90, 147, 81, 98, 81].

In [89, 88], blind identification is accomplished in two steps. First, existing MIMO blind identification techniques are used to determine the input signal within a matrix ambiguity, $\mathbf{T}$, and then this constant matrix ambiguity $\mathbf{T}$ is resisted through a 0th order PARMC. In this subsection, we study the possibility of employing a proper order PARMC so that the input signal $\mathbf{X}(z)$ can be directly identified from the output signal $\mathbf{Y}(z)$ using a closed-form algebraic algorithm.

The input signal blind identifiability in (8.3.1) can be reformulated as follows by pre- and post- multiplying $\mathbf{H}_1^{-1}(z)$ and $\mathbf{X}^{-1}(z)$, respectively, to both sides:

$$\mathbf{H}_1^{-1}(z)\mathbf{H}(z)\mathbf{G}(z) = \mathbf{G}(z)\mathbf{X}_1(z)\mathbf{X}^{-1}(z) \quad \text{implies} \quad \mathbf{X}_1(z)\mathbf{X}^{-1}(z) = \alpha I_K, \tag{8.3.2}$$

for some nonzero constant α, where $\mathbf{H}_1^{-1}(z)$ is a left inverse of $\mathbf{H}_1(z)$, i.e., $\mathbf{H}_1^{-1}(z)\mathbf{H}_1(z) = I_N$. Note that (8.3.1) is stronger than (8.3.2) since

$$\mathbf{H}_1(z)\mathbf{G}(z)\mathbf{X}_1(z) = \mathbf{H}(z)\mathbf{G}(z)\mathbf{X}(z)$$

indicates

$$\mathbf{H}_1^{-1}(z)\mathbf{H}(z)\mathbf{G}(z) = \mathbf{G}(z)\mathbf{X}_1(z)\mathbf{X}^{-1}(z)$$

but not vice versa.

The $N \times N$ matrix $\mathbf{H}_1^{-1}(z)\mathbf{H}(z)$ is almost surely a nonzero polynomial matrix. If $\mathbf{H}_1^{-1}(z)\mathbf{H}(z)$ has order at most r, then as long as $\mathbf{G}(z)$ is rth order polynomial ambiguity resistant, (8.3.2) implies $\mathbf{X}_1(z)\mathbf{X}^{-1}(z) = \alpha(z)I_K$, i.e., $\mathbf{X}_1(z) = \alpha(z)\mathbf{X}(z)$ for a nonzero polynomial $\alpha(z)$ of order at most r. This implies that a rth order PARMC $\mathbf{G}(z)$ can reduce the $M \times N$ polynomial matrix ambiguity into a scalar polynomial ambiguity. Under the assumption that the gcd of all components of $\mathbf{X}_1(z)$ is a nonzero constant, we can easily reduce $\alpha(z)$ to a scalar, α. This proves that, if a signal $\mathbf{X}_1(z)$ with the gcd of all its components as a nonzero constant, and $\mathbf{Y}(z) = \mathbf{H}_1(z)\mathbf{G}(z)\mathbf{X}_1(z)$, then $\mathbf{X}_1(z) = \alpha\mathbf{X}(z)$ for a nonzero constant, in other words, the input signal $\mathbf{X}(z)$ is blindly identifiable.

The above discussions imply that, when $\mathbf{G}(z)$ is rth order polynomial ambiguity resistant, the input signal $\mathbf{X}(z)$ can be blindly identified from the output $\mathbf{Y}(z)$ and the MC $\mathbf{G}(z)$. In order to choose a proper MC $\mathbf{G}(z)$, it is important to estimate the minimal order r of the polynomial matrix $\mathbf{H}_1^{-1}(z)\mathbf{H}(z)$ given the ISI channel order of $\mathbf{H}(z)$, Q_h.

It is known that the order $Q_{h^{-1}}$ of $\mathbf{H}^{-1}(z)$ satisfies

$$Q_{h^{-1}} \geq \frac{NQ_h + N - M}{M - N},$$

see for example [91, 81]. Therefore, the total order r of $\mathbf{H}_1^{-1}(z)\mathbf{H}(z)$ satisfies

$$r \geq \frac{NQ_h + N - M}{M - N} + Q_h = \frac{NQ_h}{M - N}.$$

On the other hand, if $\mathbf{V}(z)$ in Equation (8.1.2) has a nontrivial solution $\mathbf{V}(z) \neq \alpha(z)I_K$, the inputs $\mathbf{X}(z)$ and $\mathbf{X}_1(z)$ with $\mathbf{X}(z) = \mathbf{V}(z)\mathbf{X}_1(z)$ and $\mathbf{H}_1(z) = \mathbf{H}(z)\mathbf{E}(z)$ satisfy

$$\mathbf{Y}(z) = \mathbf{H}_1(z)\mathbf{G}(z)\mathbf{X}_1(z) = \mathbf{H}(z)\mathbf{G}(z)\mathbf{X}(z).$$

Therefore, it is not possible for the identification of the input signal. The above results are summarized in the following theorem.

Theorem 8.3 *Assume the ISI channel $\mathbf{H}(z)$ is an $M \times N$ irreducible polynomial matrix with order Q_h. If $\mathbf{G}(z)$ is a rth order polynomial ambiguity resistant MC, then the input signal $\mathbf{X}(z)$ in Fig.8.1 is blindly identifiable from the output signal $\mathbf{Y}(z)$ and the MC $\mathbf{G}(z)$, where*

$$r = \lceil \frac{NQ_h}{M - N} \rceil. \tag{8.3.3}$$

Contrarily, if the input signal $\mathbf{X}(z)$ in Fig.8.1 is blindly identifiable from the output signal $\mathbf{Y}(z)$ and the MC $\mathbf{G}(z)$, then $\mathbf{G}(z)$ must be a polynomial ambiguity resistant MC of a certain order.

Similar arguments apply to the blind identifiability for both the channel inverse $\mathbf{H}^{-1}(z)$ and the input signal $\mathbf{X}(z)$ by using strong PARMC: $\mathbf{Y}(z) = \mathbf{H}_1(z)\mathbf{G}(z)\mathbf{X}_1(z) = \mathbf{H}(z)\mathbf{G}(z)\mathbf{X}(z)$ if and only if $\mathbf{H}_1^{-1}(z)\mathbf{H}(z) = \alpha(z)I_N$ and $\mathbf{X}_1(z)\mathbf{X}^{-1}(z) = \alpha(z)I_k$, i.e., $\mathbf{H}_1^{-1}(z) = \alpha(z)\mathbf{H}^{-1}(z)$ and $\mathbf{X}_1(z) = \alpha(z)\mathbf{X}(z)$ for some nonzero polynomial $\alpha(z)$. Following the proof of Theorem 8.3 about the gcd division, $\alpha(z)$ can be found from $\mathbf{X}_1(z) = \alpha(z)\mathbf{X}(z)$, and then $\mathbf{H}^{-1}(z)$ can be found from $\mathbf{H}_1^{-1}(z) = \alpha(z)\mathbf{H}^{-1}(z)$. The necessity is also similar to the one for Theorem 8.3. This proves the following result.

Theorem 8.4 *Assume the ISI channel $\mathbf{H}(z)$ is an $M \times N$ irreducible polynomial matrix with order Q_h. If the MC $\mathbf{G}(z)$ is strong rth order polynomial matrix ambiguity resistant, then, the input signal $\mathbf{X}(z)$ and the ISI channel inverse $\mathbf{H}^{-1}(z)$ in Fig.8.1 are blindly identifiable from the output signal $\mathbf{Y}(z)$ and the MC $\mathbf{G}(z)$, where r is defined in (8.3.3). Contrarily, if the input signal $\mathbf{X}(z)$ and the channel inverse $\mathbf{H}^{-1}(z)$ in Fig.8.1 are blindly identifiable from the output signal $\mathbf{Y}(z)$ and the MC $\mathbf{G}(z)$, then $\mathbf{G}(z)$ must be a strong polynomial ambiguity resistant MC of a certain order.*

As a remark on the blind identifiability, since $\mathbf{H}(z)$ is not a square matrix, its inverse $\mathbf{H}^{-1}(z)$ is not unique. The above blind identifiability means the unique solution (up to a nonzero constant difference) for the input signal $\mathbf{X}(z)$ and a solution for the inverse $\mathbf{H}^{-1}(z)$ of $\mathbf{H}(z)$. As such, although the overall solutions for $\mathbf{X}(z)$ and $\mathbf{H}^{-1}(z)$ may not be unique due to the non-uniqueness of $\mathbf{H}^{-1}(z)$, the input signal part $\mathbf{X}(z)$ is always unique.

8.3.2 An Algebraic Blind Identification Algorithm

Results in the previous section suggest an algebraic algorithm for the blind identification: solve for $\mathbf{X}_1(z)$ in the equation $\mathbf{Y}(z) = \mathbf{H}_1(z)\mathbf{G}(z)\mathbf{X}_1(z)$ from the known output $\mathbf{Y}(z)$ and the MC $\mathbf{G}(z)$; and then remove the scalar polynomial, $\alpha(z)$, from $\mathbf{X}_1(z)$ to obtain $\alpha\mathbf{X}(z)$.

Although the input and output signals $\mathbf{X}(z)$ and $\mathbf{Y}(z)$ are in matrix forms in the previous sections, they can also be column vectors by equating corresponding columns in the matrices. To derive a time-domain closed-form algorithm, we adopt the vector representation for the input and output in the following discussion. More specifically, we consider

$$\mathbf{Y}(z) = \mathbf{H}(z)\mathbf{G}(z)\mathbf{X}(z), \tag{8.3.4}$$

where $\mathbf{X}(z)$ is of size $K \times 1$ and $\mathbf{Y}(z)$ is of size $M \times 1$. $\mathbf{H}(z)$ is the $M \times N$ irreducible ISI channel of order Q_h, and $\mathbf{G}(z)$ is a strong rth order PARMC,

where r takes the value in (8.3.3). The parameters K, N, M satisfy the inequalities $K < N < M$.

It was established in the previous section that solutions of

$$\hat{\mathbf{H}}_1^{-1}(z)\mathbf{Y}(z) = \mathbf{G}(z)\hat{\mathbf{X}}_1(z), \tag{8.3.5}$$

satisfy $\hat{\mathbf{X}}_1(z) = \alpha_1(z)\mathbf{X}(z)$ and $\hat{\mathbf{H}}_1^{-1}(z)\mathbf{H}(z) = \alpha_1(z)\mathbf{I}(z)$. Replacing $\mathbf{Y}(z)$ with $z^r\mathbf{Y}(z)$ in the above equation yields

$$\hat{\mathbf{H}}_2^{-1}(z)z^r\mathbf{Y}(z) = \mathbf{G}(z)\hat{\mathbf{X}}_2(z). \tag{8.3.6}$$

Clearly, $\hat{\mathbf{X}}_2(z) = z^r\alpha_2(z)\mathbf{X}(z)$. To exploit the MC structure and remove the scalar polynomial from the input estimate in one shot, consider the following equation set

$$\begin{cases} \hat{\mathbf{H}}_1^{-1}(z)\mathbf{Y}(z) &= \mathbf{G}(z)\hat{\mathbf{X}}(z) \\ \hat{\mathbf{H}}_2^{-1}(z)z^r\mathbf{Y}(z) &= \mathbf{G}(z)\hat{\mathbf{X}}(z) \end{cases} \tag{8.3.7}$$

Then $\hat{\mathbf{X}}(z) = \alpha_1(z)\mathbf{X}(z)$ and at the same time, $\hat{\mathbf{X}}(z) = z^r\alpha_2(z)\mathbf{X}(z)$. Since $\alpha_1(z)$ and $\alpha_2(z)$ are of order at most r, it is not difficult to show that $\hat{\mathbf{X}}(z)$ must be of form $\alpha\mathbf{X}(z)$. Hence, the input sequence can be uniquely identified by solving the above linear equation set in the time domain.

Denote $\mathbf{F}(z) = \mathbf{H}^{-1}(z)$. From previous discussion, the minimum order of $\mathbf{F}(z)$, Q_f is given by

$$Q_f = \lceil \frac{NQ_h + N - M}{M - N} \rceil. \tag{8.3.8}$$

Let

$$\mathbf{F}(z) = \sum_{m=0}^{Q_f} F(m)z^{-m} \quad \text{and } \mathbf{G}(z) = \sum_{m=0}^{Q_g} G(m)z^{-m},$$

$$\mathbf{X}(z) = \sum_{m=0}^{Q_x} X(m)z^{-m} \quad \text{and } \mathbf{Y}(z) = \sum_{m=0}^{Q_y} Y(m)z^{-m}.$$

Then from $\mathbf{F}(z)\mathbf{Y}(z) = \mathbf{G}(z)\mathbf{X}(z)$ we have,

$$\sum_m \left(\sum_{l=0}^{Q_f} F(l)Y(m-l) \right) z^{-m} = \sum_m \left(\sum_{l=0}^{Q_g} G(l)X(m-l) \right) z^{-m},$$

i.e.,

$$\sum_{l=0}^{Q_f} F(l)Y(m-l) = \sum_{l=0}^{Q_g} G(l)X(m-l), \quad m \in \mathbf{Z}, \tag{8.3.9}$$

where $F(m)$, $0 \le m \le Q_f$, and $X(m)$, $0 \le m \le Q_g$, are unknowns to solve. For each m, let

$$F(m) = \begin{bmatrix} f_{1,m} \\ f_{2,m} \\ \vdots \\ f_{N,m} \end{bmatrix},$$

where $f_{l,m}$ is the lth row of the matrix $F(m)$. Denote $\mathcal{F}$ a *super* column vector containing all unknowns in matrices $F(m)$, $0 \le m \le Q_f$, i.e.,

$$\mathcal{F} = (f_{1,0}, \cdots, f_{N,0}, f_{1,1}, \cdots, f_{N,1}, \cdots, f_{1,Q_f}, \cdots, f_{N,Q_f})^T. \tag{8.3.10}$$

The size of $\mathcal{F}$ is $(MN(Q_f+1)) \times 1$. Let $\mathcal{Y}(m)$ be the following block matrix of size $N \times (MN(Q_f+1))$ for each integer m:

$$\mathcal{Y}(m) = \begin{bmatrix} Y^T(m) & \cdots & Y^T(m-Q_f) & 0 & \cdots & 0 \\ 0 & \cdots & 0 & Y^T(m) & \cdots & Y^T(m-Q_f) \\ \vdots & \vdots & \vdots & \vdots & \vdots & \vdots \\ 0 & \cdots & 0 & 0 & \cdots & 0 \end{bmatrix}$$

$$\begin{matrix} \cdots & 0 & \cdots & 0 \\ \cdots & 0 & \cdots & 0 \\ \vdots & \vdots & \vdots & \vdots \\ \cdots & Y^T(m) & \cdots & Y^T(m-Q_f) \end{matrix} \Bigg] \tag{8.3.11}$$

Then, the time-domain equivalent of Equation (8.3.7) is given by

$$\mathcal{Y}(m)\mathcal{F}_1 = (G(0) \cdots G(f)) \begin{bmatrix} \hat{X}(m) \\ \vdots \\ \hat{X}(m-Q_g) \end{bmatrix}, \quad m \ge 0, \tag{8.3.12}$$

and

$$\mathcal{Y}(m+r)\mathcal{F}_2 = (G(0) \cdots G(f)) \begin{bmatrix} \hat{X}(m) \\ \vdots \\ \hat{X}(m-Q_g) \end{bmatrix}, \quad m \ge 0. \tag{8.3.13}$$

Upon defining $\mathcal{Y}_i = [\mathcal{Y}^T(i) \cdots \mathcal{Y}^T(Q_x - r)]^T$, we are able to combine the above equations and establish a linear equation set with respect to all un-

knowns as follows,

$$\begin{bmatrix} \mathcal{Y}_0 & \mathbf{0} & -\mathcal{G} \\ \mathbf{0} & \mathcal{Y}_r & -\mathcal{G} \\ \mathcal{Y}_0 & -\mathcal{Y}_r & \mathbf{0} \end{bmatrix} \begin{bmatrix} \mathcal{F}_1 \\ \mathcal{F}_2 \\ X(0) \\ \vdots \\ X(Q_x - r) \end{bmatrix} = \mathbf{0}, \tag{8.3.14}$$

where $\mathcal{G}$ is the following generalized Sylvester matrix:

$$\mathcal{G} =$$

$$\begin{bmatrix} G(0) & 0 & 0 & \cdots & 0 & 0 & \cdots & 0 \\ G(1) & G(0) & 0 & \cdots & 0 & 0 & \cdots & 0 \\ \vdots & \vdots & \vdots & \vdots & \vdots & \vdots & \vdots & \vdots \\ G(Q_g) & G(Q_g-1) & G(Q_g-2) & \cdots & G(0) & 0 & \cdots & 0 \\ 0 & G(Q_g) & G(Q_g-1) & \cdots & G(1) & G(0) & \cdots & 0 \\ \vdots & \vdots & \vdots & \vdots & \vdots & \vdots & \vdots & \vdots \\ 0 & 0 & 0 & \cdots & 0 & G(Q_g) & \cdots & G(0) \end{bmatrix}. \tag{8.3.15}$$

The input signal as well as the 0-delay and maximum-delay zero-forcing equalizers can be readily determined. It can be easily verified that when the number of data vectors increases, there are more equations than unknowns in the above linear homogeneous system, which renders an overdetermined system with a unique solution.

8.4 Applications in Communication Systems

In this section, we will apply the theory previously developed to the blind identification of a baud-rate sampled communication system and an undersampled system with multiple receivers (antennas). The application to the space-time coding discussed in Chapter 6 for multiple transmit and receive antennas follows automatically by considering the general MIMO system in Fig.8.1. Contrasting to most existing blind identification techniques, the use of PARMC allows the blind identification to be accomplished without output diversities.

8.4.1 Applications in Single-Receiver, Baud-Rate Sampled Systems

A MC coded single-receiver communication system is shown in Fig.8.2 , where the baud-rate sampled ISI channel is characterized by a polynomial $H(z)$ of order q_h.

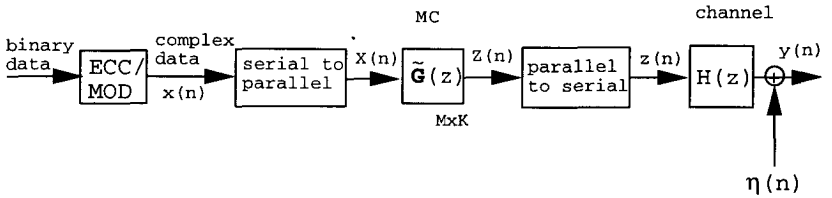

Figure 8.2: A single-receiver communication system with baud-rate sampling.

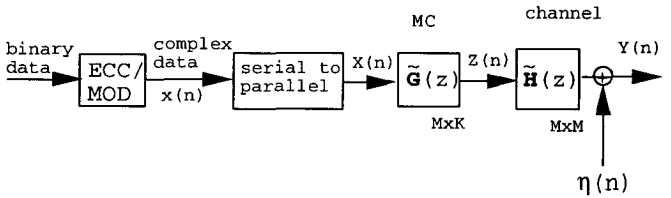

Figure 8.3: A blocked single-receiver system with baud-rate sampling.

To apply the blind techniques developed in the previous section, we need to formulate the above system and transfer it into the one shown in Fig.8.1. To achieve this, we block the output signal $y(n)$ with block size M (from serial to parallel) into an M-element vector, $Y(n)$. The system in Fig.8.2 can then be represented as in Fig.8.3, where $\tilde{\mathbf{H}}(z)$ is the blocked version of the channel $H(z)$ in Fig.8.2, as we have seen in Section 2.3:

$$\tilde{\mathbf{H}}(z) = \begin{bmatrix} H_0(z) & z^{-1}H_{M-1}(z) & \cdots & z^{-1}H_1(z) \\ H_1(z) & H_0(z) & \cdots & z^{-1}H_2(z) \\ \vdots & \vdots & \vdots & \vdots \\ H_{M-2}(z) & H_{M-3}(z) & \cdots & z^{-1}H_{M-1}(z) \\ H_{M-1}(z) & H_{M-2}(z) & \cdots & H_0(z) \end{bmatrix}, \qquad (8.4.1)$$

where $H_l(z)$ is the lth polyphase component of $H(z)$ as follows

$$H_l(z) = \sum_n H(Mn+l)z^{-n}, \quad 0 \le l \le M-1. \tag{8.4.2}$$

The matrix $\tilde{\mathbf{H}}(z)$ is pseudo-circulant and can be diagonalized the same as in (2.3.10). Let $\mathbf{W}_M$ be the $M \times M$ DFT matrix, i.e.,

$$\mathbf{W}_M \triangleq (W_M^{jk})_{0 \le j,k \le M-1},$$

where

$$W_M = e^{-2\pi\sqrt{-1}/M};$$

$\Lambda_M(z)$ the diagonal polynomial matrix

$$\Lambda_M(z) \triangleq \text{diag}\left(1, z^{-1}, \cdots, z^{-M+1}\right);$$

and $\mathbf{V}(z)$ the following diagonal polynomial matrix in terms of the polynomial $H(z)$:

$$\mathbf{V}(z) \triangleq \text{diag}\left(H(z), H(zW_M), \cdots, H(zW_M^{M-1})\right). \tag{8.4.3}$$

Then,

$$\tilde{\mathbf{H}}(z^M) = \left(\mathbf{W}_M^* \Lambda_M(z)\right)^{-1} \mathbf{V}(z) \mathbf{W}_M^* \Lambda_M(z). \tag{8.4.4}$$

For an MC to resist the polynomial ambiguity, $\tilde{\mathbf{G}}(z)$ and $\tilde{\mathbf{H}}(z)$ must be rearranged so that the channel becomes a tall and irreducible polynomial matrix. Clearly, when $H(z)$ is not a nonzero constant, the polynomial matrix $\tilde{\mathbf{H}}(z)$ is not irreducible. Although this is true, it was proved in Section 2.3 that any $M \times N$ submatrix of $\tilde{\mathbf{H}}(z)$ is irreducible as long as two rotations of the zero set of the polynomial $H(z)$ at the angles W_M^m for $0 \le m \le M-1$ do not intersect (Theorem 2.1). Since this condition is satisfied almost surely for a polynomial $H(z)$, we may assume that all $M \times N$ submatrices $\mathbf{H}(z)$ of $\tilde{\mathbf{H}}(z)$ are irreducible when $N < M$. Hence we can design the $M \times K$ MC in Figs.8.2-8.3 to be

$$\tilde{\mathbf{G}}(z) = \begin{bmatrix} I_N \\ 0_{(M-N)\times N} \end{bmatrix} \mathbf{G}(z), \tag{8.4.5}$$

where $\mathbf{G}(z)$ is an $N \times K$ PARMC studied previously. Consequently, the system in Fig.8.3 can be described as follows:

$$\mathbf{Y}(z) = \mathbf{H}(z)\mathbf{G}(z)\mathbf{X}(z), \quad \text{and} \quad \mathbf{H}(z) = \tilde{\mathbf{H}}(z) \begin{bmatrix} I_N \\ 0_{(M-N)\times N} \end{bmatrix}, \tag{8.4.6}$$

where $\mathbf{H}(z)$ is actually an $M \times N$ submatrix of the $M \times M$ pseudo-circulant matrix $\tilde{\mathbf{H}}(z)$ in (8.4.1), which is irreducible. From (8.4.6), it is clear that the system in Fig.8.3 is reduced to the one in Fig.8.1. The theory/algorithm developed in the previous section becomes readily applicable to the above single-receiver system in Fig.8.2.

Given the order of the ISI channel polynomial $H(z)$, g_h, the order of MC $\mathbf{G}(z)$, r, can be determined as follows. From (8.4.1)-(8.4.2), the order of the pseudo-circulant matrix $\tilde{\mathbf{H}}(z)$ and its submatrix $\mathbf{H}(z)$ is

$$Q_h = \lceil \frac{q_h}{M} \rceil.$$

From (8.3.3), the corresponding parameters of the MC in (8.2.7) can be set as

$$r = \lceil \frac{N\lceil \frac{q_h}{M} \rceil}{M-N} \rceil, \quad K = N-1, \quad \text{and} \quad M > N. \tag{8.4.7}$$

With these parameters, the output data rate relative to the input signal rate for the above MC coded single-receiver system is $(N/K)(M/N) = M/(N-1)$, where M can be chosen as $N+1$. Thus, the relative data rate increase is $2/(N-1)$, which approaches 0, i.e., no expansion, when N is large. This proves the following theorem.

Theorem 8.5 *For any $\epsilon > 0$, there exists a positive integer N for the MC $\mathbf{G}(z)$ in (8.2.7) such that the overall data rate expansion for the single antenna receiver system in Fig.8.2 is less than ϵ and at the same time, the input signal $\mathbf{X}(z)$ can be blindly identified from the output $\mathbf{Y}(z)$ using the closed-form algorithm in Section 8.3.2.*

Notice that the existing blind identification techniques require the data rate to be at least twice the input symbol rate at the receiver.

8.4.2 Applications in Undersampled Antenna Array Receiver Systems

Having shown that blind identification can be accomplished with a minimum amount of bandwidth expansion using MC coding techniques, we now study the possibility of perfect signal recovery when the received signals are undersampled.

Without loss of generality, an undersampled antenna array system is shown in Fig.8.4, where $H_l(z)$ for $l = 1, 2, ..., M$ are the ISI channel transfer polynomials of the M antennas, and $N \downarrow$ means downsampling by factor N, i.e., taking one sample from each N samples. Clearly, only partial

information of the input is available in each antenna output. It was proved in [89, 88] that it is impossible to recover the input blindly from the M outputs without using any assistance at the transmitter.

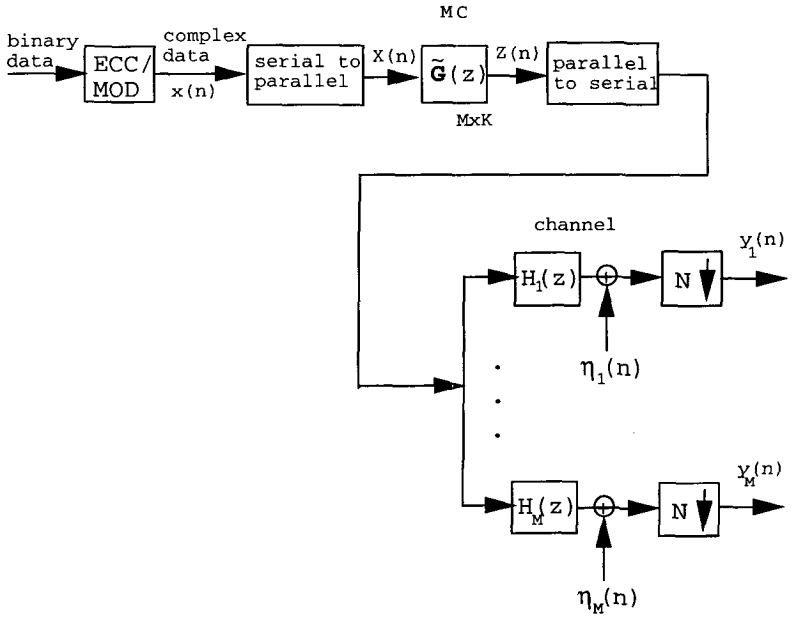

Figure 8.4: An undersampled antenna array system.

The system in Fig.8.4 can be converted to the one in Fig.8.5, where $\mathbf{H}(z)$ is the $M \times N$ polyphase matrix of the M polynomials $H_l(z)$, $1 \leq l \leq M$: $\mathbf{H}(z) = (H_{l,n}(z))_{M \times N}$. Here

$$H_{l,n}(z) = \sum_k H_l(Nk + n)z^{-k}$$

is the nth polyphase component of the lth polynomial

$$H_l(z) = \sum_m H_l(m)z^{-m},$$

and $Y(n) = (y_1(n), y_2(n), \cdots, y_M(n))^T$. As discussed before, when $M > N$ this matrix $\mathbf{H}(z)$ is almost surely irreducible. From Fig.8.5, one can see that the undersampled antenna array receiver system in Fig.8.4 can be cast into

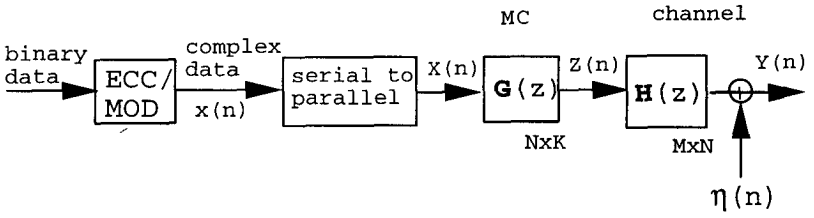

Figure 8.5: An equivalent undersampled antenna array system.

the exact same framework of Fig.8.1, allowing direct applications of the theory/algorithm developed in Section 8.2 and Section 8.3.

Assume q_h is the maximum of the orders of the M polynomials $H_l(z)$ for the M antennas. The order Q_h of the polyphase matrix $\mathbf{H}(z)$ is

$$Q_h = \lceil \frac{q_h}{N} \rceil.$$

For blind identification, the parameters for the MC $\mathbf{G}(z)$ in (8.2.7) can be chosen as

$$r = \lceil \frac{N\lceil \frac{q_h}{N} \rceil}{M-N} \rceil, \quad K = N-1, \quad \text{and} \quad M > N. \tag{8.4.8}$$

It should be noticed that the number of antennas, M, in a system is usually fixed. Because $N < M$ is required, this seems providing a lower bound for the data rate expansion in the transmitter, which requires $0 < K < N < M$. With the minimum bandwidth expansion setup: $K = N - 1, N = M - 1$, at least $1/(M-1)$ data rate increase is needed for the blind equalization given the number of antennas, M. In the following, we show that this limitation can be lifted by blocking the vector output sequence $Y(n) = [y_1(n), y_2(n), \cdots, y_M(n)]^T$ in Fig.8.5 similar to the method for the single antenna system studied in the previous subsection. The blocked equivalent system of the undersampled antenna array receiver system in Fig.8.5 is shown in Fig.8.6, where the block size is L and the matrix $[\mathbf{H}(z)]_L$ is the blocked version of the matrix $\mathbf{H}(z)$ in Fig.8.5:

$$[\mathbf{H}(z)]_L = \begin{bmatrix} \mathbf{H}_0(z) & z^{-1}\mathbf{H}_{M-1}(z) & \cdots & z^{-1}\mathbf{H}_1(z) \\ \mathbf{H}_1(z) & \mathbf{H}_0(z) & \cdots & z^{-1}\mathbf{H}_2(z) \\ \vdots & \vdots & \vdots & \vdots \\ \mathbf{H}_{M-2}(z) & \mathbf{H}_{M-3}(z) & \cdots & z^{-1}\mathbf{H}_{M-1}(z) \\ \mathbf{H}_{M-1}(z) & \mathbf{H}_{M-2}(z) & \cdots & \mathbf{H}_0(z) \end{bmatrix}, \tag{8.4.9}$$

where the notation $\mathcal{H}(z) = [\mathbf{H}(z)]_L$ was used in Chapter 6. Here, $\mathbf{H}_l(z)$ is the lth polyphase component of the matrix $\mathbf{H}(z)$ as follows

$$\mathbf{H}_l(z) = \sum_n H(Ln+l)z^{-n}, \quad 0 \le l \le L-1,$$

where $H(m)$ are the $M \times N$ constant coefficient matrices in $\mathbf{H}(z) = \sum_m H(m)z^{-m}$. Matrix $[\mathbf{H}(z)]_L$ is block pseudo-circulant. $[Y]_L(n)$ and $[\eta]_L(n)$ with size $NL \times 1$ in Fig.8.6 are the blocked forms of the vector sequences $Y(n)$ and $\eta(n)$, respectively. Correspondingly, the minimum rate-increase MC $\mathbf{G}(z)$ has size $NL \times (NL-1)$. Therefore, if the blocked channel polynomial matrix $[\mathbf{H}(z)]_L$ in Fig.8.6 is still irreducible, then the system in Fig.8.6 is cast again to the one in Fig.8.1.

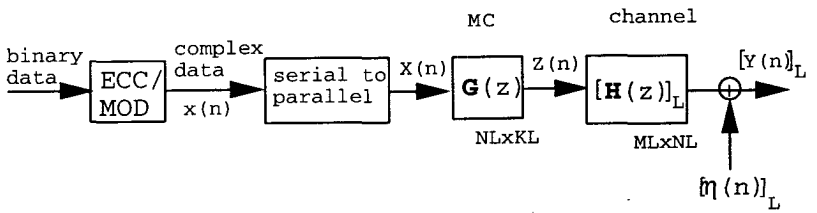

Figure 8.6: A blocked undersampled antenna array system.

Before proving the irreducibility of the matrix $[\mathbf{H}(z)]_L$, let us investigate the effects of the blocking operations above. Notice that the overall data rate expansion in Fig.8.6 is $1/((M-1)L)$ by choosing $N = M-1$ and $K = NL-1$, which approaches zero when the block size L is large. The advantage is that the data rate expansion at the transmitter can be reduced by employing the above blocking procedure, even when the number of antennas is fixed.

We now need to prove that the blocked version $[\mathbf{H}(z)]_L$ of $\mathbf{H}(z)$ is irreducible when $\mathbf{H}(z)$ itself is irreducible. Since $[\mathbf{H}(z)]_L$ is block pseudo-circulant, by permuting its rows and columns, it can be converted into the block matrix with MN blocks and each of the blocks, $B_{m,n}(z)$, is an $L \times L$ pseudo-circulant matrix:

$$[\mathbf{H}(z)]_L = P_l(B_{m,n}(z))_{M \times N} P_r,$$

where P_l and P_r are the row and column block permutation matrices. Similar to (8.4.3)-(8.4.4) the $L \times L$ pseudo-circulant matrix $B_{m,n}(z^L)$ can be diagonalized as

$$B_{m,n}(z^L) =$$

$$(\mathbf{W}_L^*\Lambda_L(z))^{-1}\text{diag}(H_{m,n}(z), H_{m,n}(zW_L), \cdots, H_{m,n}(zW_L^{L-1}))\mathbf{W}_L^*\Lambda_L(z),$$

where $H_{m,n}(z)$ come from matrix $\mathbf{H}(z) = (H_{m,n}(z))_{M\times N}$. Therefore,

$$[\mathbf{H}(z^L)]_L$$

$$= P_l[\mathbf{W}]_L^{-1}\left(\text{diag}(H_{m,n}(z), H_{m,n}(zW_L), \cdots, H_{m,n}(zW_L^{L-1}))\right)_{M\times N}[\mathbf{W}]_L P_r$$

where

$$[\mathbf{W}]_L = \text{diag}(\mathbf{W}_L^*\Lambda_L(z), \cdots, \mathbf{W}_L^*\Lambda_L(z)).$$

By implementing the same permutations,

$$[\mathbf{H}(z^L)]_L = P_l[\mathbf{W}]_L^{-1}P_l\text{diag}(\mathbf{H}(z), \mathbf{H}(zW_L), \cdots, \mathbf{H}(zW_L^{L-1}))P_r[\mathbf{W}]_L P_r.$$

Since matrices $P_l[\mathbf{W}]_L^{-1}P_l$ and $P_r[\mathbf{W}]_L P_r$ are irreducible, matrix $[\mathbf{H}(z)]_L$ is irreducible if and only if $\mathbf{H}(z)$ is irreducible. This proves the following lemma.

Lemma 8.1 *The blocked version* $[\mathbf{H}(z)]_L$ *in (8.4.9) of* $\mathbf{H}(z)$ *is irreducible if and only if* $\mathbf{H}(z)$ *is irreducible.*

This lemma and the previous discussion on data rate expansion in the transmitter lead to the following result.

Theorem 8.6 *For any* $\epsilon > 0$, *there exists a positive integer* N *for the MC* $\mathbf{G}(z)$ *in (8.2.7) such that the data rate expansion at the transmitter for the antenna array system in Fig.8.4 is less than* ϵ *and at the same time, the input signal* $\mathbf{X}(z)$ *can be blindly identified from the undersampled outputs* $y_l(n)$, $1 \le l \le M$, *of the* M *antennas with the undersampling factor* $N = M - 1$ *using the closed-form algorithm in Section 8.3.2.*

It should be noticed that, although the blind identifiability in the above two theorems hold theoretically for an arbitrary small amount of data (or bandwidth) expansion, the implementation of the closed-form algorithm in Section 8.3.2 may become prohibitive when the sizes of the MC get larger. This is also due to the possibility of a linear system being ill-posed when its size gets larger. We want to emphasize that the focus of this chapter is on feasibility studies rather than algorithm development. There is an evident need for more sophisticated MC coding-based blind identification algorithms which are of practical importance.

Another remark we want to make here is the following observation. When the order Q_h of the ISI channel $\mathbf{H}(z)$ is large, the size of the linear system (8.3.14) is also large due to the large number of unknowns in $\mathcal{F}$ in (8.3.10) for $\mathbf{H}^{-1}(z)$. In this case, it might be better to use a current MIMO

blind identification method to reduce the large order ISI channel $\mathbf{H}(z)$ into a nonsingular constant matrix, i.e., a zero order ISI channel $\mathbf{T}$. Then, the technique developed in [89, 88], or 0th order polynomial matrix ambiguity resistant MC in this paper can be used to blindly identify the input signal and the constant ambiguity matrix $\mathbf{T}$. The trade-off between these two approaches is under our current investigation.

Last but not the least, we want to point out that the MC proposed in (8.2.7) have some interesting features which are essential to practice applications. For example, assuming that the input data to the MC are modulated complex values, such as $e^{j2\pi k/4}$, $k = 0, 1, 2, 3$, in QPSK modulation, since the MC in (8.2.7) only sums the current sample $X(n)$ and the past $X(n-r-1)$ as $X(n) + X(n-r-1)$, the output data $Z(n)$ from the MC, which are to be transmitted after a pulse shaping filter, preserves the modulation symbol patterns except some occasional 0 symbols. This implies that the MC coding in Fig.8.2 and Fig.8.4 can be implemented without introducing undue complexity.

8.5 Numerical Examples

In this section, we want to present two numerical examples to verify the theory/algorithm developed in the previous sections. Simulated outputs from a baud-rate sampled single-receiver system and an undersampled antenna array system are used for blind identification. The results presented here are to illustrate the feasibility rather than efficiency of the proposed MC coding and blind identification techniques, although some robustness in handling noisy data is demonstrated by the proposed algorithm.

8.5.1 Single Antenna Receiver with Baud Sampling Rate

In this example, we set the order of the baud-rate sampled ISI channel to be 4. The ISI channel is randomly selected, which in this example is

$$H(z) = 0.9275 - 0.5174z^{-1} + 0.2343z^{-2} + 0.7955z^{-3} + 0.1551z^{-4}.$$

The parameters in Fig.8.2 and Fig.8.3 and (8.4.5)-(8.4.6) are $K = 2, N = 3, M = 4$. In this case, the channel matrix $\mathbf{H}(z)$ in (8.4.6) is

$$\mathbf{H}(z) =$$

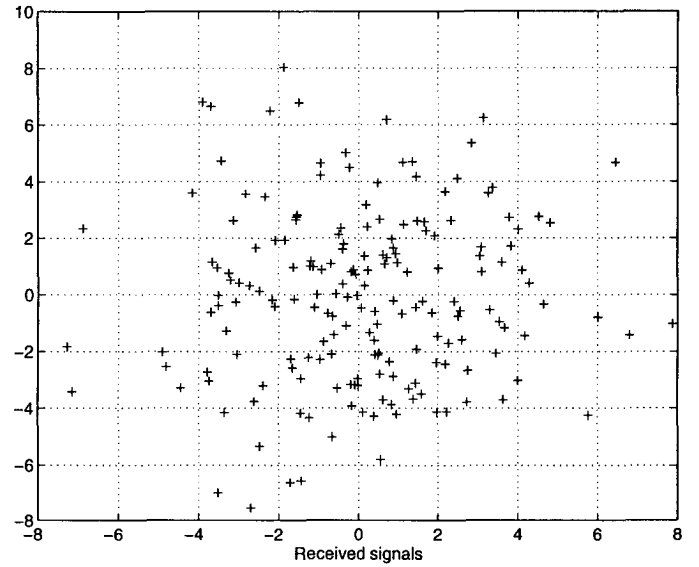

(a)

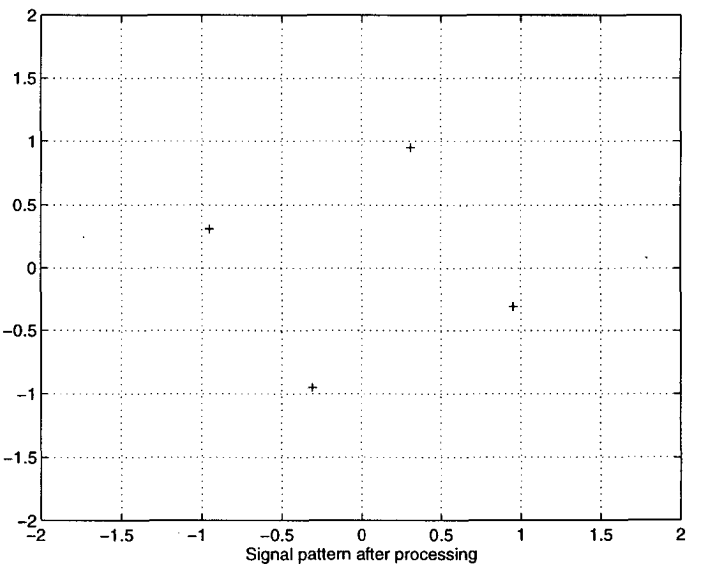

(b)

Figure 8.7: (a) ISI channel outputs with baud sampling; (b) recovered signal after blind identification using MC coding techniques.

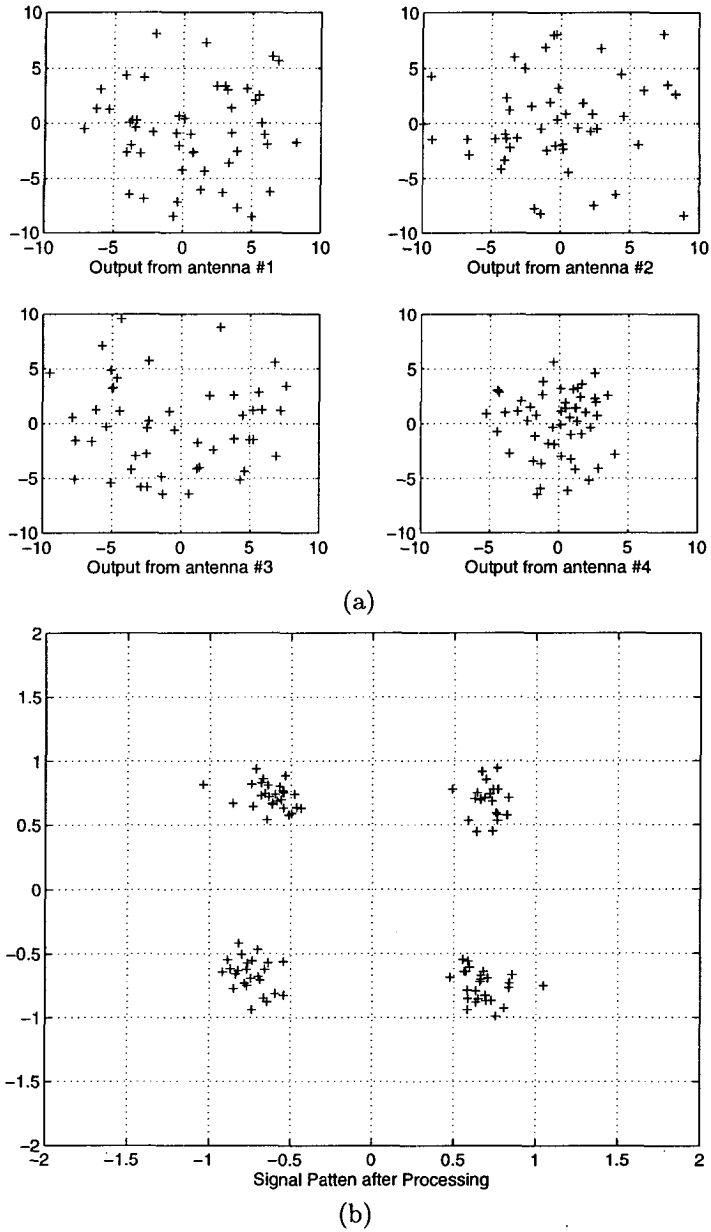

Figure 8.8: (a) Undersampled antenna outputs before blind identification; (b) recovered signal after blind identification using MC coding techniques.

$$\begin{bmatrix} 0.9275+0.1551z^{-1} & 0.7955z^{-1} & 0.2343z^{-1} \\ -0.5174 & 0.9275+0.1551z^{-1} & 0.7955z^{-1} \\ 0.2343 & -0.5174 & 0.9275+0.1551z^{-1} \\ 0.7955 & 0.2343 & -0.5174 \end{bmatrix}.$$

The order of $\mathbf{H}(z)$, Q_h, is thus 1. Based on (8.4.7), it is adequate to use $r = 3$ for the MC $\mathbf{G}(z)$ in (8.2.7). The order of $\mathbf{G}(z)$ is $r + 1 = 4$. $\mathbf{G}(z)$ is capable of resisting any 3rd order polynomial matrix ambiguity.

QPSK signals are used as the input signal in this example. The received data without identification is shown in Fig.8.7(a). The processed data after applying the proposed blind technique is shown in Fig.8.7(b). In this particular example, we use noise-free observations to demonstrate that the proposed techniques can provide closed-form solution with a finite number of data samples.

8.5.2 Undersampled Antenna Array Receivers

In this example, we use 4 antennas and undersampled the received signals by a factor of 3, i.e., $M = 4$ and $N = 3$ in Figs.8.4-8.5. Four ISI channels $H_l(z)$, $l = 1, 2, 3, 4$, are randomly chosen, which in this example are

$$\begin{aligned}
H_1(z) &= (0.3323+0.3446j)+(-0.2337+0.7782j)z^{-1} \\
&\quad +(0.1551+0.2511j)z^{-2}+(-0.5945+1.1582j)z^{-3} \\
&\quad +(-0.5398-1.2997j)z^{-4}+(-1.5044-2.7960j)z^{-5}; \\
H_2(z) &= (0.5589-0.7233j)+(1.4499+2.1805j)z^{-1} \\
&\quad +(-0.9646-0.3105j)z^{-2}+(0.1302+0.8625j)z^{-3} \\
&\quad +(1.8800+0.3066j)z^{-4}+(-0.0954+0.6967j)z^{-5}; \\
H_3(z) &= (0.8999+1.2682j)+(1.8361+0.4378j)z^{-1} \\
&\quad +(0.0388-0.9230j)z^{-2}+(0.0350-1.0347j)z^{-3} \\
&\quad +(-1.0038+0.9690j)z^{-4}+(0.3967+3.2069j)z^{-5}; \\
H_4(z) &= (-0.2009-0.0312j)+(-0.3829+1.3333j)z^{-1} \\
&\quad +(0.7655-0.3848j)z^{-2}+(-0.6247-0.1927j)z^{-3} \\
&\quad +(-0.4974-0.7473j)z^{-4}+(-0.5271+0.5360j)z^{-5}.
\end{aligned}$$

In this case, the channel matrix $\mathbf{H}(z)$ in Fig.8.5 is of order $Q_h = 1$. Similar to the previous example, the parameter r in (8.2.7) is set to be 3, which enables the MC $\mathbf{G}(z)$ to resist a 3rd order polynomial matrix ambiguity.

Instead of noise-free data, we apply the proposed blind identification algorithm to a minimum amount of output vectors, 50, under 30dB SNR.

The signal patterns before and after the identification are compared in Figs.8.8(a) and (b).

Chapter 9

Characterization and Construction of Polynomial Ambiguity Resistant Modulated Codes

In Chapter 8, we introduced PARMC that were channel independent and used at the transmitter such that the receiver is able to blindly identify the input signal no matter what the input symbol constellation is. In this chapter, we present more properties, characterizations, and canonical forms of PARMC, which are useful in the PARMC construction. The results in this chapter are from [186, 172]

9.1 PAR-Equivalence and Canonical Forms for Irreducible Polynomial Matrices

Let us first see an equivalence for PARMC, which is first introduced in [186] for the ambiguity resistant precoder canonical forms. Let $\mathcal{M}_{N\times K}(z)$ denote the set of all $N \times K$ polynomial matrices.

Definition 9.1 *The transformation* $T_{\mathbf{P},\mathbf{Q}}$ *of* $\mathcal{M}_{N\times K}(z)$ *defined by*

$$T_{\mathbf{P},\mathbf{Q}}(\mathbf{A}(z)) = \mathbf{P}\mathbf{A}(z)\mathbf{Q}(z),\ \forall\ \mathbf{A}(z) \in \mathcal{M}_{N\times K}(z),$$

where $\mathbf{P}$ *is an* $N \times N$ *nonsingular constant matrix and* $\mathbf{Q}(z)$ *is a* $K \times K$ *unimodular polynomial matrix, is called a PAR-equivalence transformation, and* $T_{\mathbf{P},\mathbf{Q}}(\mathbf{A}(z))$ *and* $\mathbf{A}(z)$ *are called PAR-equivalent.*

One can see that a PAR-equivalence transformation includes all three row elementary operations with constant multipliers and all three column elementary operations where an operation of multiplying a nonzero degree polynomial to a column is not included. From the PAR-equivalence definition, we have the following result.

Theorem 9.1 *A PAR-equivalence transformation preserves the (strong) rth PARMC property, i.e., an* $N \times K$ *polynomial matrix* $\mathbf{G}(z)$ *is (strong) rth PARMC if and only if* $\mathbf{PG}(z)\mathbf{Q}(z)$ *is (strong) rth PARMC for any* $N \times N$ *nonsingular constant matrix* $\mathbf{P}$ *and any unimodular polynomial matrix* $\mathbf{Q}(z)$.

Proof. Consider equation

$$\mathbf{E}(z)\mathbf{PG}(z)\mathbf{Q}(z) = \mathbf{PG}(z)\mathbf{Q}(z)\mathbf{V}(z).$$

Then

$$\mathbf{P}^{-1}\mathbf{E}(z)\mathbf{P} \cdot \mathbf{G}(z) = \mathbf{G}(z) \cdot \mathbf{Q}(z)\mathbf{V}(z)\mathbf{Q}(z)^{-1}.$$

If $\mathbf{G}(z)$ is (strong) rth PARMC, then we have

$$(\mathbf{P}^{-1}\mathbf{E}(z)\mathbf{P} = \alpha(z)I_N), \quad \mathbf{Q}(z)\mathbf{V}(z)\mathbf{Q}(z)^{-1} = \alpha(z)I_K$$

for some polynomial $\alpha(z)$ of order at most r, i.e., $\mathbf{PG}(z)\mathbf{Q}(z)$ is (strong) rth PARMC.

On the other hand, if $\mathbf{PG}(z)\mathbf{Q}(z)$ is (strong) rth PARMC, then from

$$\mathbf{E}(z)\mathbf{G}(z) = \mathbf{G}(z)\mathbf{V}(z)$$

we have

$$\mathbf{PE}(z)\mathbf{P}^{-1} \cdot \mathbf{PG}(z)\mathbf{Q}(z) = \mathbf{PG}(z)\mathbf{Q}(z) \cdot \mathbf{Q}(z)^{-1}\mathbf{V}(z)\mathbf{Q}(z).$$

So, we have $(\mathbf{PE}(z)\mathbf{P}^{-1} = \alpha(z)I_N)$, $\mathbf{Q}(z)^{-1}\mathbf{V}(z)\mathbf{Q}(z) = \alpha(z)I_K$ for some polynomial $\alpha(z)$ of order at most r, i.e., $\mathbf{G}(z)$ is (strong) rth PARMC. ■

Lemma 9.1 *Any polynomial matrix* $\mathbf{A}(z) \in \mathcal{M}_{N\times K}(z)$ *with rank* $= K$ *is PAR-equivalent to*

$$\begin{bmatrix} g_{1,1}(z) & 0 & 0 & \cdots & 0 \\ g_{2,1}(z) & g_{2,2}(z) & 0 & \cdots & 0 \\ g_{3,1}(z) & g_{3,2}(z) & g_{3,3}(z) & \cdots & 0 \\ \cdots & \cdots & \cdots & \cdots & \cdots \\ g_{K,1}(z) & g_{K,2}(z) & g_{K,3}(z) & \cdots & g_{K,K}(z) \\ \cdots & \cdots & \cdots & \cdots & \cdots \\ g_{N,1}(z) & g_{N,2}(z) & g_{N,3}(z) & \cdots & g_{N,K}(z) \end{bmatrix} \tag{9.1.1}$$

where $\deg(g_{1,1}(z)) \le \deg(g_{2,2}(z)) \le \cdots \le \deg(g_{K,K}(z))$. *Furthermore,*

$$\deg(g_{i,j}(z)) < \deg(g_{i,i}(z)) \quad \textit{for any } j < i.$$

Proof. Let $\mathbf{A}(z)$ be an $N \times K$ matrix with entries $a_{ij}(z)$. Let $d_i(z) = \gcd(a_{i1}(z), \cdots, a_{iK}(z))$. By row permutation only we may assume that $d_i(z) \neq 0$ and $\deg d_i$ is nondecreasing with i for $i = 1, \cdots, K$. Now $\mathbf{A}(z)$ is PAR-equivalent to (by only column transforms)

$$\begin{bmatrix} d_1(z) & 0 & \cdots & 0 \\ b_{21}(z) & b_{22}(z) & \cdots & b_{2K}(z) \\ \cdots & \cdots & \cdots & \cdots \\ b_{N1}(z) & b_{N2}(z) & \cdots & b_{NK}(z) \end{bmatrix}.$$

Furthermore, for $i = 2, \cdots, N$,

$$\deg[\gcd(b_{i2}(z), \cdots, b_{iK}(z))] \ge \deg[\gcd(b_{i1}(z), \cdots, b_{iK}(z))]$$

$$\ge \deg d_i \ge \deg d_1(z).$$

Similarly we can deal with the submatrix

$$\mathbf{B}(z) = \begin{bmatrix} b_{22}(z) & \cdots & b_{2K}(z) \\ \cdots & \cdots & \cdots \\ b_{N2}(z) & \cdots & b_{NK}(z) \end{bmatrix}$$

with $rank(\mathbf{B}) = K - 1$. By induction the lemma is proved. ■

Lemma 9.2 *For* L *polynomials* $f_1(z) \neq 0, f_2(z), \cdots, f_L(z)$, *if*

$$\deg(\gcd(cf_1 + f_2, f_3, \cdots, f_L)) \ge \deg f_1$$

for any constant c, *then* $f_1 | f_2$, $f_1 | f_3$, $\cdots$, $f_1 | f_L$.

Proof. We first prove the case $L = 3$. It is obvious if f_1 is a constant. Now suppose $\deg f_1 \geq 1$ and $d_c(z) \equiv \gcd(cf_1 + f_2, f_3)$. Then $\deg d_c \geq 1$. Let $d = \gcd(f_1, f_2, f_3)$. Then

$$f_1 = dg_1, f_2 = dg_2, f_3 = dg_3,$$

$$\gcd(g_1, g_2, g_3) = 1,$$

and

$$\deg(\gcd(cg_1 + g_2, g_3)) \geq \deg g_1.$$

Let $\alpha_1, \cdots, \alpha_k$ be the all zeroes of g_3. If $g_1(\alpha_j) = 0$ for some $j \in \{1, \cdots, k\}$, then $g_2(\alpha_j) \neq 0$. Let $C_2 > 0$ such that

$$|g_2(\alpha_j)| < C_2$$

for any $1 \leq j \leq k$ and let $C_1 > 0$ such that

$$\min_{g_1(\alpha_j) \neq 0} \{|g_1(\alpha_j)|\} > C_1$$

(if $g_1(\alpha_j) = 0$ for $1 \leq j \leq k$, we can take any $C_1 > 0$). Take

$$c > \frac{C_2}{C_1}.$$

For any α_j, we have two cases: if $g_1(\alpha_j) = 0$, then

$$cg_1(\alpha_j) + g_2(\alpha_j) = g_2(\alpha_j) \neq 0;$$

if $g_1(\alpha_j) \neq 0$, then

$$|cg_1(\alpha_j) + g_2(\alpha_j)| > \frac{C_2}{C_1} \cdot C_1 - C_2 = 0.$$

Hence the above two cases mean $\gcd(cg_1 + g_2, g_3) = 1$. Therefore we have

$$\gcd(cf_1 + f_2, f_3) = d_c = d \times \gcd(cg_1 + g_2, g_3) = d.$$

Now $\deg d \geq \deg f_1$ and $d | f_1$ imply $d(z) = cf_1(z)$ for some nonzero constant c. Hence $f_1 | f_2$, $f_1 | f_3$. For general L we know

$$\deg(\gcd(cf_1 + f_2, f_3, \cdots, f_L)) = \deg(\gcd(cf_1 + f_2, \gcd(f_3, \cdots, f_L))).$$

By the above proof, $f_1 | f_2, f_1 | \gcd(f_3, \cdots, f_L)$. Hence $f_1 | f_2, f_1 | f_3, \cdots, f_1 | f_L$. ■

Lemma 9.3 *If* $\mathbf{G}(z) = (g_{ij}(z))$ *is a nonzero matrix in* $\mathcal{M}_{N\times K}(z)$ *of the form* (9.1.1) *and if* $g_{11}(z) \neq 0$ *is an element of* $\mathbf{G}(z)$ *with* $m = \deg(g_{11}) \leq \deg(g_{ij})$ *for any* $g_{ij}(z)$, *then either* $g_{11}(z)$ *divides all* $g_{ij}(z)$, *or else there exists a PAR-equivalence transform* T *such that*

$$T(\mathbf{G}(z)) = \mathbf{Q}(z) = (q_{ij})$$

has the form (9.1.1) *and* $q_{11}(z) \neq 0$ *is of degree less than* m.

Proof. Suppose $g_{11}(z)$ does not divide every element of $\mathbf{G}(z)$. By Lemma 9.2, there exists a constant c and $i, 2 \leq i \leq N$ such that

$$\deg(\gcd(cg_{11} + g_{i1}, g_{i2}, \cdots, g_{ii}, \cdots, g_{iK}) < \deg g_{11} = m.$$

This means that $\mathbf{G}(z)$ is PAR-equivalent to a matrix with i-row

$$(cg_{11} + g_{i1}, g_{i2}, \cdots, g_{ii}, \cdots, g_{iK}).$$

Now Lemma 9.1 guarantees that $\mathbf{G}(z)$ is PAR-equivalent to $\mathbf{Q}(z)$ of form (9.1.1) with $\deg q_{11} \leq \deg(\gcd(cg_{11} + g_{i1}, g_{i2}, \cdots, g_{ii}, \cdots, g_{iK})) < m$. ■

Combining Lemma 9.1 and Lemma 9.3 we obtain the following result.

Theorem 9.2 *Any nonzero matrix* $\mathbf{A}(z) \in \mathcal{M}_{N\times K}(z)$ *with rank* $= K$ *is PAR-equivalent to a matrix of the following form*

$$\begin{bmatrix} g_{11}(z) & 0 & 0 & \cdots & 0 & 0 & \cdots & 0 \\ g_{21}(z) & g_{22}(z) & 0 & \cdots & 0 & 0 & \cdots & 0 \\ \cdots & \cdots & \cdots & \cdots & \cdots & \cdots & \cdots & \cdots \\ g_{k1}(z) & g_{k2}(z) & g_{k3}(z) & \cdots & g_{kk}(z) & 0 & \cdots & 0 \\ \cdots & \cdots & \cdots & \cdots & \cdots & \cdots & \cdots & \cdots \\ g_{N1}(z) & g_{N2}(z) & g_{N3}(z) & \cdots & g_{Nk}(z) & 0 & \cdots & 0 \end{bmatrix}$$

with $g_{ii}|g_{(i+1)(i+1)}, g_{ii}|g_{ji}$ *for any* $i = 1, 2, \cdots, k-1$ *and* $j \geq i$.

Proof. Obviously, $\mathbf{A}(z)$ is PAR-equivalent to a matrix of form $[\mathbf{B}\ \mathbf{0}]$ where $\mathbf{B}$ is an $N \times k$ matrix with $rank(\mathbf{B}) = k$. By Lemma 9.1, we have that any nonzero matrix is PAR-equivalent to a matrix as above such that $g_{11}(z)$ has the minimum degree. If $g_{ii}(z)$ divides all $g_{kl}(z)$ for any $k, l \geq i$, Theorem 9.2 is proved. If $g_{ii}(z)$ does not divide some $g_{kl}(z)$ for some $k, l \geq i$, we then consider the submatrix:

$$\begin{bmatrix} g_{ii}(z) & 0 & 0 & \cdots & 0 \\ g_{(i+1)i}(z) & g_{(i+1)(i+1)}(z) & 0 & \cdots & 0 \\ \cdots & \cdots & \cdots & \cdots & \cdots \\ g_{ki}(z) & g_{k(i+1)}(z) & g_{k(i+2)}(z) & \cdots & g_{kk}(z) \\ \cdots & \cdots & \cdots & \cdots & \cdots \\ g_{Ni}(z) & g_{N(i+1)}(z) & g_{N(i+2)}(z) & \cdots & g_{Nk}(z) \end{bmatrix}.$$

Therefore, by Lemma 9.3, under PAR-equivalence we have that $g_{ii}(z)$ divides all $g_{kl}(z)$ for any $k, l \geq i$. ■

By the above theorem, for irreducible matrices, we have the following result.

Theorem 9.3 *Any irreducible matrix in $\mathcal{M}_{N\times K}(z)$ is PAR-equivalent to a polynomial matrix of the following form*

$$\begin{bmatrix} 1 & 0 & 0 & \cdots & 0 & 0 \\ 0 & 1 & 0 & \cdots & 0 & 0 \\ \cdots & \cdots & \cdots & \cdots & \cdots & \cdots \\ 0 & 0 & 0 & \cdots & 1 & 0 \\ g_{K1}(z) & g_{K2}(z) & g_{K3}(z) & \cdots & g_{K(K-1)}(z) & g_{KK}(z) \\ \cdots & \cdots & \cdots & \cdots & \cdots & \cdots \\ g_{N1}(z) & g_{N2}(z) & g_{N3}(z) & \cdots & g_{N(K-1)}(z) & g_{NK}(z) \end{bmatrix} \tag{9.1.2}$$

with

$$gcd(g_{KK}, g_{(K+1)K}, \cdots, g_{NK}) = 1$$

and

$$\deg g_{KK} \leq \deg g_{(K+1)K} \leq \cdots \leq \deg g_{NK}.$$

Furthermore, $g_{kl}(z)$ can be either 0 or a nonconstant polynomial (i.e., $\deg g_{kl} \geq 1$) for $K \leq k \leq N$ and $1 \leq l \leq K-1$, and

$$g_{N1}(z) = \cdots = g_{N(L-1)}(z) = 0,\ 1 \leq \deg g_{NL} < \cdots < \deg g_{NK}$$

for some L with $1 \leq L \leq K$.

Proof. By Theorem 9.2, if g_{ii} is not a nonzero constant, then there exists α such that $g_{ii}(\alpha) = 0$. So $g_{ji}(\alpha) = 0$ for any $j = 1, 2, \cdots, N$ which contradicts with the irreducibility of $\mathbf{G}(z)$. Similar arguments can prove that $\gcd(g_{KK}, g_{(K+1)K}, \cdots, g_{NK}) = 1$. When $g_{kl}(z)$ is a nonzero constant for some k, l with $K \leq k \leq N$ and $1 \leq l \leq K-1$, it can be reduced to zero by implementing a constant elementary row operation, i.e., $g_{kl}(z)$ can be reduced to zero by an AR-equivalence transformation. ■

Remark, The result in Theorem 9.3 is the simplest form we can have, which can not be improved further. For example, we can directly check that

$$\begin{bmatrix} 1 & 0 \\ z^{-1} & z^{-2} \\ z^{-2} & z^{-3}+1 \end{bmatrix}$$

is an irreducible matrix, we can not simplify it further under AR-equivalence transformations. This polynomial matrix is actually a strong 0th order PARMC from Theorem 9.8 to be shown later.

Definition 9.2 *If* $\mathbf{A}(z)$ *is PAR-equivalent to* $\mathbf{G}(z)$ *of the form* (9.1.2), *then* $\mathbf{G}(z)$ *is called the canonical form of* $\mathbf{A}(z)$. *If* $g_{KK} = 1$, *we call* $\mathbf{G}(z)$ *the systematic form of* $\mathbf{A}(z)$.

With the above canonical form, to consider a PARMC we only need to consider a PARMC of the form (9.1.2).

To conclude this section, we generalize the linear independence as follows.

Definition 9.3 *A set of polynomials* $\{g_i(z)\}_{1\le i\le n}$ *are called* r*th order linearly independent (*r*th LID) if*

$$\sum_{i=1}^{n} e_i(z)g_i(z) = 0 \Longleftrightarrow e_i(z) = 0,\ i = 1, 2, \cdots, n,$$

where $\{e_i(z)\}_{1\le i\le n}$ *are polynomials of orders at most* r.

9.2 (Strong) rth PARMC with $N > K$

In this section, we want to present a relationship between rth PARMC and strong rth PARMC. We also derive a sufficient condition for the strong rth PARMC with $N > K$.

Theorem 9.4 *Let* $\mathbf{G}(z)$ *be of the canonical form (9.1.2). If* $\mathbf{G}(z)$ *is* r*th PARMC, then*

$$\max_{K\le i\le N}(\deg\, g_{iK}) > r.$$

Proof. If $\deg g_{iK} \le r$ for any i with $K \le i \le N$, let

$$\mathbf{E}(z) = \begin{bmatrix} 1 & 0 & \cdots & 0 & 0 & \cdots & 0 \\ 0 & 1 & \cdots & 0 & 0 & \cdots & 0 \\ \cdots & \cdots & \cdots & \cdots & \cdots & \cdots & \cdots \\ 0 & 0 & \cdots & 1 & 0 & \cdots & 0 \\ g_{KK}(z) & g_{KK}(z) & \cdots & g_{KK}(z) & 1 & \cdots & 0 \\ \cdots & \cdots & \cdots & \cdots & \cdots & \cdots & \cdots \\ g_{NK}(z) & g_{NK}(z) & \cdots & g_{NK}(z) & 0 & \cdots & 1 \end{bmatrix}$$

and

$$\mathbf{V}(z) = \begin{bmatrix} 1 & 0 & \cdots & 0 & 0 \\ 0 & 1 & \cdots & 0 & 0 \\ \cdots & \cdots & \cdots & \cdots & \cdots \\ 0 & 0 & \cdots & 1 & 0 \\ 1 & 1 & \cdots & 1 & 1 \end{bmatrix}.$$

Then we can check that $\mathbf{E}(z)\mathbf{G}(z) = \mathbf{G}(z)\mathbf{V}(z)$, and $\mathbf{E}(z)$ is an $N \times N$ polynomial matrix of order at most r. This is contradictory to the rth PARMC of $\mathbf{G}(z)$. ∎

From this theorem, one can clearly see that any constant matrix can not be PARMC of any order. If we have a rth PARMC $\mathbf{G}(z)$ of size $N \times K$, it is easy to construct rth PARMC of size $M \times K$ with $M > N$.

Theorem 9.5 *If an $M \times K$ polynomial matrix $\mathbf{A}(z)$ is PAR-equivalent to*

$$\begin{bmatrix} \mathbf{G}(z) \\ \mathbf{0}_{(M-N)\times K} \end{bmatrix},$$

and $\mathbf{G}(z)$ is rth PARMC, then $\mathbf{A}(z)$ is also rth PARMC. However, $\mathbf{A}(z)$ must not be strong rth PARMC, even when $\mathbf{G}(z)$ is strong rth PARMC.

Proof. From the equation

$$\begin{bmatrix} \mathbf{E}_{11}(z) & \mathbf{E}_{12}(z) \\ \mathbf{E}_{21}(z) & \mathbf{E}_{22}(z) \end{bmatrix} \begin{bmatrix} \mathbf{G}(z) \\ \mathbf{0}_{(M-N)\times K} \end{bmatrix} = \begin{bmatrix} \mathbf{G}(z) \\ \mathbf{0}_{(M-N)\times K} \end{bmatrix} \mathbf{V}(z),$$

we have $\mathbf{E}_{11}(z)\mathbf{G}(z) = \mathbf{G}(z)\mathbf{V}(z)$. Since $\mathbf{G}(z)$ is rth PARMC, so $\mathbf{V}(z) = \alpha(z)I_K$ for some polynomial $\alpha(z)$ of order at most r, i.e.,

$$\begin{bmatrix} \mathbf{G}(z) \\ \mathbf{0}_{(M-N)\times K} \end{bmatrix}$$

is rth PARMC. However, since

$$\begin{bmatrix} I_N & \mathbf{0} \\ \mathbf{0} & 2I_{M-N} \end{bmatrix} \begin{bmatrix} \mathbf{G}(z) \\ \mathbf{0}_{(M-N)\times K} \end{bmatrix} = \begin{bmatrix} \mathbf{G}(z) \\ \mathbf{0}_{(M-N)\times K} \end{bmatrix} I_K,$$

where $\mathbf{E}(z)$ is not equal to any $\alpha(z)I_N$, i.e.,

$$\begin{bmatrix} \mathbf{G}(z) \\ \mathbf{0}_{(M-N)\times K} \end{bmatrix}$$

is not strong 0th PARMC. So it is not strong rth PARMC either. ∎

We now see a connection between rth strong PARMC and rth PARMC.

Theorem 9.6 *Suppose that $\mathbf{G}(z)$ has the form (9.1.2) with $N > K$. If $\mathbf{G}(z)$ is rth PARMC, and $\{g_{KK}, \cdots, g_{NK}\}$ are rth order linearly independent, then $\mathbf{G}(z)$ is also strong rth PARMC.*

Proof. $\mathbf{G}(z)$ can be written as

$$\mathbf{G}(z) = \begin{bmatrix} I_{K-1} & \mathbf{0} \\ \mathbf{G}_{11}(z) & \mathbf{G}_{12}(z) \end{bmatrix}$$

where

$$\mathbf{G}_{11}(z) = \begin{bmatrix} g_{K1}(z) & \cdots & g_{K(K-1)}(z) \\ \cdots & \cdots & \cdots \\ g_{N1}(z) & \cdots & g_{N(K-1)}(z) \end{bmatrix} \text{ and } \mathbf{G}_{12}(z) = \begin{bmatrix} g_{KK}(z) \\ \vdots \\ g_{NK}(z) \end{bmatrix}.$$

Consider the equation

$$\begin{bmatrix} \mathbf{E}_{11}(z) & \mathbf{E}_{12}(z) \\ \mathbf{E}_{21}(z) & \mathbf{E}_{22}(z) \end{bmatrix} \begin{bmatrix} I_{K-1} & \mathbf{0} \\ \mathbf{G}_{11}(z) & \mathbf{G}_{12}(z) \end{bmatrix} = \begin{bmatrix} I_{K-1} & \mathbf{0} \\ \mathbf{G}_{11}(z) & \mathbf{G}_{12}(z) \\ \mathbf{G}_{11}(z) & \mathbf{G}_{12}(z) \end{bmatrix} \mathbf{V}(z),$$

where $\mathbf{E}_{11}(z), \mathbf{E}_{12}(z), \mathbf{E}_{21}(z)$ and $\mathbf{E}_{22}(z)$ are polynomial matrices of orders at most r. If $\mathbf{G}(z)$ is rth PARMC, then $\mathbf{V}(z) = \alpha(z)I_K$ for some polynomial $\alpha(z)$ of order at most r. Therefore,

$$\begin{aligned} \mathbf{E}_{11}(z) + \mathbf{E}_{12}(z)\mathbf{G}_{11}(z) &= \alpha(z)I_{K-1}, && (9.2.1) \\ \mathbf{E}_{21}(z) + \mathbf{E}_{22}(z)\mathbf{G}_{11}(z) &= \alpha(z)\mathbf{G}_{11}(z), && (9.2.2) \\ \mathbf{E}_{12}(z)\mathbf{G}_{12}(z) &= \mathbf{0}, && (9.2.3) \\ \mathbf{E}_{22}(z)\mathbf{G}_{12}(z) &= \alpha(z)\mathbf{G}_{12}(z). && (9.2.4) \end{aligned}$$

Since $\{g_{KK}, \cdots, g_{NK}\}$ are rth LID, so from (9.2.3) and (9.2.4), we have $\mathbf{E}_{12}(z) = \mathbf{0}$ and $\mathbf{E}_{22}(z) = \alpha(z)I_{N-K+1}$. Substituting $\mathbf{E}_{12}(z)$ and $\mathbf{E}_{22}(z)$ into (9.2.1) and (9.2.2), we obtain $\mathbf{E}_{11}(z) = \alpha(z)I_{K-1}$ and $\mathbf{E}_{21}(z) = \mathbf{0}$. So $\mathbf{G}(z)$ is strong rth PARMC. ■

Theorem 9.7 *Suppose that $\mathbf{G}(z)$ has the form (9.1.2) with $N > K$. If*

$$A_{i^{(1)},i^{(2)}} \triangleq \{g_{mK}g_{i^{(1)}K}, g_{nK}g_{i^{(2)}K}, g_{mK}(g_{i^{(1)}l}g_{i^{(2)}K} - g_{i^{(2)}l}g_{i^{(1)}K}),$$

$$1 \le l \le K-1,\ K \le m, n \le N, \text{ and } n \ne i^{(1)}\}$$

are rth order linearly independent for some $i^{(1)}$ and $i^{(2)}$ with $K \le i^{(1)} < i^{(2)} \le N$, then $\mathbf{G}(z)$ is strong rth PARMC.

Proof. Consider equation $\mathbf{E}(z)\mathbf{G}(z) = \mathbf{G}(z)\mathbf{V}(z)$, where $\mathbf{E}(z)$ is an $N \times N$ nonzero polynomial matrix of order at most r, and $\mathbf{V}(z)$ is a $K \times K$

polynomial matrix. Denote $\mathbf{E}(z) = (e_{ij})_{N\times N}$ and $\mathbf{V}(z) = (v_{ij})_{K\times K}$, then we have the following equations:

$$e_{ij} + \sum_{m=K}^{N} e_{im}g_{mj} = v_{ij},\ 1 \le i,j \le K-1, \tag{9.2.5}$$

$$e_{ij} + \sum_{m=K}^{N} e_{im}g_{mj} = \sum_{n=1}^{K} v_{nj}g_{in},$$
$$K \le i \le N,\ 1 \le j \le K-1, \tag{9.2.6}$$

$$\sum_{m=K}^{N} e_{im}g_{mK} = v_{iK},\ 1 \le i \le K-1, \tag{9.2.7}$$

$$\sum_{m=K}^{N} e_{im}g_{mK} = \sum_{n=1}^{K} v_{nK}g_{in},\ K \le i \le N. \tag{9.2.8}$$

From (9.2.8) we have

$$\left(\sum_{m=K}^{N} e_{i^{(1)}m}g_{mK} - \sum_{n=1}^{K-1} v_{nK}g_{i^{(1)}n}\right) g_{i^{(2)}K}$$

$$= \left(\sum_{m=K}^{N} e_{i^{(2)}m}g_{mK} - \sum_{n=1}^{K-1} v_{nK}g_{i^{(2)}n}\right) g_{i^{(1)}K}. \tag{9.2.9}$$

Substituting (9.2.7) to (9.2.9), we get

$$\sum_{m=K}^{N} e_{i^{(1)}m}g_{mK}g_{i^{(2)}K} - \sum_{n=1}^{K-1}\sum_{m=K}^{N} e_{nm}g_{mK}g_{i^{(1)}n}g_{i^{(2)}K}$$

$$= \sum_{m=K}^{N} e_{i^{(2)}m}g_{mK}g_{i^{(1)}K} - \sum_{n=1}^{K-1}\sum_{m=K}^{N} e_{nm}g_{mK}g_{i^{(2)}n}g_{i^{(1)}K},$$

i.e.,

$$(e_{i^{(1)}i^{(1)}} - e_{i^{(2)}i^{(2)}})g_{i^{(1)}K}g_{i^{(2)}K}$$
$$+ \sum_{\substack{m=K\\ m\neq i^{(1)}}}^{N} e_{i^{(1)}m}g_{mK}g_{i^{(2)}K} - \sum_{\substack{m=K\\ m\neq i^{(2)}}}^{N} e_{i^{(2)}m}g_{mK}g_{i^{(1)}K}$$
$$- \sum_{n=1}^{K-1}\sum_{m=K}^{N} e_{nm}g_{mK}(g_{i^{(1)}n}g_{i^{(2)}K} - g_{i^{(2)}n}g_{i^{(1)}K}) = 0.$$

Since $A_{i^{(1)},i^{(2)}}$ are rth LID, so $e_{i^{(1)}i^{(1)}} = e_{i^{(2)}i^{(2)}}$, $e_{i^{(1)}m} = 0$ and $e_{i^{(2)}n} = 0$ for $K \le m, n \le N$ with $m \neq i^{(1)}$ and $n \neq i^{(2)}$, and $e_{ij} = 0$ for $1 \le i \le K-1$ and $K \le j \le N$. Also we can obtain $v_{KK} = e_{i^{(1)}i^{(1)}} = e_{i^{(2)}i^{(2)}}$ and $v_{iK} = 0$ for $1 \le i \le K-1$.

Now from (9.2.5) and (9.2.6) we have

$$e_{ij} = v_{ij},\ 1 \le i, j \le K-1, \tag{9.2.10}$$

$$e_{i^{(1)}j} + e_{i^{(1)}i^{(1)}} g_{i^{(1)}j} = \sum_{n=1}^{K} v_{nj} g_{i^{(1)}n},\ 1 \le j \le K-1, \tag{9.2.11}$$

$$e_{i^{(2)}j} + e_{i^{(2)}i^{(2)}} g_{i^{(2)}j} = \sum_{n=1}^{K} v_{nj} g_{i^{(2)}n},\ 1 \le j \le K-1. \tag{9.2.12}$$

From (9.2.11) and (9.2.12) we get

$$\left(e_{i^{(1)}j} + e_{i^{(1)}i^{(1)}} g_{i^{(1)}j} - \sum_{n=1}^{K-1} v_{nj} g_{i^{(1)}n} \right) g_{i^{(2)}K}$$

$$= \left(e_{i^{(2)}j} + e_{i^{(2)}i^{(2)}} g_{i^{(2)}j} - \sum_{n=1}^{K-1} v_{nj} g_{i^{(2)}n} \right) g_{i^{(1)}K}$$

for any j with $1 \le j \le K-1$, i.e.,

$$e_{i^{(1)}j} g_{i^{(2)}K} - e_{i^{(2)}j} g_{i^{(1)}K} + (e_{i^{(1)}i^{(1)}} - e_{jj})(g_{i^{(1)}j} g_{i^{(2)}K} - g_{i^{(2)}j} g_{i^{(1)}K})$$

$$- \sum_{\substack{n=1 \\ n \neq j}}^{K-1} e_{nj} (g_{i^{(1)}n} g_{i^{(2)}K} - g_{i^{(2)}n} g_{i^{(1)}K}) = 0,\ 1 \le j \le K-1. \tag{9.2.13}$$

The rth LID of $A_{i^{(1)},i^{(2)}}$ implies that $\{g_{i^{(2)}K} g_{i^{(1)}K}, g_{i^{(2)}K}^2, g_{i^{(2)}K}(g_{i^{(1)}l} g_{i^{(2)}K} - g_{i^{(2)}l} g_{i^{(1)}K}), 1 \le l \le K-1\}$ are rth LID, i.e., $\{g_{i^{(1)}K}, g_{i^{(2)}K}, g_{i^{(1)}l} g_{i^{(2)}K} - g_{i^{(2)}l} g_{i^{(1)}K}, 1 \le l \le K-1\}$ are rth LID. So from (9.2.13) we have $e_{i^{(1)}i^{(1)}} = e_{jj}$, $e_{i^{(1)}j} = e_{i^{(2)}j} = 0$ and $e_{nj} = 0$ for $1 \le j \ne n \le K-1$. Thus we get $\mathbf{V}(z) = e_{i^{(1)}i^{(1)}} I_K$, i.e., $\mathbf{G}(z)$ is rth PARMC.

From the rth LID of $A_{i^{(1)},i^{(2)}}$ again, we know that $\{g_{mK} g_{i^{(1)}K}, K \le m \le N\}$ are rth LID, i.e., $\{g_{KK}, g_{(K+1)K}, \cdots, g_{NK}\}$ are rth LID. According to Theorem 9.6, $\mathbf{G}(z)$ is also strong rth PARMC. ■

The above theorem provides us a new and more general sufficient condition for constructing $N \times K$ strong rth PARMC for a general N with $N > K$.

9.3 (Strong) rth PARMC with $N = K + 1$

In this section, we discuss polynomial matrices only with $N = K + 1$. The following sufficient condition for strong 0th PARMC with $N = K + 1$ was obtained in [186].

Theorem 9.8 *Let $\mathbf{G}(z)$ have the canonical form (9.1.2) with $N = K + 1$. If $g_{N1}(z) = \cdots = g_{N(L-1)}(z) = 0$ and $1 \leq \deg g_{NL} < \cdots < \deg g_{NK}$ for some L, $1 \leq L \leq K$, and if*

$$\{1, g_{K1}, g_{K2}, \cdots, g_{K(L-1)}, g_{NL}, \cdots, g_{N(K-1)}\}$$

are 0th order linearly independent, and $W_1 \cap W_2 = \{0\}$, where

$$W_1 = \text{span}\{g_{NK}, g_{NK}g_{K1}, \cdots, g_{NK}g_{K(K-1)}\},$$

$$W_2 = \text{span}\{g_{KK}, g_{KK}g_{K1}, \cdots, g_{KK}g_{K(L-1)}, g_{KK}g_{NL}, \cdots, g_{KK}g_{N(K-1)}\},$$

where span means the set of all linear combinations with constant coefficients, then $\mathbf{G}(z)$ is strong 0th order PARMC.

Proof. By $\mathbf{EG}(z) = \mathbf{G}(z)\mathbf{V}(z)$ we get the following equations:

$$\begin{aligned}
e_{ij} + e_{iK}g_{Kj}(z) + e_{iN}g_{Nj}(z) &= v_{ij}(z), \\
&\quad 1 \leq i, j \leq K-1, && (9.3.1)\\
e_{Kj} + e_{KK}g_{Kj}(z) + e_{KN}g_{Nj}(z) &= \sum_{m=1}^{K} g_{Km}(z)v_{mj}(z), \\
&\quad 1 \leq j \leq K-1, && (9.3.2)\\
e_{Nj} + e_{NK}g_{Kj}(z) + e_{NN}g_{Nj}(z) &= \sum_{m=1}^{K} g_{Nm}(z)v_{mj}(z), \\
&\quad 1 \leq j \leq K-1, && (9.3.3)\\
e_{iK}g_{KK}(z) + e_{iN}g_{NK}(z) &= v_{iK}(z), \\
&\quad 1 \leq i \leq K-1, && (9.3.4)\\
e_{KK}g_{KK}(z) + e_{KN}g_{NK}(z) &= \sum_{m=1}^{K} g_{Km}(z)v_{mK}(z), && (9.3.5)\\
e_{NK}g_{KK}(z) + e_{NN}g_{NK}(z) &= \sum_{m=1}^{K} g_{Nm}(z)v_{mK}(z). && (9.3.6)
\end{aligned}$$

Substituting (9.3.4) to (9.3.6) we obtain

$$e_{NK}g_{KK}(z) + e_{NN}g_{NK}(z)$$

$$= \sum_{m=1}^{K-1} g_{Nm}(z)(e_{mK}g_{KK}(z) + e_{mN}g_{NK}(z)) + v_{KK}(z)g_{NK}(z),$$

i.e.,

$$\left(e_{NN} - v_{KK}(z) - \sum_{m=1}^{K-1} e_{mN}g_{Nm}(z)\right) g_{NK}(z)$$

$$= \left(\sum_{m=1}^{K-1} e_{mK}g_{Nm}(z) - e_{NK}\right) g_{KK}(z).$$

So $\gcd(g_{NK}, g_{KK}) = 1$ implies

$$g_{NK}(z) | (\sum_{m=1}^{K-1} e_{mK}g_{Nm}(z) - e_{NK}).$$

Hence $1 \leq \deg g_{NL} < \cdots < \deg g_{NK}$ implies $e_{NK} = 0$ and $e_{iK} = 0$ for $i = L, \cdots, K-1$ and

$$v_{KK}(z) = e_{NN} - \sum_{m=1}^{K-1} e_{mN}g_{Nm}(z). \tag{9.3.7}$$

Plugging (9.3.4) and (9.3.7) into (9.3.5) we get

$$\left(e_{KN} - \sum_{m=1}^{K-1} e_{mN}g_{Km}(z)\right) g_{NK}(z)$$

$$= \left(e_{NN} - e_{KK} + \sum_{m=1}^{K-1} (e_{mK}g_{Km} - e_{mN}g_{Nm}(z))\right) g_{KK}(z),$$

or

$$\left(e_{KN} - \sum_{m=1}^{K-1} e_{mN}g_{Km}(z)\right) g_{NK}(z)$$

$$= \left(e_{NN} - e_{KK} + \sum_{m=1}^{L-1} e_{mK}g_{Km} - \sum_{m=L}^{K-1} e_{mN}g_{Nm}(z)\right) g_{KK}(z). \tag{9.3.8}$$

Now $W_1 \cap W_2 = \{0\}$ and the 0th LID of

$$\{1, g_{K1}, \cdots, g_{K(L-1)}, g_{NL}, \cdots, g_{N(K-1)}\}$$

mean $e_{KK} = e_{NN}, e_{iK} = 0$ for $i = 1, \cdots, L-1$, $e_{mN} = 0$ for $m = L, \cdots, K-1$. So

$$e_{KN} - \sum_{m=1}^{K-1} e_{mN} g_{Km}(z) = e_{KN} - \sum_{m=1}^{L-1} e_{mN} g_{Km}(z) = 0$$

implies $e_{KN} = 0$, $e_{mN} = 0$ for $m = 1, \cdots, L-1$ by the linear independence of $\{1, g_{K1}, \cdots, g_{K(L-1)}\}$. Hence we obtain $e_{iN} = 0$ for $i = 1, 2, \cdots, K$, $e_{KN} = 0, e_{KK} = e_{NN}, e_{iK} = 0$ for $i = 1, 2, \cdots, K-1$. Then (9.3.1) becomes

$$v_{ij}(z) = e_{ij}, \quad i, j = 1, 2, \cdots, K-1, \tag{9.3.9}$$

(9.3.2) becomes

$$e_{Kj} + e_{KK} g_{Kj}(z) = \sum_{m=1}^{K} g_{Km}(z) v_{mj}(z), \quad 1 \le j \le K-1, \tag{9.3.10}$$

(9.3.3) becomes

$$e_{Nj} + e_{NN} g_{Nj}(z) = \sum_{m=1}^{K} g_{Nm}(z) v_{mj}(z)$$

$$= \sum_{m=L}^{K} g_{Nm}(z) v_{mj}(z), \quad 1 \le j \le K-1. \tag{9.3.11}$$

Plugging (9.3.9) into (9.3.11) we get $e_{NN} = e_{jj} = v_{jj}$, $v_{ij}(z) = e_{ij} = 0$ for $i = L, \cdots, K, j = 1, 2, \cdots, K-1, i \neq j$. In this case (9.3.10) becomes

$$e_{Kj} + e_{KK} g_{Kj}(z) = \sum_{m=1}^{L-1} g_{Km}(z) e_{mj} + \sum_{m=L}^{K} g_{Km}(z) e_{mj}.$$

This means that $e_{ij} = 0$ if $i = 1, \cdots, L-1, j = 1, 2, \cdots, K-1, i \neq j$. This proves that $E = e_{11} I_{K+1}, V(z) = e_{11} I_K$. ∎

Note that the above conditions are not necessary from the following counter example:

$$\mathbf{G}(z) = \begin{bmatrix} 1 & 0 & 0 \\ 0 & 1 & 0 \\ z^{-1} & z^{-2} & 1 + z^{-3} \\ 0 & z^{-1} & z^{-5} \end{bmatrix}. \tag{9.3.12}$$

Clearly, $\{1, g_{31}, g_{42}\}$ are not linearly independent, but $\mathbf{G}(z)$ is actually strong 0th PAR as we will see later.

Theorem 9.9 *Let* $\mathbf{G}(z)$ *have the form (9.1.2) with* $N = K + 1$. *Then* $\mathbf{G}(z)$ *is* r*th PARMC if and only if* $\mathbf{G}(z)$ *is strong* r*th PARMC.*

Proof. The sufficiency is obvious. Now we prove the necessity. If $\mathbf{G}(z)$ is rth PARMC, according to Theorem 9.6, we only need to prove that $\{g_{KK}, g_{NK}\}$ are rth order linearly independent (rth LID).

If there exist polynomials $e_1(z)$ and $e_2(z)$ of orders at most r such that

$$e_1(z)g_{KK}(z) + e_2(z)g_{NK}(z) = 0,$$

since $gcd(g_{KK}, g_{NK}) = 1$ from the canonical form, we have $g_{NK}(z)/e_1(z)$ and $g_{KK}(z)/e_2(z)$. According to Theorem 9.4, $\max(\deg g_{KK}, \deg g_{NK}) > r$. So $e_1(z) = 0$ and $e_2(z) = 0$, i.e., $\{g_{KK}, g_{NK}\}$ are rth LID. This proves the necessity. ■

The following theorem can be derived from Theorem 9.7 directly.

Theorem 9.10 *Suppose that* $\mathbf{G}(z)$ *has the form (9.1.2) with* $N = K + 1$. *If*

$$A_{K,N} \triangleq \{g_{KK}g_{NK}, g_{KK}^2, g_{NK}^2, g_{KK}(g_{NK}g_{Kn} - g_{KK}g_{Nn}),$$

$$g_{NK}(g_{NK}g_{Kn} - g_{KK}g_{Nn}), 1 \le n \le K - 1\}$$

are r*th order linearly independent, then* $\mathbf{G}(z)$ *is strong* r*th PARMC.*

As a remark, the condition in Theorem 9.10 is sharper than the conditions in Theorem 9.8. Let us see the example in (9.3.12). We know $\mathbf{G}(z)$ does not satisfy the conditions in Theorem 9.8. But

$$A_{3,4} \triangleq \{z^{-8} + z^{-5}, z^{-6} + 2z^{-3} + 1, z^{-10},$$

$$z^{-9} + z^{-6}, z^{-10} - 2z^{-4} - z^{-1}, z^{-11}, z^{-12} - z^{-9} - z^{-5}\}$$

are actually 0th LID, i.e., $\mathbf{G}(z)$ is strong 0th PARMC by Theorem 9.10. Moreover, we can show that $A_{K,N}$ are 0th LID if the conditions in Theorem 9.8 are true. In fact, if there exist constants a, b, c, d_n and e_n ($1 \le n \le K - 1$) such that

$$ag_{KK}g_{NK} + bg_{KK}^2 + cg_{NK}^2 + \sum_{n=1}^{K-1} d_n g_{KK}(g_{NK}g_{Kn} - g_{KK}g_{Nn})$$

$$+ \sum_{n=1}^{K-1} e_n g_{NK}(g_{NK}g_{Kn} - g_{KK}g_{Nn}) = 0,$$

then

$$\frac{g_{NK}}{\left(bg_{KK}^2 - \sum_{n=1}^{K-1} d_n g_{KK}^2 g_{Nn}\right)}.$$

From the assumption in Theorem 9.8, we get $b = 0$, $d_n = 0$ for $L \leq n \leq K-1$, and

$$ag_{KK} + cg_{NK} + \sum_{n=1}^{L-1} d_n g_{KK} g_{Kn} + \sum_{n=1}^{K-1} e_n (g_{NK} g_{Kn} - g_{KK} g_{Nn}) = 0,$$

i.e.,

$$\left(c + \sum_{n=1}^{K-1} e_n g_{Kn}\right) g_{NK} = g_{KK} \left(-a - \sum_{n=1}^{L-1} d_n g_{Kn} + \sum_{n+L}^{K-1} e_n g_{KK} g_{Nn}\right).$$

Since $W_1 \cap W_2 = \{0\}$ and $\{1, g_{K1}, \cdots, g_{K(L-1)}, g_{NL}, \cdots, g_{N(K-1)}\}$ are 0th LID, we get $c = 0$, $a = 0$, $d_n = 0$ and $e_n = 0\,(1 \leq n \leq K-1)$. So $A_{K,N}$ are 0th LID.

The rth LID of $A_{K,N}$ implies that

$$\{g_{KK}, g_{NK}, g_{NK} g_{Kn} - g_{KK} g_{Nn},\ 1 \leq n \leq K-1\}$$

is rth LID. In fact, the rth LID of

$$\{g_{KK}, g_{NK}, g_{NK} g_{Kn} - g_{KK} g_{Nn},\ 1 \leq n \leq K-1\}$$

is also necessary for the rth PARMC of $\mathbf{G}(z)$, and is certainly necessary for the strong rth PARMC of $\mathbf{G}(z)$.

Theorem 9.11 *If $\mathbf{G}(z)$ has the form (9.1.2) with $N = K+1$, and $\mathbf{G}(z)$ is rth PARMC, then $\{g_{KK}, g_{NK}, g_{NK} g_{Kn} - g_{KK} g_{Nn},\ 1 \leq n \leq K-1\}$ are rth order linearly independent.*

Proof. Assume that $\{g_{KK}, g_{NK}, g_{NK} g_{Kn} - g_{KK} g_{Nn},\ 1 \leq n \leq K-1\}$ are not rth LID, then there exist polynomials a, b and c_n, $1 \leq n \leq K-1$, of order at most r such that

$$ag_{KK} + bg_{NK} + \sum_{n=1}^{K-1} c_n (g_{NK} g_{Kn} - g_{KK} g_{Nn}) = 0,$$

i.e.,

$$\left(b + \sum_{n=1}^{K-1} c_n g_{Kn}\right) g_{NK} = g_{KK} \left(-a + \sum_{n=1}^{K-1} c_n g_{Nn}\right).$$

So

$$\frac{g_{KK}}{\left(b + \sum_{n=1}^{K-1} c_n g_{Kn}\right)} \text{ and } \frac{g_{NK}}{\left(-a + \sum_{n=1}^{K-1} c_n g_{Nn}\right)}.$$

Now let $\mathbf{E}(z) = (e_{ij})_{N\times N}$, where $e_{NN} = e_{KK}$, $e_{NK} = 0, e_{KN} = 0$, $e_{nK} = 0$ and $e_{nN} = 0$ for $1 \le n \le K-1$, and for any j with $1 \le j \le K-1$, $e_{jj} = e_{KK} - c_j$, $e_{Kj} = b$, $e_{Nj} = -a$, and $e_{nj} = -c_n$, $1 \le n \le K-1$ for $n \ne j$. Let $\mathbf{V}(z) = (v_{ij})_{K\times K}$, where $v_{KK} = e_{NN}$, $v_{ij} = e_{ij}$ for $1 \le i, j \le K-1$, and for any j with $1 \le j \le K-1$,

$$v_{Kj} = \frac{\left(b + \sum_{n=1}^{K-1} c_n g_{Kn}\right)}{g_{KK}} \text{ or } \frac{\left(-a + \sum_{n=1}^{K-1} c_n g_{Nn}\right)}{g_{NK}}.$$

We can check that $\mathbf{E}(z)\mathbf{G}(z) = \mathbf{G}(z)\mathbf{V}(z)$. It is obvious that $\mathbf{V}(z) \ne \alpha(z)I_K$. This is contradictory to $\mathbf{G}(z)$ is rth PARMC. ■

Combining Theorems 9.10 and 9.11, we have the following corollary.

Corollary 9.1 *If* $\mathbf{G}(z)$ *has the systematic form, i.e.,*

$$\mathbf{G}(z) = \begin{bmatrix} 1 & 0 & 0 & \cdots & 0 \\ 0 & 1 & 0 & \cdots & 0 \\ 0 & 0 & 1 & \cdots & 0 \\ \cdots & \cdots & \cdots & \cdots & \cdots \\ 0 & 0 & 0 & \cdots & 1 \\ g_{(K+1)1}(z) & g_{(K+1)2}(z) & g_{(K+1)3}(z) & \cdots & g_{(K+1)K}(z) \end{bmatrix}_{(K+1)\times K},$$

then $\mathbf{G}(z)$ *is strong* r*th PARMC, if and only if*

$$\{1, g_{(K+1)1}, g_{(K+1)2}, \cdots, g_{(K+1)K}\}$$

are r*th order linearly independent.*

Proof. The necessity comes from Theorem 9.11 immediately. Now we prove the sufficiency. According to Theorem 9.10, we need to prove that

$$\{1, g_{(K+1)n}, g_{(K+1)K}g_{(K+1)n}, 1 \le n \le K\}$$

are rth LID.

With PAR-equivalence transformations, we can assume $\deg g_{(K+1)n} < \deg g_{(K+1)K}$ for $1 \le n \le K-1$. If there exist polynomials a, b_n and c_n, $1 \le n \le K$, of orders at most r such that

$$a + \sum_{n=1}^{K} b_n g_{(K+1)n} + \sum_{n=1}^{K} c_n g_{(K+1)K} g_{(K+1)n} = 0, \tag{9.3.13}$$

then

$$\frac{g_{(K+1)K}}{\left(a + \sum_{n=1}^{K-1} b_n g_{(K+1)n}\right)}.$$

From the rth LID of $\{1, g_{(K+1)1}, g_{(K+1)2}, \cdots, g_{(K+1)K}\}$, we have $a = 0$ and $b_n = 0$ for $1 \le n \le K-1$. Using (9.3.13) again, we have $b_K = 0$ and $c_n = 0$ for $1 \le n \le K$. So $\{1, g_{(K+1)1}, g_{(K+1)2}, \cdots, g_{(K+1)K}\}$ are rth LID. ■

The special case when $r = 0$ in the above corollary was obtained in [186]. The following corollary can be checked easily by using Theorem 9.10, which provides a convenient way to construct nonsystematic strong rth PARMC with $N = K + 1$.

Corollary 9.2 *Suppose that* $\mathbf{G}(z)$ *has the form (9.1.2) with* $N = K + 1$. *If* $g_{N1}(z) = \cdots = g_{N(L-1)}(z) = 0$ *for some* L $(1 \le L \le K)$, *and*

$$\deg g_{Kn} < \deg g_{K(n+1)} + r, \quad 1 \le n < L - 1,$$

$$\deg g_{Nn} < \deg g_{N(n+1)} + r, \quad L \le n < K,$$

and $\deg g_{K(L-1)} < \deg g_{NL} + r$, *then* $\mathbf{G}(z)$ *is strong* r*th PARMC.*

Chapter 10

An Optimal Polynomial Ambiguity Resistant Modulated Code Design

In Chapter 9, we characterized and constructed PARMC. Although any PARMC is good enough in theory to be used to blindly cancel the ISI without additive noise, different PARMC may have performance differences when there is additive noise in the channel. The question, then, becomes which PARMC performs "better," where "better" means better symbol error rate performance at the receiver after equalization. In this chapter, we propose a criterion for PARMC design by introducing a distance concept for a PARMC and then study the optimal design based on the criterion. The results in this chapter are summarized from [163, 177].

10.1 A Criterion for PARMC Design

If the ISI channel is known, the criterion for the optimal MC is to maximize the free distance of the combined MC of the encoder MC and the ISI channel. However, when the ISI channel is not known, this criterion and the criterion in Chapter 4 using the joint DFE do not apply to PARMC. In the following, we propose a different criterion for the PARMC design for resisting both ISI and additive noise, which is to maximize the mean distance of all the different PARMC encoded symbols. The motivation is as follows.

Consider the general MIMO system in Fig.8.1, where $\mathbf{X}(z)$ is the $K \times$

1 polynomial matrix of the z-transform of the input vectors, $\mathbf{G}(z)$ is an (N, K) PARMC, $\mathbf{H}(z)$ is the $M \times N$ polynomial matrix of the ISI channel, $\eta(z)$ is the $M \times 1$ polynomial matrix of the z-transform of the additive white noise vectors, and $\mathbf{Y}(z)$ is the $M \times 1$ polynomial matrix of the z-transform of the channel output vectors. Let

$$\mathbf{G}(z) = \sum_{n=0}^{Q_G} G(n)z^{-n}, \ \mathbf{H}(z) = \sum_{n=0}^{Q_H} H(n)z^{-n},$$

$$\mathbf{X}(z) = \sum_{n} X(n)z^{-n}, \ \mathbf{Y}(z) = \sum_{n} Y(n)z^{-n}.$$

Let

$$\mathbf{V}(z) \triangleq \mathbf{G}(z)\mathbf{X}(z) = \sum_{n} V(n)z^{-n},$$

the z-transform of the PARMC output vector sequence, and

$$\mathbf{U}(z) \triangleq \mathbf{H}(z)\mathbf{V}(z) = \sum_{n} U(n)z^{-n},$$

the z-transform of the ISI channel output vector sequence. Notice that all $X(n), Y(n), V(n), V(n), \eta(n)$ are constant column vectors while $G(n), H(n)$ are constant matrices. The performance of the above system in resisting the additive noise depends on the minimal distance of all the sequences of $U(n)$, which clearly depend on the unknown ISI channel $H(n)$. Therefore, it is not possible to consider the minimal distance if the ISI channel is not known. The next candidate is the mean distance between all different sequences $U(n)$ by assuming the ISI channel $H(n)$ random, which is basically determined by the mean power of the PARMC encoded sequences and therefore is fixed for a normalized PARMC. We now consider the mean distance between all possible symbols $U(n)$ rather than sequences.

To study the mean distance for the output symbols in $U(n)$, let us use matrix representations for linear transformations. By concatenating all vectors $X(n)$ together, all vectors $V(n)$ together, all vectors $U(n)$ together, all vectors $\eta(n)$ together, and all vectors $Y(n)$ together, we obtain larger block vectors $\mathcal{X} = (x(n))$, $\mathcal{V} = (v(n))$, $\mathcal{U} = (u(n))$, $\eta = (\eta(n))$, and $\mathcal{Y} = (y(n))$, respectively. Let $\mathcal{G}$ and $\mathcal{H}$ denote the generalized Sylvester matrices, respectively:

$$\mathcal{G} = \begin{bmatrix} G(Q_G) & \cdots & G(0) & \cdots & 0 \\ \vdots & \ddots & \ddots & \ddots & \vdots \\ 0 & \cdots & G(Q_G) & \cdots & G(0) \end{bmatrix},$$

$$\mathcal{H} = \begin{bmatrix} H(Q_H) & \cdots & H(0) & \cdots & 0 \\ \vdots & \ddots & \ddots & \ddots & \vdots \\ 0 & \cdots & H(Q_H) & \cdots & H(0) \end{bmatrix}. \tag{10.1.1}$$

Then,

$$\mathcal{V} = \mathcal{G}\mathcal{X}, \quad \mathcal{U} = \mathcal{H}\mathcal{V}, \quad \mathcal{Y} = \mathcal{U} + \eta. \tag{10.1.2}$$

In what follows, for convenience we assume the input signal $x(n)$ is an i.i.d. random process with mean zero and variance σ_x^2. Thus, random processes $v(n)$ and $u(n)$ have mean zero. We also assume all coefficients in the ISI channel $\mathbf{H}(z)$ are i.i.d. with mean zero and variance σ_H^2 and they are independent of $x(n)$. Notice that this assumption is only used to simplify the following analysis and it does not apply to the single receiver system in Fig.8.2, where the corresponding channel matrix $\mathbf{H}(z)$ has the pseudo-circulant structure in (2.3.3).

The mean distances between all values of $u(n)$ and all values of $v(n)$ are

$$d_v \triangleq \left(\mathrm{E}(\sum_{m,n} |v(m) - v(n)|^2) \right)^{1/2}, \; d_u \triangleq \left(\mathrm{E}(\sum_{m,n} |u(m) - u(n)|^2) \right)^{1/2}, \tag{10.1.3}$$

respectively. By the i.i.d. assumption on the coefficients of $\mathbf{H}(z)$, it is not hard to see the following relationship between the mean distance d_u of the ISI channel output values $u(n)$ and the mean distance d_v of the PARMC output values (or the ISI channel input values) $v(n)$:

$$d_u = \sigma_H d_v. \tag{10.1.4}$$

Based on the above mean distance formula, we have the following definition for optimal PARMC.

Definition 10.1 *A normalized (N, K) PARMC $\mathbf{G}(z)$ is called* optimal *if the mean distance d_v of all the PARMC output symbols is the maximal among all normalized (N, K) PARMC.*

The squared mean distance d_v can be calculated as

$$d_v^2 = \sum_{m,n} \mathrm{E}|v(m) - v(n)|^2$$

$$= 2(LN-1) \sum_n \mathrm{E}(|v(n)|^2) - 2 \sum_{m \neq n} \mathrm{E}\left(v(m)v^*(n)\right), \tag{10.1.5}$$

where L is the length of the PARMC output vector sequence $V(n)$ and N is the PARMC size. Let $R(m,n)$ be the correlation function of the random process $v(n)$, i.e.,

$$R(m,n) = \mathrm{E}(v(m)v^*(n)).$$

Let $\mathcal{R}$ be the correlation matrix of $v(n)$, i.e.,

$$\mathcal{R} = (R(m,n)) = \mathrm{E}\left(\mathcal{GX}\,(\mathcal{GX})^\dagger\right) = \mathcal{G}\mathrm{E}(\mathcal{X}\mathcal{X})^\dagger\mathcal{G}^\dagger = \sigma_x^2\mathcal{G}\mathcal{G}^\dagger, \qquad (10.1.6)$$

where † means the conjugate transpose. One can see that the first term and the second term in the right hand side of (10.1.5) for the distance d_v are the sum of all the diagonal elements, i.e., the trace, of the matrix $\mathcal{G}\mathcal{G}^\dagger$ multiplied by $2\sigma_x^2$, and the sum of all the off diagonal elements of the matrix $\mathcal{G}\mathcal{G}^\dagger$ multiplied by $2\sigma_x^2$, respectively. The trace of $\mathcal{G}\mathcal{G}^\dagger$ of a normalized MC is nothing else but N from (2.1.5). In formula, the squared mean distance d_v can be calculated as

$$\begin{aligned} d_v^2 &= 2\sigma_x^2\left((LN-1)\mathrm{trace}(\mathcal{G}\mathcal{G}^\dagger) - \sum_{m\neq n}(\mathcal{G}\mathcal{G}^\dagger)_{mn}\right) \\ &= 2\sigma_x^2\left(LN\mathrm{trace}(\mathcal{G}\mathcal{G}^\dagger) - \sum_{m,n}(\mathcal{G}\mathcal{G}^\dagger)_{mn}\right) \qquad (10.1.7) \end{aligned}$$

where $(\mathcal{G}\mathcal{G}^\dagger)_{mn}$ denotes the element at the mth row and the nth column of $\mathcal{G}\mathcal{G}^\dagger$. We next want to further simplify d_v in (10.1.7). For a PARMC $\mathbf{G}(z)$, define

$$\begin{aligned} D_G &\triangleq \text{sum of all coefficients of} \\ &\quad \text{all coefficient matrices of } \mathbf{G}(z)\mathbf{G}^\dagger(1/z), \qquad (10.1.8) \\ E_G &\triangleq \text{sum of all magnitude squared coefficients} \\ &\quad \text{of all coefficient matrices of } \mathbf{G}(z), \qquad (10.1.9) \end{aligned}$$

where $\mathbf{G}^\dagger(z)$ means the conjugate transpose of all coefficient matrices of $\mathbf{G}(z)$. Then, by (10.1.1), it is not hard to see that

$$\mathrm{trace}(\mathcal{G}\mathcal{G}^\dagger) = LE_G, \quad \text{and} \quad \sum_{m,n}(\mathcal{G}\mathcal{G}^\dagger)_{mn} = LD_G. \qquad (10.1.10)$$

Therefore,

$$d_v^2 = 2\sigma_x^2 L(LNE_G - D_G). \qquad (10.1.11)$$

Based on formula (10.1.11) on the mean distance d_v of the PARMC output symbols, we define the distance for a PARMC as follows.

Definition 10.2 *For an (N, K) PARMC $\mathbf{G}(z)$, its* distance *is defined by*

$$d(G) \triangleq N - \frac{D_G}{E_G},$$

where D_G and E_G are defined in (10.1.8)-(10.1.9).

Based on Definitions 10.1 and 10.2 and (10.1.11), a PARMC is optimal if and only if its distance is maximal.

Let us see an example. Consider the PARMC $\mathbf{G}(z)$ in (8.2.7). It is not hard to see that $E_G = 2(N-1)$, and when $N > 2$,

$$\mathbf{G}(z)\mathbf{G}^\dagger(1/z)$$

$$= \begin{bmatrix} 1 & z^{r+1} & 0 & \cdots & 0 & 0 & 0 \\ z^{-r-1} & 2 & z^{r+1} & \cdots & 0 & 0 & 0 \\ 0 & z^{-r-1} & 2 & \cdots & 0 & 0 & 0 \\ \vdots & \vdots & \vdots & & \vdots & \vdots & \vdots \\ 0 & 0 & 0 & \cdots & z^{-r-1} & 2 & z^{r+1} \\ 0 & 0 & 0 & \cdots & 0 & z^{-r-1} & 1 \end{bmatrix}_{N \times N}.$$

Thus, when $N > 2$, $D_G = 4(N-1)$. Therefore, when $N > 2$,

$$d(G) = N - \frac{4(N-1)}{2(N-1)} = N - 2.$$

Since the PARMC output vector length L, the PARMC size N, and the input signal variance σ_x^2 are fixed, the following theorem is straightforward from (10.1.11).

Theorem 10.1 *An (N, K) PARMC $\mathbf{G}(z)$ is optimal if and only if the total sum D_G of all the coefficients of all the coefficient matrices of the product matrix $\mathbf{G}(z)\mathbf{G}^\dagger(1/z)$ is minimal when the total sum E_G of all the magnitude squared coefficients of all coefficient matrices of $\mathbf{G}(z)$ is fixed.*

We now want to find a family of column operations of a PARMC so that they do not change the distance property.

Corollary 10.1 *Let $\mathbf{U}(z)$ be a $K \times K$ paraunitary matrix with*

$$\mathbf{U}(z)\mathbf{U}^\dagger(1/z) = I_K.$$

If $\mathbf{G}(z)$ is an (N, K) PARMC with distance $d(G)$, then $\mathbf{G}(z)\mathbf{U}(z)$ is also a PARMC with distance $d(G)$, i.e., $d(GU) = d(G)$. If $\mathbf{G}(z)$ is an optimal $N \times K$ PARMC, then so is $\mathbf{G}(z)\mathbf{U}(z)$.

Proof. From (10.1.8), clearly $D_G = D_{GU}$. Since the sum of all magnitude squared coefficients of all coefficient matrices of $\mathbf{G}(z)$ is equal to the sum of all diagonal elements of the coefficient matrix of the constant term z^{-0} in the matrix $\mathbf{G}(z)\mathbf{G}^\dagger(1/z)$ and $\mathbf{G}(z)\mathbf{U}(z)\mathbf{U}^\dagger(1/z)\mathbf{G}^\dagger(1/z) = \mathbf{G}(z)\mathbf{G}^\dagger(1/z)$, we have $E_G = E_{GU}$. Thus, we have $d(G) = d(GU)$. ■

Notice that

$$\sigma_x^2 L D_G = \sigma_x^2 \sum_{m,n} (\mathcal{G}\mathcal{G}^\dagger)_{mn} = \sum_{m,n} \mathrm{E}(v(m)v^*(n)) = \mathrm{E}\left|\sum_n v(n)\right|^2 \geq 0. \tag{10.1.12}$$

Using (10.1.11), the following upper bound for the mean distance d_v is proved.

Theorem 10.2 *The mean distance d_v of the PARMC output symbols for an (N, K) PARMC $\mathbf{G}(z)$ is upper bounded by*

$$d_v \leq \sigma_x L\sqrt{2N}\sqrt{E_G}, \tag{10.1.13}$$

where σ_x^2 is the input signal variance, L is the length of the PARMC output vector sequence, and E_G is defined by (10.1.9), i.e., the total energy of all coefficients in $\mathbf{G}(z)$. The upper bound for the distance of an (N, K) PARMC $\mathbf{G}(z)$ is $d(G) \leq N$.

Now the question is: can the above upper bound be reached? Clearly the PARMC that reach the upper bound in (10.1.13) are the optimal. In the next section, we will answer this question positively. Notice that when there is no MC coding, i.e., $\mathbf{G}(z) = I_K$, we have

$$\mathrm{E}\left|\sum_n v(n)\right|^2 = \sum_n \mathrm{E}|v(n)|^2 = \sum_n \mathrm{E}|x(n)|^2 = LK\sigma_x^2 > 0,$$

the mean distance of the PARMC output values is

$$d_v = \left(\sum_{m,n} \mathrm{E}|v(m) - v(n)|^2\right)^{1/2} = \sigma_x\sqrt{2(LK-1)LK},$$

and the PARMC distance is $d(G) = K - 1$ in this case.

10.2 Optimal Systematic PARMC

In this section, we determine all optimal systematic PARMC by using the criterion proposed previously. We have the following result.

Theorem 10.3 *An $N \times (N-1)$ systematic PARMC $\mathbf{G}(z)$ in (9.1.2) with*

$$g_{Nk}(z) = \sum_{l=0}^{n_k} a_{kl} z^{-l},\ a_{kn_k} \neq 0,\ 1 \leq k \leq N-1,\ n_1 > n_2 > \cdots > n_{N-1} \geq 1, \tag{10.2.1}$$

is optimal if and only if

$$\sum_{l=0}^{n_k} a_{kl} = -1, \quad \textit{for } k = 1, 2, ..., N-1. \tag{10.2.2}$$

Moreover, for the above optimal PARMC, the mean distance d_v of the PARMC output symbols and the PARMC distance $d(G)$ are

$$d_v = \sigma_x L \sqrt{2N} \sqrt{E_F}, \quad \textit{and} \quad d(G) = N, \tag{10.2.3}$$

where σ_x^2 is the variance of the input signal, L is the length of the PARMC output vector sequence and

$$E_G = N - 1 + \sum_{k=1}^{N-1} \sum_{l=0}^{n_k} |a_{kl}|^2. \tag{10.2.4}$$

Proof. E_G in (10.2.4) is clearly the total sum of all the magnitude squared coefficients in all coefficient matrices of the PARMC $\mathbf{G}(z)$. To calculate D_G in (10.1.8) for $\mathbf{G}(z)$, the product matrix $\mathbf{G}(z)\mathbf{G}^\dagger(1/z)$ is

$$\mathbf{G}(z)\mathbf{G}^\dagger(1/z)$$

$$= \begin{bmatrix} 1 & 0 & \cdots & 0 & g_{N1}^*(1/z) \\ 0 & 1 & \cdots & 0 & g_{N2}^*(1/z) \\ \cdots & \cdots & \cdots & \cdots & \cdots \\ 0 & 0 & \cdots & 1 & g_{N,N-1}^*(1/z) \\ g_{N1}(z) & g_{N2}(z) & \cdots & g_{N,N-1}(z) & g_0(z) \end{bmatrix}_{N \times N},$$

where

$$g_{Nk}^*(1/z) = \sum_{l=0}^{N-1} a_{kl}^* z^l,$$

and

$$g_0(z) = \sum_{k=1}^{N-1} g_{Nk}(z) g_{Nk}^*(1/z) = \sum_{k=1}^{N-1} \sum_{l_1=0}^{n_k} \sum_{l_2=0}^{n_k} a_{kl_1} a_{kl_2}^* z^{-(l_1 - l_2)}.$$

Thus, it is not hard to see that

$$\begin{aligned} D_G &= N-1+\sum_{k=1}^{N-1}\sum_{l=0}^{n_k}(a_{kl}+a_{kl}^*)+\sum_{k=1}^{N-1}\sum_{l_1=0}^{n_k}\sum_{l_2=0}^{n_k}a_{kl_1}a_{kl_2}^* \\ &= \sum_{k=1}^{N-1}\left|\sum_{l=0}^{n_k}a_{kl}+1\right|^2. \end{aligned}$$

Therefore, the minimum of D_G over all $\mathbf{G}(z)$ in (10.2.1) is reached if and only if $D_G = 0$. In other words, D_G is minimal if and only if (10.2.2) holds, where E_G in (10.2.4) is fixed.

When $D_G = 0$, i.e., the PARMC $\mathbf{G}(z)$ is optimal, the optimal mean distance formula (10.2.3) for the PARMC $\mathbf{G}(z)$ follows from (10.1.11). ■

This theorem also implies that there exist PARMC that reach the upper bound (10.1.13), i.e., $D_G = 0$. By (10.1.12), the following corollary is straightforward.

Corollary 10.2 *The following statements are equivalent:*

(i) An $N \times K$ PARMC $\mathbf{G}(z)$ is optimal;

(ii) $D_G = 0$, i.e., the total sum of all coefficients of all coefficient matrices of $\mathbf{G}(z)\mathbf{G}^\dagger(1/z)$ is zero;

(iii) The distance of the PARMC $\mathbf{G}(z)$ is $d(G) = N$.

Given size N, the simplest optimal $N \times (N-1)$ systematic PARMC are

$$\begin{bmatrix} 1 & 0 & \cdots & 0 \\ 0 & 1 & \cdots & 0 \\ \cdots & \cdots & \cdots & \cdots \\ 0 & 0 & \cdots & 1 \\ -z^{-n_1} & -z^{-n_2} & \cdots & -z^{-n_{N-1}} \end{bmatrix}_{N\times(N-1)} \tag{10.2.5}$$

where $n_1 > n_2 > \cdots > n_{N-1} \geq 1$.

10.3 Numerical Examples

In this section, we want to present some examples to illustrate the theory obtained in the previous sections. Since all numerical simulations in this section are only used to prove the concepts of resisting additive channel random errors, some simplifications are made. These simplifications include

that an MIMO system identification algorithm has been implemented, i.e., there is only a nonsingular constant matrix ambiguity in the ISI channel.

We consider the undersampled communication system in Fig.8.4 with 5 antennas, and downsampling by factor 4. After an MIMO system identification algorithm is implemented, the ISI channel matrix becomes a 4×4 nonsingular constant matrix. Thus, we simply assume the ISI channel matrix as a 4×4 nonsingular constant matrix and then a white noise $\eta(n)$ is added to the ISI channel output, as shown in Fig.10.1(a). Notice that the 4×4 ISI channel constant matrix corresponds to 4 antenna array receivers, where each channel has 4 tap ISI by using the interpretation of the combination of the polyphase components [142], as shown in Fig.10.1(b).

We now consider the following five $(4,3)$ PARMC:

$$\mathbf{G}_1(z) = \begin{bmatrix} 1 & 0 & 0 \\ z^{-1} & 1 & 0 \\ 0 & z^{-1} & 1 \\ 0 & 0 & z^{-1} \end{bmatrix}, \quad \mathbf{G}_2(z) = \begin{bmatrix} 1 & 0 & 0 \\ 0 & 1 & 0 \\ 0 & 0 & 1 \\ z^{-3} & z^{-2} & z^{-1} \end{bmatrix},$$

$$\mathbf{G}_3(z) = \begin{bmatrix} 1 & 0 & 0 \\ 0 & 1 & 0 \\ 0 & 0 & 1 \\ \frac{1}{\sqrt{2}}(z^{-3}+z^{-2}) & \frac{1}{\sqrt{2}}(z^{-2}+z^{-1}) & \frac{1}{\sqrt{2}}(z^{-1}+1) \end{bmatrix},$$

$$\mathbf{G}_4(z) = \begin{bmatrix} 1 & 0 & 0 \\ 0 & 1 & 0 \\ 0 & 0 & 1 \\ -z^{-3} & -z^{-2} & -z^{-1} \end{bmatrix},$$

$$\mathbf{G}_5(z) = \begin{bmatrix} 1 & 0 & 0 \\ 0 & 1 & 0 \\ 0 & 0 & 1 \\ az^{-3}+bz^{-2} & cz^{-2}+dz^{-1} & -z^{-1} \end{bmatrix},$$

where

$$a = -\frac{\sqrt{3}+3}{4}, \quad b = \frac{\sqrt{3}-1}{4}, \quad c = -\frac{\sqrt{3}+1}{4}, \quad d = \frac{\sqrt{3}-3}{4}.$$

By Theorem 10.3, the PARMC $\mathbf{G}_4(z)$ and $\mathbf{G}_5(z)$ are optimal. All $E_{G_i} = 6$ for $i = 1, 2, ..., 5$ for all these PARMC. Their distances are

$$d(G_1) = d(G_2) = 4 - 2 = 2, d(G_4) = d(G_5) = 4$$

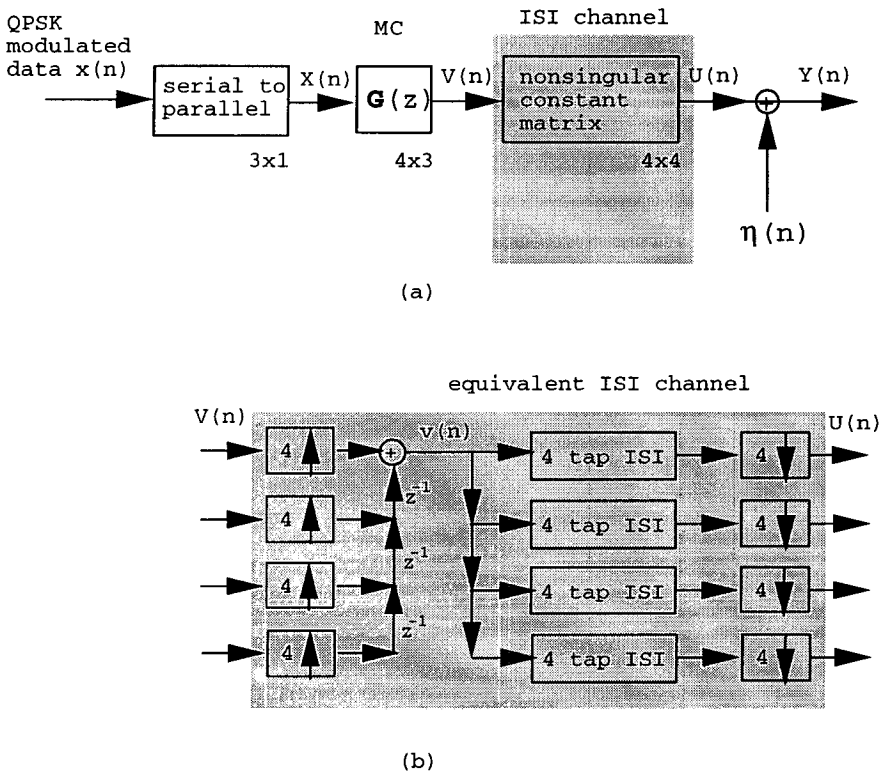

Figure 10.1: Simplified undersampled antenna receiver system.

and

$$d(G_3) = 4 - \frac{3(\sqrt{2}+1)^2}{6} = \frac{5-2\sqrt{2}}{2} \approx 1.0858.$$

QPSK signaling is used for the input signal of the PARMC. The *linear* closed-form equalization algorithm developed in Section 8.3.2 is used for the decoding. For more about closed-form blind equalization, see for example [90]. Three hundred Monte Carlo iterations are used. Fig.10.2 shows the QPSK symbol error rate comparison of these five PARMC via the SNR for the additive channel white noise. Clearly, the two optimal PARMC $\mathbf{G}_4(z)$ and $\mathbf{G}_5(z)$ outperform the other nonoptimal PARMC $\mathbf{G}_i(z)$ for $i = 1, 2, 3$. Since $d(G_1) = d(G_2)$, theoretically these two PARMC should have the same symbol error rate performance. From Fig.10.2, one can see that the performance difference between these two MCs is small. Notice that the

theory developed in Chapters 8, 9, and 10 holds for general modulation schemes as mentioned earlier.

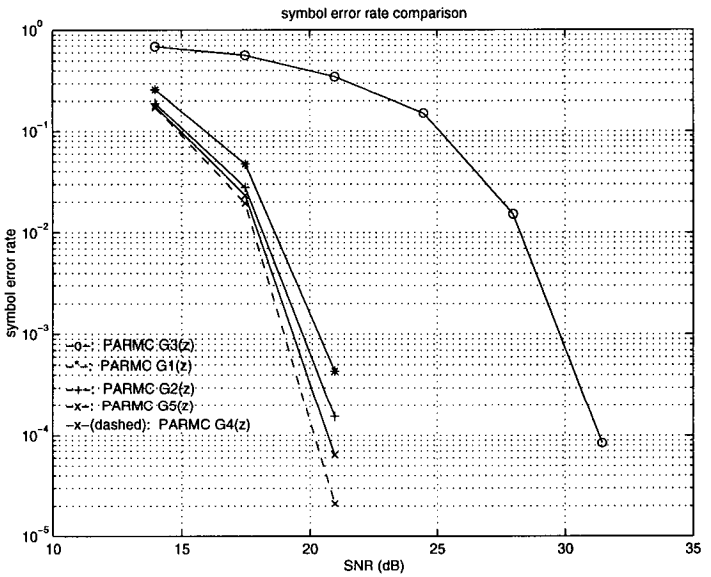

Figure 10.2: Symbol error rate comparison: Solid line with $*$ is for $\mathbf{G}_1(z)$; solid line with $+$ is for $\mathbf{G}_2(z)$; solid line with o is for $\mathbf{G}_3(z)$; dashed line with x is for $\mathbf{G}_4(z)$; solid line with x is for $\mathbf{G}_5(z)$.

Chapter 11

Conclusions and Some Open Problems

In this book, we introduced modulated codes (MC) for ISI channels. MC are convolutional codes defined over the complex field and can be naturally combined with an ISI channel and therefore can be optimally designed for a given ISI channel. We introduced several optimal MC design methods. An optimal design method usually depends on a decoding method at the receiver. There are two classes of such methods. One class of methods are the optimal MC design methods that depend on the input signal constellations, such as the joint MLSE design method using the joint MLSE decoding as in Chapter 2 and Chapter 3. The design complexity of this class of methods is usually high. However, the performance is optimal. The other class of methods are the optimal MC design methods that do not depend on any input signal constellations, such as the joint DFE design method using the joint DFE decoding at the receiver as in Chapter 4. The design complexity of this class of methods is usually low as we have seen in Chapter 4 but its performance is not as good as the ones when the signal constellation is considered.

In Chapter 2, we have shown that an MC does not provide any coding gain (i.e., advantage), in the AWGN channel over the uncoded system, however for any finite tap ISI channel there always exists an MC with coding gain compared to the uncoded AWGN channel. In Chapter 5, we have also shown that the MC coded ISI channel may have higher information rates than the original ISI channel does at low channel SNR, which implies that the achievable transmission data rates of the MC coded ISI channel may be higher than the ones of the original ISI channel. Our simulation results

have confirmed this theoretical result by employing the turbo coding before the binary-to-complex mapping. Surprisingly, by using a turbo code and a proper MC for an ISI channel, the performance may be above the capacity of the AWGN channel at low channel SNR.

Another advantage of the MC combined with an ISI channel is that it is possible to design channel independent MC such that the receiver is able to blindly identify the input signal. Such MC have been named polynomial ambiguity resistant MC (PARMC) and were studied in Chapters 8-10. We have shown that an MC to be a PARMC is necessary and sufficient for the blind identifiability. Surprisingly, we have shown that any block MC is not a PARMC. In other words, using a block MC at the transmitter, the receiver is not able to always recover an input signal, where the input signal constellation is not in the consideration. We have characterized PARMC in many cases and introduced an algebraic blind identification algorithm.

Using an optimally designed MC for a given ISI channel, both the transmitter and the receiver need to know the ISI channel. Using a PARMC, neither the transmitter nor the receiver needs to know the ISI channel. We have also introduced a channel independent MC coded OFDM system, where the MC encoding may be able to remove some of the spectral nulls and therefore improve the OFDM system performance for spectral null channels and wireless frequency-selective multipath fading channels. For the MC coded OFDM system, the receiver, however, needs to know the ISI channel in the decoding.

Since in the optimal MC design, the ISI channel information is needed, which is certainly possible when the ISI channel is known in priori, such as storage channels and some wireline channels. It is also expected, however, that the MC introduced in this book may be useful even in wireless channels since the simplicity of the MC encoding may be able to provide the convenience updating the MC at the transmitter and the receiver.

The results in this book are mainly summarized from our last few year's research work on MC. There are still many important open problems to be solved. We list a few of them as follows.

Open Problem 1: Fast optimal MC searching algorithm for a given ISI channel.

We have introduced an efficient searching algorithm of the optimal MC for a given ISI channel in Section 3.4. However, this algorithm is still slow for a reasonably long ISI channel or large-sized MC. The complexity comes from the large size of an error-pattern trellis due to the large size of the difference symbols of the input information symbols. It is very important to have a fast searching algorithm for the optimal MC in applications.

Open Problem 2: The higher rate MC existence with coding gain

compared to the uncoded AWGN channel.

Although it has been proved in Chapter 2 that for any finite tap ISI channel there exists an MC with coding gain compared to the uncoded AWGN channel, the rates of the MC in the proof are mainly either $1/\Gamma$ or $2/\Gamma$, where Γ is the ISI channel length. It will be interesting to prove that, for any rate r and any finite tap ISI channel there always exists a rate r MC with coding gain compared to the uncoded AWGN channel, which is conjectured true.

Open Problem 3: Sharper upper bounds of the coding gain of the MC in ISI channels.

In Section 2.4, we have shown that the coding gain of any MC in an ISI channel compared to the uncoded AWGN channel is upper bounded by the length of the ISI channel. This upper bound is sharpened for some special cases in Section 2.5. A general sharper upper bound of the coding gain or the proof of the tightness of the ISI channel length will be interesting.

Open Problem 4: Improved blind identification algorithm using a PARMC over the least square solution algorithm.

In Section 8.3.2, we introduced a least square solution algorithm for blindly identifying the input signal using a PARMC. This algorithm, however, may not perform well when the channel SNR is not high. Any improved blind identification algorithm is certainly interesting.

Appendix A

Some Fundamentals on Multirate Filterbank Theory

In this appendix, we want to briefly introduce some basic concepts and properties of multirate filterbank theory that was used as a precoding for an ISI channel in, for example, [165, 53, 89, 88, 171, 172, 77, 118]. For more details on multirate filterbank theory, we refer the reader to [32, 141, 2, 142, 46, 152, 126, 95, 13, 148, 106, 104, 26, 31, 99, 124, 125, 149, 150, 151, 140, 139, 38, 102, 146, 103, 73, 145, 143, 144, 96, 94, 87, 174, 173, 105]. References listed here are some early works on multirate filterbank theory for one dimensional signals and do not cover recent developments on the subject, such as multidimensional multirate filterbank theory and time-varying filterbank theory.

A.1 Some Basic Building Blocks

We first want to introduce some basic building blocks in multirate filterbank theory. Before going to the details, let us first introduce a notation for polynomial matrices. For a polynomial matrix $\mathbf{H}(z)$, its *tilde operation* $\tilde{\mathbf{H}}(z)$ denotes $\mathbf{H}^\dagger(1/z^*)$, i.e.,

$$\tilde{\mathbf{H}}(z) = \sum_n \mathbf{H}_n^\dagger z^n, \quad \text{if} \quad \mathbf{H}(z) = \sum_n \mathbf{H}_n z^{-n}.$$

A.1.1 Decimator and Expander

An M-fold decimator (or downsampling) and L-fold expander (or upsampling) are depicted in Fig.A.1(a) with an example in Fig.A.1(b), and Fig.A.1(c) with an example in Fig.A.1(d), respectively, where

$$y_D(n) = x(Mn),$$

and

$$y_E(n) = \begin{cases} x[n/L], & \text{if } n \text{ is a multiple of } L, \\ 0, & \text{otherwise.} \end{cases}$$

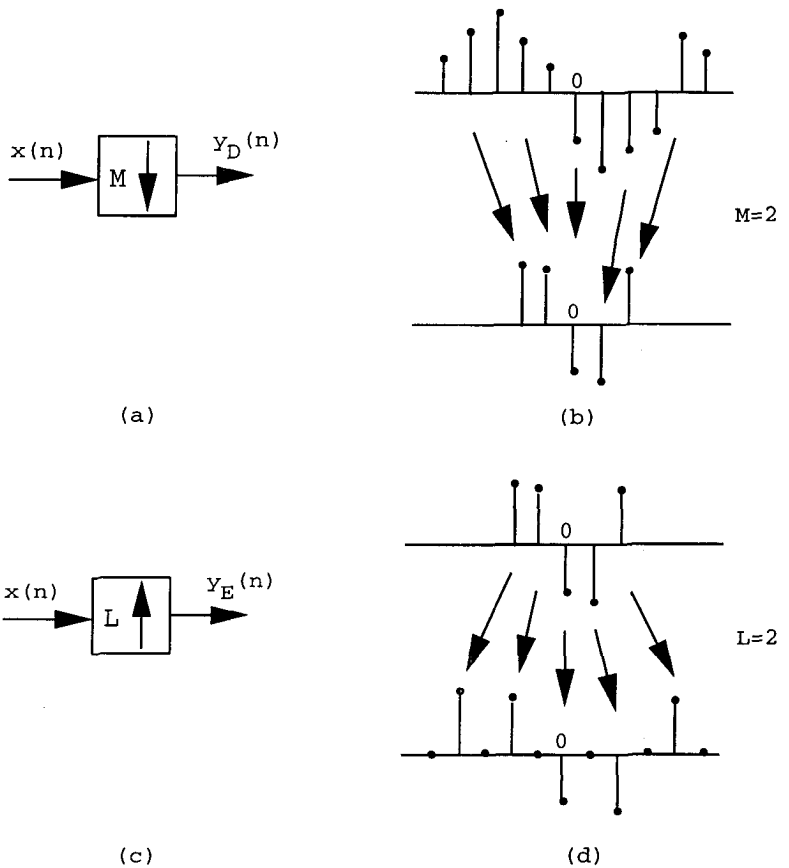

Figure A.1: Decimator and expander.

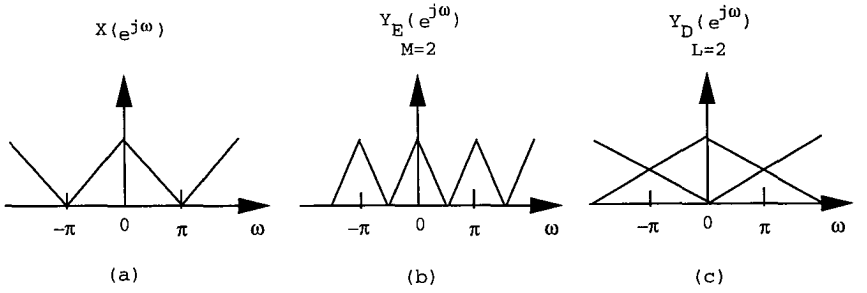

Figure A.2: The frequency domain representation examples of the decimator and expander.

In the frequency and z-transform domains, see for example [142],

$$Y_D(e^{j\omega}) = \sum_n y_D(n)e^{-j\omega n} = \frac{1}{M}\sum_{k=0}^{M-1} X(e^{j(\omega-2\pi k)/M}), \qquad \text{(A.1.1)}$$

and

$$Y_E(z) = \sum_n y_E(n)z^{-n} = X(z^L), \quad \text{and } Y_E(e^{j\omega}) = X(e^{j\omega L}).$$

The graphical meaning for the expander is that the DTFT of the expanded $y_E(n)$ is an L-fold compressed version of the uncompressed $X(e^{j\omega})$ shown in Fig.A.2(a),(b). The graphical meaning for the decimator is the following (shown in Fig.A.2(a),(c)):

(i) Stretch $X(e^{j\omega})$ by a factor M to obtain $X(e^{j\omega/M})$;

(ii) Create $M-1$ copies of this stretched version by shifting it uniformly in successive amounts of 2π;

(iii) Add all these shifted and stretched versions to the original unshifted and stretched version $X(e^{j\omega/M})$, and divide by M.

The $M-1$ shifted and stretched versions of $X(e^{j\omega})$ in (A.1.1) are the aliasing created by the downsampling.

A.1.2 Noble Identities

The following two Noble identities play important roles in the multirate filterbank theory. They tell us when the orders of the decimator/expander

and an LTI system can be switched. The two Noble identities are shown in Fig.A.3, where $y_1(n) = y_2(n)$ and $y_3(n) = y_4(n)$.

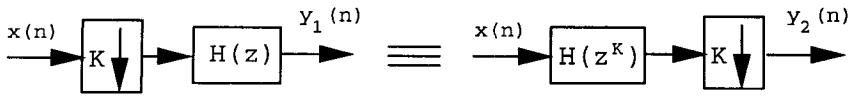

(a) Noble identity for decimator

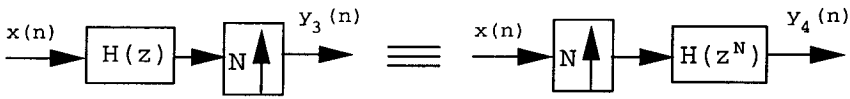

(b) Noble identity for expander

Figure A.3: The Noble identities.

A.1.3 Polyphase Representations

The polyphase representation was first invented by Bellanger et. al. [13] and Vary [148] and later recognized by Vaidyanathan and Vetterli in the simplifications of multirate filterbank theory studies. It can be briefly described as follows. For any given integer N, any filter $H(z)$ can be decomposed into

$$H(z) = \sum_{l=0}^{N-1} z^{-l} E_l(z^N), \tag{A.1.2}$$

where

$$E_l(z) = \sum_n h[Nn + l] z^{-n},$$

and $h[n]$ is the impulse response of $H(z)$. The decomposition (A.1.2) is called the *Type 1 polyphase representation* of $H(z)$. Meanwhile, $H(z)$ can also be decomposed into

$$H(z) = \sum_{l=0}^{N-1} z^{-N+1+l} R_l(z^N), \tag{A.1.3}$$

where $R_l(z) = E_{N-1-l}(z)$, which is called the *Type 2 polyphase representation* of $H(z)$. For $l = 0, 1, ..., N-1$, $E_l(z)$ and $R_l(z)$ are called the lth Type 1 and Type 2 *polyphase components* of $H(z)$, respectively. We will see later that the Type 1 polyphase representation is for the analysis bank and the Type 2 polyphase representation is for the synthesis bank in a multirate filterbank.

The main purpose for introducing the above polyphase representations is to move the decimator from the right side of an LTI filter to the left side (expander from the left side of an LTI filter to the right side) by using the Noble identities in Fig.A.3. In the Noble identities, the power of the variable z in an LTI filter needs to rise, which usually does not hold for an LTI filter but holds for the polyphase representations of an LTI filter as shown in (A.1.2)-(A.1.3).

A.2 M-Channel Multirate Filterbanks

A general M-channel multirate filterbank is depicted in Fig.A.4, where the left side is an analysis bank and the right side is a synthesis bank, each of which has M LTI filters. In many applications, such as frequency division multiple access (FDMA), these M LTI filters occupy M different frequency bands as shown in Fig.A.5.

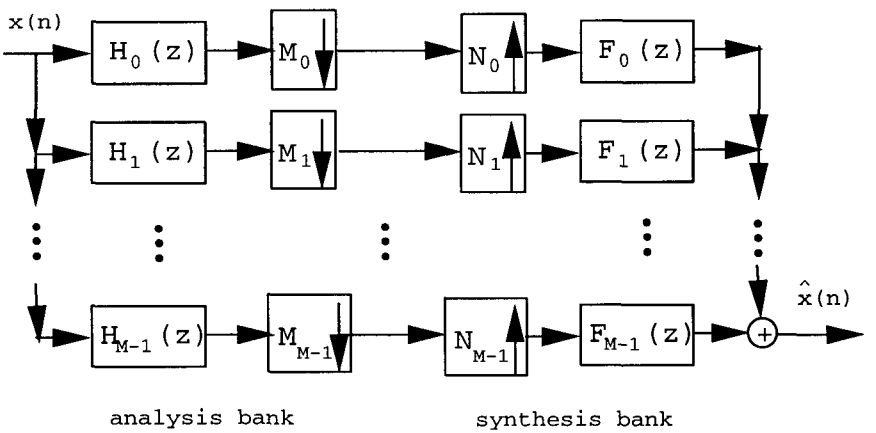

Figure A.4: A general M-channel multirate filterbank.

There are several cases for an M-channel multirate filterbank in Fig.A.4:

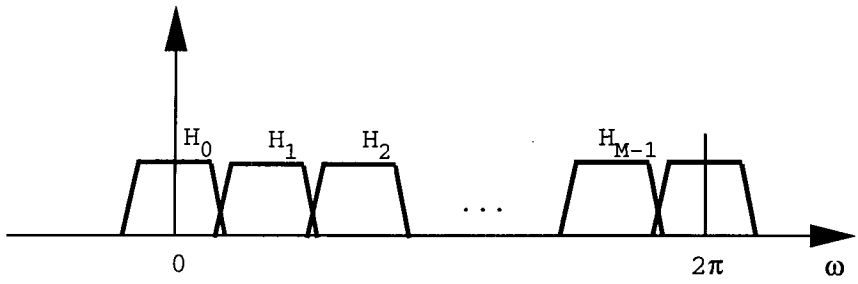

Figure A.5: M-channel analysis filter frequency response example.

(i) when $M_0 = M_1 = \cdots = M_{M-1} = N_0 = N_1 = \cdots = N_{M-1} = M$, the filterbank is called maximally decimated;

(ii) when $M_0 = M_1 = \cdots = M_{M-1} = N_0 = N_1 = \cdots = N_{M-1} < M$, the filterbank is called nonmaximally decimated;

(iii) when $M_0 = M_1 = \cdots = M_{M-1} = N_0 = N_1 = \cdots = N_{M-1} > M$, the filterbank is called over decimated;

(iv) when M_k and N_l are not all equal, the filterbank is called nonuniformally decimated.

In this section, we focus on the first case for convenience, i.e., maximally decimated multirate filterbanks.

A.2.1 Maximally Decimated Multirate Filterbanks: Perfect Reconstruction and Aliasing Component Matrix

An M-channel maximally decimated multirate filterbank is shown in Fig.A.6. A multirate filterbank in Fig.A.6 is called perfect reconstruction (PR) if and only if $\hat{x}(n) = cx(n - n_0)$ for a nonzero constant c and an integer n_0.

The question now becomes how to construct a PR multirate filterbank, in other words, what conditions on $H_m(z)$ and $F_m(z)$ are for the PR. Since in many applications, such as transmultiplexing and image analysis and coding, FIR filters are preferred, in what follows we are only interested in FIR filters $H_m(z)$ and $F_m(z)$ in Fig.A.6. In this case, the multirate filterbank is called FIR. Examples of 2-channel PR filterbanks were first obtained by Smith and Barnwell [124] and Mintzer [99], independently.

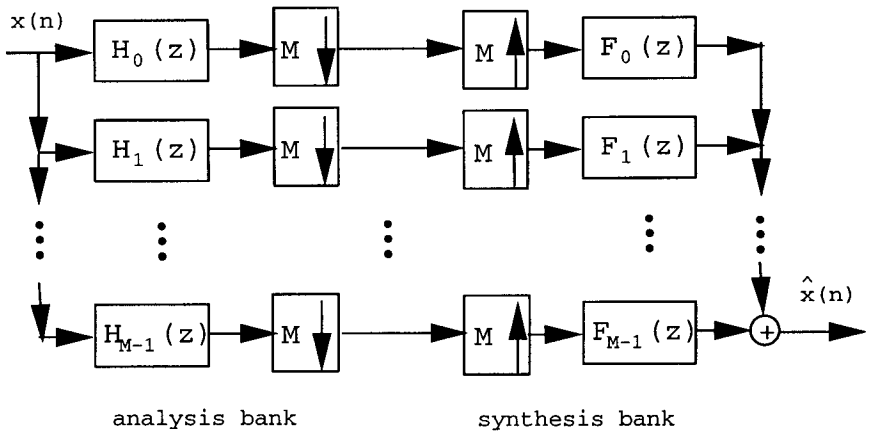

Figure A.6: M-channel maximally decimated multirate filterbank.

In the z-transform domain, the PR property becomes

$$\hat{X}(z) = cz^{-n_0}X(z). \tag{A.2.1}$$

In terms of an input signal $X(z)$, using (A.1.1) the output $\hat{X}(z)$ in Fig.A.6 can be formulated as follows:

$$\hat{X}(z) = A_0(z)X(z) + \sum_{l=1}^{M-1} A_l(z)X(zW_M^l), \tag{A.2.2}$$

where

$$A_l(z) = \frac{1}{M}\sum_{k=0}^{M-1} H_k(zW_M^l)F_k(z), \quad 0 \le l \le M-1. \tag{A.2.3}$$

Clearly, the second term in the right-hand side of (A.2.2) is the aliasing term. For the PR property (A.2.1), we need

$$A_0(z) = cz^{-n_0} \quad \text{and} \quad A_l(z) = 0 \quad \text{for } 1 \le l \le M-1. \tag{A.2.4}$$

We now want to simplify the PR condition (A.2.4). To do so, let

$$\mathbf{t}(z) = [cz^{-n_0}, 0, \cdots, 0]^T,$$

$$\mathbf{f}(z) = [F_0(z), F_1(z), \cdots, F_{M-1}(z)]^T,$$

and

$$\mathbf{H}(z) = \begin{bmatrix} H_0(z) & \cdots & H_{M-1}(z) \\ \vdots & \vdots & \vdots \\ H_0(zW_M^{M-1}) & \cdots & H_{M-1}(zW_M^{M-1}) \end{bmatrix}. \quad \text{(A.2.5)}$$

Then

$$\mathbf{H}(z)\mathbf{f}(z) = M\mathbf{t}(z). \quad \text{(A.2.6)}$$

Thus, given an analysis bank, $H_0(z), ..., H_{M-1}(z)$, if the matrix polynomial $\mathbf{H}(z)$ has an FIR inverse, then the synthesis bank $\mathbf{f}(z)$ can be solved from the equation (A.2.6). In other words, the multirate filterbank in Fig.A.6 with this synthesis is PR. The matrix polynomial $\mathbf{H}(z)$ in (A.2.5) is called the *aliasing component* (AC) matrix. In conclusion, we have the following theorem.

Theorem A.1 *An FIR multirate filterbank in Fig. 16 is perfect reconstruction if and only if its AC matrix* $\mathbf{H}(z)$ *has FIR inverse.*

One can see that the AC matrix $\mathbf{H}(z)$ is a structured matrix, where its components are not free but related. This limits the study and construction of PR multirate filterbanks. We next want to use the polyphase representations and Noble identities introduced in Section A.1.2 and convert the AC matrix to the polyphase matrix in which all components are free.

A.2.2 Maximally Decimated Multirate Filterbanks: Perfect Reconstruction and Polyphase Matrix

The analysis in Section A.2.1 is a direct analysis of the relationship between the input and the output in Fig.A.6. We next want to first simplify the block diagram in Fig.A.6 by using some properties of building blocks studied in Section A.1, such as Noble identities and polyphase representations, and then study the PR property for the simplified system. The main idea for the simplification is to switch the orders of decimator/expander and FIR filters, and then convert the multirate filterbank into a multi-input and multi-output (MIMO) system.

For each analysis filter $H_m(z)$ in Fig.A.6, let $E_{m,k}(z)$ be its kth Type 1 polyphase component, and for each synthesis filter $F_m(z)$ in Fig.A.6, let $R_{l,m}(z)$ be its lth Type 2 polyphase component, for $0 \leq m, k, l \leq M-1$. Let

$$\mathbf{E}(z) = (E_{m,k}(z))_{0\leq m,k\leq M-1}, \quad \text{and } \mathbf{R}(z) = (R_{l,m}(z))_{0\leq l,m\leq M-1},$$

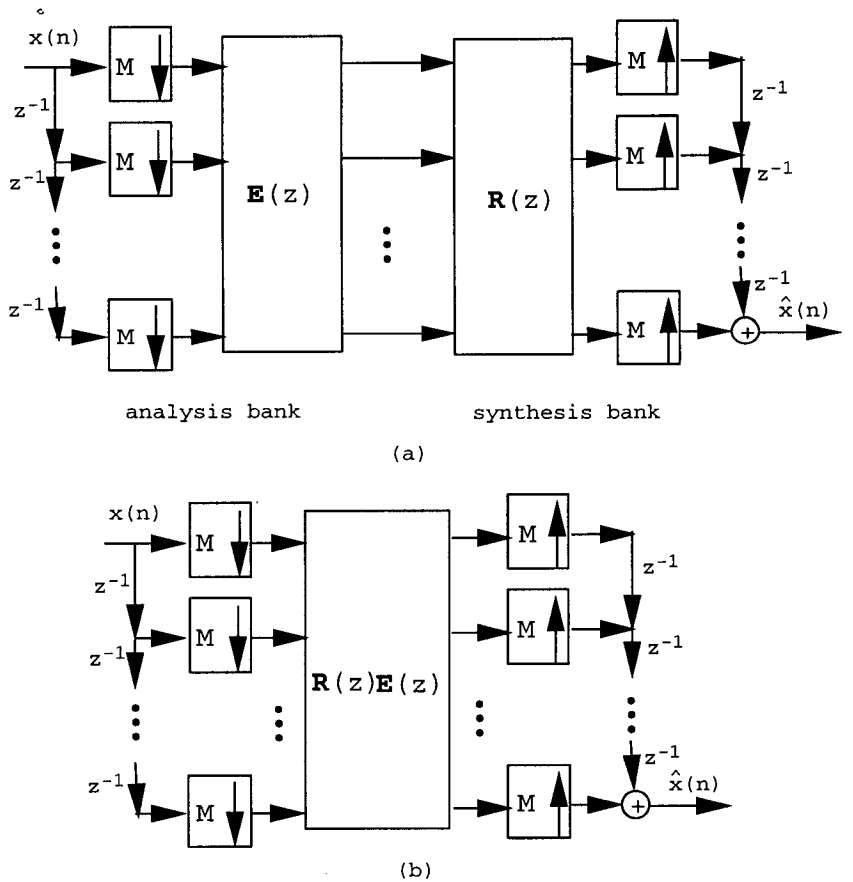

Figure A.7: Polyphase representation of M-channel maximally decimated multirate filterbank.

which are called the *polyphase matrices* of the analysis bank and the synthesis bank in Fig.A.6, respectively. Then it is not hard to see that

$$\mathbf{h}(z) = \mathbf{E}(z^M)\mathbf{e}(z) \quad \text{and } \mathbf{f}(z) = \tilde{\mathbf{e}}(z)\mathbf{R}(z^M), \tag{A.2.7}$$

where $\mathbf{h}(z) = (H_0(z), \cdots, H_{M-1}(z))^T$, $\mathbf{e}(z) = (1, z^{-1}, \cdots, z^{-M+1})^T$, $\mathbf{f}(z) = (F_0(z), \cdots, F_{M-1}(z))^T$, and $\tilde{\mathbf{e}}(z)$ is the tilde operation of $\mathbf{e}(z)$. Thus, by using the Noble identities, the multirate filterbank in Fig.A.6 is the same as the one shown in Fig.A.7(a), which is called the polyphase representation of the multirate filterbank in Fig.A.6.

Let $\mathbf{P}(z) = \mathbf{R}(z)\mathbf{E}(z)$, then the multirate filterbank in Fig.A.6 is equivalent to the MIMO system in Fig.A.7(b) with system transform matrix $\mathbf{P}(z)$. Clearly, the PR property is equivalent to the invertibility of the polyphase matrix $\mathbf{E}(z)$.

Theorem A.2 *An FIR multirate filterbank in Fig.A.6 is perfect reconstruction if and only if the polyphase matrix* $\mathbf{E}(z)$ *has FIR inverse.*

Theorem A.1 deals with the AC matrix $\mathbf{H}(z)$ while Theorem A.2 deals with the polyphase matrix $\mathbf{E}(z)$. From (A.2.7), it is not hard to see the following relationships between these two matrices:

$$\mathbf{H}(z) = \mathbf{W}_M^{\dagger}\mathbf{D}(z)\mathbf{E}^T(z^M) \quad \text{and } \mathbf{E}(z^M) = \mathbf{H}^T(z)\mathbf{W}_M\mathbf{D}(z^{-1}), \tag{A.2.8}$$

where $\mathbf{W}_N$ is the DFT matrix and $\mathbf{D}(z)$ is the diagonal matrix polynomial:

$$\mathbf{D}(z) = \text{diag}(1, z^{-1}, \cdots, z^{-M+1}).$$

From (A.2.8), it is clear that the FIR invertibilities of the AC matrix $\mathbf{H}(z)$ and the polyphase matrix $\mathbf{E}(z)$ are equivalent. Unlike matrix $\mathbf{H}(z)$, matrix $\mathbf{E}(z)$ does not have any relationship between its components, which leads to the systematic construction and factorization discussed later.

In some applications, such as the cross-talk cancellation in transmultiplexers [142], PR may not be necessary as long as the aliasing (cross-talk) is cancelled in a multirate filterbank, i.e., the second term at the right hand side of (A.2.2) is zero. A necessary and sufficient condition on such filterbanks was obtained by Vaidyanathan and Mitra [145], which is stated as follows. A square matrix polynomial $\mathbf{P}(z)$ is called *pseudo-circulant* if and only if it has the following form:

$$\mathbf{P}(z) = \begin{bmatrix} P_0(z) & P_{M-1}(z) & \cdots & P_1(z) \\ z^{-1}P_1(z) & P_0(z) & \cdots & z^{-1}P_2(z) \\ \vdots & \vdots & \vdots & \vdots \\ z^{-1}P_{M-2}(z) & z^{-1}P_{M-3}(z) & \cdots & P_{M-1}(z) \\ z^{-1}P_{M-1}(z) & z^{-1}P_{M-2}(z) & \cdots & P_0(z) \end{bmatrix}.$$

Notice that, when there are no z^{-1} in the above $\mathbf{P}(z)$, it is circulant.

Theorem A.3 *An M-channel multirate filterbank in Fig.A.6 is aliasing free if and only if the polyphase matrix $\mathbf{P}(z) = \mathbf{R}(z)\mathbf{E}(z)$ is pseudo-circulant. Under this condition, the filterbank output and the input are related by $\hat{X}(z) = \mathbf{A}_0(z)\mathbf{X}(z)$ as in (A.2.2), where*

$$\mathbf{A}_0(z) = z^{-M+1}(P_0(z^M) + z^{-1}P_1(z^M) + \cdots + z^{-M+1}P_{M-1}(z^M)).$$

A.3 Perfect Reconstruction FIR Multirate Filterbank Factorization and Construction

From the studies in Section A.2, PR FIR M-channel multirate filterbanks are converted to $M \times M$ matrix polynomials. In this section, we focus on $M \times M$ matrix polynomials $\mathbf{E}(z) = (E_{k,l}(z))_{0 \le k,l \le M-1}$. Without loss of generality, in what follows we only consider FIR and causal matrix polynomials, i.e.,

$$\mathbf{E}(z) = \sum_{n=0}^{L} \mathbf{E}_{k,l} z^{-n}, \quad L \text{ is a nonnegative integer.}$$

As studied in Section A.2, when the polyphase matrices of analysis banks have FIR inverses, the corresponding synthesis banks can be obtained by using the inverses for the PR multirate filterbanks, i.e., PR FIR multirate filterbanks are constructed. In this section, we first study general $\mathbf{E}(z)$ with FIR inverses and then study paraunitary matrix polynomials $\mathbf{E}(z)$ that are corresponding to paraunitary multirate filterbanks.

A.3.1 Factorization of FIR Polyphase Matrices with FIR Inverses

The goal of this subsection is to characterize all FIR causal $M \times M$ matrix polynomials with FIR inverses. Since the determinant of the FIR inverse of an $M \times M$ matrix polynomial is the inverse of its determinant, we have the following lemma.

Lemma A.1 *An FIR matrix polynomial has FIR inverse if and only if its determinant is cz^{-n_0} for a nonzero constant c and an integer n_0.*

Let $\mathbf{H}(z)$ be an FIR causal matrix polynomial with FIR inverse. If $\det(\mathbf{H}(z)) = cz^{-\rho}$, then ρ is called its *McMillan degree*, the minimal number of delay elements to implement the MIMO system [142]. A matrix polynomial $\mathbf{H}(z)$ is called *unimodular* if and only if its McMillan degree is 0, i.e., its determinant is a nonzero constant. To introduce the complete factorization of FIR matrix polynomials with FIR inverses, let us first introduce three types of elementary operations.

Three elementary row (column) operations:

Type 1: Interchange two rows (or columns).

Type 2: Multiply a row (or column) with a nonzero constant c.

Type 3: Add a polynomial multiple of a row (or column) to another row (or column).

The corresponding matrices of the above elementary operations are called elementary matrices, which have the following forms.

Let $\mathbf{e}_i$ be the M dimensional vector with its ith entry 1 and other entries 0 for $i = 1, 2, ..., M$, i.e.,

$$\mathbf{e}_i = (0 \quad \cdots \quad 0 \underset{i}{1} 0 \quad \cdots \quad 0)^T.$$

A Type 1 elementary matrix $\mathbf{A}$ can be written as

$$\mathbf{A} = \mathbf{I} + (\mathbf{e}_i - \mathbf{e}_j)(\mathbf{e}_j - \mathbf{e}_i)^\dagger,$$

for certain $i \neq j$ and $1 \leq i, j \leq M$.

A Type 2 elementary matrix $\mathbf{A}$ can be written as

$$\mathbf{A} = \mathbf{I} + c\mathbf{e}_i\mathbf{e}_i^\dagger,$$

for certain $c \neq -1$ and a certain i, $1 \leq i \leq M$.

A Type 3 elementary matrix $\mathbf{U}(z)$ can be written as

$$\mathbf{U}(z) = \mathbf{I} + \alpha(z)\mathbf{e}_i\mathbf{e}_j^\dagger,$$

where $\alpha(z)$ is a polynomial of z^{-1} and $i \neq j$ with $1 \leq i, j \leq M$.

With these three elementary operations/matrices, any $M \times N$ matrix polynomial can be diagonalized and the resulted decomposition is called the *Smith-McMillan decomposition*, which is stated as follows. An $M \times N$

matrix polynomial has the following Smith-McMillan decomposition (see, for example, [142]):

$$\mathbf{H}(z) = \mathbf{W}(z) \begin{bmatrix} \gamma_0(z) & 0 & \cdots & 0 & 0 & \cdots & 0 \\ 0 & \gamma_1(z) & \cdots & 0 & 0 & \cdots & 0 \\ \vdots & \vdots & \vdots & \vdots & \vdots & \vdots & \vdots \\ 0 & 0 & \cdots & \gamma_p(z) & 0 & \cdots & 0 \\ 0 & 0 & \cdots & 0 & 0 & \cdots & 0 \\ \vdots & \vdots & \vdots & \vdots & \vdots & \vdots & \vdots \\ 0 & 0 & \cdots & 0 & 0 & \cdots & 0 \end{bmatrix} \mathbf{U}(z), \quad \text{(A.3.1)}$$

where $\mathbf{W}(z)$ and $\mathbf{U}(z)$ are products of some elementary matrix polynomials with sizes $M \times M$ and $N \times N$, respectively, $\gamma_i(z)$ are polynomials of z^{-1}, $\gamma_i(z)$ divides $\gamma_{i+1}(z)$, for $i = 0, 1, ..., p-1$, i.e.,

$$\gamma_i(z) | \gamma_{i+1}(z), \ i = 0, 1, ..., p-1,$$

and

$$\gamma_i(z) = \frac{\Delta_{i+1}(z)}{\Delta_i(z)},$$

where $\Delta_0(z) = 1$, and $\Delta_i(z)$ for $i > 0$ is the greatest common divisor of all the $i \times i$ minors of $\mathbf{H}(z)$.

When $\mathbf{H}(z)$ is a square causal matrix polynomial with FIR inverse, the diagonal matrix in the Smith-McMillan decomposition has the form of

$$\text{diag}(c_1 z^{-n_1}, \cdots, c_M z^{-n_M})$$

where $n_m \geq 0$ and $c_m \neq 0$ for $1 \leq m \leq M$, and $0 \leq n_1 \leq \cdots \leq n_M$. Although this is a complete characterization of all square causal matrix polynomials with FIR inverses, the factorization in (A.3.1) is not convenient to be incorporated in the optimal design studied later. We next want to introduce another factorization. For more details, see [143, 144]. We define three kinds of basic matrices.

Class I.

$\mathcal{O} \triangleq \{\mathbf{V}(z) : \mathbf{V}(z) = \mathbf{I} - \mathbf{v}\mathbf{v}^\dagger + z^{-1}\mathbf{v}\mathbf{v}^\dagger$ where $\mathbf{v}$ is an $M \times 1$ constant vector with unit norm $\}$.

Let $\mathbf{V}(z) = \mathbf{I} - \mathbf{v}\mathbf{v}^\dagger + z^{-1}\mathbf{v}\mathbf{v}^\dagger \in \mathcal{O}$. Then its inverse $\mathbf{V}^{-1}(z) = \mathbf{I} - \mathbf{v}\mathbf{v}^\dagger + z\mathbf{v}\mathbf{v}^\dagger$.

Class II.

$\mathcal{U} \triangleq \{\mathbf{U}(z) : \mathbf{U}(z) = \mathbf{I} + \alpha z^{-m}\mathbf{e}_i\mathbf{e}_j^\dagger$ where α is a constant, m is a nonnegative integer and $i \neq j$ with $1 \leq i, j \leq M$ $\}$.

Let $\mathbf{U}(z) = \mathbf{I} + \alpha z^{-m}\mathbf{e}_i\mathbf{e}_j^\dagger \in \mathcal{U}$. Then, its inverse $\mathbf{U}^{-1}(z) = \mathbf{I} - \alpha z^{-m}\mathbf{e}_i\mathbf{e}_j^\dagger$.

Class III.

$\mathcal{A} \triangleq \{\mathbf{A} : \mathbf{A} = \mathbf{I} + (\mathbf{e}_i - \mathbf{e}_j)(\mathbf{e}_j - \mathbf{e}_i)^\dagger$ for certain $i \neq j$ and $1 \leq i, j \leq M$ or $\mathbf{A} = \mathbf{I} + c\mathbf{e}_i\mathbf{e}_i^\dagger$ for certain $c \neq -1$ and a certain i, $1 \leq i \leq M$ $\}$.

Let $\mathbf{A} = \mathbf{I} + (\mathbf{e}_i - \mathbf{e}_j)(\mathbf{e}_j - \mathbf{e}_i)^\dagger \in \mathcal{A}$. Then, its inverse $\mathbf{A}^{-1} = \mathbf{A}$. Let $\mathbf{A} = \mathbf{I} + c\mathbf{e}_i\mathbf{e}_i^\dagger \in \mathcal{A}$. Then, its inverse $\mathbf{A}^{-1} = \mathbf{I} - \frac{c}{c+1}\mathbf{e}_i\mathbf{e}_i^\dagger$.

With these three cases of matrices, we have the following complete factorization.

Theorem A.4 *A causal FIR $M \times M$ matrix polynomial $\mathbf{H}(z)$ has FIR inverse if and only if $\mathbf{H}(z)$ has the following form*

$$\mathbf{H}(z) = \mathbf{V}_\rho(z) \cdots \mathbf{V}_1(z)\mathbf{A}_\sigma\mathbf{U}_\sigma(z) \cdots \mathbf{A}_1\mathbf{U}_1(z), \tag{A.3.2}$$

where ρ is the McMillan degree of $\mathbf{H}(z)$, σ is a certain nonnegative integer, $\mathbf{V}_i(z) \in \mathcal{O}$ for $i = 1, 2, ..., \rho$, $\mathbf{A}_i \in \mathcal{A}$ and $\mathbf{U}_i(z) \in \mathcal{U}$ for $i = 1, 2, ..., \sigma$.

A.3.2 Factorization of Paraunitary FIR Matrix Polynomials

In this subsection, we introduce paraunitary matrix polynomials and corresponding multirate filterbanks, which are special FIR multirate filterbanks with FIR inverses.

An $M \times N$ matrix polynomial $\mathbf{H}(z)$ is called *paraunitary* if and only if

$$\tilde{\mathbf{H}}(z)\mathbf{H}(z) = d\mathbf{I}_N, \quad \text{for all complex values } z,$$

where d is a positive constant and $\mathbf{I}_N$ is the $N \times N$ identity matrix. When we restrict the complex value z on the unit circle, i.e., in the Fourier transform domain, it becomes the concept of lossless matrices. An $M \times N$ matrix polynomial $\mathbf{H}(z)$ is called *lossless* if and only if

$$\mathbf{H}^\dagger(e^{j\omega})\mathbf{H}(e^{j\omega}) = d\mathbf{I}_N, \quad \text{for all real values } \omega,$$

where d is a positive constant. When $\mathbf{H}(z)$ is FIR, "lossless" is equivalent to "paraunitary." When $\mathbf{H}(z)$ exists for all $z = e^{j\omega}$ but not all complex values z, "lossless" is not equivalent to "paraunitary," while "paraunitary" always implies "lossless." Since we are interested in FIR $\mathbf{H}(z)$, we only consider paraunitary matrix polynomials in this subsection. An example of paraunitary matrix polynomial is:

$$\mathbf{H}(z) = \begin{bmatrix} z^{-1}+1 & z^{-1}-1 \\ z^{-1}-1 & z^{-1}+1 \end{bmatrix}, \text{ in this case } \tilde{\mathbf{H}}(z) = \begin{bmatrix} z+1 & z-1 \\ z-1 & z+1 \end{bmatrix},$$

and

$$\tilde{\mathbf{H}}(z)\mathbf{H}(z) = 4\mathbf{I}_2.$$

A paraunitary multirate filterbank is shown in Fig.A.8.

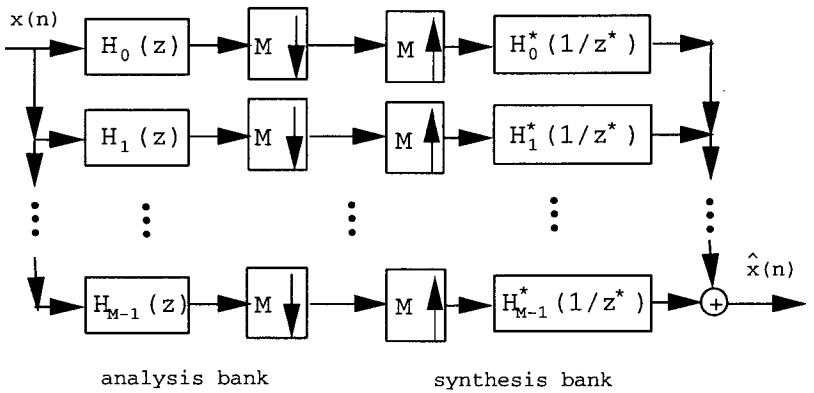

Figure A.8: Paraunitary M-channel maximally decimated multirate filterbank.

Similar to orthogonal transformations (matrices), the advantages of paraunitary multirate filterbanks include that they preserve signal energies in the decompositions (or transformations) and the synthesis banks (or inverse transformations) are simply the tilde operations of the analysis banks. In this sense, paraunitary multirate filterbanks are generalizations of orthogonal transformations, such as DFT, by adding delay variables (or memory) into the transformations. In the following, we want to present a complete characterization of all paraunitary matrix polynomials obtained by Vaidyanathan.

Theorem A.5 *(Vaidyanathan) An $M \times M$ causal FIR matrix polynomial $\mathbf{H}(z)$ is paraunitary if and only if it can be factorized as*

$$\mathbf{H}(z) = d\mathbf{V}_\rho(z)\cdots\mathbf{V}_1(z)\mathbf{H}_0, \tag{A.3.3}$$

where d is a positive constant, ρ is the McMillan degree of $\mathbf{H}(z)$, $\mathbf{H}_0$ is an $M \times M$ unitary constant matrix, $\mathbf{V}_i(z) \in \mathcal{O}$ for $i = 1, 2, ..., \rho$, and if $\rho = 0$ then $\mathbf{H}(z) = d\mathbf{H}_0$.

For a nonsquare paraunitary matrix polynomial, the following similar factorization holds (see [38, 142, 173] for more details).

Theorem A.6 *An $M \times N$ causal FIR matrix polynomial $\mathbf{H}(z)$ is paraunitary if and only if it can be factorized as*

$$\mathbf{H}(z) = d\mathbf{V}_\rho(z) \cdots \mathbf{V}_1(z)\mathbf{H}_0,$$

where d is a positive constant, $\mathbf{H}_0$ is an $M \times N$ unitary constant matrix, $\mathbf{V}_i(z) \in \mathcal{O}$ for $i = 1, 2, ..., \rho$, and if $\rho = 0$ then $\mathbf{H}(z) = d\mathbf{H}_0$.

For 2-channel paraunitary matrix polynomials, the above factorization is simplified as the following lattice representation, see [142].

Corollary A.1 *A 2×2 causal FIR matrix polynomial $\mathbf{H}(z)$ is paraunitary if and only if it can be factorized as*

$$\mathbf{H}(z) = d\mathbf{R}_\rho \Lambda(z) \cdots \mathbf{R}_1 \Lambda(z) \mathbf{R}_0 \begin{bmatrix} 1 & 0 \\ 0 & \pm 1 \end{bmatrix},$$

where d is a positive constant, ρ is the McMillan degree of $\mathbf{H}(z)$, and

$$\mathbf{R}_i = \begin{bmatrix} \cos\theta_i & \sin\theta_i \\ -\sin\theta_i & \cos\theta_i \end{bmatrix}, \quad \textit{and} \quad \Lambda(z) = \begin{bmatrix} 1 & 0 \\ 0 & z^{-1} \end{bmatrix},$$

and θ_i is an angle for $i = 0, 1, 2, ..., \rho$.

A lattice realization of a 2-channel paraunitary analysis bank is shown in Fig.A.9, where $\alpha = \sqrt{d}$, $c_i = \cos\theta_i$ and $s_i = \sin\theta_i$ for $i = 0, 1, ..., \rho$, where ρ delays are needed.

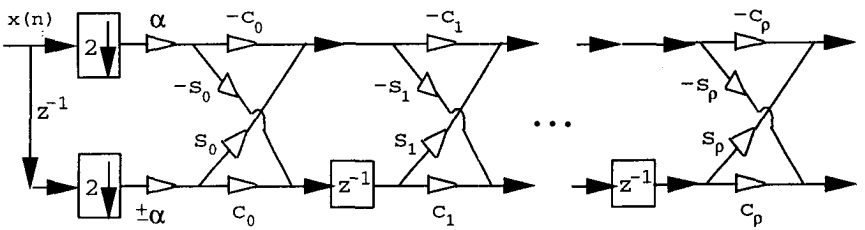

Figure A.9: Lattice realization of 2-channel paraunitary analysis bank.

A.3.3 Perfect Reconstruction Multirate Filterbank Design

After the complete characterizations of PR multirate filterbanks, the next important issue is the design of a desired PR multirate filterbank. In this

subsection, we want to briefly describe a method for the design. The goal here is to design an M-channel PR multirate filterbank such that all analysis filters have good filter properties, i.e., with good passband and stopband attenuation properties. What one can do is to use the factorizations (A.3.2) and (A.3.3) to parameterize these analysis filters and then formulate the minimization problem for the parameters:

$$\min \sum_{m=0}^{M-1} \int_{m\text{th stopband}} |H_m(e^{j\omega})|^2 d\omega. \tag{A.3.4}$$

For design examples, see [142, 126].

A.4 DFT and Cosine Modulated Filterbanks

In Section A.3, we have studied general M-channel maximally decimated multirate filterbanks, where the Fourier spectra of M analysis filters may not necessarily have the same shape. In many applications, such as FDMA communication systems, it is however quite often that all M analysis filters are derived from a single prototype filter and therefore have the same shape of their Fourier spectra. The advantage of such systems is the implementation simplicity. In this section, we introduce two kinds of such filterbanks. One is the discrete Fourier transform (DFT) filterbank, where analysis filters are single-sided shifts of a prototype filter in the frequency domain (or exponential modulation). The other is the cosine modulated filterbank, where analysis filters are double-sided shifts of a prototype filter.

A.4.1 DFT Filterbanks

DFT filterbanks form a class of the simplest multirate filterbanks, where all analysis filters are shifted from a single prototype filter in the frequency domain. The question then becomes when DFT filterbanks are PR. To study this question, let us formulate the analysis filters. Let

$$P(z) = \sum_{n=0}^{L-1} p(n) z^{-n},$$

be an FIR filter with length L, which is usually a good lowpass filter. The M analysis filters are

$$H_m(z) = P(zW_M^m) = \sum_{n=0}^{L-1} p(n) W_M^{-mn} z^{-n}, \quad 0 \le m \le M-1, \tag{A.4.1}$$

where their Fourier spectra are illustrated in Fig.A.5. Notice that M analysis filter coefficients $h_m(n) = W_M^{-mn}p(n)$ are no longer real even when the prototype filter coefficients $p(n)$ are real.

Let $P_l(z)$, $0 \leq l \leq M-1$, be the Type 1 polyphase components of the prototype filter $P(z)$ with total M components. Then it is not hard to see that the polyphase matrix of the analysis bank $H_m(z)$, $0 \leq m \leq M-1$, in (A.4.1) is

$$\mathbf{E}(z) = \mathbf{W}_M^{\dagger}\text{diag}(P_0(z), P_1(z), \cdots, P_{M-1}(z)),$$

which is shown in Fig.A.10 with $\mathbf{P}(z)$ =diag$(P_0(z), P_1(z), \cdots, P_{M-1}(z))$.

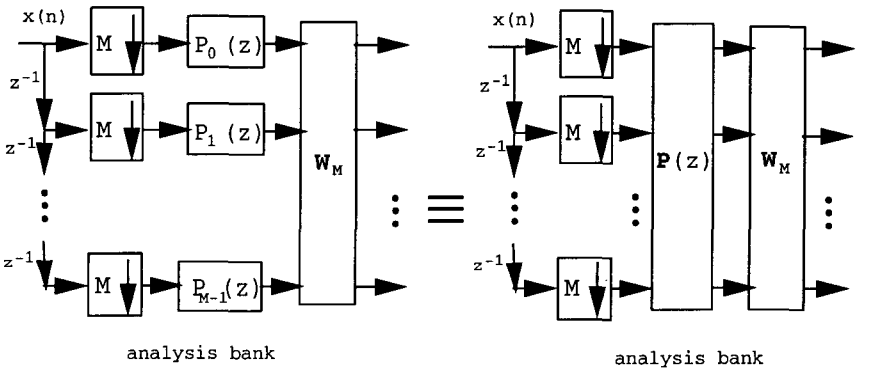

Figure A.10: DFT analysis bank.

By the study in Section A.2, it is clear that the DFT filterbanks are PR *if and only if*

$$P_m(z) = c_m z^{-n_m}, \quad c_m \neq 0, \ 0 \leq m \leq M-1, \quad \text{for some integer } n_m$$

or

$$P(z) = \sum_{m=0}^{M-1} c_m z^{-Mn_m - m}, \quad c_m \neq 0. \tag{A.4.2}$$

The paraunitariness of the above DFT filterbank forces $|c_m| = c \neq 0$ for all $0 \leq m \leq M-1$, which is basically equivalent to the DFT. When $P_m(z) = 1/\sqrt{M}$ for $0 \leq m \leq M-1$, the DFT filterbank is precisely reduced to the DFT as shown in Fig.A.11, which is the reason for the name of the DFT filterbanks.

One can see that the condition on the prototype filter $P(z)$ in (A.4.2) for the PR property is very restrictive and usually limits their applications.

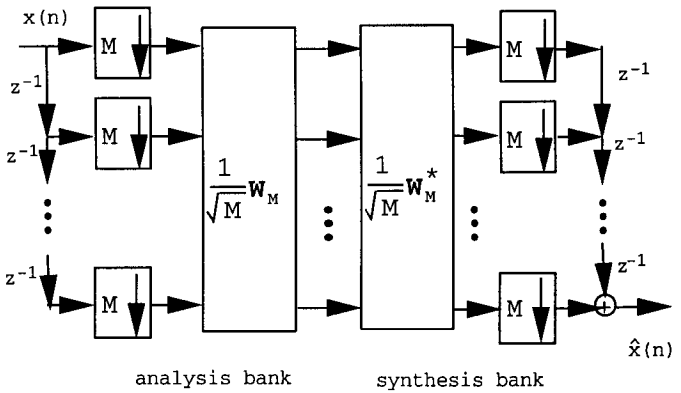

Figure A.11: DFT (analysis bank) and IDFT (synthesis bank).

There are three ways to get around this condition. The first one, which is also the most intuitive, is to design $P(z)$ with excellent lowpass property. Then the DFT filterbank is almost PR because the whole frequency band is almost divided with a wall-cut manner by M analysis filters. The second way is to use nonmaximally decimated DFT filterbanks, i.e., the decimation factor is less than the number of channels (or users), which corresponds to oversampled short-time Fourier transforms or discrete Gabor transforms, see for example, [106, 156, 109]. The third way is to use double-sided shifts instead of the single-sided shifts as in (A.4.2), which leads to cosine modulated filterbanks as we shall see in the next subsection.

A.4.2 Cosine Modulated Filterbanks

The DFT filterbanks in Section A.4.1 have two disadvantages. One is that analysis filter coefficients are complex-valued and the other is that the PR condition is too restrictive. We now want to use double-sided shifts or cosine modulations to construct M analysis filters with real coefficients and better filter properties in PR multirate banks.

Let $P(z)$ be a prototype filter with length L as before. Let

$$U_m(z) = P(zW_{2M}^{m+0.5}) \quad \text{and} \quad V_m(z) = P(zW_{2M}^{-(m+0.5)}), \quad 0 \le m \le M-1,$$

and for $0 \le m \le M-1$,

$$H_m(z) = a_m U_m(z) + a_m^* V_m(z) = \sum_{n=0}^{L-1} 2\ \text{real}(a_m W_{2M}^{-(m+0,5)n}) p(n) z^{-n}.$$

This tells us that the analysis filter coefficients are all real. Furthermore, let

$$a_m = W_{2M}^{(m+0.5)(L-1)/2+(-1)^m\pi/4}.$$

Then the analysis filter coefficients are

$$h_m(n) = 2\cos\left[\frac{\pi}{M}(m+0.5)(n-\frac{L-1}{2}) + (-1)^m\frac{\pi}{4}\right]p(n). \qquad \text{(A.4.3)}$$

The corresponding synthesis filter coefficients are

$$f_m(n) = 2\cos\left[\frac{\pi}{M}(m+0.5)(n-\frac{L-1}{2}) - (-1)^m\frac{\pi}{4}\right]p(n). \qquad \text{(A.4.4)}$$

From these filters, one can see why they are called cosine modulated filterbanks. We now present a necessary and sufficient condition for the PR property, which was obtained in [73]. For details, see [142].

Theorem A.7 *Let $P_l(z)$, $0 \le l \le 2M-1$, be the Type 1 polyphase components of a prototype filter $P(z)$ of length L with $2M$ total components. If $L = 2KM+1$ for some positive integer K and M analysis filters and synthesis filters are defined in (A.4.3) and (A.4.4), respectively, then the cosine modulated filterbank is paraunitary if and only if*

$$\tilde{P}_m(z)P_m(z) + \tilde{P}_{m+M}(z)P_{m+M}(z) = \alpha, \quad 0 \le m \le M-1, \qquad \text{(A.4.5)}$$

for a constant $\alpha > 0$.

This theorem suggests the following method to construct paraunitary cosine modulated filterbanks. Define

$$\mathbf{Q}_m(z) = \begin{bmatrix} P_m(z) \\ P_{m+M}(z) \end{bmatrix}, \quad m = 0, 1, 2, ..., M-1,$$

then condition (A.4.5) is equivalent to

$$\tilde{\mathbf{Q}}_m(z)\mathbf{Q}_m(z) = \alpha, \quad m = 0, 1, 2, ..., M-1,$$

i.e., all $\mathbf{Q}_m(z)$ are 2×1 paraunitary matrix polynomials. They have been completely characterized in Section A.3.2 and the factorization in Theorem A.6 can be used to construct optimal cosine modulated filterbanks similar to those studied in Section A.3.3. For design examples, see [142].

Bibliography

[1] K. Abed-Meraim, W. Qiu, and Y. Hua. Blind system identification. *Proceedings of the IEEE*, 85:1310–1322, Aug. 1997.

[2] A. Akansu and R. Haddad. *Multiresolution Signal Decomposition: Transforms, Subbands, and Wavelets.* Academic Press Inc., New York, 1992.

[3] A. N. Akansu, O. Duhamel, X. Lin, and M. de Courville. Orthogonal transmultiplexers in communications: A review. *IEEE Trans. Signal Processing*, 46:979–995, April 1998.

[4] N. Al-Dhahir and J. M. Cioffi. MMSE-decision-feedback equalizers: Finite-length results. *IEEE Trans. on Information Theory*, 41(4):961–975, July 1995.

[5] N. Al-Dhahir and J. M. Cioffi. Block transmission over dispersive channels: Transmit filter optimization and realization, and MMSE-DFE receiver performance. *IEEE Trans. on Information Theory*, 42(1):137–160, Jan. 1996.

[6] N. Al-Dhahir and J. M. Cioffi. Efficient computation of the delay-optimized finite length MMSE-DFE. *IEEE Trans. on Signal Processing*, 44:1288–1292, May 1996.

[7] S. L. Ariyavisitakul and Y. Li. Joint coding and decision feedback equalization for broadband wireless channels. *IEEE J. Select. Areas in Commun.*, 16:1670–1678, Dec. 1998.

[8] S. L. Ariyavisitakul, J. Winters, and I. Lee. Optimum space-time processors with dispersive interference-unified analysis and required filter span. In *Proc. of ICC'99*, Vancouver, Canada, June 6-10 1999.

[9] T. Aulin and C. E. Sundberg. On the minimum Euclidean distance for a class of signal space codes. *IEEE Trans. on Information Theory*, 28:43–55, 1982.

[10] M. E. Austin. Decision-feedback equalization for digital communication over dispersive channels. Technical Report 437, MIT Lincoln Lab., Lexington, MA, Aug. 1967.

[11] K. Balachandran and J. B. Anderson. Mismatched decoding of intersymbol interference using a parallel concatenated scheme. *IEEE J. Select. Areas in Commun.*, 16:255–259, Feb. 1998.

[12] C. A. Belfiore and J. H. Park. Decision feedback equalization. *Proceedings of the IEEE*, 67:1143–1156, Aug. 1979.

[13] M. Bellanger, G. Bonnerot, and M. Coudreuse. Digital filtering by polyphase network: application to sample rate alteration and filter banks. *IEEE Trans. Acoust. Speech Signal Process.*, 24:109–114, 1976.

[14] S. Benedetto, D. Divsalar, G. Montorsi, G. Pollara, and F. Pollara. A soft-input soft-output APP module for iterative decoding of concatenated codes. *IEEE Comm. Letters*, 1:22–24, Jan. 1997.

[15] S. Benedetto and G. Montorsi. Unveiling turbo codes: Some results on parallel concatenated coding schemes. *IEEE Trans. Inform. Theory*, 42:409–429, May 1996.

[16] C. Berrou and A. Glavieux. Near optimum error correcting coding and decoding: Turbo-codes. *IEEE Trans. on Communications*, 44(10):1261–1271, Oct. 1996.

[17] E. Biglieri, D. Divsalar, P. J. McLane, and M. K. Simon. *Introduction to Trellis-Coded Modulation with Applications.* Macmillan Publishing Company, New York, 1991.

[18] J. A. C. Bingham. Multicarrier modulation for data transmission: An idea whose time has come. *IEEE Commun. Mag.*, 28:4–14, May 1990.

[19] R. S. Blum. Analytical tools for the design of space-time convolutional codes. 2000.

[20] D. M. Brady. An adaptive coherent diversity receiver for data transmission through dispersive media. In *Proc. of ICC'70*, pages 21.35–21.40, San Francisco, CA, June 1970.

[21] L. H. Brandenburg and A. D. Wyner. Capacity of the Gaussian channel with memory: The multivariate case. *Bell System Technical Journal*, 53:745–778, May-June 1974.

[22] A. R. Calderbank, C. Heegard, and T. A. Lee. Binary convolutional codes with application to magnetic recording. *IEEE Trans. on Information Theory*, 32, Nov. 1986.

[23] P. R. Chevillat and E. Eleftheriou. Decoding of trellis-encoded signals in the presence of intersymbol interference and noise. *IEEE Trans. on Communications*, 37:669–676, July 1989.

[24] J. Chow, J. M. Cioffi, and J. Bingham. A discrete multitone transceiver system for HDSL applications. *IEEE J. Select. Areas Commun.*, 9:895–908, Aug. 1991.

[25] P. S. Chow, J. C. Tu, and J. M. Cioffi. Performance evaluation of a multichannel transceiver system for ADSL and VHDSL services. *IEEE J. Select. Areas Commun.*, 9:909–919, Aug. 1991.

[26] P. L. Chu. Quadrature mirror filter design for an arbitrary number of equal bandwidth channels. *IEEE Trans. Acoust. Speech Signal Process.*, 33:203–218, 1985.

[27] L. J. Cimini. Analysis and simulation of digital mobile channel using orthogonal frequency division multiple access. *IEEE Trans. Commun.*, pages 665–675, July 1985.

[28] J. M. Cioffi, G. P. Dudevoir, M. V. Eyuboglu, and G. D. Forney (Jr). MMSE decision-feedback equalizers and coding II: Coding results. *IEEE Trans. on Commun.*, 43:2595–2604, Oct. 1995.

[29] J. M. Cioffi, G. P. Dudevoir, M. V. Eyuboglu, and G. D. Forney (Jr). MMSE decision-feedback equalizers and coding I: Equalization results. *IEEE Trans. on Commun.*, 43:2582–2594, Oct. 1995.

[30] J. M. Cioffi and G. D. Forney (Jr). Generalized decision-feedback equalization for packet transmission with ISI and Gaussian noise. In *Communications, Computation, Control and Signal Processing*, pages 79–127, Boston, 1997. Kluwer Academic Publishers, Boston. Chapter 4, A. Paulraj, V. Roychowdhury, and C. D. Schaper Eds.

[31] R. V. Cox. The design of uniformly and nonuniformly spaced pseudo QMF. *IEEE Trans. Acoust. Speech Signal Process.*, 34:1090–1096, 1986.

[32] R. E. Crochiere and L. R. Rabiner. *Multirate Digital Signal Processing.* Prentice-Hall, Englewood Cliffs, NJ, 1983.

[33] Z. Ding, C. R. Johnson (Jr.), and R. A. Kennedy. On the (non)existence of undesirable equilibria of Godard blind equalizers. *IEEE Trans. on Signal Processing*, 40:2425–2432, 1992.

[34] Z. Ding, R. A. Kennedy, B. D. O. Anderson, and C. R. Johnson (Jr.). Ill-convergence of Godard blind equalizers in data communication systems. *IEEE Trans. on Communications*, 39:1313–1327, 1991.

[35] Z. Ding and Y. Li. On channel identification based on second-order cyclic spectra. *IEEE Trans. on Signal Processing*, 42:1260–1264, May 1994.

[36] Z. Ding and Y. Li. *Blind Equalization and Identification.* Marcel Dekker, Inc., 2000.

[37] D. Divsalar and F. Pollara. Turbo codes for PCS applications. In *Int. Conf. Communications*, pages 54–59, Seattle, WA, June 1995.

[38] Z. Doğanata, P. P. Vaidyanathan, and T. Q. Nguyen. General synthesis procedures for FIR lossless transfer matrices. *IEEE Trans. Acoust. Speech Signal Process.*, 36:1561–1574, 1988.

[39] C. Douillard, M. Jézéquel, and C. Berrou. Iterative correction of intersymbol interference: Turbo-equalization. *European Trans. Telecommun.*, 6(5):507–511, Sept./Oct. 1995.

[40] A. Duel-Hallen and C. Heegard. Delayed decision-feedback sequence estimation. *IEEE Trans. on Communications*, 37:428–436, May 1989.

[41] M. V. Eyuboglu and G. D. Forney (Jr.). Trellis precoding : Combined coding, precoding and shaping for intersymbol interference channel. *IEEE Trans. Inform. Theory*, 38:301–314, Mar. 1992.

[42] M. V. Eyuboglu and S. U. H. Qureshi. Reduced-state sequence estimation with set partitioning and decision feedback. *IEEE Trans. on Communications*, 36:13–20, Jan. 1988.

[43] D. D. Falconer and G. J. Foschini. Theory of minimum mean-squared-error QAM systems employing decision feedback equalization. *Bell Syst. Tech. J.*, 52:1821–1849, Dec. 1973.

[44] P. Fan and X.-G. Xia. Some new results on coding gain of modulated codes over ISI channels. Technical Report 98-6-2, Department of Electrical and Computer Engineering, University of Delaware, Newark, Delaware, June 1998.

[45] P. Fan and X.-G. Xia. Capacity and information rates of the discrete-time Gaussian channel with intersymbol interference and modulated code encoding. Technical Report 98-5-1, Department of Electrical and Computer Engineering, University of Delaware, Newark, Delaware, May 1999.

[46] N. J. Fliege. *Multirate Digital Signal Processing.* John Wiley & Sons, New York, 1994.

[47] B. L. Floch, M. Alard, and C. Berrou. Coded orthogonal frequency division multiplex. *Proc. of the IEEE*, 83:982–996, June 1995.

[48] S. A. Fredricsson. Optimum transmitting filter in digital PAM systems with a Viterbi decoder. *IEEE Trans. on Information Theory*, 20:479–489, July 1974.

[49] J. Garcia-Frias. *Combined hidden Markov models and turbo codes.* Ph.D. Dissertation, Dept. of Electrical Engineering, UCLA, Los Angeles, California, 1999.

[50] J. Garcia-Frias and J. D. Villasenor. Combining hidden Markov source models and parallel concatenated codes. *IEEE Comm. Letters*, pages 111–113, July 1997.

[51] J. Garcia-Frias and J. D. Villasenor. Combined blind equalization and turbo decoding. In *Proc. Internal. Conf. Comm.*, Vancouver, Canada, June 6-10 1999.

[52] W. A. Gardner. A new method of channel identification. *IEEE Trans. on Communications*, 39:813–817, 1991.

[53] G. B. Giannakis. Filterbanks for blind channel identification and equalization. *IEEE Signal Processing Letters*, 4:184–187, June 1997.

[54] R. D. Gitlin and S. B. Weinstein. Fractionally-spaced equalizations: An improved digital transversal equalizer. *Bell System. Tech. J.*, 60:275–296, Feb. 1981.

[55] D. N. Godard. Self-recoving equalization and carrier tracking in two-dimensional data communication systems. *IEEE Trans. on Communications*, 28, Nov. 1980.

[56] G. H. Golub and C. F. V. Loan. *Matrix Computations.* Johns Hopkins University Press, Baltimore, 1983.

[57] H. Harashima and H. Miyakawa. Matched-transmission technique for channels with intersymbol interference. *IEEE Trans. Commun.*, 30:774–780, Aug. 1972.

[58] D. Hatzinakos and C. L. Nikias. Estimation of multipath channel response in frequency selective channels. *IEEE J. Select. Areas Communications*, 7:12–19, Jan. 1989.

[59] W. Hirt and J. L. Massey. Capacity of the discrete-time Gaussian channel with intersymbol interference. *IEEE Trans. Inform. Theory*, 34:380–388, May 1988.

[60] B. M. Hochwald and T. L. Marzetta. Unitary space-time modulation for multiple-antenna communications in Rayleigh flat fading. *IEEE Trans. on Information Theory*, 1998. Submitted.

[61] B. M. Hochwald, T. L. Marzetta, T. L. Richardson, W. Sweldens, and R. Urbanke. Systematic design of unitary space-time constellation. *IEEE Trans. on Information Theory*, 1999. Submitted.

[62] B. M. Hochwald and W. Sweldens. Differential unitary space-time modulation. *IEEE Trans. on Communications*, 1999. Submitted.

[63] Y. Hua. Fast maximum likelihood for blind identification of multiple FIR channels. *IEEE Trans. Signal Processing*, 44:661–672, Mar. 1996.

[64] Y. Hua. Blind identification and equalization of channels driven by colored signals. 2000.

[65] B. L. Hughes. Differential space-time modulation. *IEEE Trans. on Information Theory*, 1999. Submitted.

[66] B. L. Hughes. Optimal space-time constellations from groups. *IEEE Trans. on Information Theory*, 2000. Submitted.

[67] R. Johannesson and K. S. Zigangirov. *Fundamentals of Convolutional Coding.* IEEE Press, New York, 1999.

[68] G. D. Forney (Jr). Maximum-likelihood sequence estimation of digital sequences in the presence of intersymbol interference. *IEEE Trans. on Information Theory*, 18:363–378, May 1972.

[69] G. D. Forney (Jr.) and M. V. Eyuboglu. Combined equalization and coding using precoding. *IEEE Commun. Mag.*, pages 25–34, Dec. 1991.

[70] G. J. Foschini (Jr.) and M. J. Gans. On limits of wireless communication in a fading environment when using multiple antennas. *Wirelss Personal Commun.*, 6:311–335, Mar. 1998.

[71] T. Kailath. *Linear Systems.* Prentice-Hall, Englewood Cliffs, NJ, 1980.

[72] S. Kasturia, J. T. Aslanis, and J. M. Cioffi. Vector coding for partial response channels. *IEEE Trans. on Information Theory*, 36(4):741–762, July 1990.

[73] R. D. Koilpillai and P. P. Vaidyanathan. Cosine-modulated FIR filter banks satisfying perfect reconstruction. *IEEE Trans.on Signal Processing*, 40:770–783, 1992.

[74] R. Laroia, S. A. Tretter, and N. Farvardin. A simple and effective precoding scheme for noise whitening on intersymbol interference channels. *IEEE Trans. on Communications*, 41:1460–1463, Oct. 1993.

[75] T. Larsson. Optimal state-space partitioning for reduced-state sequence detection. Technical Report 101, Dept. Computer Eng., Chalmers Univ. of Technol.,Göteborg, Sweden, 1990.

[76] E. A. Lee and D. G. Messerschmitt. *Digital Communication.* Kluwer Academic Publishers, Boston, 1994. 2nd Ed.

[77] T. Li and Z. Ding. Joint transmitter-receiver optimization for partial response channels based on nonmaximally decimated filterbank precoding technique. *IEEE Trans. on Signal Processing*, 47(9):2407–2414, Sept. 1999.

[78] Y. Li, J. Chuang, and N. R. Sollenberger. Transmitter diversity for OFDM systems and its impact on high-rate wireless networks. *IEEE J. Select. Areas Commun.*, 17:1233–1243, July 1999.

[79] Y. Li and Z. Ding. Convergence analysis of finite length blind adaptive equalizers. *IEEE Trans. on Signal Processing*, 43:2120–2129, Sept. 1995.

[80] Y. Li and Z. Ding. Global convergence of fractionally spaced Godard (CMA) adaptive equalizers. *IEEE Trans. on Signal Processing*, 44:818–826, April 1996.

[81] Y. Li and K. J. R. Liu. On blind MIMO channel identification using second-order statistics. In *Proc. of 30th Conf. on Info. Sci. and Systems*, Princeton Univ., Princeton, NJ, Mar. 1996.

[82] Y. Li and K. J. R. Liu. Static and dynamic convergence behavior of adaptive blind equalizers. *IEEE Trans. on Signal Processing*, 44:2736–2745, Nov. 1996.

[83] Y. Li, K. J. R. Liu, and Z. Ding. Length and cost dependent local minima of unconstrained blind channel equalizers. *IEEE Trans. on Signal Processing*, 43:2726–2735, Nov. 1996.

[84] Y. Li, N. Seshadri, and S. Ariyavisitakul. Channel estimation for OFDM systems with transmitter diversity in mobile wireless channels. *IEEE J. Select. Areas Commun.*, 17:461–471, Mar. 1999.

[85] Y. Li and N. R. Sollenberger. Adaptive antenna arrays for OFDM systems with cochannel interference. *IEEE Trans. Commun.*, 47:217–229, Feb. 1999.

[86] S. Lin and D. J. Costello (Jr). *Error Control Coding: Fundamentals and Applications.* Prentice-Hall, Englewood Cliffs, New Jersey, 1983.

[87] Y.-P. Lin and P. P. Vaidyanathan. Linear phase cosine modulated maximally decimated filter banks with perfect reconstruction. *IEEE Trans. Signal Processing*, 43:2525, 1995.

[88] H. Liu and X.-G. Xia. Precoding techniques for undersampled multi-receiver communication systems. In *Proc. of Asilomar'97*, pages 1043–1047, Pacific Grove, California, Nov. 1997.

[89] H. Liu and X.-G. Xia. Precoding techniques for undersampled multi-receiver communication systems. *IEEE Trans. on Signal Processing*, 48:1853–1863, July 2000.

[90] H. Liu and G. Xu. Closed-form blind symbol estimation in digital communications. *IEEE Trans. on Signal Processing*, 43:2714–2723, Nov. 1995.

[91] H. Liu and G. Xu. Multiuser blind channel estimation and spatial channel pre-equalization. In *Proc. of ICASSP'95*, Detroit, MI, May 1995.

[92] R. Liu and L. Tong. Special Issue on Blind Systems Identification and Estimation. *Proceedings of the IEEE*, 86(10), Oct. 1998.

[93] R.W. Lucky. Automatic equalization for digital communications. *Bell Syst. Tech. J.*, 44:547–588, April 1965.

[94] H. S. Malvar. Lapped transforms for efficient transform/subband coding. *IEEE Trans. Acoust. Speech Signal Process.*, 38:969–978, 1990.

[95] H. S. Malvar. *Signal Processing with Lapped Transforms.* Artech House, Boston, MA, 1992.

[96] H. S. Malvar and D. H. Staelin. The LOT: Transform coding without blocking effects. *IEEE Trans. Acoust. Speech Signal Process.*, 37:553–559, 1989.

[97] J. H. Manton and Y. Hua. A frequency domain deterministic approach to channel identification. *IEEE Signal Processing Letters*, 6:323–326, Dec. 1999.

[98] K. A. Meraim, P. Loubaton, and E. Moulines. A subspace method for certain blind identification problems. *IEEE Trans. on Information Theory*, 43:499–511, 1997.

[99] F. Mintzer. Filters for distortion-free two-band multirate filter banks. *IEEE Trans. Acoust. Speech Signal Process.*, 33:626–630, 1985.

[100] S. K. Mitra and R. Gnanasekaran. Block implementation of recursive digital filters-New structures and properties. *IEEE Trans. on Circuits and Systems*, 25:200–207, April 1978.

[101] E. Moulines, P. Duhamel, J. Cardoso, and S. Mayrargue. Subspace methods for the blind identification of multichannel FIR filters. *IEEE Trans. on Signal Processing*, 43:516–525, Feb. 1995.

[102] T. Q. Nguyen and P. P. Vaidyanathan. Two-channel perfect reconstruction FIR QMF structures which yield linear phase FIR analysis and synthesis filters. *IEEE Trans. Acoust. Speech Signal Process.*, 37:676–690, 1989.

[103] T. Q. Nguyen and P. P. Vaidyanathan. Structures for M-channel perfect reconstruction FIR QMF banks which yield linear phase analysis filters. *IEEE Trans. Acoust. Speech Signal Process.*, 38:433–446, 1990.

[104] H. J. Nussbaumer. Pseudo QMF filter bank. *IBM Tech. Disclosure Bulletin*, 24:3081–3087, 1981.

[105] S.-M. Phoong and P. P. Vaidyanathan. Paraunitary filter banks over finite fields. *IEEE Trans. Signal Processing*, 45:1443–1457, 1997.

[106] M. R. Portnoff. Time-frequency representation of digital signals and systems based on short-time fourier analysis. *IEEE Trans. Acoust. Speech Signal Process.*, 28:55–69, 1980.

[107] R. Price. Nonlinearly feedback-equalized pam vs. capacity. In *Proc. of ICC'72*, pages 22.12–22.17, Philadelphia, Penn., June 1972.

[108] J. G. Proakis. *Digital Communications.* New York: McGraw Hill, 1995. 3rd Ed.

[109] S. Qian and D. Chen. Discrete Gabor transform. *IEEE Trans. Signal Processing*, 41:2429–2438, 1993.

[110] D. Raphaeli and Y. Zarai. Combined turbo equalization and turbo decoding. *IEEE Comm. Letters.*, 2(4):107–109, 1998.

[111] L. Rodman. Matrix functions. *Handbook of Algebra*, Elsevier, New York 1996.

[112] M. Rouanne and D. J. Costello (Jr.). An algorithm for computing the distance spectrum of trellis codes. *IEEE J. Select. Areas Commun.*, 7:929–940, Aug. 1989.

[113] A. Said. Design of optimal signals for bandwidth-efficient linear coded modulation. Technical Report TR94-1, Electrical, Computer, and Systems Dept., Rensselaer Polytech. Inst., Troy, NY, Communication, Information and Voice Processing Report Series, Tech. Rep., 1994. Ph.D. dissertation.

[114] A. Said and J. B. Anderson. Tables of optiaml partial-response trellis modulation codes. Technical Report TR93-3, Electrical, Computer, and Systems Dept., Rensselaer Polytech. Inst., Troy, NY, Communication, Information and Voice Processing Report Series, Tech. Rep., 1993.

[115] A. Said and J. B. Anderson. Bandwidth-efficient coded modulation with optimized linear partial-response signals. *IEEE Trans. on Information Theory*, 44:701–713, 1998.

[116] J. Salz. Optimum mean-square decision feedback equalization. *Bell Syst. Tech. J.*, 52:1341–1373, Oct. 1973.

[117] Y. Sato. A method of self-recoving equalization for multi-level amplitude modulation. *IEEE Trans. on Communications*, 23, June 1975.

[118] A. Scaglione, G. B. Giannakis, and S. Barbarossa. Redundant filterbank precoders and equalizers: Part I and Part II. *IEEE Trans. on Signal Processing*, 47(7):1988–2022, July 1999.

[119] C. Schlegel. *Trellis Coding.* IEEE Press, New York, 1997.

[120] O. Shalvi and E. Weinstein. New criteria for blind deconvolution of nonminimum phase systems (channels). *IEEE Trans. on Information Theory*, 36:312–321, Mar. 1990.

[121] S. Shamai and R. Laroia. The intersymbol interference channel: Lower bounds on capacity and channel precoding loss. *IEEE Trans. Inform. Theory*, 42:1388–1404, Sept. 1996.

[122] S. Shamai, L. H. Ozarow, and A. D. Wyner. Information rates for a discrete-time Gaussian channel with intersymbol interference and stationary inputs. *IEEE Trans. Inform. Theory*, 37:1527–1539, Nov. 1991.

[123] D. T. M. Slock. Blind joint equalization of multiple synchronous mobile users using oversampling and/or multiple antennas. In *Proc. of 28th Conf. on Info. Sci. and Systems*, pages 1154–1158, Pacific Grove, CA, Nov. 1994.

[124] M. J. T. Smith and T. P. Barnwell III. Exact reconstruction techniques for tree-structured subband coders. *IEEE Trans. Acoust. Speech Signal Process.*, 34:434–441, 1986.

[125] M. J. T. Smith and T. P. Barnwell III. A new filter-bank theory for time-frequency representation. *IEEE Trans. Acoust. Speech Signal Process.*, 35:314–327, 1987.

[126] G. Strang and T. Q. Nguyen. *Wavelets and Filter Banks.* Wellesley-Cambridge Press, 1996.

[127] G. L. Stuber. *Principles of Mobile Communication.* Kluwer, Boston, 1996.

[128] S. Talwar, M. Viberg, and A. Paulraj. Blind estimation of multiple cochannel digital signals using an antenna array. *IEEE Signal Processing Letters*, 1:29–31, Feb. 1994.

[129] V. Tarokh, H. Jafarkhani, and A. R. Calderbank. Space-time block codes from orthogonal designs. *IEEE Trans. Inform. Theory*, 45:1456–1467, Jul. 1999.

[130] V. Tarokh, A. Naguib, N. Seshadri, and A. R. Calderbank. Combined array processing and space-time coding. *IEEE Trans. Inform. Theory*, 45:1121–1128, May 1999.

[131] V. Tarokh, N. Seshadri, and A. R. Calderbank. Space-time codes for high data rate wireless communication: Performance analysis and code construction. *IEEE Trans. Inform. Theory*, 44:744–765, Mar. 1998.

[132] E. Telatar. Capacity of multiantenna Gaussian channels. Technical report, AT&T-Bell Lab. Internal Tech. Memo., June 1995.

[133] M. Tomlinson. New automatic equalizer employing modulo arithmetic. *Electron. Lett.*, 7:138–139, Mar. 1971.

[134] L. Tong, G. Xu, and T. Kailath. A new approach to blind identification and equalization of multipath channels. In *Proc. of Asilomar'91*, pages 856–860, Pacific Grove, California, Nov. 1991.

[135] L. Tong, G. Xu, and T. Kailath. Blind identification and equalization based on second-order statistics: a time domain approach. *IEEE Trans. on Information Theory*, 40, Mar. 1994.

[136] J. K. Tugnait. Blind equalization and estimation of FIR communications channels using fractional sampling. *IEEE Trans. on Communications*, 44:324–336, Mar. 1996.

[137] G. Ungerboeck. Fractional tap-spacing equalizer and consequences for clock recovery in data modems. *IEEE Trans. on Communications*, 24:856–864, Aug. 1976.

[138] G. Ungerboeck. Channel coding with multilevel/phase signals. *IEEE Trans. on Inform. Theory*, 28:55–67, 1982.

[139] P. P. Vaidyanathan. Quadrature mirror filter banks, M-band extensions and perfect-reconstruction techniques. *IEEE ASSP Mag.*, 4:4–20, 1987.

[140] P. P. Vaidyanathan. Theory and design of M-channel maximally decimated quadrature mirror filters with arbitrary M, having perfect reconstruction property. *IEEE Trans. Acoust. Speech Signal Process.*, 35:476–492, 1987.

[141] P. P. Vaidyanathan. Multirate digital filters, filter banks, polyphase networks, and applications: a tutorial. *Proc. of the IEEE*, 78:56–93, 1990.

[142] P. P. Vaidyanathan. *Multirate Systems and Filter Banks.* Prentice Hall, Englewood Cliffs, NJ, 1993.

[143] P. P. Vaidyanathan and T. Chen. Role of anticausal inverses in multirate filter-banks—Part I: System-theoretic fundamentals. *IEEE Trans.on Signal Processing*, 43:1090–1102, 1995.

[144] P. P. Vaidyanathan and T. Chen. Role of anticausal inverses in multirate filter-banks—Part II: The FIR case, factorizations, and biorthogonal lapped transforms. *IEEE Trans.on Signal Processing*, 43:1103–1115, 1995.

[145] P. P. Vaidyanathan and S. K. Mitra. Polyphase networks, block digital fitering, LPTV systems, and alias-free QMF banks: a unified approach based on pseudocirculants. *IEEE Trans. Acoust. Speech Signal Process.*, 36:381–391, 1988.

[146] P. P. Vaidyanathan, T. Q. Nguyen, Z. Doğanata, and T. Saramäki. Improved technique for design of perfect reconstruction FIR QMF banks with lossless polyphase matrices. *IEEE Trans. Acoust. Speech Signal Process.*, 37:1042–1056, 1989.

[147] A. J. van der Veen, S. Talwar, and A. Paulraj. A subspace approach to blind space-time signal processing for wireless communication systems. *IEEE Trans. on Signal Processing*, 45:173–190, Jan. 1997.

[148] P. Vary. On the design of digital filter banks based on a modified principle of polyphase. *AEU*, 33:293–300, 1979.

[149] M. Vetterli. Filter banks allowing for perfect reconstruction. *Signal Processing*, 10:219–244, 1986.

[150] M. Vetterli. A theory of multirate filter banks. *IEEE Trans. Acoust. Speech Signal Process.*, 35:356–372, 1987.

[151] M. Vetterli and D. Le Gall. Perfect reconstruction FIR filter banks: some properties and factorizations. *IEEE Trans. Acoust. Speech Signal Process.*, 37:1057–1071, 1989.

[152] M. Vetterli and J. Kovačević. *Wavelets and Subband Coding.* Prentice Hall, Englewood Cliffs, NJ, 1995.

[153] P. A. Voois, I. Lee, and J. M. Cioffi. The effect of decision delay in finite-length decision feedback equalization. *IEEE Trans. on Information Theory*, 42:618–621, Mar. 1996.

[154] G. Wang, K. Xiao, and X.-G. Xia. Performance analysis of precoded OFDM systems in frequency-selective multipath Rayleigh fading channels. 1999.

[155] L.-F. Wei. Precoding technique for partial-response channels with applications to HDTV transmission. *IEEE J. Select. Areas Commun.*, 11:127–135, Jan. 1993.

[156] J. Wexler and S. Raz. Discrete Gabor expansions. *Signal Processing*, 21:207–220, 1990.

[157] J. Winters, J. Salz, and R. D. Gitlin. The impact of antenna diversity on the capacity of wireless communication systems. *IEEE Trans. Commun.*, 42:1740–1751, Feb./Mar./Apr. 1994.

[158] A. Wittneben. Base station modulation diversity for signal simulcast. In *Proc. IEEE' VTC*, pages 505–511, May 1993.

[159] C. W.-C. Wong and J. B. Anderson. Optimal short time impulse response channels for an MLSE receiver. In *Proc. of ICC'79*, pages 25.3.1–25.3.5, Boston, MA, June 1979.

[160] G. W. Wornell. Emerging applications of multirate signal processing and wavelets in digital communications. *Proceedings of the IEEE*, 84:586–603, April 1996.

[161] J. Xavier and V. Barroso. Polyhedral concepts for deterministic blind sepration of binary signals. In *Globecom99*, Rio de Janneiro, Brazil, Dec. 1999.

[162] J. Xavier, V. Barroso, and J. M. F. Moura. Closed form blind channel identification and source separation in SDMA systems through correlative coding. *IEEE J. Select. Areas Commun.*, 16, Oct. 1998.

[163] X.-G. Xia. Ambiguity resistant precoders in ISI/multipath cancellation: Distance and optimality. In *Proc. of Asilomar'97*, pages 936–940, Pacific Grove, California, Nov. 1997.

[164] X.-G. Xia. Modulated coding and least square decoding via coded modulation and Viterbi decoding. Technical Report 97-6-2, Department of Electrical and Computer Engineering, University of Delaware, Newark, Delaware, June 1997.

[165] X.-G. Xia. New precoding for intersymbol interference cancellation using nonmaximally decimated multirate filterbanks with ideal FIR

equalizers. *IEEE Trans. on Signal Processing*, 45:2431–2441, Oct. 1997.

[166] X.-G. Xia. Coding gain for modulated codes combined with ISI channels. 1998.

[167] X.-G. Xia. Modulated-coded zero-forcing decision feedback equalizer: Performance analysis and optimal modulated code design. Technical Report 98-5-2, Department of Electrical and Computer Engineering, University of Delaware, Newark, Delaware, May 1998.

[168] X.-G. Xia. A new coded zero-forcing decision feedback equalizer using modulated codes. In *Proc. MILCOM*, Atlantic City, New Jersey, Oct. 31-Nov.3 1999.

[169] X.-G. Xia. Precoded OFDM systems robust to spectral null channels and vector OFDM systems with reduced cyclic prefix length. Technical Report 99-4-1, Department of Electrical and Computer Engineering, University of Delaware, Newark, Delaware, April 1999.

[170] X.-G. Xia, P. Fan, and Q. Xie. A new coding scheme for ISI channels: Modulated codes. In *Proc. Internal. Conf. Comm.*, Vancouver, Canada, June 6-10 1999.

[171] X.-G. Xia and H. Liu. Polynomial ambiguity resistant precoders: theory and applications in ISI/multipath cancellation. *Circuits, Systems, and Signal Processing*, 19(2):71–98, 2000.

[172] X.-G. Xia, W. Su, and H. Liu. Filterbank precoders for blind equalization: Polynomial ambiguity resistant precoders (PARP). *IEEE Trans. Circuits and Systems I*, 1999. Submitted.

[173] X.-G. Xia and B. M. Suter. FIR paraunitary filter banks given several analysis filters: factorization and construction. *IEEE Trans. Signal Processing*, 44:720–723, 1996.

[174] X.-G. Xia and B. M. Suter. Vector-valued wavelets and vector filter banks. *IEEE Trans. Signal Processing*, 44:508–518, 1996.

[175] X.-G. Xia and B. W. Suter. Multirate filterbanks with block sampling. *IEEE Trans. Signal Processing*, 44:484–496, Mar. 1996.

[176] X.-G. Xia, G. Wang, and P. Fan. Space-time modulated codes for memory channels: Capacity and information rates, zero-forcing decision feedback equalizer. Technical Report 98-5-2, Department of Electrical and Computer Engineering, University of Delaware, Newark, Delaware, May 1999.

[177] X.-G. Xia and G. C. Zhou. On optimal ambiguity resistant precoders in isi/multipath cancellation. *IEEE Trans. on Circuits and Systems II*, 2000. Inprint.

[178] Q. Xie and X.-G. Xia. Modulated codes with ISI channels. Technical Report 98-3-1, Department of Electrical and Computer Engineering, University of Delaware, Newark, Delaware, Mar. 1998.

[179] Q. Xie and X.-G. Xia. Coded MMSE decision feedback equalizer using modulated codes. In *Proc. of Conf. on Info. Sci. and Systems*, Princeton University, Mar. 15-17 2000.

[180] G. Xu, H. Liu, L. Tong, and T. Kailath. A least-square approach to blind channel identification. *IEEE Trans. on Signal Processing*, 43:2982–2993, Dec. 1995.

[181] J. Yang and S. Roy. Joint transmitter-receiver optimization for multi-input multi-output systems with decision feedback. *IEEE Trans. on Information Theory*, 40(5):1334–1347, Sept. 1994.

[182] D. Yellin, A. Vardy, and O. Amrani. Joint equalization and coding for intersymbol interference channels. *IEEE Trans. on Information Theory*, 43:409–415, Mar. 1997.

[183] H. H. Zeng, L. Tong, and C. R. Johnson (Jr.). Relationships between the constant modulus and Wiener receivers. *IEEE Trans. on Information Theory*, 44:1523–1538, July 1998.

[184] Y.-J. Zhang and X.-G. Xia. Joint turbo and modulated code encoding/decoding. 1999.

[185] Y.-J. Zhang and X.-G. Xia. A new modulated code design for ISI channels. In *Proc. of Conf. on Info. Sci. and Systems*, Princeton University, Mar. 15-17 2000.

[186] G. C. Zhou and X.-G. Xia. Ambiguity resistant polynomial matrices. *Linear Algebra and Its Applications*, 286:19–35, 1999.

[187] K. Zhou, J. G. Proakis, and F. Ling. Decision-feedback equalization of time-dispersive channels with coded modulation. *IEEE Trans. on Commun.*, 38:18–24, Jan. 1990.

[188] T. N. Zogakis, J. T. Aslanis (Jr.), and J. M. Cioffi. A coded and shaped discrete multitone system. *IEEE Trans. Commun.*, 43:2941–2949, Dec. 1995.

[189] W. Y. Zou and Y. Wu. COFDM: An overview. *IEEE Trans. on Broadcasting*, 40:1–8, Mar. 1995.

Index